

Application of Gold(I) Catalysis in the Synthesis of Bridged Carbocycles, (±)-Magellanine and (±)-Salvinorin A

Philippe McGee

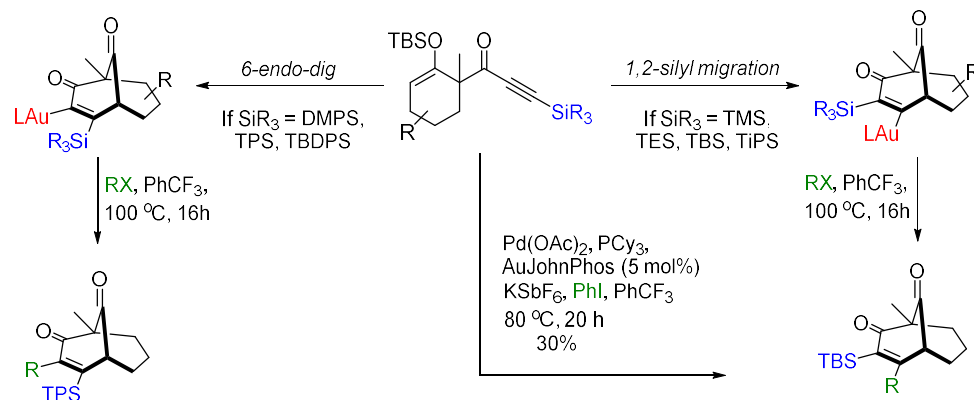
A thesis submitted in partial fulfillment of the
requirements for the Doctorate in Philosophy degree in Chemistry

Department of Chemistry and Biomolecular Science
Faculty of Science
University of Ottawa

© Philippe McGee, Ottawa, Canada, 2018

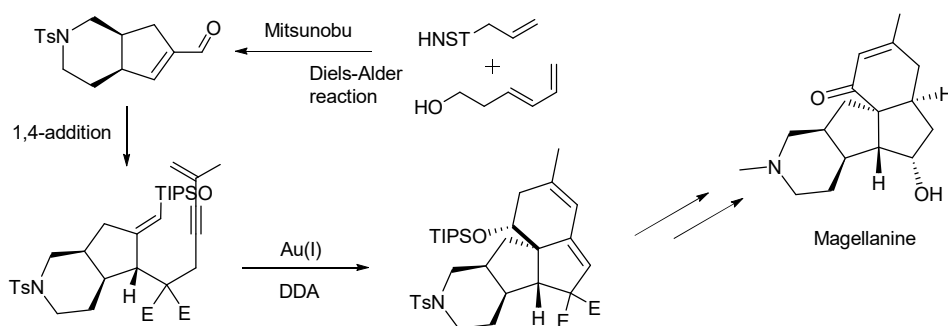
Abstract

Gold was considered for a long time to be an inert metal and was only in 1986 that the first homogeneous gold-catalyzed transformation was reported. In our laboratory, we isolated a surprisingly stable vinyl complex that resulted from an unexpected 1,2-silyl migration while working on a gold(I)-catalyzed reaction for the synthesis of polyprenylated polycyclic acylphloroglucinols (PPAPs). We herein report the isolation of a variety of organogold species where we could control the silyl migration based on the nature of the silyl group installed on the terminal alkyne. Silyl groups bearing an aromatic ring inhibited the silyl migration while the aliphatic silyl group afforded the 1,2-silyl migrated adduct. After mechanistic investigation of this intriguing migration, we believe that this process goes through a relatively rare gold vinylidene intermediate. More than 15 organogold complexes were isolated in good yield and characterized by x-ray crystallography. Investigation of their reactivity led to the formation of C(sp³)–C(sp²) bonds using electrophilic reagents without the use of Pd-based catalysts.

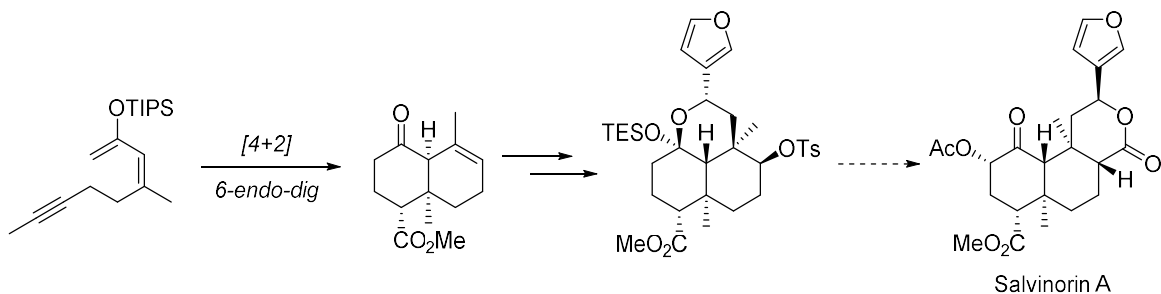


We have also developed a new gold(I)-catalyzed dehydro Diels-Alder reaction using a simple monocyclic silyl enol ether. This methodology proceeds effectively with a wide scope by the use of [JackiephosAu(NCMe)]SbF₆ in toluene. This methodology was then applied to the

synthesis of magellanine, an architecturally complexed angular natural product isolated in 1976 from the club moss *Lycopodium Magellanicum*. The key step precursor was rapidly constructed via a Mitsunobu/Diels-Alder reaction that generated the requisite carboxaldehyde. The dehydro Diels-Alder reaction afforded the molecular skeleton of magellanine diastereoselectively in 91% yield. The synthesis was successfully accomplished in 11 steps demonstrating the ability of the gold(I) salt to rapidly construct complex molecules.



Since the discovery of salvinorin A, a lot of efforts were exerted in order to optimize the biological activity for treatment of central nervous system disorders. Development of a new synthetic routes to salvinorins are essential to afford novel functionalized analogues. The decalin framework of salvinorin A was assembled with a Diels-Alder reaction with Et_2AlCl followed by a gold(I)-catalyzed 6-*endo-dig* carbocyclization with $[\text{JohnphosAu}(\text{NCMe})]\text{SbF}_6$. Further functionalization afforded an elaborated intermediate which possesses the correct stereochemistry of the natural product. Following these promising results, efforts are currently in progress for the completion of the total synthesis.



Acknowledgments

Le défi d'effectuer un doctorat n'est sans aucun doute une des épreuves les plus difficiles que j'ai vécu à ce jour. Cette étape est loin d'être un périple individuel, sans la présence des gens dans mon entourage, rien de cela n'aurait été possible. C'est pour cette raison que je tiens à faire la mention et des remerciements à plusieurs personnes et institutions qui m'ont encouragé lors de cette partie éprouvante de ma vie.

Mon superviseur, Louis Barriault, fut une inspiration incroyable tout au long de mon doctorat. Son leadership, sa persévérance, son positivisme et sa créativité à l'égard de la chimie sont surprenants. Je tiens à le remercier d'avoir cru en moi et de m'avoir accepté dans son laboratoire de recherche. Les conseils de Prof. Barriault ont été précieux et m'ont aidé tout au long de mes études.

Mes parents, Michel et Lucie, ont sans aucun doute joué un rôle primordial dans ce parcours. Dès le début, ils m'ont encouragé à effectuer des études de niveaux supérieurs. Je les remercie non seulement pour leur support financier, mais aussi pour leur soutien moral. Ce support m'a donné le courage de continuer malgré certaines épreuves difficiles. Je leur en suis extrêmement reconnaissant pour tout ce qu'ils ont fait pour moi. Merci maman et papa!

Sans oublier ma douce moitié, Sonia, qui a été présente pendant cette étape. Elle m'a toujours soutenu et encouragé tout au long de ce parcours. Sa bonne humeur et son beau sourire ont indéniablement ajouté beaucoup de positif dans ma vie. Merci de m'avoir écouté et compris lors des moments où j'avais besoin de me confier.

Ma sœur Karine, mon frère David et mon ami Philippe ont toujours démontré de l'admiration par rapport à mon progrès universitaire. Cela m'a sans aucun doute aidé à pousser mes limites pour les rendre fiers. David, même s'il a été physiquement loin, il a toujours été près de mon cœur. Les petites soirées festives "olé olé" avec eux m'ont beaucoup diverti. Un bon équilibre avec la vie sociale fut essentiel pour garder la santé morale. Merci à tous mes amis, dont Nicolas Papillon.

Je tiens aussi à souligner plusieurs de mes anciens collègues qui sont maintenant devenus des amis. J'aimerais remercier Francis Barabé qui fut un mentor lors de mes débuts, Jason fut un exemple à suivre et Joel a été un collègue de bureau hors de l'ordinaire. Boubacar a été un partenaire de hottes très inspirant, Amandine m'a ébloui avec sa personnalité exceptionnelle et je remercie Geneviève pour sa contribution en recherche. Terry a un cœur énorme et m'a beaucoup aidé avec mon anglais. Les idées innovantes de Mathieu m'ont toujours surpris. Je remercie Julie de m'avoir diverti avec ses photos de chats et Montserrat pour les spectres infrarouges. Je n'oublierai jamais les discussions intellectuelles et inspirantes avec Mike. J'aimerais aussi remercier J-P, Martin, Samantha, Huy, André, Léa, Alysson, Avery, Sherif et Tom pour leur appui lors de mes études. J'ai apprécié tous les moments passés avec eux que ce soit en réunion parlant de chimie ou même autour d'une bière.

Je tiens aussi à remercier André Beauchemin, Fabien Gagosz, Keith Fagnou et Chris Boddy qui ont eu un impact sur ma passion pour la chimie. Il ne faut tout de même pas oublier Annette et Josée au centre administratif qui me font toujours sourire en arrivant le matin. Merci aussi à Glenn Facey pour le soutien à la RMN, Ilia Korobkov pour les rayons X et Sharon au centre de spectrométrie en masse.

Les soutiens financiers offerts par le Conseil de recherche en science naturelle et génie du Canada (CRSNG), Fonds de recherche du Québec - Nature et technologies (FRQNT) et Bourse d'études supérieures de l'Ontario (BÉSO) m'ont été d'une aide indescriptible. Finalement, tous mes sincères remerciements à l'Université d'Ottawa qui m'a offert un endroit propice pour réaliser mon doctorat.

Table of contents

Chapter 1: Introduction to gold catalysis.....	1
1.1 Physical properties of gold(I).....	1
1.2 General reactivity of gold(I).....	3
1.3 Effect of counterions and ligands in gold(I) catalysis.....	7
1.4 Activation of alkyne for the construction of molecular complexity.....	7
1.4.1 Addition of ROH nucleophiles.....	8
1.4.2 Addition of R ₂ NH nucleophiles.....	10
1.4.3 Conia-ene type reactions.....	13
1.4.4 Cycloisomerization.....	14
1.5 Binuclear Au(I) in photoredox catalysis.....	18
1.6 Conclusion.....	21
1.7 References.....	21
Chapter 2: Isolation and reactivity of vinylgold complexes.....	25
2.1 Introduction to vinylgold.....	25
2.2 Unexpected vinylgold intermediates.....	26
2.3 Substrates preparations.....	28
2.4 Optimization and substrate scope.....	30
2.5 Mechanistic insights.....	34
2.6 Reactivity of vinylgold.....	37
2.7 Synergistic dual-catalysis with Au and Pd.....	39

2.8 Conclusion.....	41
2.9 References.....	42
Chapter 3: Gold(I)-catalyzed [4+2] cycloaddition and its application to the synthesis of magellanine.....	45
3.1 Introduction to gold(I)-catalyzed dehydro Diels-Alder reaction.....	45
3.2 Formation of angular cores via a gold(I)-catalyzed carbocyclization.....	47
3.2.1 Hypothesis.....	48
3.2.2 Substrate preparation.....	50
3.2.3 Optimization and substrate scope.....	51
3.2.4 Double bond isomerization.....	58
3.3 Magellanine and related alkaloids.....	59
3.3.1 Previous synthetic forays of magellanine and its congeners.....	60
3.3.2 Our retrosynthetic approach.....	63
3.3.3 Route A: Enal synthesis through Lewis acid-catalyzed [4+2].....	66
3.3.4 Route B: Enal synthesis through dehydrogenative Diels-Alder.....	67
3.3.5 Route C: Enal synthesis through one-pot Mitsunobu/Diels-Alder reaction.....	70
3.3.6 End game: Total synthesis of (±)-magellanine.....	73
3.4 Conclusion.....	76
3.5 References.....	77
Chapter 4: Towards the total synthesis of salvinorin A.....	80
4.1 Introduction.....	80
4.1.1 Structural features and biological properties.....	81
4.1.2 Structure-affinity relationship (SAR).....	82

4.1.3 Biosynthesis	84
4.1.4 Previous synthetic approaches.....	85
4.2 Progress towards Salvinorin A.....	88
4.2.1 Retrosynthetic analysis.....	88
4.2.2 Synthesis of the diene and Diels-Alder cycloaddition.....	90
4.2.3 Decalin formation via a 6- <i>endo-dig</i> gold(I)catalyzed carbocyclization.....	92
4.2.4 Enone functionalization.....	95
4.2.5 Exploring the reactivity of the acetal / lactol.....	99
4.2.6 En route towards the synthesis of salvinorin A.....	101
4.3 Future work.....	104
4.4 Conclusion.....	106
4.5 References.....	107
Chapter 5: Conclusion.....	110
Chapter 6: Additional information.....	112
6.1 Claims to original research.....	112
6.2 Publications for this work.....	112
6.3 Oral presentations.....	113
6.4 Poster presentations.....	113
Chapter 7: Experimental procedures.....	115
7.1 Isolation and reactivity of vinyl gold complexes.....	115
7.1.1 Silylation of the terminal alkynes for the preparation of 2.3.2	115
7.1.2 Removal of THP protecting groups on 2.3.2	119
7.1.3 Oxidation of the propargylic alcohols 2.3.3	121

7.1.4 Aldol reaction and Dess-Martin oxidation for the formation of 2.3.5	123
7.1.5 Aldol reaction for the formation of 2.3.8	129
7.1.6 Conjugated addition and oxidation to produce 2.3.8	132
7.1.7 Silyl enol ether formation	135
7.1.8 Vinylgold formation	145
7.1.9 Transmetalation of vinylgold with palladium	163
7.1.10 Alkylation of vinylgold	164
7.1.11 Other side products	174
7.2 Gold(I)-catalyzed [4+2] and its application to the synthesis of magellanine	175
7.2.1 Sonogashira coupling for the formation of 3.2.15	175
7.2.2 Preparation of 3.2.17 via conjugated 1,4 addition	179
7.2.3 Gold(I)-catalyzed [4+2] cycloaddition	188
7.2.4 Synthesis of magellanine: Route A	198
7.2.5 Synthesis of magellanine: Route B	204
7.2.6 Synthesis of magellanine: Route C	207
7.2.7 End game: Total synthesis of (±)-magellanine	211
7.3 Towards the total synthesis of salvinorin A	223
7.3.1 Synthesis of the diene and Diels-Alder cycloaddition	223
7.3.2 Preparation of allylic alcohol 4.2.4	226
7.3.3 Exploring the reactivity of the acetal / lactol	234
7.3.4 En route towards the synthesis of salvinorin A	239
Collective spectral data	247

Schemes

Scheme 1.1 - Lewis acidity and backdonation ability of Au(I).....	3
Scheme 1.2- General catalytic cycle for alkyne functionalization using gold(I) salts	4
Scheme 1.3- Stages according to Xu and Hammond.....	6
Scheme 1.4 - Hydration of alkynes with Au(I).....	9
Scheme 1.5 - Total synthesis of (±)-bryostatin 6.....	10
Scheme 1.6 - Gold(I)-catalyzed intermolecular hydroamination.....	11
Scheme 1.7 - Ligand-controlled gold-catalyzed reaction of ureas	11
Scheme 1.8 - Synthesis of (-)-quinocarcin.....	12
Scheme 1.9- Gold-catalyzed Conia-ene reaction of β-ketoesters	13
Scheme 1.10 - Regioselective cyclization of silyl enol ethers.....	13
Scheme 1.11 - Total synthesis of (+)-lycopoladine.....	14
Scheme 1.12 - General pathways for cycloisomerization of 1,6-enynes	15
Scheme 1.13- Regioselective double cycloisomerization of 1,11-dien-3,9-diynes	16
Scheme 1.14 - Total synthesis of (-)-englerin A	17
Scheme 1.15 - Proposed mechanism for the formation of the oxatricyclic core.....	18
Scheme 1.16- Photoredox cyclizations with binuclear gold complex.....	19
Scheme 1.17 - Proposed oxidative quenching catalytic cycle.....	20
Scheme 1.18 - Total synthesis of (±)-triptolide.....	20
Scheme 2.1 - The first isolated vinylgold intermediates.....	25
Scheme 2.2 - Relative rate of protodeauration.....	26
Scheme 2.3 - Total synthesis of polycyclic prolynated acylphloroglucinol (PPAPs).....	27

Scheme 2.4 - A chromatographically stable vinylgold complex	28
Scheme 2.5 - Substrate preparation bearing different silyl substituents	29
Scheme 2.6 - Preparation of sterically hindered substrates	30
Scheme 2.7 - Ligand optimization in the isolation of vinylgold species	32
Scheme 2.8 - Controlled 1,2-silyl migration	33
Scheme 2.9 - Crossover experiment	35
Scheme 2.10 - Experiment for interconversion of 2.4.1k and 2.4.2a	36
Scheme 2.11 - Proposed mechanisms	36
Scheme 2.12 - Synergistic dual catalysis with Au and Pd	39
Scheme 2.13 - First attempt of dual-catalysis	40
Scheme 2.14 - Control experiment	40
Scheme 2.15 - Optimized conditions	41
Scheme 3.1 - General dehydro Diels-Alder reaction (DDA)	43
Scheme 3.2 – Echavarren’s gold(I)-catalyzed intramolecular [4+2] cycloadditions	44
Scheme 3.3 – Tetracycle formation via cyclization of 1-aryl-6,8-dien-1-ynes	46
Scheme 3.4 - Domino cyclization for the synthesis of polyaromatic heterocycles	47
Scheme 3.5 - Envisaged gold(I)-catalyzed process for the construction of angular core	49
Scheme 3.6 - Synthesis of substituted propargyl malonates	50
Scheme 3.7 - Precursors synthesis for the gold(I)-catalysed transformation	51
Scheme 3.8 – Model substrate investigation by Geneviève Bétournay	52
Scheme 3.9 - Substrate scope for gold(I)-catalyzed carbocyclization	54
Scheme 3.10 - Proposed mechanism for the formation of the naphthalene derivative	57
Scheme 3.11 - Reaction condition for NMR experiment	58

Scheme 3.12 - Prins-pinacol rearrangement by Overman	61
Scheme 3.13 - Formal [4+2] cycloaddition by Paquette's and co-workers	61
Scheme 3.14 - Total synthesis of magellanine by Liao	62
Scheme 3.15 – Pauson-Khand key step by Takahashi	62
Scheme 3.16 - Pauson-Khand reaction key steps by Mukai	63
Scheme 3.17 - Site specific aldol reaction by Yang	64
Scheme 3.18 - Palladium catalyzed olefin insertion by Yan	64
Scheme 3.19 - Retrosynthetic approach of (±)-magellanine	65
Scheme 3.20 – Geneviève Bétounay's approach to the synthesis of enal 3.3.36	66
Scheme 3.21 - Overview of the route A	67
Scheme 3.22 - Dehydrogenative Diels-Alder reaction by Christina White	68
Scheme 3.23 - Dehydrogenative Diels-Alder reaction approach	69
Scheme 3.24 - Overview of the route B	70
Scheme 3.25 - Hypothetical Mitsunobu/Diels-Alder reaction sequence	71
Scheme 3.26 - Optimized route of enal preparation	73
Scheme 3.27 - Overview of the route C	73
Scheme 3.28 - Key steps of the tetracyclic core formation	74
Scheme 3.29 - Functional group manipulation for (±)-magellanine synthesis	75
Scheme 3.30 - Last steps of (±)-magellanine synthesis	76
Scheme 4.1 - Epimerization of salvinorin A	81
Scheme 4.2 - Simplified biosynthetic pathway for salvinorin A	83
Scheme 4.3 - Synthesis of salvinorin A by Evans	84
Scheme 4.4 - Synthesis of salvinorin A by Hagiwara	86

Scheme 4.5 - Synthesis of salvinorin A by Forsyth	87
Scheme 4.6 - Synthesis of salvinorin A by Metz	88
Scheme 4.7 - Retrosynthetic analysis of salvinorin A	89
Scheme 4.8 - Synthesis of the diene 4.2.8	90
Scheme 4.9 - Possible products from 4.2.8	92
Scheme 4.10 - Preparation of the α -bromo acetal 4.2.3	97
Scheme 4.11 - Lactol vs 1,4-hydroxyaldehyde	99
Scheme 4.12 - Attempts to trap the opened lactol 4.2.25	100
Scheme 4.13 - Successful transformations from 4.2.25 or 4.2.2	101
Scheme 4.14 - Attempts to form a nitrile at the C-8 position	102
Scheme 4.15 - Incorporation of the furan moiety and attempt to install the nitrile	103
Scheme 4.16 - Substitution from the enone 4.2.4	104
Scheme 4.17 - Alternative preparation of salvinorin A	105
Scheme 4.18 – Summary of the current approach	106

Figures

Figure 1.1- Consequences of the relativistic effect on orbitals.....	2
Figure 1.2- General correlation of ion pair with reactivity.....	5
Figure 1.3- Ligand structures that modulate different stages of gold-catalyzed reactions.....	7
Figure 1.4 - Total syntheses using gold catalysis.....	8
Figure 3.1 - Natural product possessing a polycyclic angular core.....	48
Figure 3.2 - Proposed transition state for the diastereoselectivity found in the isolated products....	53
Figure 3.3 - Additives used in Table 3.1.....	54
Figure 3.4 - Reaction progress quantified by NMR.....	59
Figure 3.5 - Structures of magellanine, magellanineone and paniculatine.....	60
Figure 3.6 - Reviewed disconnection of (±)-magellanine synthesise.....	77
Figure 4.1 - Structure of salvinorin A-C.....	80
Figure 4.2 - Salvinorin A proposed binding site.....	82
Figure 4.3 - Structural modification tolerance from the structure-activity relationship.....	83
Figure 4.4 - Structure comparison of salvinorin A with MOM-Sal B and RB-64.....	84
Figure 4.5 - Proposed complexes for the selective epoxidation.....	96

Tables

Table 2.1 - Optimization of vinylgold formation.....	31
Table 2.2 – Vinylgold complexes cross-coupling reaction.....	38
Table 3.1 – Isomerization optimization.....	53
Table 3.2 - Ligand optimization for the DDA reaction.....	55
Table 3.3 - Optimization of the Mitsunobu and Diels-Alder reaction.....	72
Table 4.1 - Optimization of the Diels-Alder cycloaddition.....	91
Table 4.2 - Solvent optimization of the gold-catalyzed carbocyclization.....	93
Table 4.3 - Ligand optimization.....	94
Table 4.4 - Epoxidation of 4.2.8	95
Table 4.5 - Optimization of the radical cyclization.....	98

Abbreviations

Ac:	acetyl
ACH:	acetone cyanohydrine
Ad:	adamantane
ADDP:	1,1'-(Azodicarbonyl)dipiperidine
AIBN:	2,2'-Azobis(2-methylpropionitrile)
BARF:	tetrakis[3,5-bis(trifluoromethyl)phenyl]borate
BC:	before Christ
BHT:	butylated hydroxytoluene
Bn:	benzyl
BQ:	benzoquinone
Bz:	benzoyl
Boc:	<i>tert</i> -butyloxycarbonyl
BOM:	benzyloxymethyl acetal
Bpy:	2,2'-Bipyridine
Cy:	cyclohexyl
CNS:	central nervous system
CSA:	camphor-10-sulfonic acid
CMMP:	(cyanomethylene)trimethylphosphorane
DCM:	dichloromethane
DCE:	1,2-dichloroethane

DDA:	dehydro Diels-Alder
DDQ:	2,3-Dichloro-5,6-dicyano-1,4-benzoquinone
DAIB:	(diacetoxyiodo)benzene
DBU:	1,8-diazabicyclo[5.4.0]undec-7-ene
DIAD:	diisopropyl azodicarboxylate
DIPEA:	<i>N,N</i> -diisopropylethylamine
DMDO:	dimethyldioxirane
DMAP:	4-(dimethylamino)pyridine
DMF:	dimethylformamide
DMP:	Dess-Martin periodinane
DMPS:	dimethyphenylsilyl
DMS:	dimethyl sulfide
DMSO:	dimethyl sulfoxide
DOXP:	1-deoxy-D-xylulose-5-phosphate pathway
Dppm:	bis(diphenylphosphino)methane
DPS:	<i>tert</i> -butyldiphenyl
E:	ethyl ester
Et:	ethyl
GGPP:	geranylgeranyl pyrophosphate
HAT:	hydrogen atom abstraction
HMDS:	hexamethyldisilazane
IMDA:	intramolecular Diels-Alder
IPP:	isopentenyl pyrophosphate

<i>i</i> Pr:	isopropyl
KOPr:	kappa opioid receptor
L:	ligand
LDA:	lithium diisopropylamide
LED:	light-emitting diode
LUMO:	lowest occupied molecular orbital
MAV:	mevalonate pathway
<i>m</i> -CPBA:	<i>m</i> -chloroperoxybenzoic acid
Me:	methyl
MS:	molecular sieves
MOM:	methoxymethylacetal
Napht:	napthalene
NBS:	<i>N</i> -bromosuccinimide
NFSI:	<i>N</i> -fluorobenzylsulfonimide
NHC:	<i>N</i> -heterocyclic carbene
NIS:	<i>N</i> -iodosuccinimide
NMO:	4-methylmorpholine <i>N</i> -oxide
NMR:	nuclear magnetic resonance
Nu:	nucleophile
ODMP:	oxa-di- π -methane
OTf:	trifluoromethanesulfonate
PCC:	pyridinium chlorochromate
Ph:	phenyl

Piv:	pivaloate
PNB:	<i>p</i> -nitrobenzyl
PMP:	1,2,2,6,6-pentamethylpiperidine
PPAPs:	polyprenylated polycyclic acylphloroglucinols
Ppy:	2-phenylpyridinato- C^2,N
<i>p</i> TSA:	<i>p</i> -toluenesulfonic acid
SET:	single electron transfert
TBS:	<i>tert</i> -butyldimethylsilyl
<i>t</i> -Bu:	<i>tert</i> -butyl
TES:	triethylsilyl
TBAF:	tetrabutylammonium fluoride
Tf:	trifluoromethanesulfonyl
TFA:	trifluoroacetic acid
THF:	tetrahydrofuran
THP:	tetrahydropyran
TMAD:	tetramethylazodicarboxamide
TMS:	trimethylsilyl
TIPS:	triisopropylsilyl
TPS:	triphenylsilyl
TOF:	turnover frequency
Ts:	toluenesulfonyl
UVA:	ultraviolet A

CHAPTER 1

Introduction to gold catalysis

1.1 Physical properties of gold(I)

Due to the molten properties of early Earth, it is thought that much of the planet's gold sank into the planetary core.¹ Thus, much of the gold that is present in the Earth's crust and mantle today was delivered to Earth by asteroid impacts during the Late Heavy Bombardment period, approximately 4 billion years ago. As a result, humans currently have limited access to small portions of the gold contained within the Earth's crust. The first documented human-made gold artifact was found in the Varna Necropolis, Bulgaria; it is believed to be from the 4th millennium BC.^{2a} For ages, gold in its pure form was admired for its bright, soft, and malleable properties along with its resistance towards oxidation. In 2017, a total of 190,040 tonnes of gold were estimated to be mined from the Earth's crust. Nowadays, the world's distribution of gold is estimated to be about 48% jewellery, 21% in investment, and 17% in industry.^{2b} Gold is also the subject of many misconceptions. For example, gold is considered a rare element, but it is more abundant than palladium, platinum, rhodium, and many other precious metals.

Along with gold's rarity, it was considered to be an inert metal and consequently, the first chemical transformations of gold salts was not reported before the late 20th century. The benefits of gold as a homogeneous catalyst for the synthesis of fine chemicals have emerged in a spectacular fashion.³ With the atomic number of 79, gold has the following electronic configuration: $[\text{Xe}]4f^{14}5d^{10}6s^1$, with most stable oxidation states being 0, +1, and +3. The remarkable reactivity of gold salts was attributed to its relativistic effect.⁴ The effect takes place

when the electron velocity becomes close to the speed of light. According to Dirac's theory, the increased velocity of the **s** and **p** electrons of gold results in a gain of mass. Since, the Bohr radius of an electron is inversely proportional to the mass of an electron, the resulting mass increases lead to energetic stabilization and radial contraction of the **s** and **p** orbitals. Consequently, this creates a stronger shielding of the nucleus and results in less attraction of the **f** and **d** orbitals. Hence, the described destabilization leads to the expansion of the **f** and **d** orbitals, as illustrated in *Figure 1.1*.

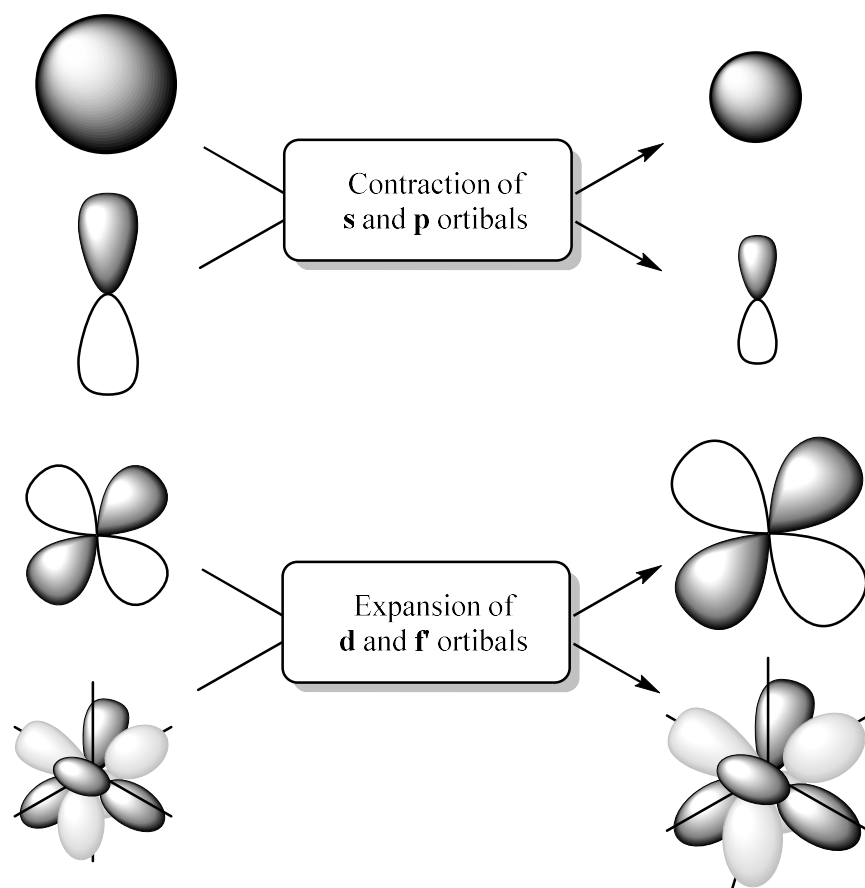
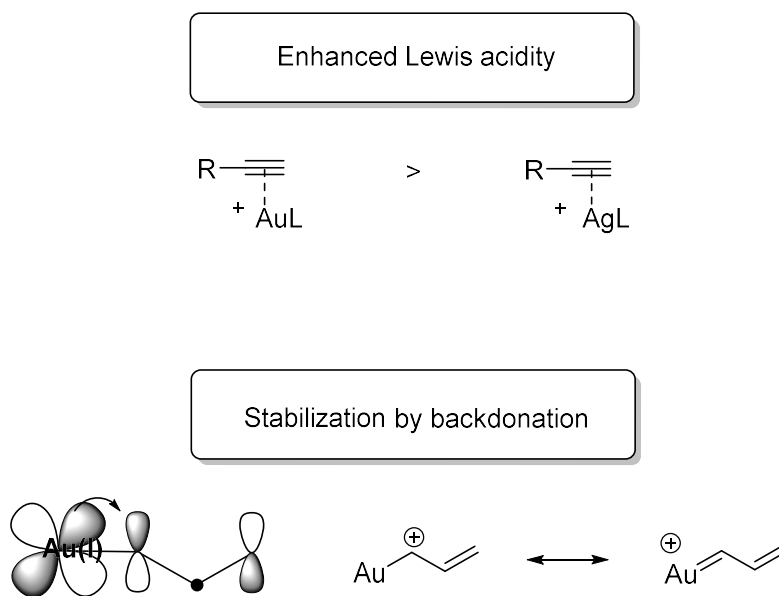


Figure 1.1- Consequences of the relativistic effect on orbitals

Although the relativistic effects have consequences on the **p** and **f** orbitals, the **6s** and **5d** orbitals are responsible for most of the chemical reactivity and physical properties observed with gold complexes. For instance, the excitation of the filled **5d** orbital occurs with a band gap of 2.38

eV; blue light is therefore absorbed which explains the bright yellow colour of gold. Moreover, the contraction of the valence **s** orbital leads to the soft Lewis-acidity of Au(I) complexes due to the low-lying lowest unoccupied molecular orbital (LUMO) (*Scheme 1.1*). In addition, the over-sized **d** orbitals allow the delocalization of electron density, explaining the ability of Au(I) complexes to stabilize nearby cationic charges by backdonation.

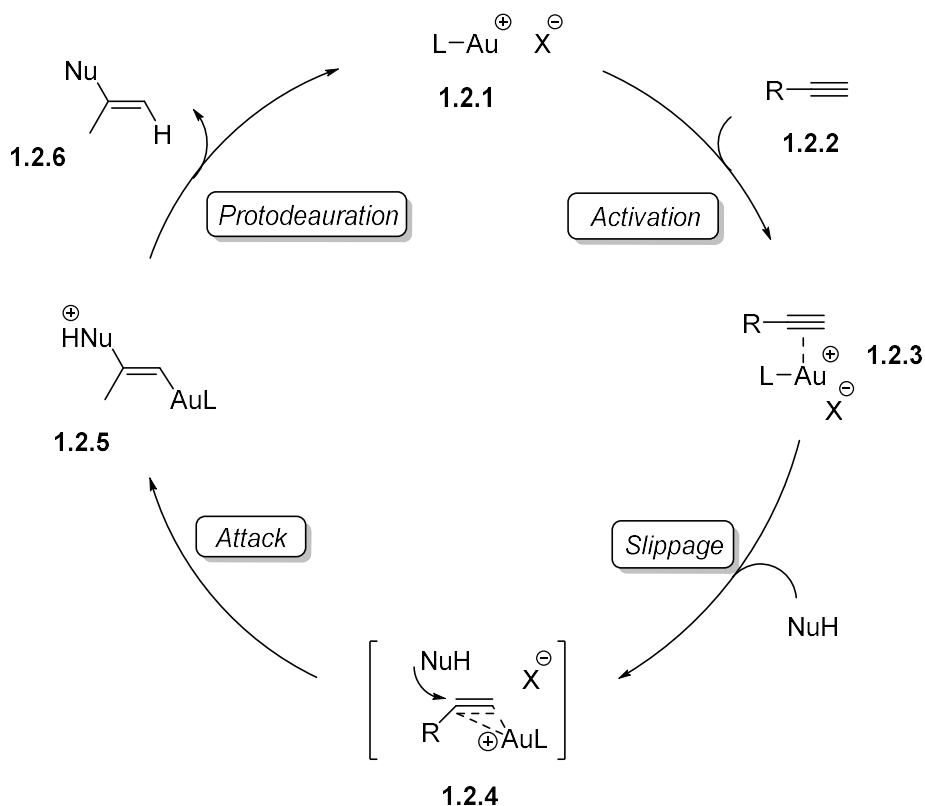


Scheme 1.1 - Lewis acidity and backdonation ability of Au(I)

1.2 General reactivity of gold(I)

The robustness, versatility, and the unique π -acidity of gold makes it a superior choice for activation of alkyne, allene, and alkene moieties as compared to other group 11 metals.^{4d} The chemoselectivity of transformations mediated by Au(I) complexes allow reactivity to occur under mild conditions and also minimizes the need for protecting groups manipulation. Generally, the catalytic cycle for the functionalization of alkyne **1.2.2** by cationic gold salt **1.2.1** to give the Au-complexed **1.2.3** starts with π -activation of the substrate **1.2.2** (*Scheme 1.2*).⁵ The electron deficient

alkyne complex **1.2.3** is now susceptible to outer-sphere attack by adequate nucleophiles such as alcohols, amines, π -bonds, and N-oxides. The addition will generate the *trans* alkynyl-gold intermediate **1.2.5** which is now subject to protodemetalation with release of the final product **1.2.6** and regenerates the active gold specie **1.2.1**.



Scheme 1.2- General catalytic cycle for alkyne functionalization using gold(I) salts

1.3 Effect of counterions and ligands in gold(I) catalysis

In 1986, Ito and Hayashi reported the first chemical reaction performed with homogeneous gold(I) catalysis.⁶ More than one decade later the first examples of alkyne activation by gold(I) salts were reported by Teles⁷ and Tanaka.⁸ Since these discoveries, the groups of Fürstner, Toste,

Echavarren, Gagosz, Blum, Hammond, Hashmi, and Zhang (just to name a few) have significantly contributed to the expansion and understanding of gold(I) catalyzed organic transformations.³

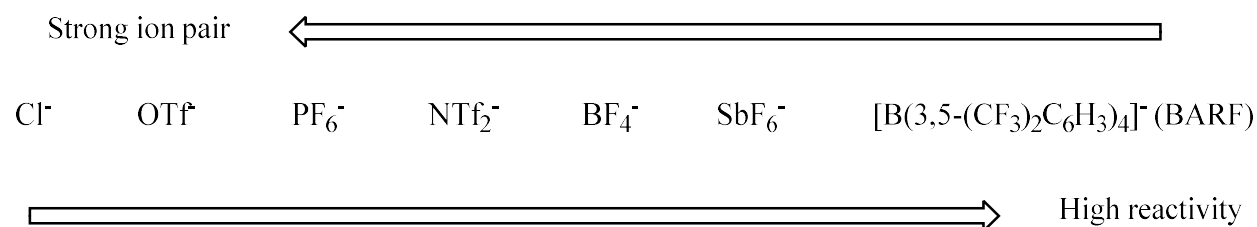
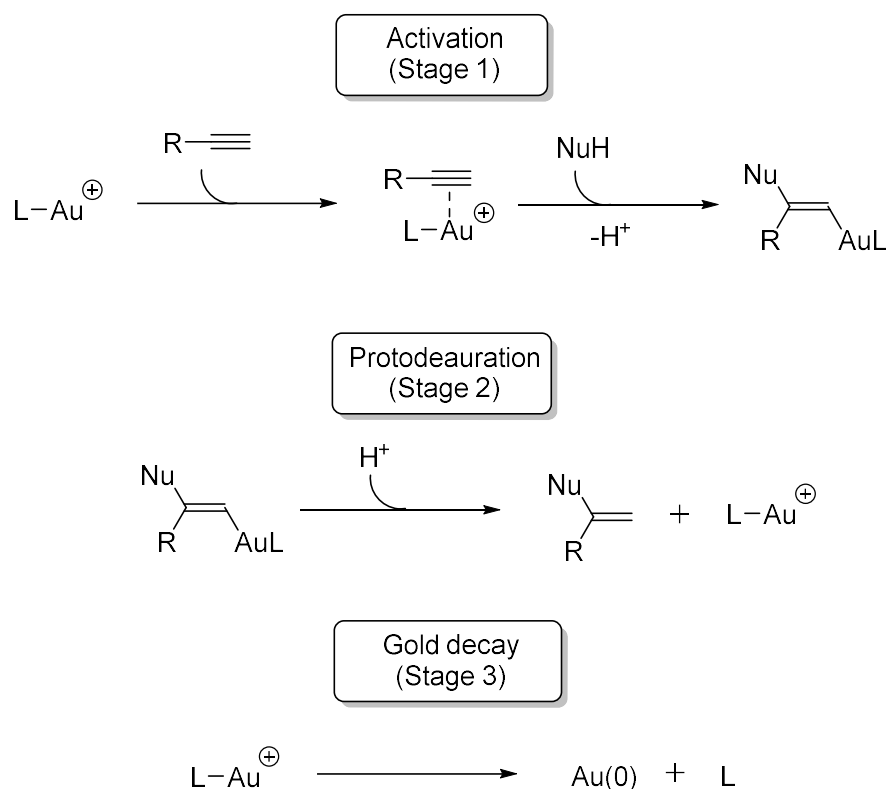


Figure 1.2- General correlation of ion pairing with reactivity

The ligand and counterion adorned on the gold(I) salts have significant impacts on efficiency and regioselectivity of gold(I) transformations. Many researchers have demonstrated the importance of the counterion in gold-catalyzed processes and all came to similar conclusions.⁹ AuCl could be used to catalyze transformations but could not efficiently activate π -bonds. The non-cationic character reduces the Lewis acidity, thus requires harsh conditions and *in-situ* activation to form the cationic gold salt. Cationic metal catalysts exist as an ion pair rather than “free” ions. Consequently, there is a charge separation between Au⁺ and X⁻ during the activation of substrates. In general, a catalyst that contains a weakly coordinating counterion such as SbF₆⁻ will exhibit stronger Lewis acidity and higher reactivity, as illustrated in *Figure 1.2*.

So far, we have highlighted the importance of the counterion and omitted the crucial role of ligands in gold(I)-catalyzed process. A detailed study by Xu and Hammond demonstrated the importance of the ligand’s electronic properties with Au(I) in each stage of a gold catalyzed reaction.¹⁰ Most gold(I)-catalyzed transformations (alkyne activation shown) proceed through three major stages: 1) electronic activation of the alkyne; 2) protodeauration to regenerate the cationic gold species; 3) degradation of the gold catalyst (*Scheme 1.3*).



Scheme 1.3- Stages according to Xu and Hammond

Ligands which adorn gold cationic species have significant impacts on the rate of each stage. *Stage 1:* the study reveals that on less activated substrates combined with a weak nucleophile (a relatively slow reaction), electron poor ligands will accelerate the overall rate of the reaction. An electron deficient ligand will enhance the cationic gold character, resulting in better affinity for the π -bond and in a higher turn over frequency (TOF). Therefore, a ligand such as **L1** (Figure 1.3) will be benefit for such chemical transformations.¹¹ *Stage 2:* in the case of slow protodeauration of the vinyl gold intermediate, usually caused by electron withdrawing properties or stabilization by the substrate, a different ligand should be used. In this scenario, the vinyl gold could be observed by NMR spectroscopy and occasionally chromatographically stable. To circumvent low turnover, a more electron rich ligand such as tricyclohexyl phosphine **L2**

accelerates the protodeauration step.¹² *Stage 3*: the third situation is considered a fast deactivation of the gold catalyst. More elaborated complexes are then necessary to avoid degradation of the gold catalysts to Au(0). It was reported that n^2 -interactions, such as those from Buchwald-type ligands, afford a higher stability by the biphenyl moiety, as illustrated by the structure of Jackiephos (**L3**).¹³ Counterions can also play an important role in the degradation of catalyst. In response to these limitations, Gagosz and co-workers developed a more thermally stable catalyst bearing the NTf₂ anion.¹⁴

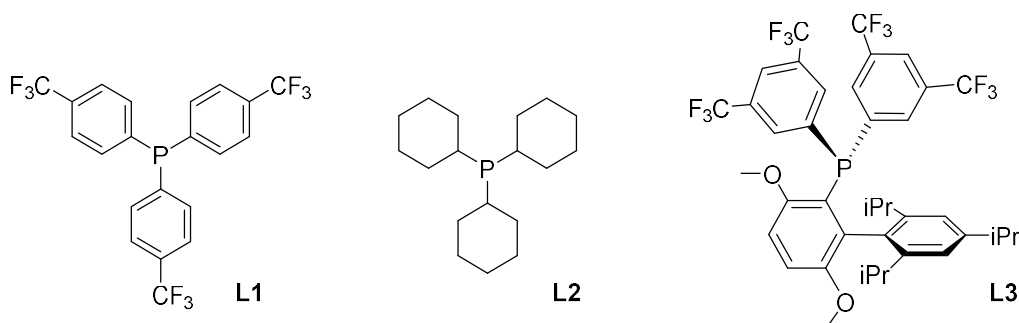


Figure 1.3- Ligand structures that modulate different stages of gold-catalyzed reactions

N-Heterocyclic carbene (NHC) ligands can also be installed on Au(I) to generate another interesting class of complexes. They differ by their electronic properties; NHCs are good σ -donors that result in less π -backdonation in comparison with phosphine ligands. Examples of regioselective transformations using carbene ligands will be discussed later in this chapter.

1.4 Activation of alkynes for the construction of molecular complexity

A broad variety of chemical reactions have been developed over the past two decades.³ This section will mostly focus on the different categories of transformations using gold catalysis. In each section, the first reported transformation, a regioselective transformation by ligand

modulation, and an application in synthesis will be presented, if available. Practicality and efficiency of gold salts in the catalysis of key transformations is demonstrated by the substantial amount of total syntheses of natural products reported, where several examples are illustrated in *Figure 1.4*.¹⁵

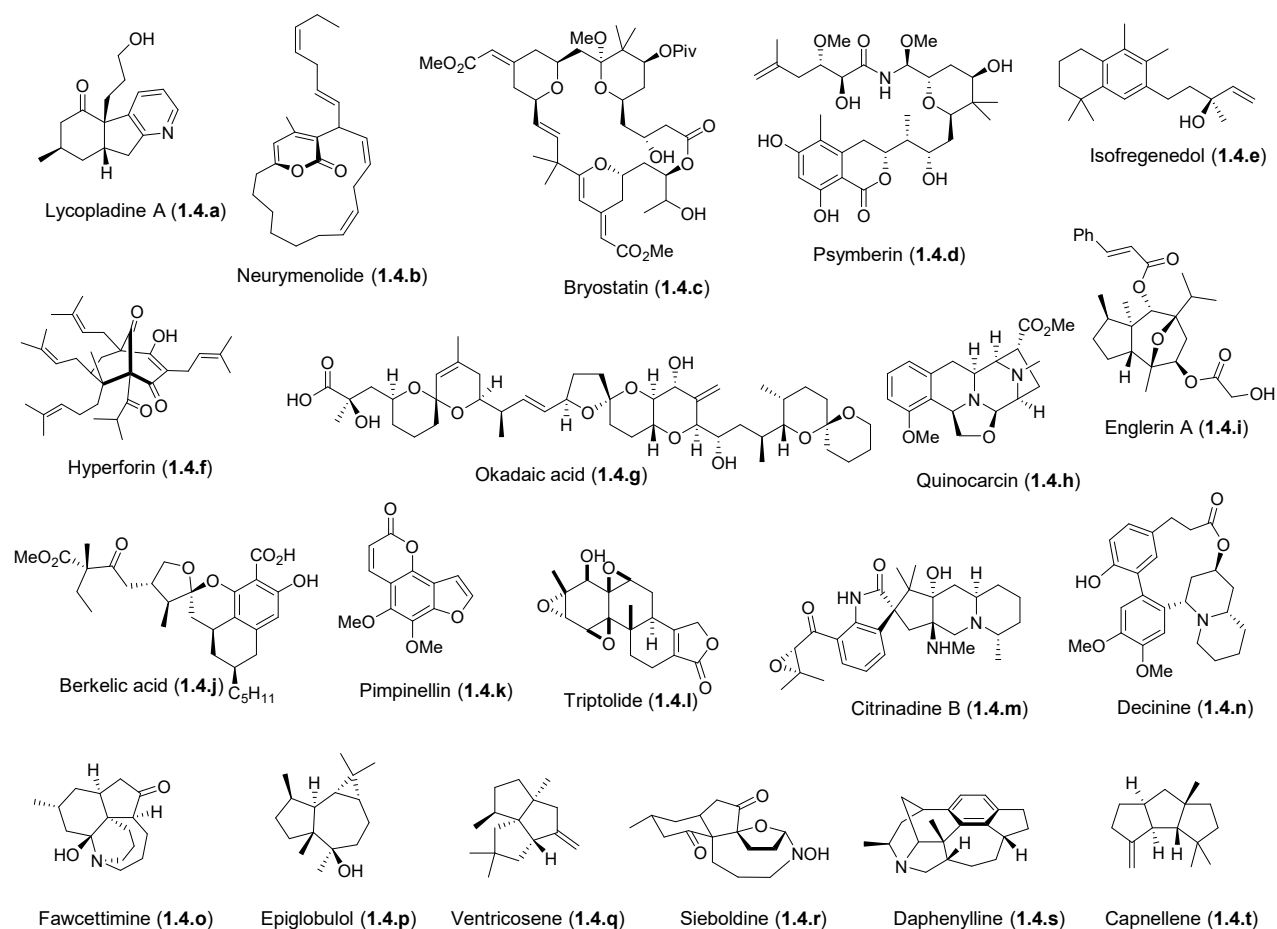
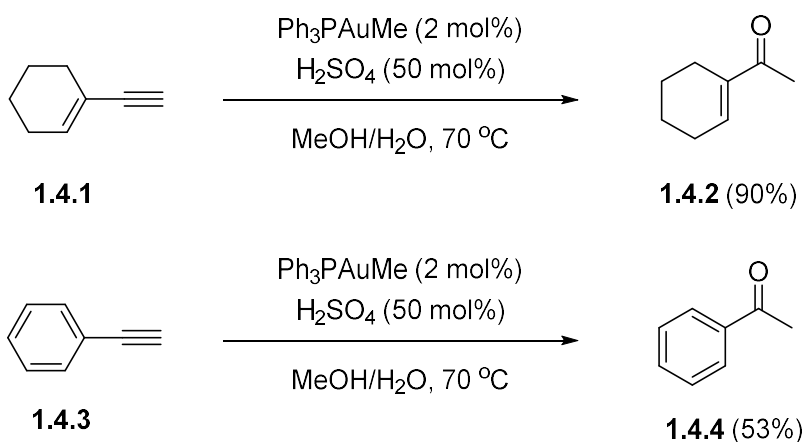


Figure 1.4 - Total syntheses using gold catalysis

1.4.1 Addition of ROH nucleophiles

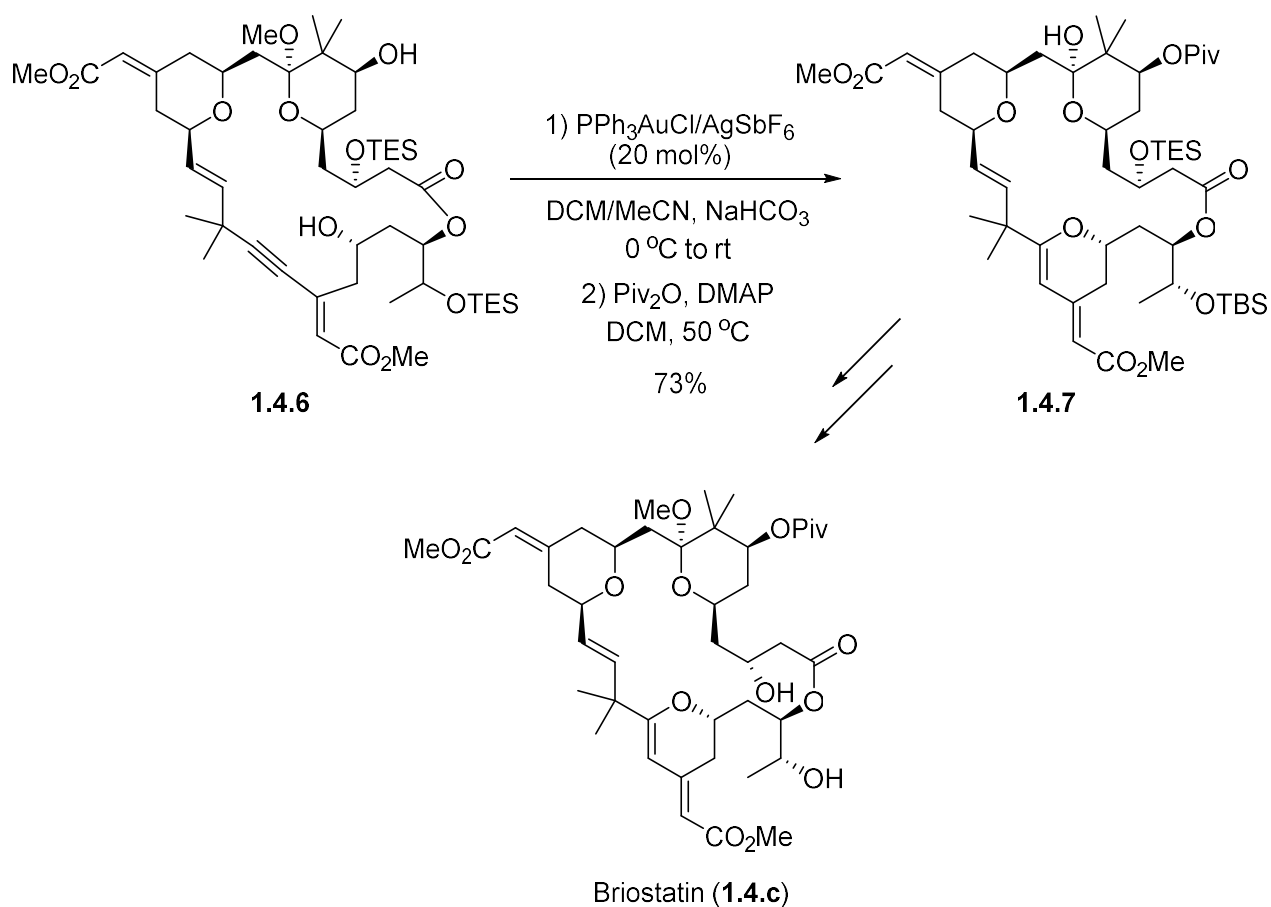
Due to the relativistic effect, gold salts possess high π -affinity and low oxophilicity and are able to activate C-C in the presence of H₂O and alcohols. The first examples of alcohol and water additions into alkynes using gold salts were reported in 1998 by the group of Tales and Tanaka

(Scheme 1.4).⁷⁻⁸ The Markovnikov-type addition was observed by the formation of **1.4.2** and **1.4.4**. It was proposed that the transformation proceeded first by the *in-situ* formation of a cationic gold species, which then activated the alkyne. Methanol addition followed by protodeauration afforded the enol ether and then hydrolysis led to the ketone. In contrast with previous work, this methodology doesn't require toxic reagents such as Hg(I) salts under acidic conditions.¹⁶



Scheme 1.4 - Hydration of alkynes with Au(I)

The efficiency of gold-catalyzed hydroxylation of alkynes in presence of various functional groups was demonstrated by Trost in 2008.^{15c} The C-ring formation of bryostatin **1.4.c** via a challenging gold-catalyzed 6-*endo-dig* carbocyclization is shown in Scheme 1.5. The transformation of **1.4.5** proceeded smoothly using an *in-situ* activated cationic gold species to afford the dihydropyran **1.4.6** in 73% yield. The selectivity for the 6-*endo-dig* pathway over the 5-*exo-dig* cyclization is presumably mediated by the Markovnikov-type addition on the polarized alkyne. Notably, due to the Lewis acidity of the catalyst in presence of water, the methyl ketal moiety was hydrolyzed under these reaction condition.

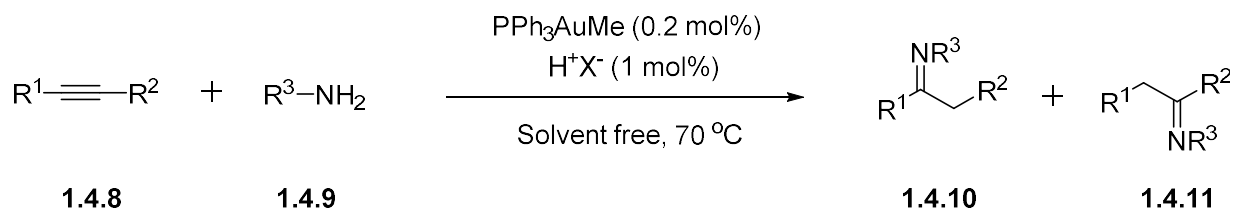


Scheme 1.5 - Total synthesis of (±)-bryostatin 6

1.4.2 Addition of R_2NH nucleophiles

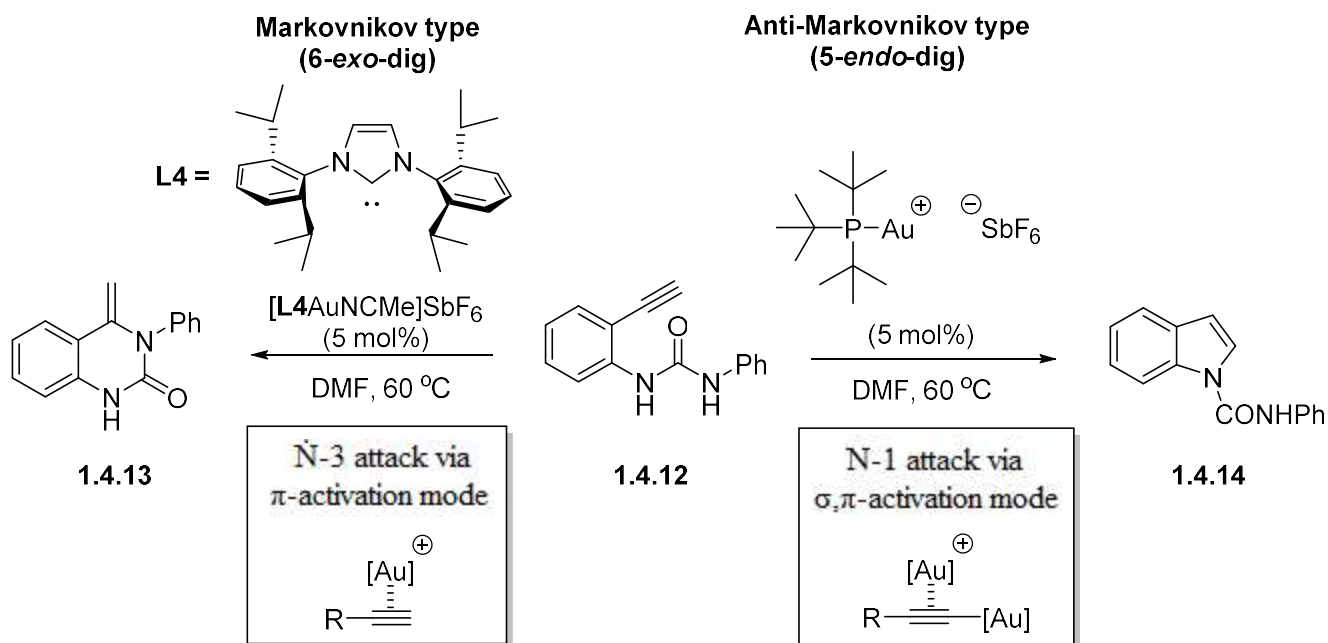
Since 1987 gold(III)-catalyzed hydroamination of terminal alkynes has been known,¹⁷ however, it was not until 2003 that Hayashi and Tanaka developed the first gold(I)-catalyzed intermolecular amination of alkynes **1.4.8** with anilines **1.4.9** to form imines **1.4.10** and **1.4.11**, respectively (Scheme 1.6).¹⁸ Cationic gold salts have a stronger azaphilicity than oxophilicity. Therefore, more nucleophilic anilines react slowly which could be explained by catalyst poisoning, caused by the active site of the gold complex being coordinated by the nitrogen atom. Preferably,

less nucleophilic *N*-nucleophiles should be used in gold(I)-catalyzed transformations to maximize reactivity.



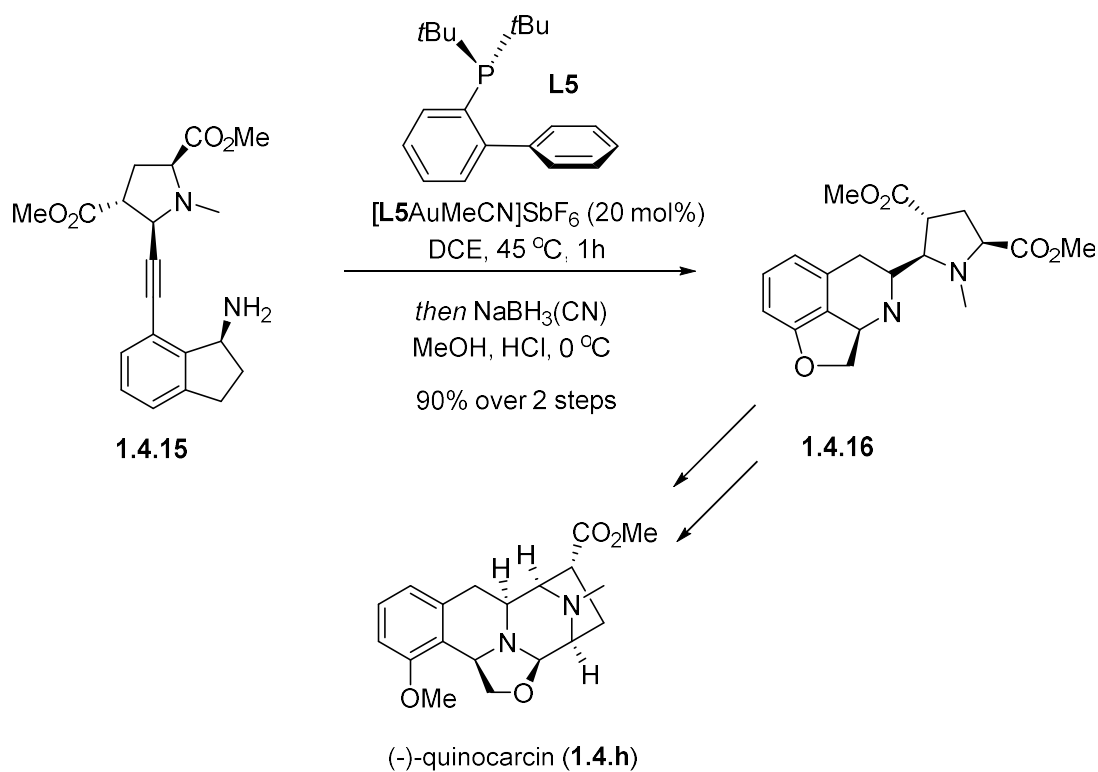
Scheme 1.6 - Gold(I)-catalyzed intermolecular hydroamination

In 2009, the group of Medio-Simónn demonstrated the divergent preparation of **1.4.13** and **1.4.14** could be accomplished from **1.4.12** through modification of the ligands' electronic properties using 1-(o-ethynylaryl)ureas, (*Scheme 1.7*).¹⁹ They have reported that either 6-*exo* or 5-*endo-dig* gold-mediated cyclizations could be performed using different activation modes.



When NHC-stabilized gold(I) complexes were used, the process went through the known π -activation mode and led to the formation of **1.4.13** via nucleophilic attack of N-3. On the other hand, activation of **1.4.12** proceeded through a dual σ,π -activation mode employing $P(t\text{-Bu})_3$ as the ligand to favour the *N*-1 attack, generating **1.4.14** selectively.

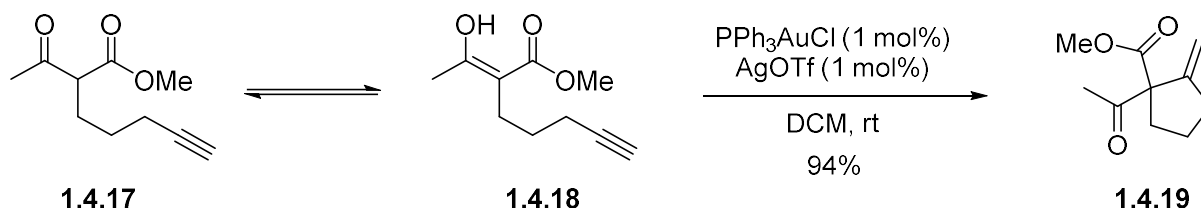
The ability of gold(I) to construct nitrogen containing heterocycles has been demonstrated in many total syntheses. For instance, Ohno and co-workers reported an efficient application of gold(I)-catalyzed intramolecular hydroamination in the total synthesis of (-)-quinocarcin (**1.4.h**).^{15h} Amine **1.4.15** was converted into **1.4.16** through *in situ* iminium reduction (*Scheme 1.8*). The amine **1.4.15** in the presence of $[L5AuMeCN]SbF_6$ lead exclusively to the 6-*endo-dig* product. The 5-*exo-dig* product was not observed due to the ring strain found in the product.



Scheme 1.8 - Synthesis of (-)-quinocarcin

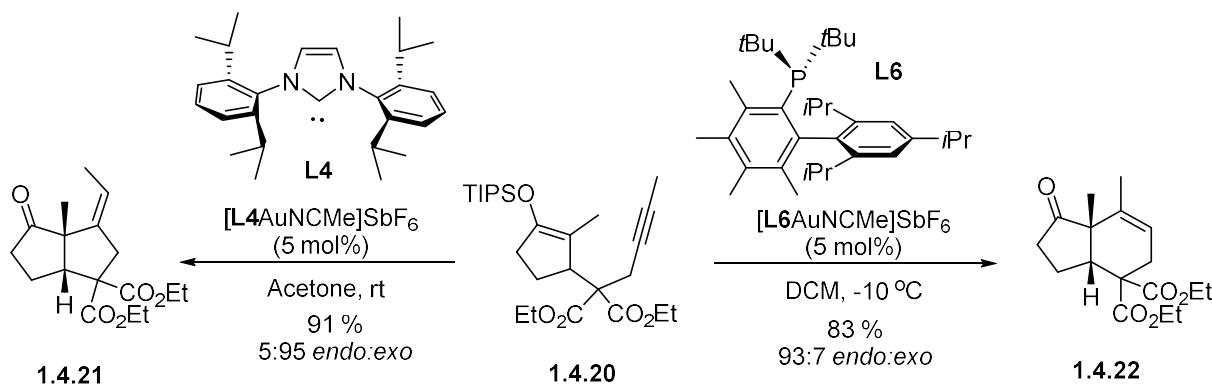
1.4.3 Conia-ene type reactions

Conia-ene type reactions are also catalyzed by gold(I), which can be considered as the cyclization of 1,6-enynes via the corresponding enol tautomer, as illustrated in *Scheme 1.9*. In 2004, Toste reported a Conia-ene reaction catalyzed by $[\text{PPh}_3\text{Au}]\text{Cl}$ and AgOTf .²⁰ The β -ketoester **1.4.17** in equilibrium with its enol form **1.4.18** underwent gold(I)-catalyzed cyclization to afford **1.4.19** in 94% yield. The intramolecular cyclization of the enol onto the unactivated alkyne proceeded selectively via a 5-*exo-dig* pathway. Notably the 6-*endo-dig* carbocyclization pathway was not observed due to Markovnikov type addition with $\text{Au}(\text{I})$.



Scheme 1.9- Gold-catalyzed Conia-ene reaction of β -ketoesters

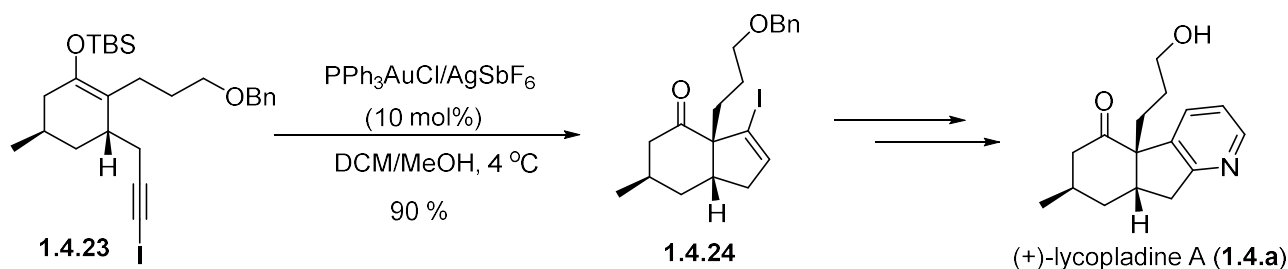
Silyl enol ethers can react in a similar way to β -ketoesters for their addition onto alkynes.²¹ In 2011, Barriault *et al.* reported a ligand-controlled carbocyclization of **1.4.20** (*Scheme 1.10*).²²



Scheme 1.10 - Regioselective cyclization of silyl enol ethers

The electron rich NHC ligand (**L4**) led preferentially to the 5-*exo-dig* product **1.4.21** whereas using a bulkier phosphine ligand (**L6**) favoured the 6-*endo-dig* product **1.4.22**. The divergence in pathway while using more hindered phosphine ligands was attributed to the distorted linearity of the L-Au-X bond at the transition state.²³ Therefore, diminishing the ligand's ability to stabilize the gold(I) intermediate by backdonation and consequently, proceeded through a more likely cationic process.

The efficiency and application of Conia-ene type reactions have been demonstrated through the total synthesis of the polycyclic alkaloid (+)-lycopoladine A (*Scheme 1.11*).^{15a} Treatment of the monocyclic silyl enol ether **1.4.23** with [PPh₃Au]Cl/AgSbF₆ undergoes 5-*endo-dig* cyclization to afford the desired polycyclic compound **1.4.24**, as the sole diastereomer. Subsequent Suzuki coupling followed by electrocyclization produced to the desired (+)-lycopoladine A.

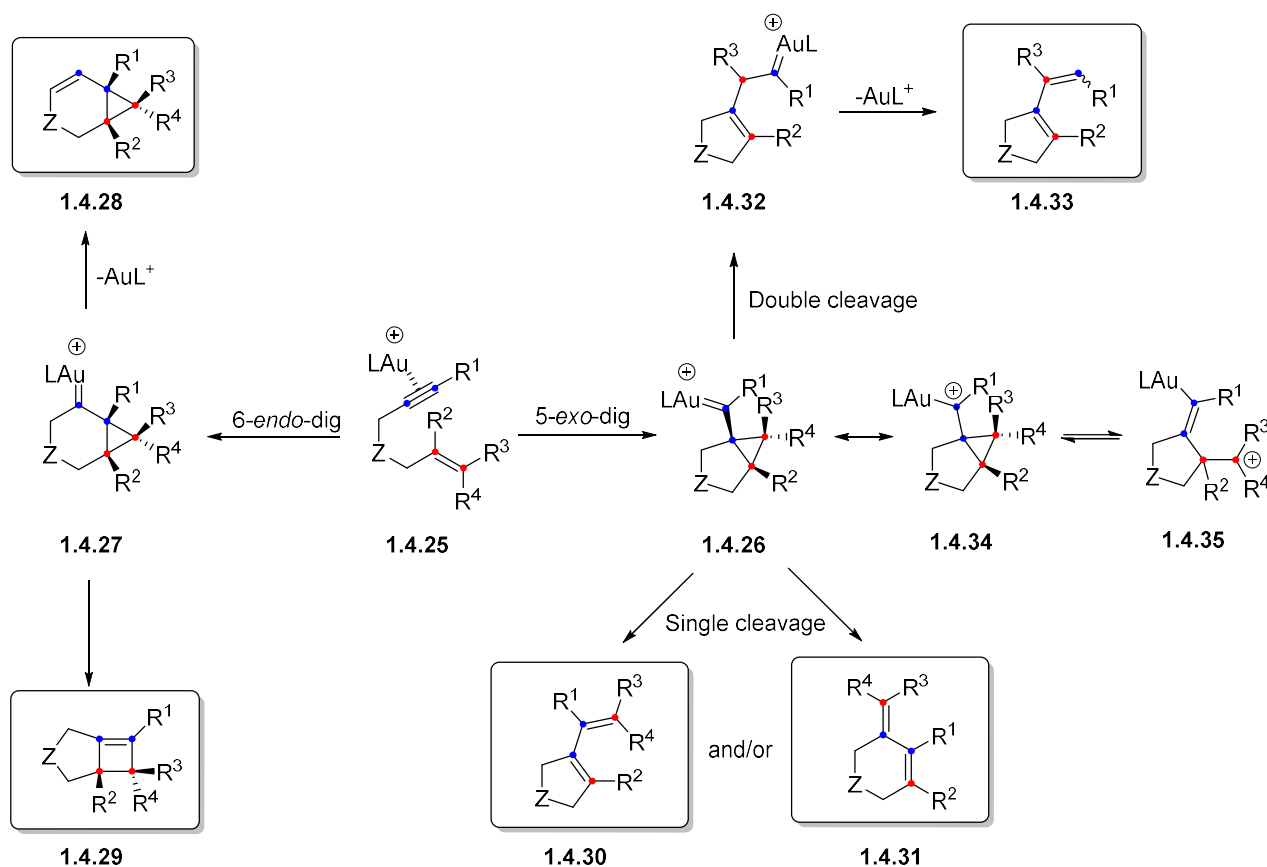


Scheme 1.11 - Total synthesis of (+)-lycopoladine

1.4.4 Cycloisomerization-type reactions

1,*n*-Enynes represent an important structural motif for construction of molecular complexity. The first example of this kind was reported in the 1980s using a palladium-based catalyst.²⁴ In contrast with palladium or platinum, gold(I)-catalyzed alkyne transformations go

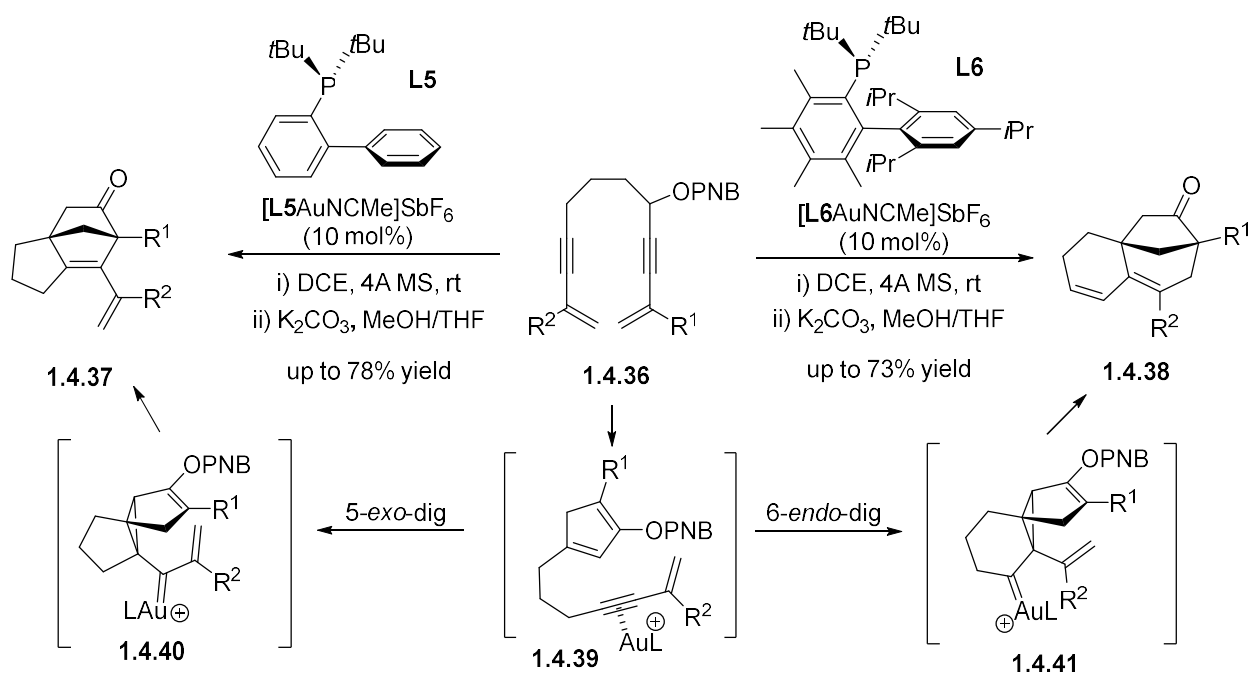
through n^2 -alkyne activation, which is then susceptible to nucleophilic attack. In absence of an internal or external nucleophile, enynes such as **1.4.25** generate products derived from different skeletal rearrangements (*Scheme 1.12*).²⁵ As a general pathway, enyne **1.4.25** will undergo 5-*exo-dig* or 6-*endo-dig* carbocyclizations to form **1.4.26** or **1.4.27**, respectively. On one hand, protodeauration of **1.4.27**, bicyclo[4.1.0]heptene derivative **1.4.28** will be observed.



Scheme 1.12 - General pathways for cycloisomerization of 1,6-enynes

Alternatively, isomerization of the gold(I) carbene **1.4.27** by ring expansion of the cyclopropane moiety could afford the cyclobutene **1.4.29**. On the other hand, a single-cleavage skeletal rearrangement via the opening of **1.4.26** would generate **1.4.30** and/or **1.4.31**. Moreover, the intermediate **1.4.26** could undergo a double cleavage rearrangement, which would lead to **1.4.33**

after protodeauration. It is important to note that 5-*exo-dig* adduct is usually the predominant product observed in gold(I)-catalyzed processes. 6-*endo-dig* carbocyclization could also be achieved by careful choice of the ligand on the gold complex. Gold(I) carbenoid intermediates, as shown in the structure of **1.4.26**, have been subject to much debate in the literature. It is important to emphasize that these types of species (**1.4.26**, **1.4.27**, and **1.4.32**) show highly delocalized structures and are strongly dependent on the nature of the R-groups (surrounding functionality) along with the ligand found on gold. π -Backdonation of gold(I) to the carbon center is generally poor and is shown in the structure of **1.4.34**, which is probably more adequate.²⁶ There are few complexes containing relatively short Au–C bonds that exhibit carbene-like structures that have been characterized, as illustrated by **1.4.26**.²⁷

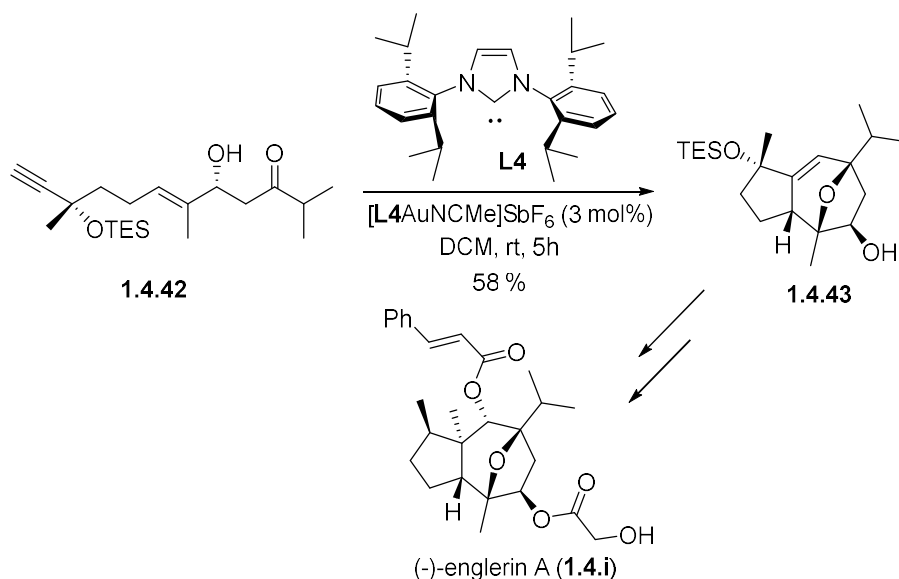


Scheme 1.13- Regioselective double cycloisomerization of 1,11-dien-3,9-diynes

Fine tuning of the steric and electronic proprieties of the gold catalyst can drastically affect the selectivity during the cycloisomerization reaction. As illustrated in *Scheme 1.13*, Chan's group

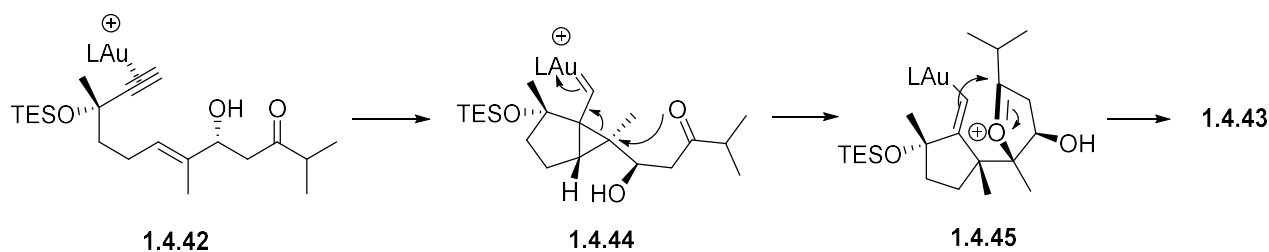
reported the selective preparation of tricyclic bridged hexenone (**1.4.37**) and heptenone (**1.4.38**) from 1,11-dien-3,9-diyne **1.4.36**.²⁸ It is proposed that **1.4.36** undergoes 1,3-acyloxy migration/metallo-Nazarov cyclization to generate the common intermediate **1.4.39**. Using [L5AuNCMe]SbF₆ complex, the carbocyclization of cyclopentadiene **1.4.39** proceeded in a 5-*exo-dig* manner to generate **1.4.37**. Interestingly, when using a more sterically hindered complex such as [L6AuNCMe]SbF₆, the reaction undergoes a selective 6-*endo-dig* cyclization.

Since 2006, Echavarren and co-workers demonstrated the remarkable application of gold(I)-catalyzed cycloisomerizations²⁹ by successfully accomplishing numerous total syntheses such as (+)-oriental F, pubinernoid B, and (-)-englerin A.¹⁵ⁱ⁻³⁰ The oxatricyclic sesquiterpene (-)-englerin A, isolated from the African plant *Phylanthus enfleri*, has been prepared using the linear precursor **1.4.42** (Scheme 1.14). Upon treatment with [L4AuNCMe]SbF₆ the carbocyclization took place to afford **1.4.43** in 58% yield.



Scheme 1.14 - Total synthesis of (-)-englerin A

It was proposed that the activation of the 1,5-enyne moiety on **1.4.42** by the cationic gold(I) complex formed the cyclopropyl metal carbene intermediate **1.4.44** through a 5-*exo-dig* cyclization (*Scheme 1.15*). Nucleophilic opening of the cyclopropane ring **1.4.44** by the carbonyl group then formed the oxonium cation **1.4.45**, which gave the key intermediate **1.4.43** after an intramolecular Prins-type reaction followed by protodeauration.

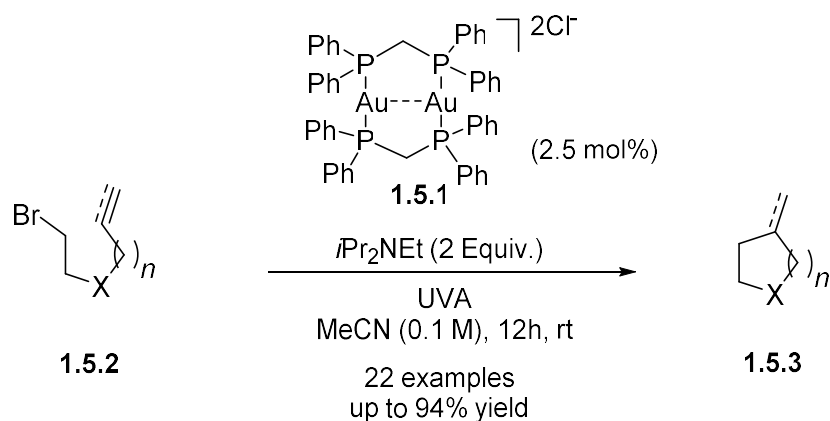


Scheme 1.15 - Proposed mechanism for the formation of the oxatricyclic core

1.5 Binuclear Au(I) in photoredox catalysis

In the last decade, photoredox catalysis has emerged as an efficient tool for the construction of C–C bonds. These light-enabled methods use photoactive transition-metal complexes and organic-based dyes, which upon irradiation undergo oxidative or reductive quenching mechanisms to generate carbon-centered radicals through single electron transfer (SET). In 1989, Che and co-workers reported that binuclear gold complexes such as $[\text{Au}_2(\mu\text{-dppm})_2]\text{Cl}_2$, possess unique photoluminescent properties.³¹ Following their work, Barriault's group³² and others³³ have demonstrated that such complexes can be used as photoredox catalysts in chemical transformations. It was demonstrated that the first excited state of $[\text{Au}_2(\mu\text{-dppm})_2]\text{Cl}_2$ (**1.5.1**) was a superior reductant than other typical ruthenium- and iridium-based photoredox catalysts, allowing the cleavage those of nonactivated C–Br bonds.

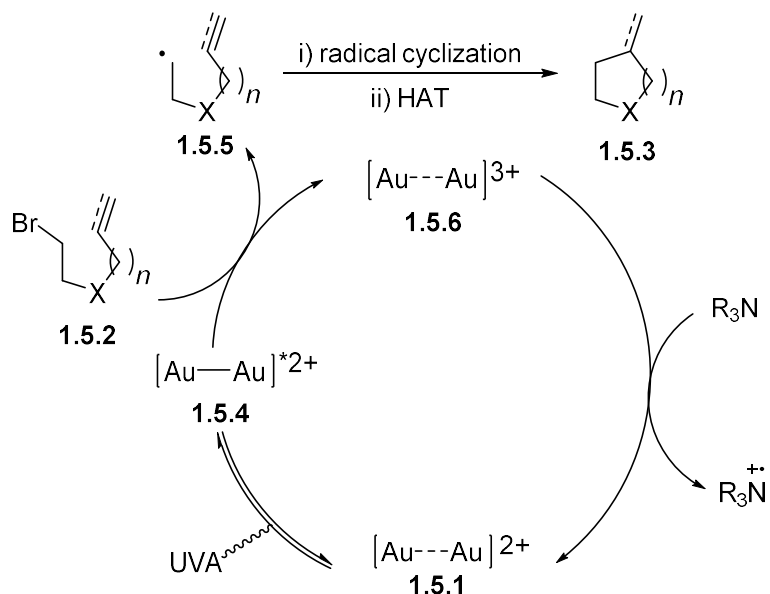
The first application of the binuclear gold(I) complex in photoredox catalysis was demonstrated by the intramolecular cyclization of bromoalkene **1.5.2** (Scheme 1.16).^{32a} Control experiments demonstrated that every reaction component was necessary for the reaction to occur. In addition, they validated that popular photocatalysts such as Ir(ppy)₃ and [Ru(bpy)₃](Cl)₂ were ineffective to reduce the C–Br bonds under standard conditions.



Scheme 1.16- Photoredox cyclizations with binuclear gold complex

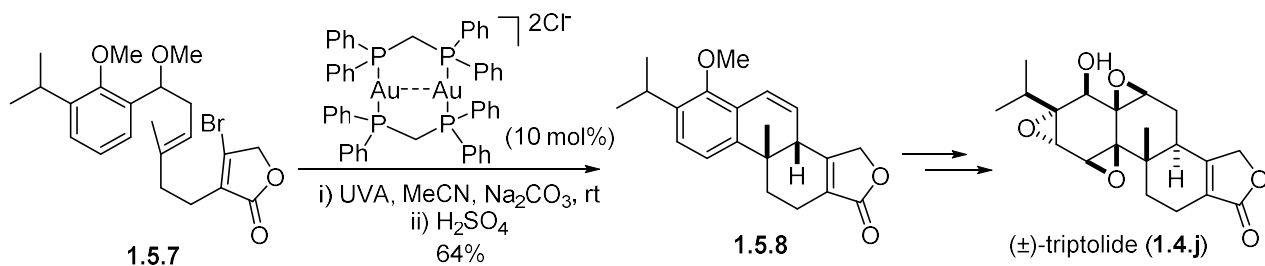
Once irradiated with the proper wavelength, the photoexcited gold complex can reduce C–Br bonds through a single electron transfer process (SET) to generate the corresponding carbon-centered radical. Mechanistic studies revealed that this process can proceed either via an inner-sphere oxidative or reductive quenching cycle.^{32e} From mechanistic insights, they proposed that the photoexcitation of the catalyst **1.5.1** with UVA would generate a covalent bond between the two gold atoms to form **1.5.4** (Scheme 1.17)^{4c} which could then reduce the C–Br of **1.5.2** via SET to generate the carbon-centered radical **1.5.5** (oxidative quenching cycle). The latter would undergo an intramolecular cyclization to create the new C(sp³)–C(sp²) bond in **1.5.3**. Concomitant

oxidation of the tertiary amine and reduction of the $[\text{Au-Au}]^{3+}$ complex would regenerate the photocatalyst **1.5.1**.



Scheme 1.17 - Proposed oxidative quenching catalytic cycle

Barriault and co-workers demonstrated the efficiency of their method in the synthesis of (\pm)-triptolide (*Scheme 1.18*).^{32c} Reaction of **1.5.7** under optimal conditions followed by the addition of H_2SO_4 led to the formation of the tetracycle **1.5.8** in 64% yield. The product was converted into a late-stage intermediate, thus completing the formal synthesis of the natural product in 9 steps.



Scheme 1.18 - Total synthesis of (\pm)-triptolide

1.6 Conclusion

We clearly see a rapid expansion in the field of homogeneous gold catalysis over the past three decades. Many types of transformations were developed using various nucleophiles such as alcohols, amines and π -bonds. Standard inter- or intramolecular addition, cycloisomerisation or Conia-ene type reaction have been reported. Regioselective transformations were also achieved via the judicious choice of the ligand complexed on gold. The efficiency of Au(I)-catalyzed reactions was demonstrated by the synthesis of complex natural products. Using dimeric gold species in a photoredox system is also a relatively new field and was applied to the synthesis of triptolide.

1.7 References

- [1] M. Willbold, T. Elliot, S. Moorbath, *Nature*, **2011**, 477, 195-198.
- [2] a) A. Gopher, T. Tsuk, S. Shalev, R. Gophna, *Current Anthropology*, **1990**, 31, 436-443; b) "How much gold has been mined", *World gold council*.
- [3] For selected review: a) B. J. Gorin, B. D. Sherry, F. D. Toste, *Chem. Rev.* **2008**, 108, 3351-3378; b) M. Rudolph, A. S. K. Hashmi, *Chem. Commun.* **2011**, 47, 6536-6544; c) A. Aubert, L. Fensterbank, P. Garcia, M. Malacria, A. Simonneau, *Chem. Rev.* **2011**, 111, 1954-1993; d) N. Krause, C. Winter, *Chem. Rev.* **2011**, 111, 1994-2009; e) C. Obradors, A. M. Echavarren, *Acc. Chem. Res.* **2014**, 47, 902-912; f) L. Fensterbank, M. Malacria, *Acc. Chem. Res.* **2014**, 47, 953-965; g) Y. Zhang, T. P. Luo, Z. Yang, *Nat. Prod. Rep.* **2014**, 31, 489-503; h) R. Dorel, A. M. Echavarren, *Chem. Rev.* **2015**, 115, 9028-9072; i) 1367A. Fürstner, *Acc. Chem. Res.* **2014**, 47, 925-938; j) D. Pflasterer, A. S. K. Hashmi, *Chem. Soc. Rev.* **2016**, 45, 1331-1367.
- [4] a) P. Pyykkö, *Angew. Chem. Int. Ed.* **2002**, 41, 3573-3578; b) H. Schwarz, *Angew. Chem. Int. Ed.* **2003**, 42, 4442-4454; c) P. Pyykkö, *Angew. Chem. Int. Ed.* **2004**, 43, 4412-4456; d) D. J. Gorin, F. D. Toste, *Nature* **2007**, 446, 395-403.
- [5] L.-P. Liu, G. B. Hammond, *Chem. Soc. Rev.* **2012**, 41, 3129 – 3139.

- [6] Y. Ito, M. Sawamura, T. Hayashi, *J. Am. Chem. Soc.*, **1986**, *108*, 6405-6450.
- [7] J. H. Teles, S. Brode, M. Chabanas, *Angew. Chem. Int. Ed.* **1998**, *57*, 1415-1418.
- [8] E. Mizushima, K. Sato, T. Hayashi, M Tanaka, *Angew. Chem. Int Ed.* **2002**, *41*, 4563-4565.
- [9] a) A. Homs, C. Obradors, D. Leboeuf, A. M. Echavarren, *Adv. Synth. Catal.* **2014**, *356*, 221-228; b) A. Zhdanko, M. Maier, *ACS Catal.* **2014**, *4*, 2770-2775; c) M. Wegener, F. Huber, C. Bolli, C. Jenne, S. F. Kirsch, *Chem. Eur. J.*, **2015**, *21*, 1328-1336; d) L. Rocchigiani, M. Jia, M. Bandini, A. Macchioni, *ACS Catal.* **2015**, *5*, 3911-3915; e) Z. Lu, J. Han, O. E. Okoromoba, N. Shimizu, H. Amii, C. F. Tormena, G. B. Hammond, B. Xu, *Org. Lett.* **2017**, *19*, 5848-5851.
- [10] W. Wang, G. B. Hammond, B. Xu, *J. Am. Chem. Soc.* **2012**, *134*, 5697-5705.
- [11] Z. J. Wang, D. Benitez, E. Tkatchouk, W. A. Goddard, F. D. Toste, *J. Am. Chem. Soc.* **2010**, *132*, 13094-13071.
- [12] A. S. Hashmi, A. M. Schuster, F. Rominger, *Angew. Chem. Int. Ed.* **2009**, *48*, 8247-8249.
- [13] A. K. Buzas, F. M. Istrate, F. Gagosz, *Org. Lett.* **2007**, *9*, 985-988.
- [14] a) A. Buzas, F. Gagosz, *J. Am. Chem. Soc.* **2006**, *128*, 12614-12615; b) A. Buzas, F. Gagosz, *Synlett* **2006**, 2727-2730; c) A. Buzas, F. Istrate, F. Gagosz, *Org. Lett.* **2006**, *8*, 1957-1959; d) A. Buzas, F. Gagosz, *Org. Lett.* **2006**, *8*, 515-518.
- [15] a) S. T. Staben, J. J. Kennedy-Smith, D. Huang, B. K. Corkey, R. L. LaLonde, F. D. Toste, *Angew. Chem. Ed. Int.* **2006**, *45*, 5991-5994; b) W. Chaladaj, M. Corbet, A. Fürstner, *Angew. Chem. Int. Ed.* **2012**, *51*, 6929-6933; c) B. M. Trost and G. Dong, *Nature*, **2008**, *456*, 485-488; d) Y. Feng, X. Jiang, J. K. De Brabander, *J. Am. Chem. Soc.* **2012**, *134*, 17083-17093; e) M. Riou, L. Barriault, *J. Org. Chem.* **2008**, *73*, 7436-7439; f) G. Bellavance, L. Barriault, *Angew. Chem. Int. Ed.* **2014**, *53*, 6701-6704; g) C. Fang, Y. C. Pang, C. J. Forsyth, *Org. Lett.* **2010**, *12*, 4528-4531; h) H. Chiba, S. Oishi, N. Fujii, H. Ohno, *Angew. Chem. Int. Ed.* **2012**, *51*, 9169-9172; i) K. Molawi, N. Delpont, A. M. Echavarren, *Angew. Chem. Int. Ed.* **2010**, *49*, 3517-3519; j) M. A. Brimble, I. Haym, J. Sperry, D. P. Furkert, *Org. Lett.* **2012**, *14*, 5820-5823; k) A. Cervi, P. Aillard, N. Hazeri, L. Petit, C. L. L. Chai, A. C. Willis, M. G. Banwell, *J. Org. Chem.* **2013**, *78*, 9876-9882; l) A. Cannillo, T. R. Schwantje, M. Bégin, F. Barabé, L. Barriault, *Org. Lett.* **2016**, *18*, 2592-2595; m) K. Kong, J. A. Enquist, M. E. McCallum, G. M. Smith, T. Matsumaru, E. Menhaji-Klotz, J. L. Wood, *J. Am. Chem. Soc.* **2013**, *135*, 10890-10893; n) Z. H. Shan, J. Liu, L. M. Xu, Y. F. Tang, J. H. Chen, Z. Yang, *Org. Lett.* **2012**, *14*, 3712-3715; o) X. Linghu, J. J. Kennedy-Smith, F. D. Toste, *Angew. Chem. Int. Ed.* **2007**, *46*, 7671-7673; p) J. Carreras, M. Livendahl, P. R. McGonigal, A. M. Echavarren, *Angew. Chem. Int. Ed.* **2014**, *53*, 4896-4899; q) S. G. Sethofer, S. T. Staben, O. Y. Hung, F. D. Toste, *Org. Lett.* **2008**, *10*, 4315-4318; r) S. M. Canham, D. J. France, L. E. Overman, *J. Am. Chem. Soc.* **2010**, *132*, 7876; s) Z. Y. Lu, Y. Li, J. Deng, A. Li, *Nat. Chem.* **2013**, *5*, 679-684; t) G. Lemiere, V. Gandon, K. Cariou, A. Hours, T. Fukuyama, A. L. Dhimane, L. Fensterbank,

- M. Malacria, *J. Am. Chem. Soc.* **2009**, 131, 2993-3006.
- [16] a) W. L. Budde, R. E. Dessy, *J. Am. Chem. Soc.* **1963**, 85, 3964-3970; b) S. Uemura, H. Miyoshi, K. Okano, *J. Chem. Soc., Perkin Trans. 1*, **1980**, 1098-110.
- [17] Y. Fukuda, K. Utimoto, H. Nozaki, *Heterocycles* **1987**, 25, 297-300.
- [18] E. Mizushima, T. Hayashi, M. Tanaka, *Org. Lett.* **2003**, 5, 3349-3352.
- [19] a) A. Gimeno, M. Medio-Simón, C. Ramirez de Arellano, G. Asensio, A. B. Cuenca, *Org. Lett.* **2010**, 12, 1900-1903; b) A. Gimeno, A. B. Cuenca, M. Medio-Simón, G. Asensio, *Adv. Synth. Catal.* **2014**, 356, 229-236; c) A. Gimeno, A. B. Cuenca, S. Suárez-Pantiga, C. Ramirez de Arellano, M. Medio-Simón, G. Asensio, *Chem. Eur. J.* **2014**, 20, 683-688.
- [20] J. J. Kennedy-Smith, S. T. Staben, F. D. Toste, *J. Am. Chem. Soc.* **2004**, 126, 4526-4527.
- [21] E. C. Minnihan, S. L. Colleti, F. D. Toste, H. C. Shen, *J. Org. Chem.* **2007**, 72, 6287-6289.
- [22] a) F. Barabé, P. Levesque, I. Korobkov, L. Barriault, *Org. Lett.* **2011**, 16, 5580-5583; b) M. Morin, P. Levesque, L. Barriault, *Beilstein, J. Org. Chem.* **2013**, 9, 2625-2628.
- [23] D. Benitz, E. Tkatchouk, A. Z. Gonzalez, W. A. Goddard, F. D. Toste, *Org. Lett.*, **2009**, 11, 4798-4801.
- [24] B. M. Trost, *Acc. Chem. Res.* **1990**, 23, 34-42.
- [25] A. Escribano-Cuesta, P. Pérez-Galán, E. Herrero-Gómez, M. Sekine, A. A. C. Braga, F. Maseras, A. Echavarren, *Org. Biomol. Chem.* **2012**, 10, 6105-6111.
- [26] a) G. Seidel, B. Gabor, R. Goddard, B. Heggen, W. Thiel, A. Fürstner, *Angew. Chem., Int. Ed.* **2014**, 53, 879-882; b) G. Seidel, A. Fürstner, *Angew. Chem., Int. Ed.* **2014**, 53, 4807-4811; c) R. E. M. Brooner, R. A. Widenhoefer, *Chem. Commun.* **2014**, 50, 2420-2423; d) H. J. Harris, R. A. Widenhoefer, *Angew. Chem., Int. Ed.* **2014**, 53, 9369-9371.
- [27] (a) M. W. Hussong, F. Rominger, P. Krämer, B. F. Straub, *Angew. Chem. Int. Ed.* **2014**, 53, 9372-9375; b) M. Joost, L. Estévez, S. Mallet-Ladeira, L. Miqueu, A. Amgoune, D. Bourissou, *Angew. Chem, Int. Ed.* **2014**, 53, 14512-14516.
- [28] W. Rao, D. Susanti, B. J. Ayers, P. W. Hong Chan, *J. Am. Chem. Soc.* **2015**, 137, 6350-6355.
- [29] E. Jiménez-Núñez, C. K. Claverie, C. Nieto-Oberhuber, A. M. Echavarren, *Angew. Chem. Ed. Int.* **2006**, 45, 5452-5455
- [30] a) E. Jiménez-Núñez, K. Molawi, A. M. Echavarren, *Chem. Commun.* **2009**, 7327-7329; b) L. López-Suárez, L. Riesgo, F. Bravo, T. T. Ransom, J. A. Beutler, A. M. Echavarren, *ChemMedChem*, **2016**, 11, 1003-1007.

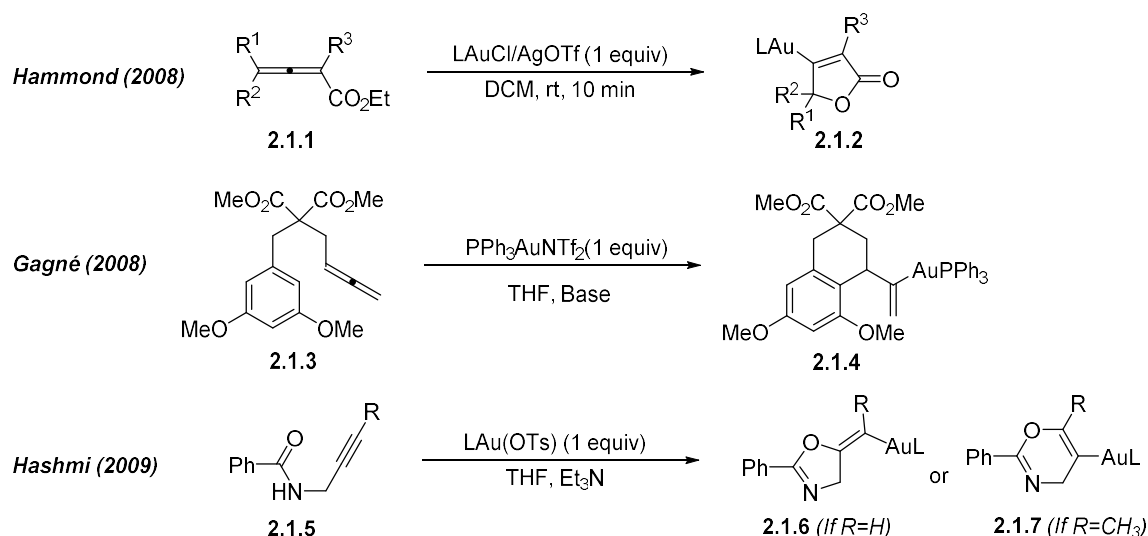
- [31] a) C. M. Che, H. L. Kwong, V. W. W. Yam, K. C. Cho, *J. Chem. Soc., Chem. Commun.* **1989**, 885-886; b) D. Li, C. M. Che, H. L. Kwong, V. W. W. Yam, *J. Chem. Soc. Dalton Trans.* **1992**, 3325-3329; c) C. S. Ma, C. T. L. Chan, W. P. To, W. M. Kwok, C. M. Che, *Chem. Eur. J.* **2015**, *21*, 13888-13893.
- [32] a) G. Revol, T. McCallum, M. Morin, F. Gagosz, L. Barriault, *Angew. Chem. Int. Ed.* **2013**, *52*, 13342-13345; b) T. McCallum, E. Slavko, M. Morin, L. Barriault, *Eur. J. Org. Chem.* **2015**, 81-85; c) S. J. Kaldas, A. Cannillo, T. McCallum, L. Barriault, *Org. Lett.* **2015**, *17*, 2864-2866; d) H. Tran, T. McCallum, M. Morin, L. Barriault, *Org. Lett.* **2016**, *18*, 4308-4311; e) C. D. McTiernan, M. Morin, T. McCallum, J. C. Scaiano, L. Barriault, *Catal. Sci. Technol.* **2016**, *6*, 201-207; f) T. McCallum, L. Barriault, *Chem. Sci.* **2016**, *7*, 4754; g) T. McCallum, S. Rohe, L. Barriault, *Synlett.* **2017**, *28*, 289-305; h) M. Zidan, T. McCallum, L. Thai-Savard, *Org. Chem. Front.* **2017**, *4*, 2092-206.
- [33] a) J. Xie, S. Shi, T. Zhang, N. Mehrkens, M. Rudolph, A. S. K. Hashmi, *Angew. Chem. Int. Ed.* **2015**, *54*, 6046; b) J. Xie, J. Li, V. Weingand, M. Rudolph, A. S. K. Hashmi, *Chem. Eur. J.* **2016**, *22*, 12646; c) F. Nzulu, S. Telitel, F. Stoffelbach, B. Graff, F. Morlet-Savary, J. Lalevee, L. Fensterbank, J.-P. Goddard, C. Ollivier, *Polym. Chem.* **2015**, *6*, 4605. d) J. Xie, J. Li, V. Weingand, M. Rudolph, A. S. K. Hashmi, *Chem. Eur. J.* **2016**, *22*, 12646-12650.

CHAPTER 2

Isolation and reactivity of vinylgold complexes

2.1 Introduction to vinylgold

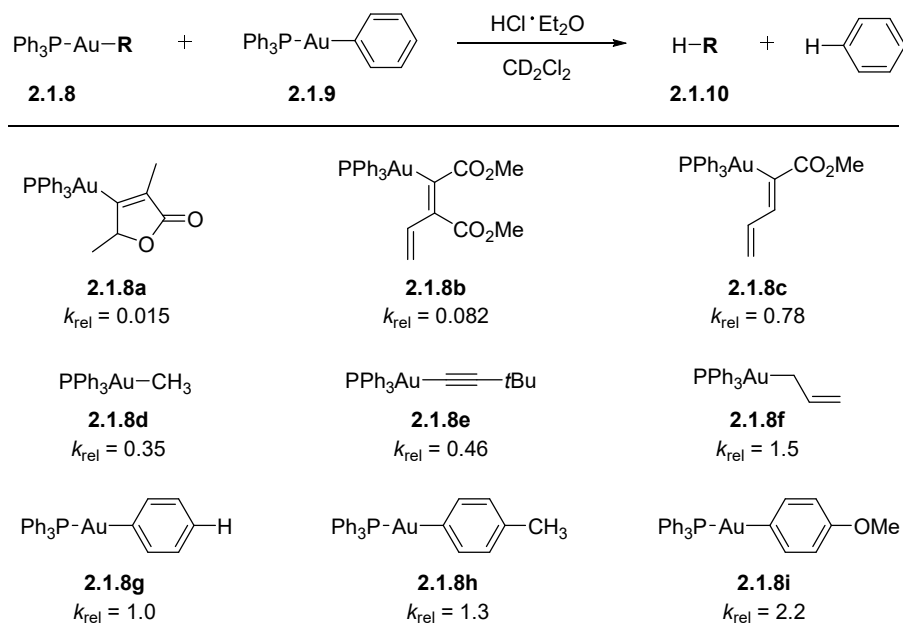
In general, complexes of organogold intermediates undergo relatively fast protodemetalation processes during typical gold Lewis acid catalyzed transformations (*vide supra*), which also regenerates the cationic gold species. In very rare cases, these intermediates can be isolated and characterized.³⁴ Hammond³⁵, Gagné³⁶ and Hashmi³⁷ reported the first chromatographically stable vinylgold complexes (*Scheme 2.1*). Preliminary results by Hammond in 2008 show that the organogold **2.1.2** were isolated upon treatment of the allenates **2.1.1** with a cationic gold(I) salt. Shortly after Hammond's results were published, Gagné's group was able to isolate vinylgold **2.1.4** from the intramolecular hydroarylation reaction of allene **2.1.3**.



Scheme 2.1 - The first isolated vinylgold intermediates

Hashmi identified that the cyclization of the substituted alkyne **2.1.5** under basic condition afforded another type of stable vinylgold intermediates, **2.1.6** and **2.1.7**. Interestingly, the unsubstituted terminal alkyne **2.1.5** led to the 5-*exo-dig* product **2.1.6** while a methyl substituent generated the 6-*endo-dig* product **2.1.7** under identical reaction conditions. Isolation of such intermediates, supported the hypothesized mechanism of gold-catalyzed processes and have provided a fertile playground for new reaction discovery such as palladium coupling with organogold complexes.³⁸

Blum and co-workers performed kinetic experiments in order to rationalize the stability of such species.³⁹ They synthesized several organogold complexes to compare the effect of the complex's hybridization and substitution to their rate of protodemetalation (*Scheme 2.2*). The unexpected stability of **2.1.8a** was attributed to the electron-deficient lactone system, which would make the subsequent protodeauration more difficult.

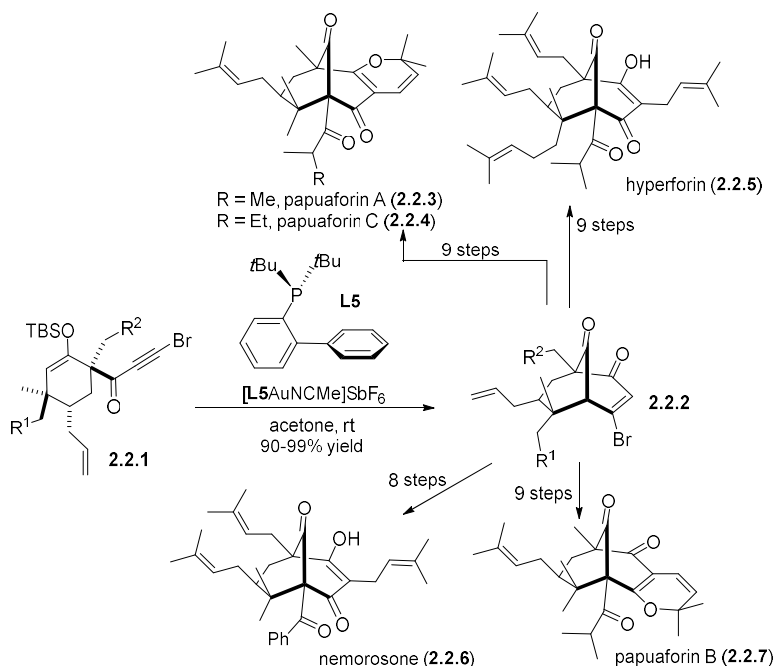


Scheme 2.2 - Relative rate of protodeauration

The electronic nature of the aromatic substituents was also investigated (**2.1.8g-i**) and demonstrated that electron rich phenyl rings generated **2.1.10** at a faster rate, which is consistent with the previous hypothesis that electron-donating substituents lead to faster protodeauration processes. These studies also revealed a strong correlation between hybridization and kinetic basicity with the organogold complex's stability, in the following trend: $sp^3 < sp < sp^2$ (aryl), as observed with compounds **2.1.8d** < **2.1.8e** < **2.1.8g**. The basicity of the conjugate acid follows a different trend which suggests that hyperconjugation in the π -system results in stabilization of the protodeauration transition-state, thus explaining the incremental changes in rate.

2.2 Unexpected vinylgold intermediates

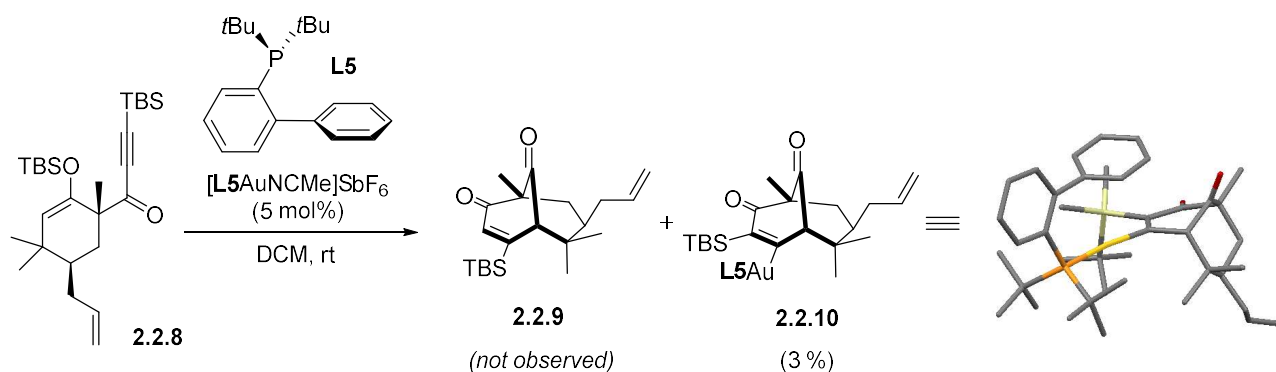
In 2009, our group developed a mild and efficient method using cationic phosphinogold(I) species to generate bicyclo[3.3.1]alkenones **2.2.2** from enol ethers **2.2.1** (Scheme 2.3).⁴⁰



Scheme 2.3 - Total synthesis of polycyclic prolynnated acylphloroglucinol (PPAPs)

This method was successfully applied in the concise total syntheses of biologically active polyprenylated polycyclic acylphloroglucinols (PPAPs) such as papuaforin A (**2.2.3**), papuaforin B (**2.2.7**), papuaforin C (**2.2.4**), hyperforin (**2.2.5**) and nemorosone (**2.2.6**).⁴¹

During these syntheses, we investigated the gold(I)-catalyzed *6-endo-dig* carbocyclization of **2.2.8** containing a substituted TBS-alkyne to produce the bridgehead ketone **2.2.9** (*Scheme 2.4*). Based on previous results, we anticipated that alkyne substitution would not affect the cyclization process. Against all odds, we isolated a very small quantity of a surprisingly stable vinylic gold intermediate **2.2.10** that resulted from an unexpected 1,2-silyl migration along with starting material (>90%). From that result, we were then interested in the mechanism of this migration with the hope of taking advantage of this strategy to assess vinylgold stability and developing new transformations.

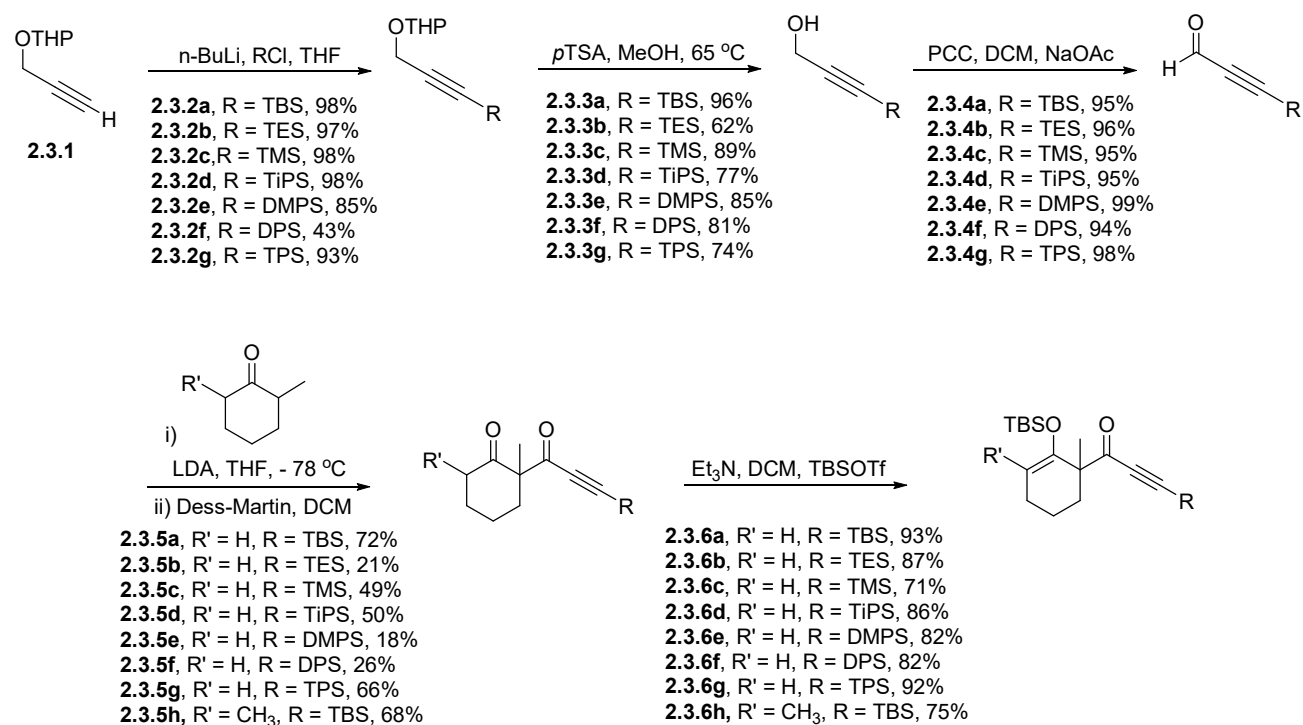


Scheme 2.4 - A chromatographically stable vinylgold complex

2.3 Substrate preparation

To further understand the nature of the 1,2-silyl migration and stability of the vinylgold complex, we synthesized several substrates having steric and electronic variants. An array of silyl groups was installed on the terminal alkyne as well as changing the bulkiness of the initial core (*Scheme 2.5*). From the commercially available protected propargyl alcohol **2.3.1**, silyl

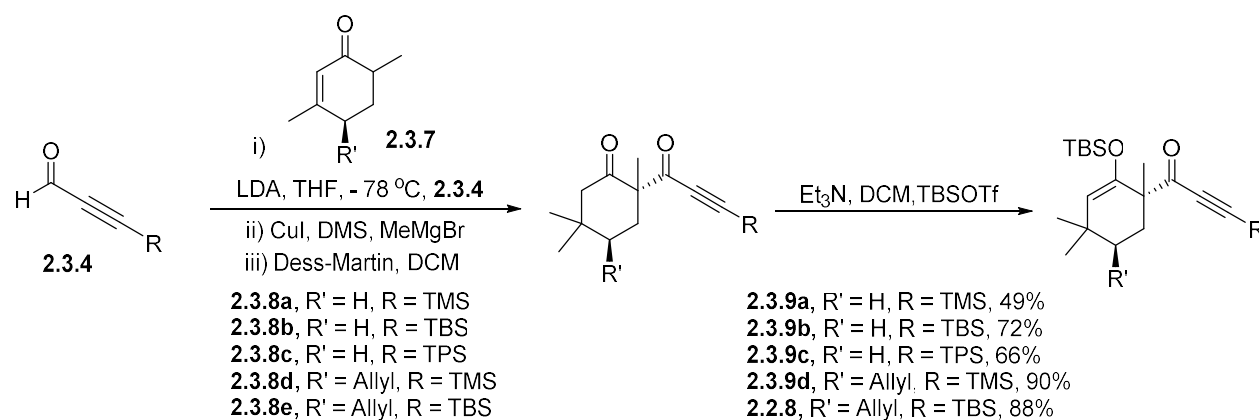
substituents were introduced using *n*-BuLi and the corresponding chlorotrialkylsilanes to generate **2.3.2a–g** in good yields. After deprotection of the pyran moiety and oxidation of the resulting alcohol by PCC, the volatile aldehydes **2.3.4a–g** were ready to be used in the aldol addition transformations. 2-Methyl cyclohexanone was deprotonated with a sub-stoichiometric amount of LDA and heated at reflux to favor the formation of the thermodynamic enolate, where the reaction intermediates were treated with various aldehydes **2.3.4**. After oxidation of the β -hydroxyketone intermediates with Dess-Martin periodinane followed by silyl enol ether formation, compounds **2.3.6a–h** were obtained in good yields. These substrates comprised the preliminary scope for the investigation of the effect of the silyl substituent on the gold-catalyzed transformation.



Scheme 2.5 - Substrate preparation bearing different silyl substituents

Moreover, we synthesized another set of substrates possessing a more hindered core (*Scheme 2.6*). The sterically congested ketone **2.3.8**, with a *gem*-dimethyl functionality, was

prepared following a known procedure.^{41a} Using a similar approach to the previously developed method (*Scheme 2.5*), the substituted enone **2.3.7** was treated with LDA and **2.3.4** for aldol addition followed by 1,4-addition of a methyl group. Further oxidation and silyl ether formation afforded the substrates **2.3.9a-d** and **2.2.8**.



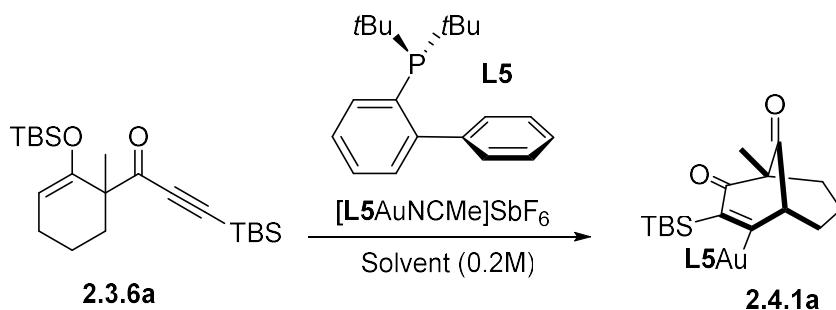
Scheme 2.6 - Preparation of sterically hindered substrates

2.4 Optimization and substrate scope

Intrigued by the vinylgold complex, we further investigated this transformation by first performing an optimization of the organogold formation using a model substrate **2.3.6a**. As a first step, we performed the reaction using a stoichiometric amount of gold complex [L5AuNCMe]SbF₆ in dichloromethane (*Table 2.1*). After 30 minutes, enol ether **2.3.6a** was fully converted to afford the vinylgold intermediate **2.4.1a** in 32% yield along with a significant amount of hydrolyzed enol ether product **2.3.5a** (>50%, entry 2). Unfortunately, lowering or increasing the temperature led to lower yields (entries 1 and 3). To prevent the hydrolysis of **2.3.6a**, the reaction was carried out in the presence of various bases (1 equivalent) such as K₂CO₃, Et₃N, and proton sponge (entries 4–6). In all of these cases, only starting material was recovered. Interestingly, this transformation does

not require basic conditions to prevent protodeauration.^{35,38a,42} Catalyst ‘poisoning’ might explain the absence of product using such reaction conditions. An increase in the amount of **2.3.6a** from 1.0 to 3.3 equivalents gave **2.4.1a** in 84% yield (entries 7–9).^[11] Substituting the DCM solvent for acetone, DCE or THF reduced the amount of product that was isolated (entries 10–12).

Table 2.1 - Optimization of vinylgold formation

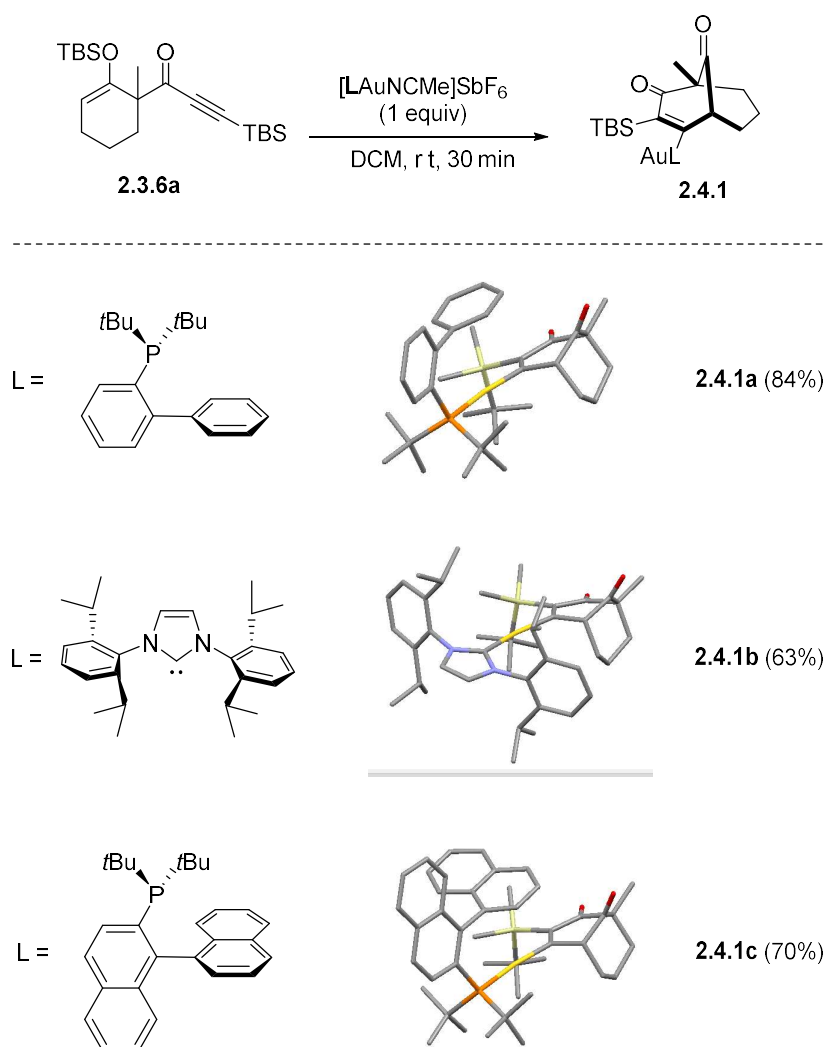


Entry	Temp.(°C)	2.3.6a (equiv)	t (min)	Additive	Solvent	Yield ^a (%)
1	0	1	30	-	DCM	5
2	20	1	30	-	DCM	32
3	60	1	30	-	DCM	27
4	20	1	30	K ₂ CO ₃	DCM	<5
5	20	1	30	Et ₃ N	DCM	<5
6	20	1	30	Proton sponge	DCM	<5
7	20	2	30	-	DCM	46
8	20	3.3	30	-	DCM	84
9	20	5	30	-	DCM	84
10	20	3.3	30	-	DCE	65
11	20	3.3	30	-	Acetone	51
12	20	3.3	30	-	THF	<5

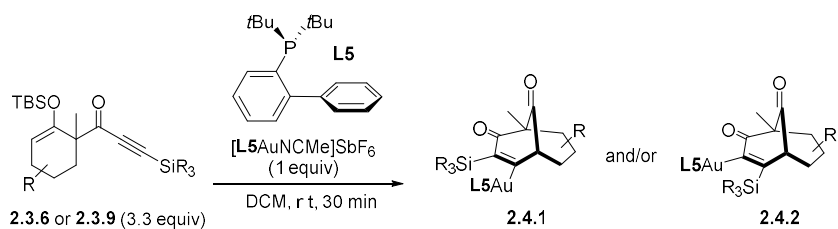
a) Isolated yield is based on Gold(I) loading

One can imagine that the vinylgold stability is attributed to the electron-deficient moiety of the complex, which has also been proposed by Hammond *et al.*⁴³ To further understand and optimize the formation of the vinylic gold species, other ligands were examined. Organogold

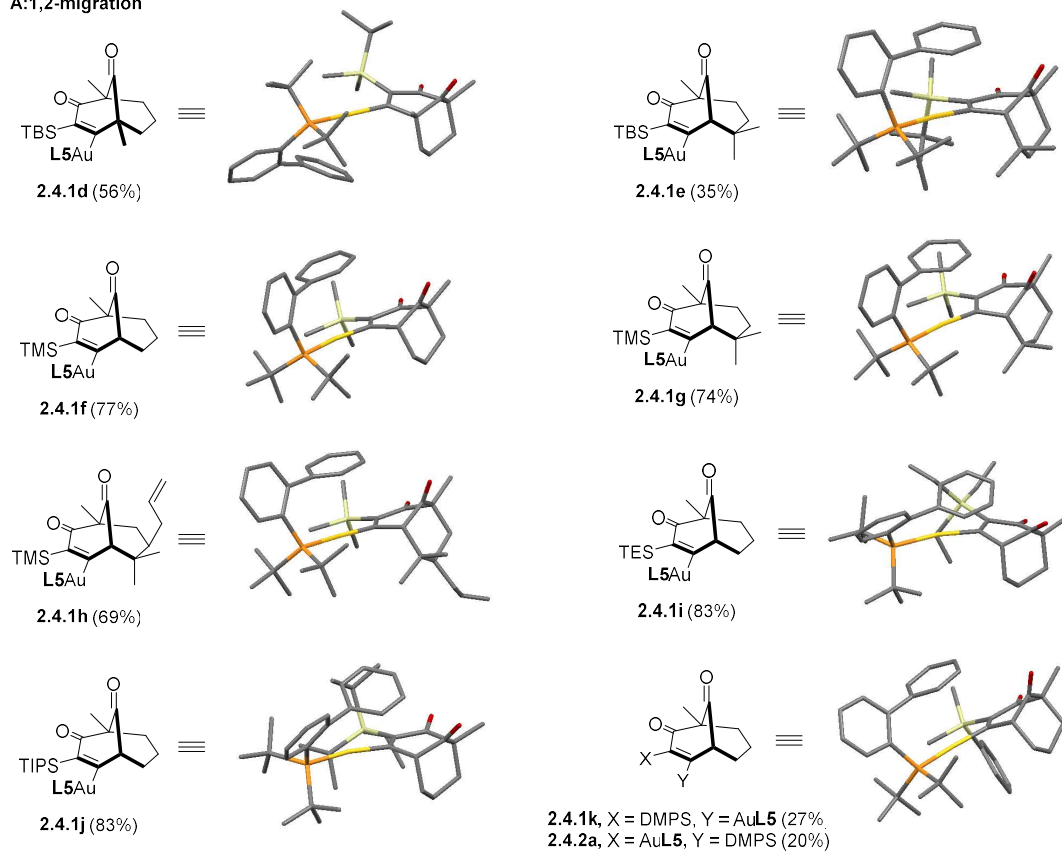
compounds bearing carbene and phosphine ligands, **2.4.1b** and **2.4.1c**, were isolated in 63% and 70% yields, respectively. Migration of the *tert*-butyldimethylsilyl group was observed in each case and was unaffected by the type of ligand. All of the structures were confirmed by single crystal X-ray diffraction.



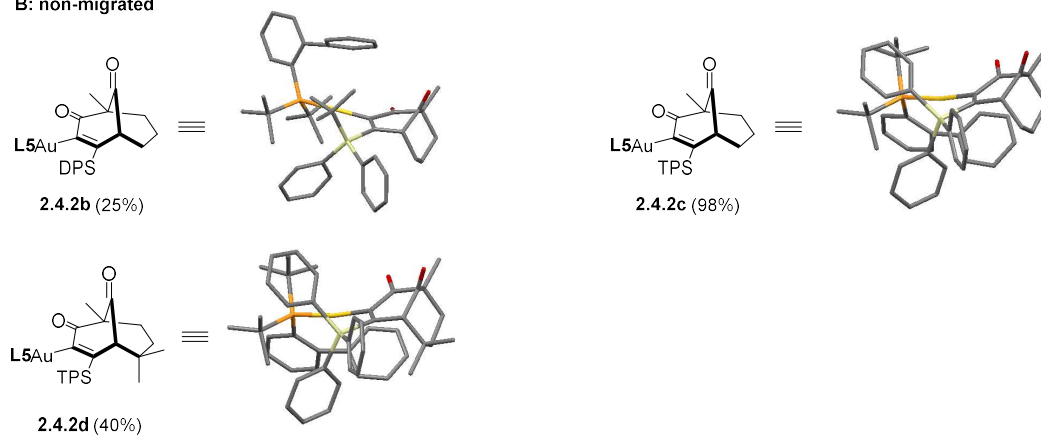
*Scheme 2.7 - Ligand optimization in the isolation of vinylgold species with 1 equivalent of $[LAuNCMe]SbF_6$ and 3.3 equivalents of **2.3.6a**.*



A: 1,2-migration



B: non-migrated



Scheme 2.8 – Controlled 1,2-silyl migration

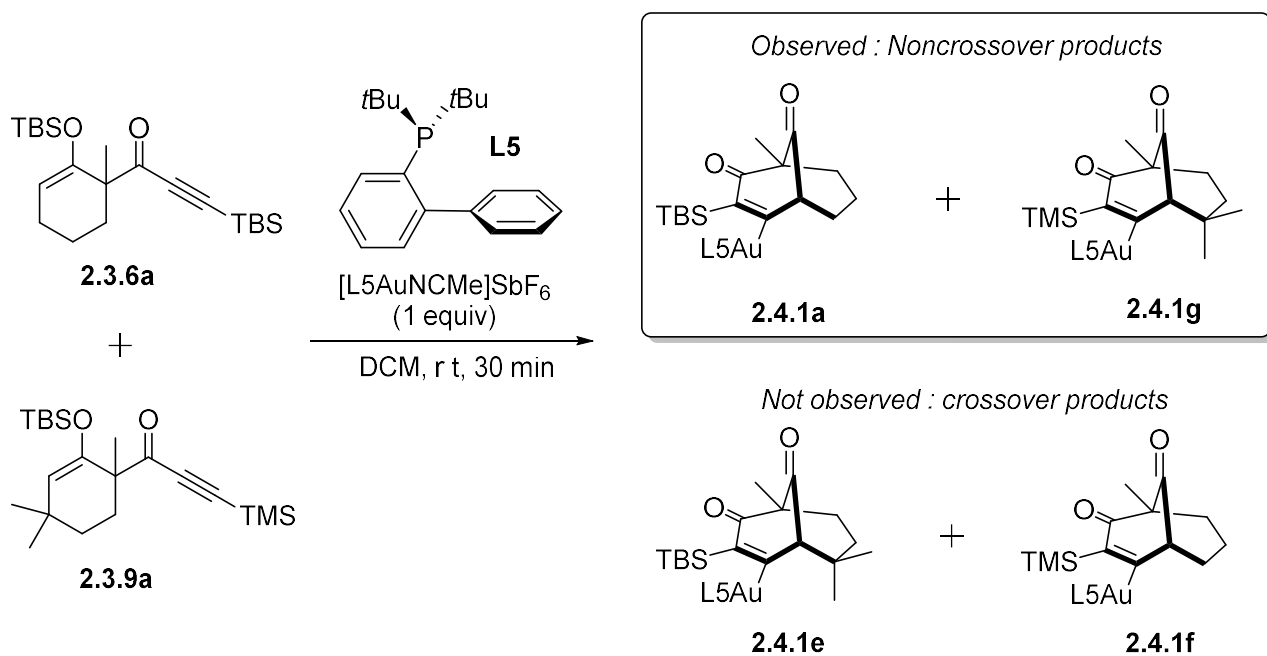
The optimized conditions were then applied to a wider variety of R₃Si-alkynes. At first glance, we found that the selectivity of the 1,2-shift was controlled by the nature of the silyl group. Noteworthy, a selective 1,2-migration/cyclization proceeded in good yields in a sterically demanding environment (*Scheme 2.8*). For example, chromatographically stable vinylgold complexes **2.4.1d-h** were isolated as the exclusive regioisomers. The replacement of TMS on the alkyne by a TES group had no effect on the reaction yield; organogold complexes **2.4.1f** and **2.4.1i** were obtained in 77% and 83% yields respectively. Increasing the R₃Si bulkiness led to a significant decrease in yield since **2.4.1e** was isolated in 35% yield. Surprisingly, the treatment of **2.3.6e** afforded a separable mixture of **2.4.1k** (27%) and **2.4.2a** (20%). When the silicon group possesses two phenyl substituents (DPS), only the non-migrated product **2.4.2b** was isolated in 25% yield. Moving from DPS to TPS, only the non-migrated products **2.4.2c** and **2.4.2d** were produced in 98% and 40% yields, respectively. These results clearly demonstrated that the nature of the silicon group on the alkyne dictates the 1,2-silyl migration. The electron deficient and hindered silyl groups led preferentially to the non-migrated products. The mechanistic aspects of this transformation will be discussed in the following section. All of the structural features of the organogold complexes mentioned above were confirmed by single crystal X-ray diffraction and NMR spectroscopic analysis.

2.5 Mechanistic insights

Independent studies from Fürstner⁴⁴ and Gervorgyan⁴⁵ reported gold(I/III)-catalyzed cascade cycloisomerizations that involved 1,2-migration of halides and silicon groups. It was proposed that the migration proceeds through the formation of a gold vinylidene intermediate. There are many examples of intermediates proceeding through alkyne-vinylidene complexes for

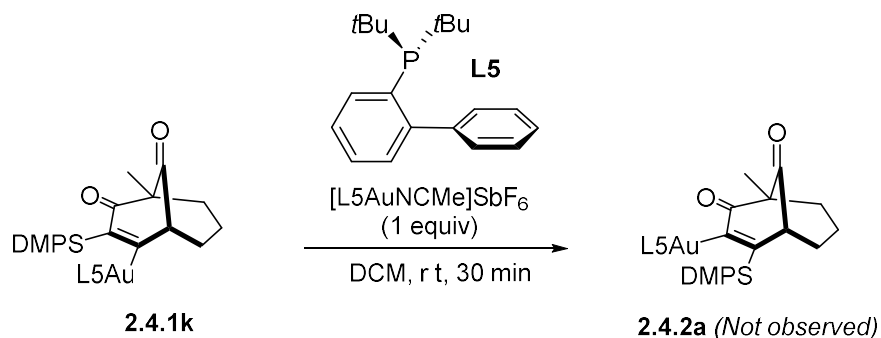
W, Ru, Rh, Mo, Ir, Co, Re and Mn complexes,⁴⁶ however, few examples exist with Au complexes.⁴⁷ In specific cases, the migration can proceed via the generation of a gold carbenoid species.⁴⁸ To the best of our knowledge, the isolation of intermediates during processes involving a silyl rearrangement has yet to be reported.

To gain more insight on the cascade 1,2-migration/cyclization, we performed crossover experiments using **2.3.6a** and **2.3.9a**. Only cyclized products **2.4.1a** and **2.4.1g** were observed in the crude reaction mixture (*Scheme 2.9*). The 1,2-migration must then proceed through an intramolecular process.



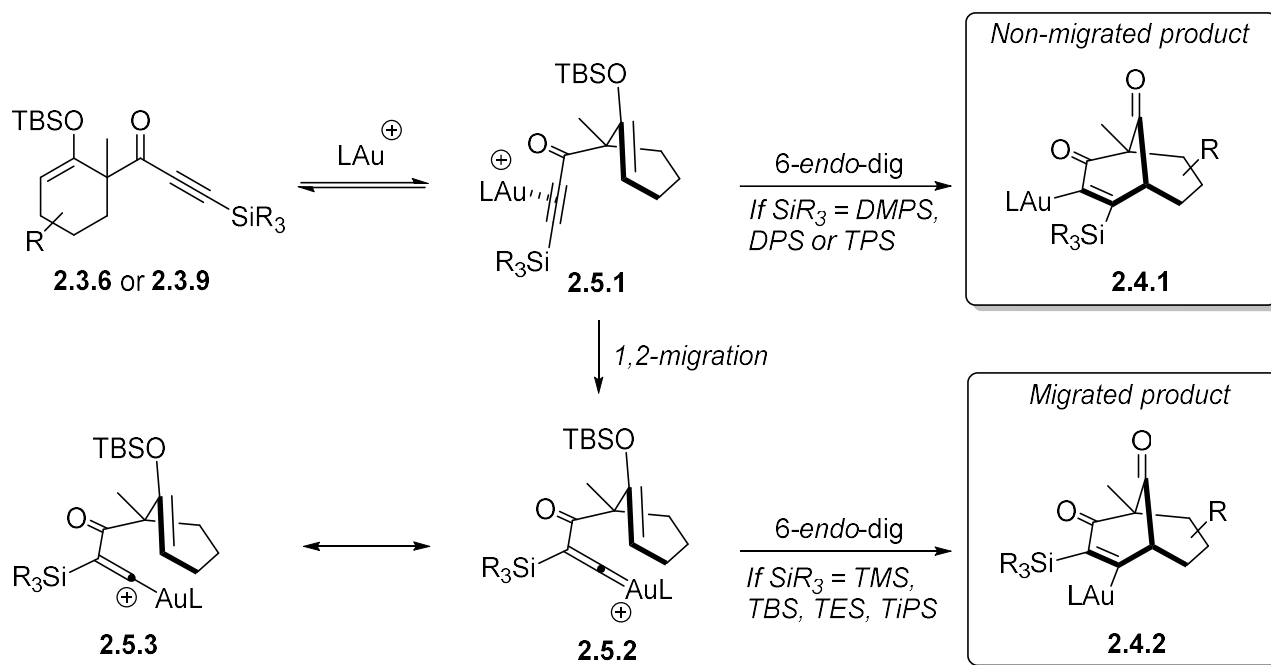
Scheme 2.9 - Crossover experiment

In addition, we envisaged the possibility that the isolated mixture of **2.4.1k** and **2.4.2a** (*Scheme 2.8*) could be the result of a thermodynamic equilibrium. The resubmission of **2.4.1k** did not lead to a combination of **2.4.1k** and **2.4.2a**. Since no interconversion was observed, it confirms that the 1,2-silyl migration occurred prior to the carbocyclization (*Scheme 2.10*).



Scheme 2.10 - Experiment for interconversion of 2.4.1k and 2.4.2a

In light of these results, one can conclude that the 1,2-silyl migration 1) occurs mainly with aliphatic silyl groups at the terminal position, 2) proceeds via an intramolecular process, and 3) occurs before the bridged core formation. Therefore, we propose two distinct pathways to explain the formation of **2.4.1** and **2.4.2** (*Scheme 2.11*).



Scheme 2.11 - Proposed mechanisms

Activation of the alkyne moiety would first generate **2.5.1** which could undergo conventional 6-*endo-dig* carbocyclization to generate **2.4.1**. On the other hand, **2.5.1** could go through the formation of a gold(I) vinylidene intermediate **2.5.2** with trialkylsilyl substituents on the terminal alkyne. With electron rich silyl groups, the existence of such vinylidene could be favored by the silicon hyperconjugation stabilization, also called beta-silicon effect,⁴⁹ of the β -carbocation found on the resonance structure **2.5.3**. Upon cyclization and protodeauration, **2.4.2** is observed.

2.6 Reactivity of vinylgold

We took advantage of the synthesis of these vinyl gold complexes to further explore their chemical reactivity (*Table 2.2*). Recently, it was shown that new C–C bonds could be generated through Pd-catalyzed cross-coupling reactions of vinylgold species with aryl and alkyl halides.⁵⁰ We identified Pd(OAc)₂ (5 mol%) and tricyclohexylphosphine (15 mol%) in PhCF₃ at 100 °C to be the optimal conditions for cross-coupling reactions. Under these conditions, the organogold complex **2.4.1a** was converted to **2.6.1a** in 83% yield (entry 1). To our surprise, **2.4.2c** proved to be inert under these conditions; only starting material was recovered. One might suggest that the transmetalation process is thwarted by steric congestion at the C–AuL₁ bond. Initial results showed that vinylgold complex **2.4.1a** can also participate in Pd-catalyzed allylic cross-coupling reactions. However, thorough control experiments demonstrated that the allylation reaction proceeded in the absence of Pd catalyst; heating of **2.3.6a** and **2.4.2a** in PhCF₃ in the presence of allylbromide gave bridgehead ketones **2.6.1b** and **2.6.2b** in 75% and 65% yields, respectively (entry 2). These results are in contrast with previous findings.^{50a-c} Other electrophiles such as propargyl bromide, methyl iodide and ethyl iodide provided the corresponding ketones **2.6.1c-e** and **2.6.2c-e** in 32%-98% yields (entries 3–5). Treatment of **2.3.6a** and **2.4.2c** with electrophilic

fluorinating agents proved to be more challenging. Vinylfluor **2.6.1f** was obtained in 33% yield whereas the conversion of **2.4.2c** gave a complex mixture (entry 6).^{50j} As expected, halogenation reactions using NBS and NIS provided the desired halogenated bridgehead ketones **2.6.1e**, **2.6.1f**, **2.6.2e** and **2.6.2f** in quantitative yields (entries 7 and 8).

Table 2.2 – Vinylgold complexes cross-coupling reaction^[a]

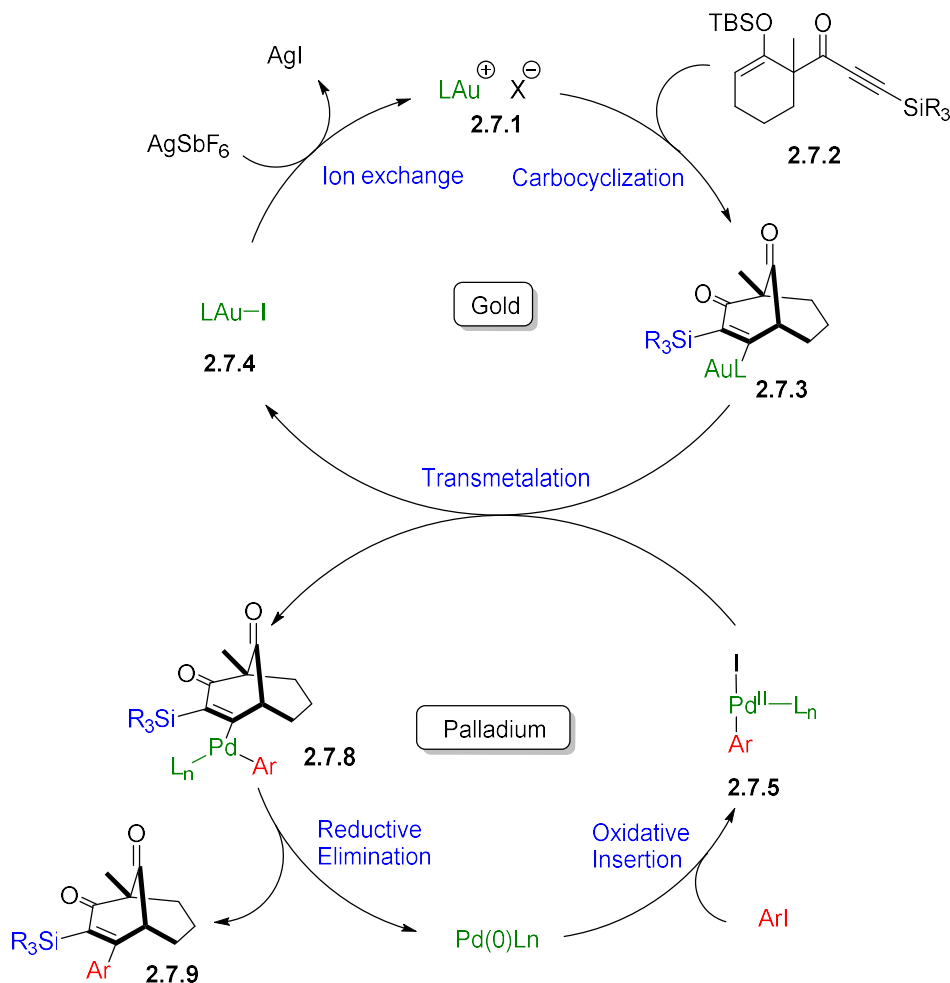
<div style="display: flex; justify-content: space-around; align-items: center;"> <div style="text-align: center;"> <p>2.4.1a → 2.6.1</p> </div> <div style="text-align: center;"> <p>2.4.2c → 2.6.2</p> </div> </div>				
Entry	RX	Product	2.6.1 (%) ^[b]	2.6.2 (%) ^[b]
1			2.6.1a (83) ^[c]	2.6.2a (–) ^[c]
2			2.6.1b (75)	2.6.2b (84)
3			2.6.1c (63)	2.6.2c (32)
4			2.6.1d (98)	2.6.2d (98)
5			2.6.1e (92)	2.6.2e (97)
6	NFSI		2.6.1f (33) ^[d]	2.6.2f (–) ^[d]
7	NBS		2.6.1g (98) ^[d]	2.6.2g (98) ^[d]
8	NIS		2.6.1h (98) ^[d]	2.6.1h (98) ^[d]

[a] RX, PhCF₃, 100 °C, 24h. [b] Isolated yield. [c] Pd(OAc)₂ (5 mol%), PCy₃ (15 mol%).

[d] Acetone, 35 °C.

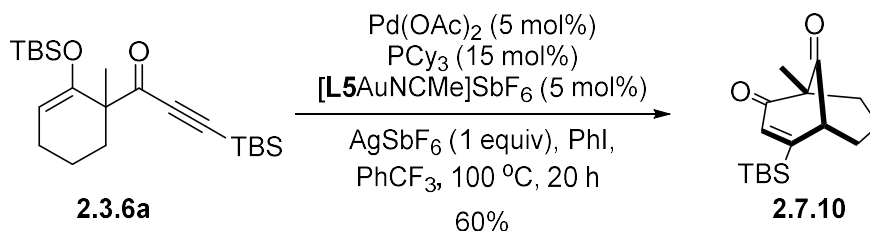
2.7 Synergistic dual-catalysis with Au and Pd

We were interested to investigate a synergistic dual-catalytic system using gold and palladium in order to directly convert **2.7.2** into **2.7.9** (Scheme 2.12). This process would start by the activation of the substrate **2.7.2** by a cationic gold species **2.7.1**, which would generate the vinylgold **2.7.3**. Oxidative insertion of Pd(0) into an aryl halide followed by transmetalation with **2.7.3** give rise to the intermediate **2.7.8** and the gold halide **2.7.4**. The desired product **2.7.9** will be obtained after reductive elimination of **2.7.8** and the active cationic gold catalyst **2.7.1** will be regenerated using a silver salt as an halogen scavenger.



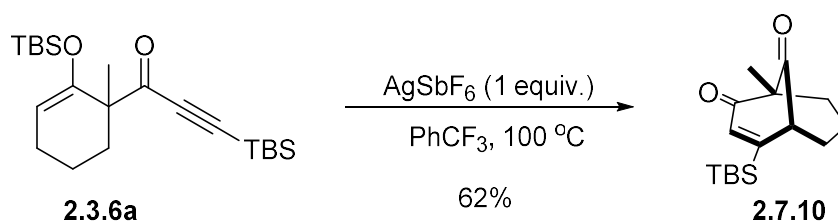
Scheme 2.12 - Synergistic dual catalysis with Au and Pd

We attempted this dual catalysis process using AgSF_6 combined with a catalytic amount of $[\text{L5AuNCMe}]\text{SbF}_6$, and our optimal conditions for the vinylgold transmetalation (*Scheme 2.13*). To our surprise no desired product was observed and the 6-*endo-dig* adduct **2.7.10** was isolated in 60% yield.



Scheme 2.13 - First attempt of dual-catalysis

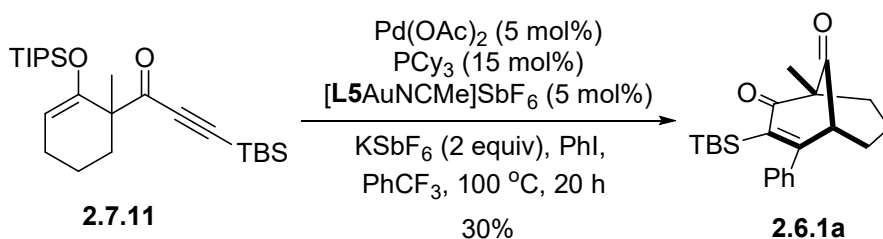
Since the non-migrated silyl **2.7.10** has never been observed during our previous investigation, we hypothesized that a side reaction was occurring with AgSbF_6 . Treatment of **2.3.6a** with AgSbF_6 in PhCF_3 at 100 °C confirmed that the formation of **2.7.10** was catalyzed by the silver salt (*Scheme 2.14*).



Scheme 2.14 - Control experiment

Hydrolysis of the TBS enol ether **2.3.6a** was problematic during our experiments, thus we opted for the more resistant TIPS enol ether **2.7.11** (*Scheme 2.15*). Other types of halogen scavengers were tested for the *in-situ* regeneration of the cationic gold species and to avoid the

undesired product **2.7.10**. NaSbF₆, KSbF₆, NaOTf, KOTf salts were investigated for the dual-catalyzed process. We found that using two equivalents of KSbF₆ led to our highest isolated yield. A modest 30% yield of the desired product **2.6.1a** was obtained, implying low turnover number of the catalysts. The main problem remains the hydrolysis of the starting material **2.7.11**.



Scheme 2.15 - Optimized conditions

Alternatively, one can imagine that treatment of Pd(0) with PhOTf instead of PhI will result in the formation of a gold cationic species after transmetalation. Unfortunately, no desired product was observed using PhOTf.

Although our work with Au(I) has not been a success, many other synergistic dual-catalysis processes with gold and other transition metals have been reported.⁵⁰⁻⁵¹

2.8 Conclusions

In summary, we reported the isolation of 15 new bicyclo[3.3.1]nonane organogold complexes characterized by X-ray crystallography. Access to these atomospherically and chromatographically stable vinylgold complexes was possible via a silyl rearrangement, which was regioselective according to the substituent of the silyl group. TBS and TPS groups offer the best yields for the rearranged and not-rearranged products, respectively. Assessment of the

chemical properties of these organogold complexes showed that they participated in Pd-catalyzed aryl cross-coupling reactions. It also led to the formation C(sp³)–C(sp²) bonds using electrophilic reagents without the use of Pd-based catalysts. We have also been able to use a synergistic Au/Pd dual-catalysis system for the formation of functionalized bridged carbocycles. However, low yields was observed due to the degradation of the starting material.

2.9 References

- [34] a) A. S. Hashmi, *Gold Bulletin*, **2009**, *41*, 275-279; b) A. S. K. Hashmi, *Angew. Chem. Int. Ed.* **2010**, *49*, 5232-5241; c) L. P. Liu, G. B. Hammond, *Chem. Soc. Rev.*, **2012**, *41*, 3129.
- [35] L.-P. Liu, B. Xu, M. S. Mashuta, G. B. Hammond. *J. Am. Chem. Soc.*, **2008**, *130*, 17642-17643.
- [36] D. Weber, M. A. Tarselli, M. R. Gagné, *Angew. Chem. Int. Ed.*, **2009**, *48*, 5733-5736
- [37] A. S. K. Hashmi, A. M. Schuster, F. Rominger, *Angew. Chem. Int. Ed.*, **2009**, *48*, 8247-8249.
- [38] a) A. S. K. Hashmi, R. Döpp, C. Lothschütz, M. Rudolph, D. Riedel, F. Rominger, *Adv. Synth. Catal.*, **2010**, *352*, 1307-1314; b) J. J. Hirner S. A. Blum, *Organometallics*, **2011**, *30*, 1299-1302; c) M. H. Pérez-Temprano, J. A. Casares, P. Espinet, *Chem. Eur. J.*, **2012**, *18*, 1864-1884; d) M. Al-Amin, k. E. Orht, S. A. Blum, *Acs. Catal.*, **2014**, *4*, 622-629; e) D. V. Patil, H. Yun, S. Shin, *Adv. Synth. Catal.*, **2015**, *357*, 2622-2628; f) A. Tlahuext-Aca, M. N. Hopkinson, R. A. Garza-Sanchez, F. Glorius, *Chem. Eur. J.*, **2016**, *22*, 5909-5913.
- [39] K. E. Roth, S. Blum, *Organometallics*, **2010**, *29*, 1712-1716.
- [40] a) F. Barabé, G. Bétournay, G. Bellavance, L. Barriault, *Org. Lett.*, **2009**, *11*, 4236–4238; b) B. Sow, G. Bellavance, F. Barabé, L. Barriault, Belstein *J. Org. Chem.*, **2011**, *7*, 1007–1013.
- [41] a) G. Bellavance, L. Barriault, *Angew. Chem. Int. Ed.* **2014**, *53*, 6701–6704; b) G. Bellavance, L. Barriault, *J. Org. Chem.*, **2018**, *83*, 7215-7230.

- [42] a) X. Zeng, R. Kinjo, B. Donnadieu, G. Bertrand, *Angew. Chem. Int. Ed.*, **2010**, *49*, 942–945; b) I. I. F. Boogaerts, S. P. Nolan, *J. Am. Chem. Soc.*, **2010**, *132*, 8858–8859; c) Y. Chen, D. Wang, J. L. Petersen, N. G. Akhmedov, X. Shi, *Chem. Commun.*, **2010**, *46*, 6147–6153; d) M. Melchionna, M. Nieger, J. Helaja, *Chem. Eur. J.*, **2010**, *16*, 8262–8267; e) A. S. K. Hashmi, A. M. Schuster, S. Gaillard, L. Cavallo, A. Poater, S. P. Nolan, *Organometallics*, **2011**, *30*, 6328–6337; f) A. S. K. Hashmi, I. Braun, P. Nösel, J. Schädlich, M. Wietek, M. Rudolph, F. Rominger, *Angew. Chem. Int. Ed.*, **2012**, *51*, 4456–4460; g) T. P. Cornell, Y. Shi, S. A. Blum, *Organometallics*, **2012**, *31*, 5990–5993; h) A. Johnson, A. Laguna, M. Concepción Gimeno, *J. Am. Chem. Soc.*, **2014**, *136*, 12812–12815.
- [43] W. Wang, G. B. Hammond, B. Xu, *J. Am. Chem. Soc.*, **2012**, *134*, 5697–5705.
- [44] V. Mamane, P. Hannen, A. Furstner, *Cent. Eur. J. Chem.*, **2004**, *10*, 4556–4575.
- [45] I. V. Seregin, V. Gevorgyan, *J. Am. Chem. Soc.*, **2006**, *128*, 12050–12051.
- [46] For selected reviews, see: a) M. I. Bruce, *Chem. Rev.*, **1991**, *91*, 197–257; b) C. Bruneau, P. H. Dixneuf, *Angew. Chem. Int. Ed.*, **2006**, *45*, 2176–2203.
- [47] a) E. Soriano, J. Marco-Contelles, *Organometallics*, **2006**, *25*, 4542–4553; b) V. Lavallo, G. D. Frey, S. Kousar, B. Donnadieu, G. Bertrand, *Proc. Natl. Acad. Sci., U.S.A.* **2007**, *104*, 13569–13573; c) I. D. Jurberg, Y. Odabachian, F. Gagosz, *J. Am. Chem. Soc.*, **2010**, *132*, 3543–3552; d) A. S. K. Hashmi, M. Wietek, I. Braun, P. Nösel, L. Jongbloed, M. Rudolph, F. Rominger, *Adv. Synth. Catal.*, **2012**, *354*, 555–562; e) A. S. K. Hashmi, M. Wietek, I. Braun, M. Rudolph, F. Rominger, *Angew. Chem. Int. Ed.*, **2012**, *51*, 10633–10637; f) L. Ye, Y. Wang, D. H. Aue, L. Zhang, *J. Am. Chem. Soc.*, **2012**, *134*, 31–34; g) M. M. Hansmann, M. Rudolph, F. Rominger, A. S. K. Hashmi, *Angew. Chem. Int. Ed.*, **2013**, *52*, 2593–2598; h) P. Morán-Poladura, E. Rubio, J. M. González, *Angew. Chem. Int. Ed.*, **2015**, *54*, 3052–3055.
- [48] a) Y. Xia, A. S. Dudnik, Y. Li, V. Gevorgyan, *Org. Lett.*, **2010**, *12*, 5538–5541; b) A. S. Dudnik, Y. Xia, Y. Li, V. Gevorgyan, *J. Am. Chem. Soc.*, **2010**, *132*, 7645–7655.
- [49] a) S. G. Wierschke, J. Chandrasekhar, W. L. Jorgensen, *J. Am. Chem. Soc.*, **1985**, *107*, 1496–1500; b) J. B. Lambert, G.-T. Wang, R. B. Finzel, D. H. Teramura, *J. Am. Chem. Soc.*, **1987**, *109*, 7838–7845; c) J. B. Lambert, Y. Shao, R. W. Emblidge, L. A. Salvador, X. Liu, J.-H. So, E. C. Chelius, *Acc. Chem. Res.*, **1999**, *32*, 183–190.
- [50] a) Y. Shi, K. E. Roth, S. D. Ramgren, S. A. Blum, *J. Am. Chem. Soc.*, **2009**, *131*, 18022–18023; b) A. S. K. Hashmi, C. Lothschütz, R. Döpp, M. Rudolph, T. D. Ramamurthi, F. Rominger, *Angew. Chem. Int. Ed.*, **2009**, *48*, 8243–8246; c) Y. Shi, S. D. Ramgren, S. A. Blum, *Organometallics*, **2009**, *28*, 1275–1277; d) A. S. K. Hashmi, R. Döpp, C. Lothschütz, M. Rudolph, D. Riedel, F. Rominger, *Adv. Synth. Catal.*, **2010**, *352*, 1307–1314; e) K. E. Roth, S. A. Blum, *Organometallics*, **2011**, *30*, 4811–4813; f) J. J. Hirner, Y.

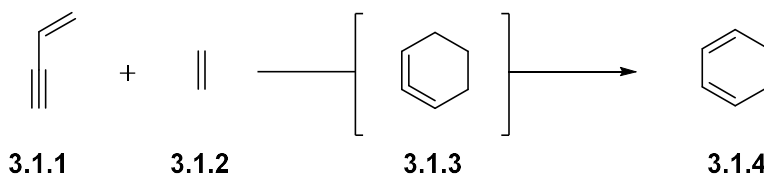
- Shi, S. A. Blum, *Acc. Chem. Res.*, **2011**, *44*, 603–613; g) J. J. Hirner, K. E. Roth, Y. Shi, S. A. Blum, *Organometallics*, **2012**, *31*, 6843–6850; h) M. Al-Amin, K. E. Roth, S. A. Blum, *ACS Catal.*, **2014**, *4*, 622–629; i) M. Al-Amin, J. S. Johnson, S. A. Blum, *Organometallics*, **2014**, *33*, 5448–5456; j) A. S. K. Hashmi, T. D. Ramamurthi, F. Rominger, *J. Organomet. Chem.*, **2009**, *694*, 592–597.
- [51] a) B. Sahoo, M. N. Hopkinson, F. Glorius, *J. Am. Chem. Soc.*, **2013**, *135*, 5505–5508; b) R. Bhattacharjee, A. Nijamudheen, A. Datta, *Org. Biomol. Chem.*, **2015**, *13*, 7412–7420; c) A. T;ahuext-Aca, M. N. Hopkinson, R. A. Garza-Sanchez, F. Glorius, *Chem. Eur. J.*, **2016**, *22*, 5909–5913; d) M. N. Hopkinson, A. Tlahuext-Aca, F. Glorius, *Acc. Chem. Res.*, **2016**, *49*, 2261–2272; e) K. S. Nalivela, M. Rudolph, E. S. Baeissa, B. G. Alhogbi, I. A. I. Mkhaliid, A. S. K. Hasmi, *A, , dv. Synth. Catal.*, **2018**, *360*, 2183–2190.

CHAPTER 3

Gold(I)-catalyzed [4+2] cycloaddition and its applications to the synthesis of magellanine

3.1 Introduction to gold(I)-catalyzed dehydro Diels-Alder reaction

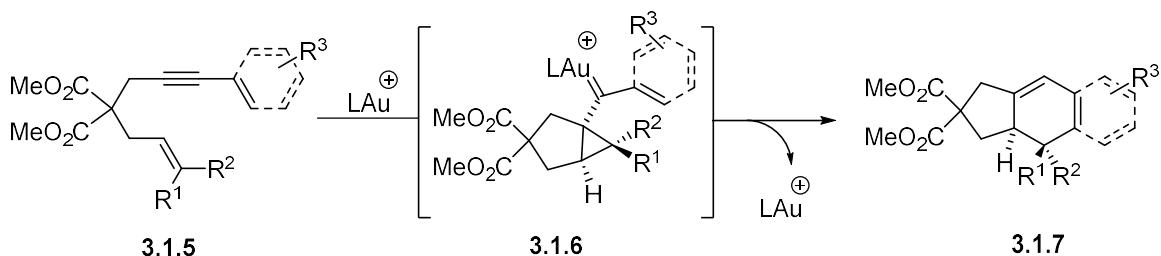
The development of new transformations for the efficient synthesis of architecturally complex scaffolds via operationally simple and practical protocols is of paramount importance in organic synthesis.⁵² In this regard, the specific affinity of cationic gold complexes for π -systems and their ability to stabilize neighboring cationic charges have stimulated the development of efficient and reliable methods for the construction C–C bonds.⁵³ The cycloaddition between an enyne **3.1.1** and an olefin **3.1.2**, known as the dehydro Diels-Alder reaction (DDA), is an expedient process for the synthesis of cyclohexadienes **3.1.4** and related carbocycles (*Scheme 3.1*).⁵⁴ While the thermal DDA reaction is well documented, the use of transition metals to catalyze this reaction remains marginal.⁵⁵



Scheme 3.1 - General dehydro Diels-Alder reaction (DDA)

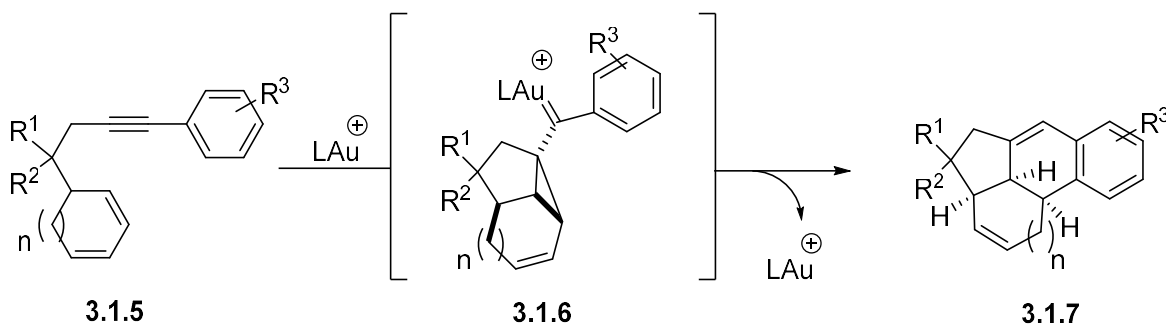
In pioneering work, Echavarren and co-workers⁵⁶ reported the Au(I)-catalyzed cyclization of arlenynes/dienynes **3.1.5** to give substituted dihydronaphthalenes **3.1.7** through a stepwise process involving a cyclopropyl gold(I)-carbene intermediate **3.1.6** (*Scheme 3.2*). Following

Echavarren's work, Gagosz's group developed a new low-cost catalyst, $[\text{PPh}_3\text{Au}]\text{NTf}_2$, possessing a better reactivity to catalyze identical transformations.⁵⁷



Scheme 3.2 – Echavarren's gold(I)-catalyzed intramolecular [4+2] cycloadditions

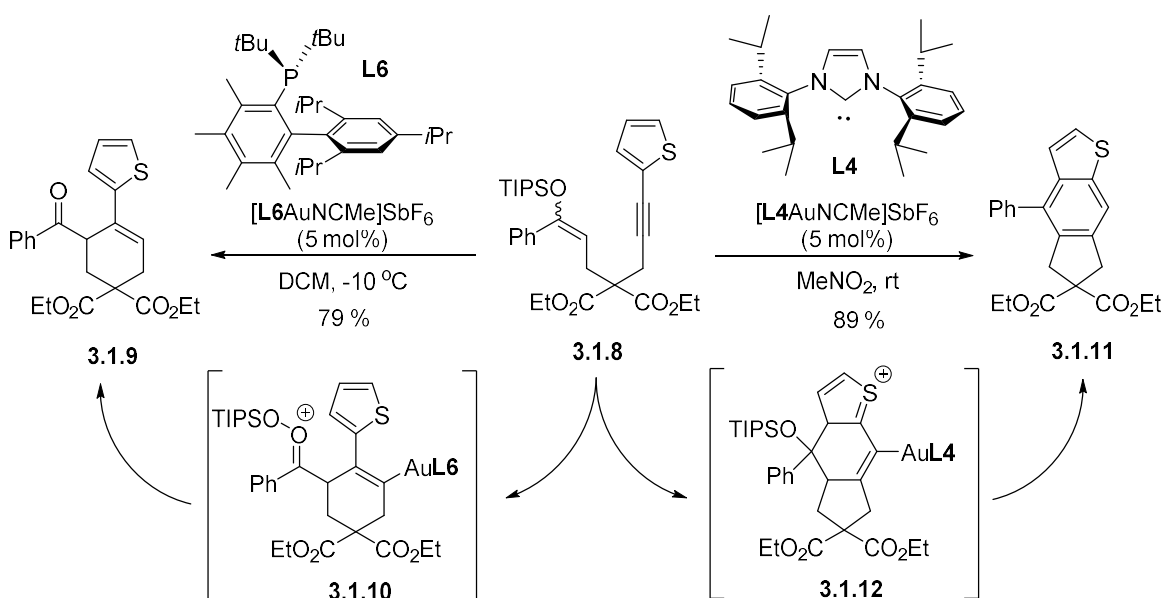
A year later, Lin's group developed a similar cycloisomerization process using cyclohexadiene **3.1.5** for the formation of tetracyclic **3.1.7** (Scheme 3.3).⁵⁸ The proposed mechanism goes through a similar pathway in which the internal aryl attacks the stabilized carbene intermediate **3.1.6** followed by aromatization to produce **3.1.7**. Moreover, an enantioselective variant of this transformation was developed in 2009 by Michelet and co-workers using chiral phosphine ligands.⁵⁹



Scheme 3.3 – Tetracycle formation via cyclization of 1-aryl-6,8-dien-1-yne

It was not until 2013 that the Barriault group reported a ligand-controlled cyclization of the silyl enol ether **3.1.8** (Scheme 3.4).⁶⁰ Following their work on regioselective 6-*endo-dig*

carbocyclizations, they identified that **3.1.9** was formed exclusively using $[\text{L6AuNCMe}]\text{SbF}_6$ with DCM as the solvent. On the other hand, with a carbene type ligand adorned on gold, $[\text{L4AuNCMe}]\text{SbF}_6$, the tricyclic compound **3.1.11** was observed. In contrast with previous work by Echavarren and others, the product undergoes aromatization via elimination of the silyl ether through the intermediate **3.1.12**.



Scheme 3.4 - Domino cyclization for the synthesis of polyaromatic heterocycles

All these transformations inspired us to develop a methodology for the synthesis of structurally more complexed scaffolds.

3.2 Formation of angular cores via a gold(I)-catalyzed carbocyclization

A substantial number of bio-active natural products having angular skeletons have been reported in the literature.⁶¹ For instance, some structurally interesting natural products are highlighted in *Figure 3.1*. The vast majority of gold-catalyzed carbocyclizations have been

designed for the formation of fused polycyclic compounds. There is a conspicuous paucity of gold(I)-catalyzed process for the construction of fused angular cores. To this end, we were interested to develop a novel gold(I)-catalyzed cycloisomerization processes for the formation of such scaffolds and demonstrate its synthetic utility in the synthesis of a complex natural product.

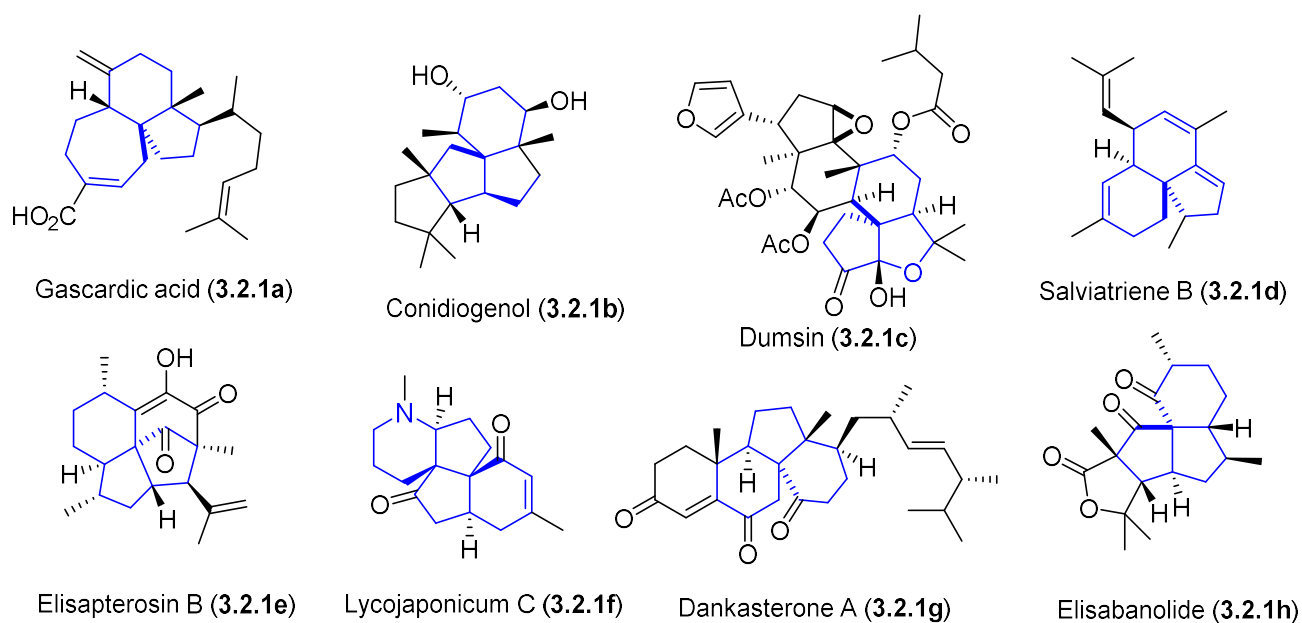
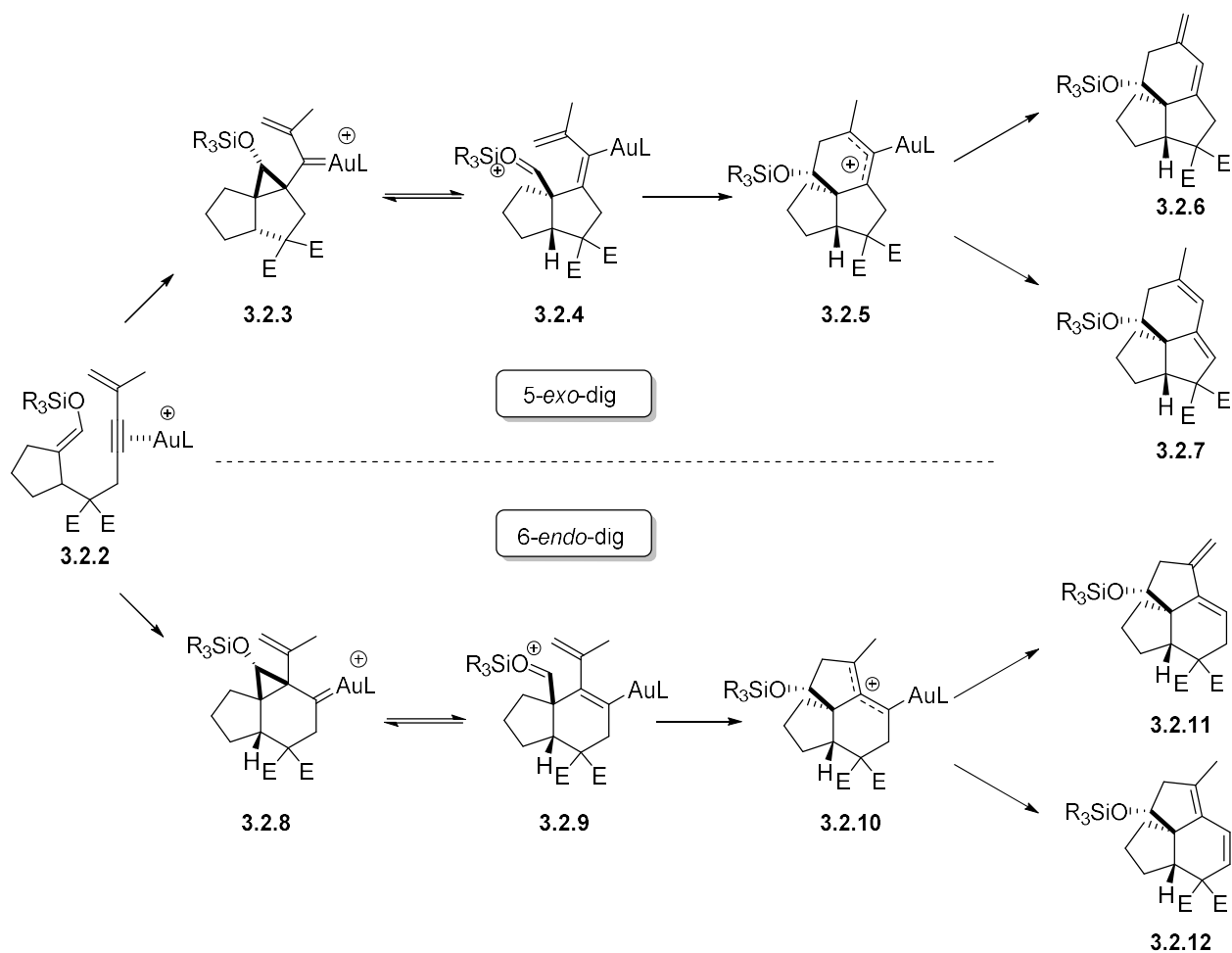


Figure 3.1 - Natural products possessing a polycyclic angular core

3.2.1 Hypothesis

We envisaged the synthesis of the angular framework from the monocyclic silyl enol ether **3.2.2** as a model substrate. Upon exposure to cationic gold(I) species, enol ether **3.2.2** could undergo a *5-exo-dig* carbocyclization to generate the cyclopropyl carbene intermediate **3.2.3**, which could be in equilibrium with **3.2.4**. A second cyclization event would take place to produce a stabilized allylic carbocation **3.2.5**. One can imagine that deprotonation from the primary or secondary carbon would generate **3.2.6** and **3.2.7**, respectively. Alternatively, a *6-endo-dig* cyclization of the silyl enol ether **3.2.2** could be observed. Following this pathway, the

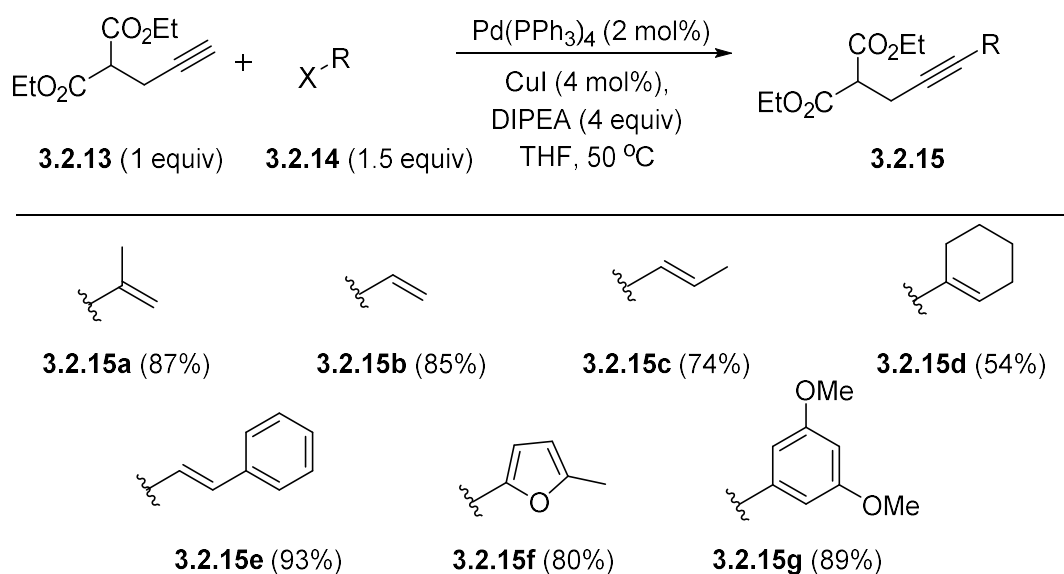
cyclopropyl-bearing intermediate **3.2.8**, in equilibrium with the oxonium cation intermediate **3.2.9**, would be produced. After a Prins-type cyclization, the cationic compound **3.2.10** should be formed. Analogous to the *5-exo-dig* pathway, deprotonation from either the primary or secondary carbon followed by protodeauration would lead to the *exo*- or the *endo*-cyclic diene **3.2.11** and **3.2.12**. In principle, proper manipulation of the reaction conditions and the use of specific cationic gold(I) catalysts could favour each pathway.



Scheme 3.5 - Envisaged gold(I)-catalyzed process for the construction of angular core

3.2.2 Substrate preparation

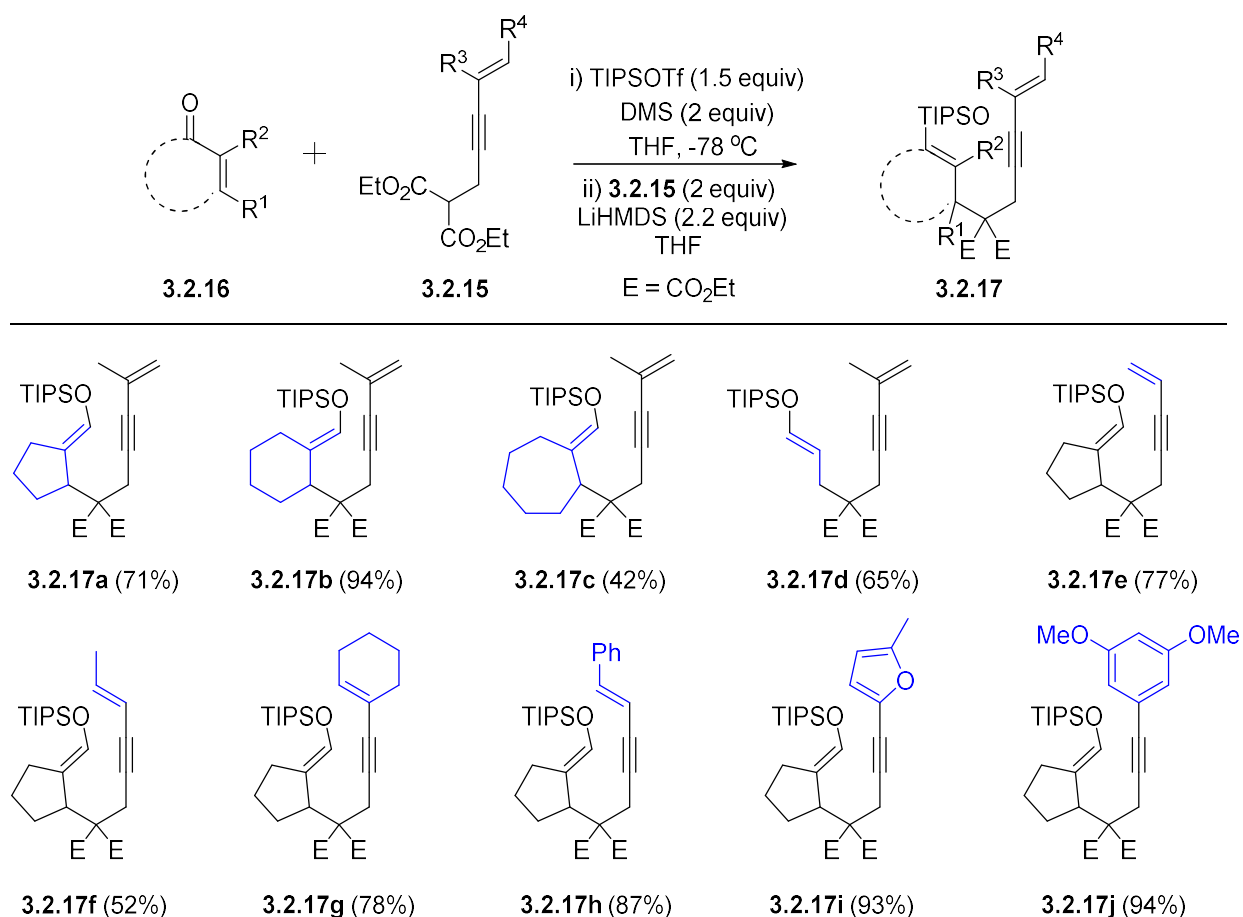
A variety of substrates were prepared in order to investigate the functional group tolerance and limitations of the gold(I)-catalyzed process. We first synthesised the substituted ethyl alpha-propargyl malonate moiety (*Scheme 3.6*). An array of vinyl bromides or aryl halides **3.2.14** were added to the alkyne **3.2.13** using the Sonogashira cross-coupling reaction. Substituted vinyl groups (**3.2.15a-e**) and electron rich aromatic rings (**3.2.15f-g**) were added in good yields (54-93%).



Scheme 3.6 - Synthesis of substituted propargyl malonates

A formal 1,4-addition of the deprotonated malonate chain **3.2.15** through the use of dimethyl sulfide and triisopropylsilyl triflate provided the desired precursors **3.2.17a-j** (*Scheme 3.7*). We immediately noticed that this reaction is highly sensitive to temperature. The intermediate formed by the addition of DMS to the enal **3.2.16** with TIPSOTf could decompose rapidly if the deprotonated malonate chain **3.2.15** is not pre-cooled and slowly added along the flask. Nonetheless, we have been able to prepare precursors of various ring sizes **3.2.17a-d** in moderate

to excellent yields (42-94%). Moreover, 1-cyclopentene-1-carboxaldehyde was chosen as the core structure to install all of the substituted propargyl malonate chains (**3.2.15b-g**). Silyl enol ethers **3.2.17e-j** were all observed in good yield (77-94%). Exclusive formation of the *E*-enol was obtained in all cases. We were then ready to attempt the gold(I)-catalyzed dehydro Diels-Alder reaction.

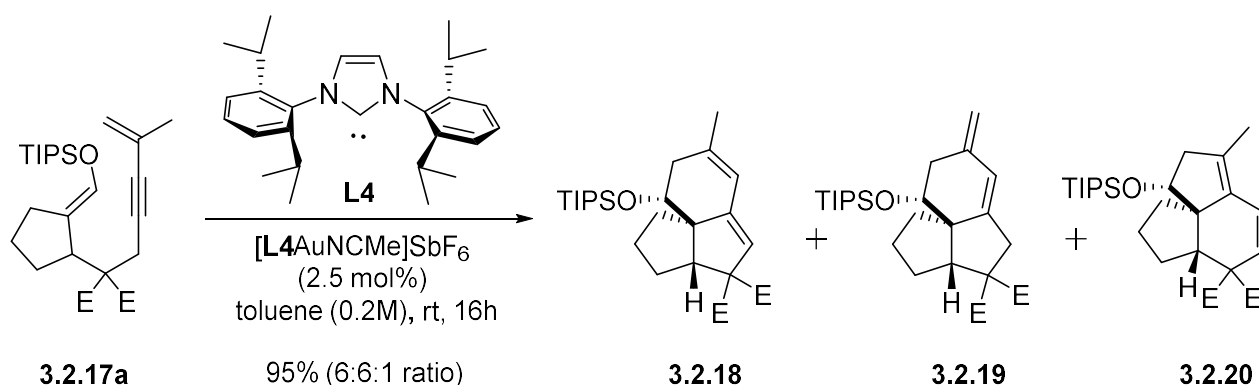


Scheme 3.7 – Precursors synthesis for the gold(I)-catalysed transformation

3.2.3 Optimization and substrate scope

Preliminary results obtained by Geneviève Bétournay⁶² demonstrated that triisopropylsilyl enols were more resistant towards decomposition under the gold(I)-catalyzed reaction condition

and afforded a better conversion. At first glance, using the $[\mathbf{L4AuNCMe}]\text{SbF}_6$ catalyst, we observed the desired product in 95% yield with a inseparable mixture of **3.2.18**, **3.2.19** and **3.2.20** in a 6:6:1 ratio (*Scheme 3.8*). She identified that; 1) toluene was the best solvent, 2) the reaction could proceed under ambient atmosphere, and 3) solvent does not need to be free of water contamination. We were satisfied to observe that the described product distribution because it confirms several aspects of the envisaged reaction mechanism (*Scheme 3.5*). 6-Membered ring formation is usually more challenging to achieve using gold(I) catalysis, thus it was not surprising to observe the 5-*exo*-dig products **3.2.18** and **3.2.19** as the major outcome.



Scheme 3.8 – Model substrate investigation by Geneviève Bétournay

In all cases, only one diastereomer was observed. We thought that this could arise from the difference in energy of the two possible transition states (**3.2.21** and **3.2.22**) during the second carbocyclization (*Figure 3.2*). The path leading to **3.2.21** would be lower in energy, notably because of the steric interaction between the bulky silyl ether group and the *cis*-fused carbocycles found on **3.2.22**.

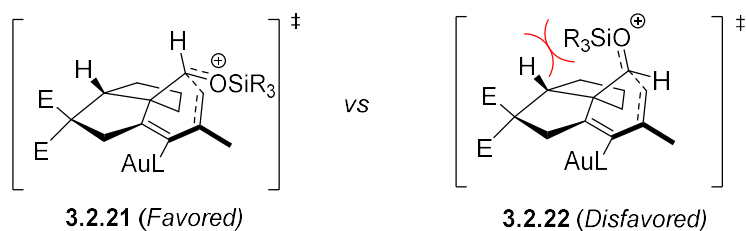


Figure 3.2 - Proposed transition state for the diastereoselectivity found in the isolated products

Although the product distribution gives us information about the mechanistic process, it is not very synthetically practical. We were interested to selectively form either **3.2.18** or **3.2.19**. We hypothesised that we could favor the formation of one of the two product by addition of a base (entries 2-4, *Table 1*). All of these attempts failed to selectively favor **3.2.18** or **3.2.19**; one can presume that the amine bases occupied the gold active site and neutralize its reactivity.

Table 3.1 – Cycloisomerization optimization

3.2.17a **L4** **[L4AuNCMe]SbF₆** (2.5 mol%)
toluene (0.2M), rt, 16h **3.2.18** **3.2.19** **3.2.20**

Entry	Additive	Additive addition time (hours)	Conversion ^[a]	Product Ratio (3.2.18 : 3.2.19 : 3.2.20)
1	None	-	> 99%	6:6:1
2	2,6-Lutidine (0.1 equiv.)	0	0 %	-
3	PMP (0.1 equiv.)	0	0 %	-
4	Cs ₂ CO ₃ (0.1 equiv.)	0	> 99%	4:6:1
5	HCl 1N (work-up)	16	> 99%	5:5:1
6	AcOH (1 equiv)	16	> 99%	7:0:1
7	HCl _{conc.} (1 equiv)	16	> 99%	8:0:1
8	TFA (1 equiv)	16	> 99%	9:0:1
9	CSA (1 equiv)	16	> 99%	13:0:1

[a] = Mesitylene was used as the internal standard

Since *endo*-cyclic olefins are known to be more thermodynamically stable,⁶³ we envisaged the possibility of *in-situ* isomerization of **3.2.19** into **3.2.18** by adding an acid upon completion of the reaction. No isomerization was observed with an acidic aqueous work-up (entry 5). One can imagine that the acid was not in physical contact with the products being in the organic layer, which does not allow the isomerization event to occur. Addition of a soluble acid in toluene was key for the isomerization to proceed (entries 6-9). We were pleased to observe complete conversion of **3.2.19** by the addition of camphor-10-sulfonic acid (entry 9).

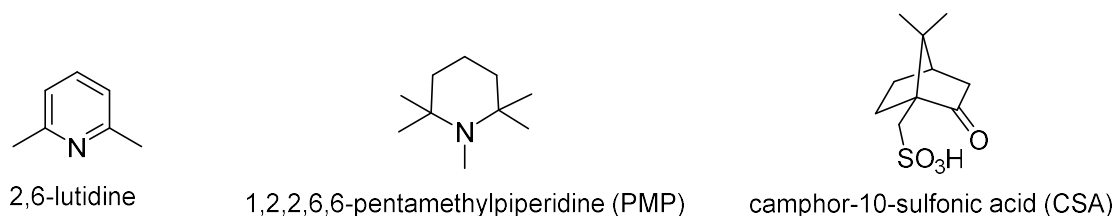


Figure 3.3 - Additives used in Table 3.1

With the solvent and additive established for the exclusive formation of **3.2.18** and **3.2.20**, we then attempted to eliminate the 6-*endo*-dig adduct by a ligand optimization for the Au(I) catalyst (Table 3.2). The catalyst loading was decreased to 1 mol% in order to identify the catalyst with the highest turn over number. **L10** adorned on gold(I) was leading to a complex mixture of products (entry 1). On the other hand, **L4**, **L5**, **L6** and **L8** produced the desired products in good conversions but mediocre selectivities (entries 2-5). Interestingly, with [PPh₃Au]NTf₂ and [L9AuNCMe]SbF₆, the regioselectivity of the transformation was optimal but incomplete conversion was obtained (entries 6 and 7). We were satisfied to observe a great conversion and selectivity using **L3** (entry 8). We hypothesized that the electron deficient ligand, having a higher π -acidity, could withdraw the electron density from the alkyne and selectively polarize the nucleophilic attack by the silyl enol ether to the 5-*exo*-dig cyclization. Therefore, this beneficial

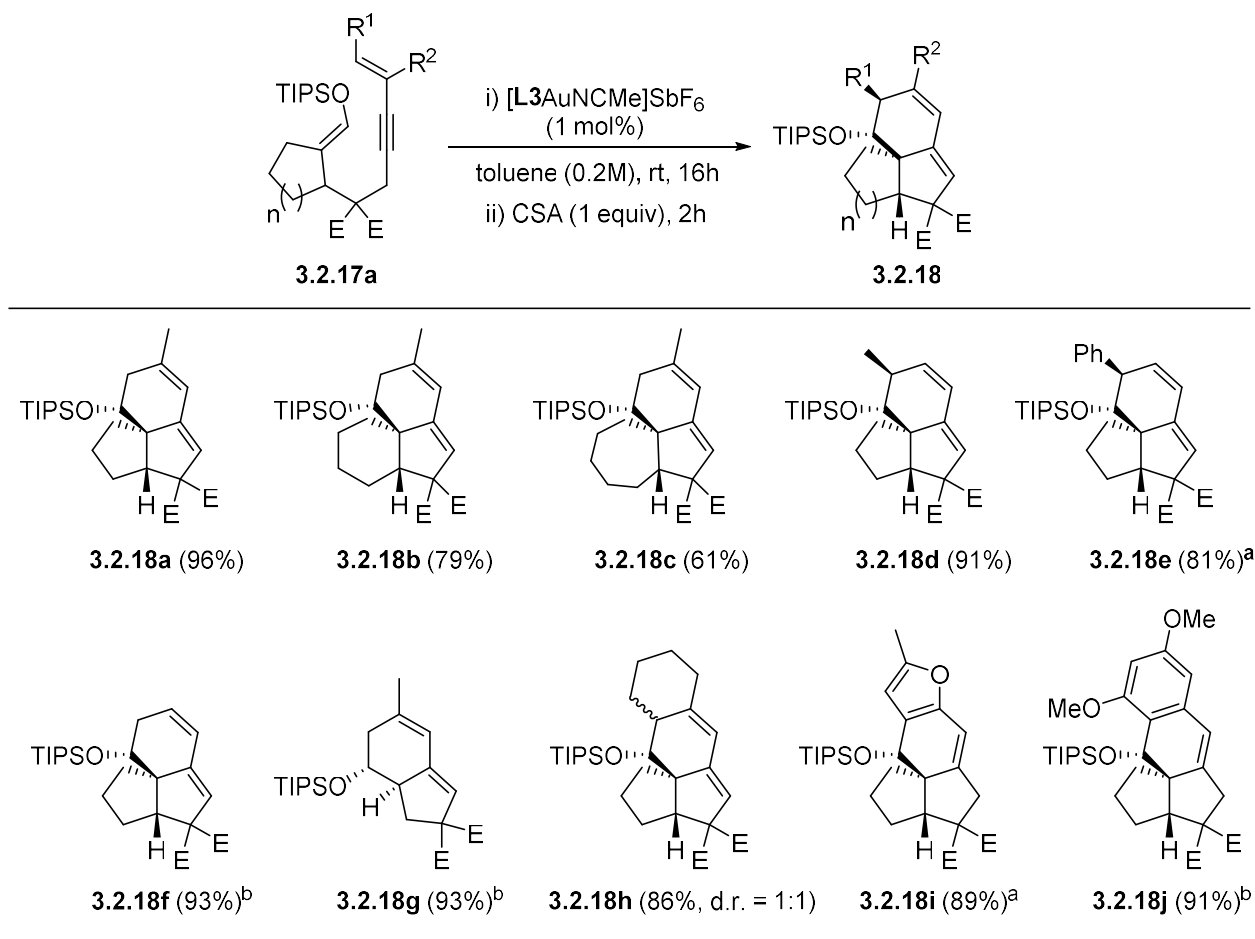
interaction explains the higher turnover number before the catalyst deactivates through other processes. This explanation would involve that activation of the alkyne is the rate determination step, which we can't confirm based on the results we have. After optimization of the additive and ligand, we were glad to obtain a perfectly controlled diastereoselectivity (>20:1) and regioselectivity (>20:1) with sole formation of the *endo*-cyclic olefins (>20:1).

Table 3.2 - Ligand optimization for the DDA reaction

3.2.17a		3.2.18	3.2.20
Entry	Ligand	Conversion ^[a]	Product Ratio (3.2.18 : 3.2.20)
1	L10	N/A	Degradation
2	L6	>99%	5:1
3	L5	>99%	9:1
4	L8	>99%	12:1
5	L4	>99%	13:1
6	PPh ₃ AuNTF ₂	68%	>20:1
7	L9	91%	>20:1
8	L3	>99%	>20:1

[a] = Mesitylene was used as the internal standard

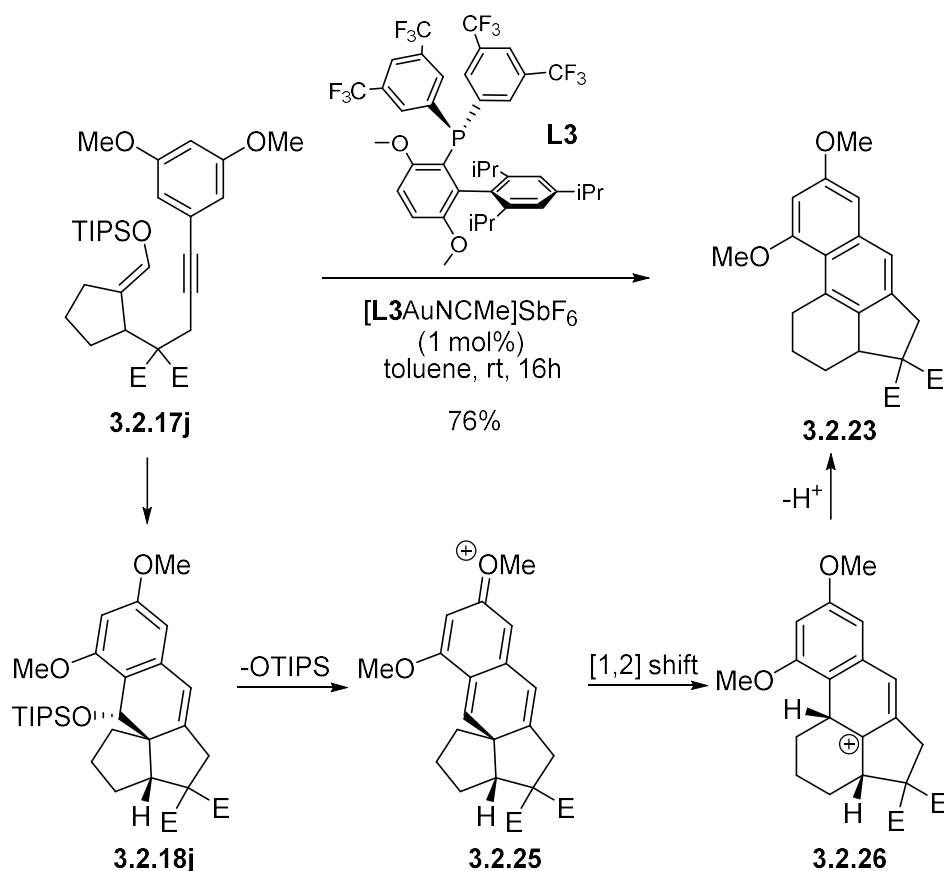
After the establishment of the optimized conditions, we examined the broad applicability of the Au(I)-catalyzed DDA reaction. Several enynes **3.2.17a-j** were subjected to the reaction conditions (*Scheme 3.9*). The model substrate **3.2.17a** gave the angular compound **3.2.18** in 96% isolated yield. Cyclization of **3.2.17b** ($n = 2$, $R^1 = \text{H}$ and $R^2 = \text{Me}$) and **3.2.17c** ($n = 3$, $R^1 = \text{H}$ and $R^2 = \text{Me}$) provided the desired tricycles **3.2.18b** and **3.2.18c** in 79% and 61% yields, respectively. It is worth noting that the cyclization of enynes having terminal substituents **3.2.17f** ($R^1 = \text{Me}$ and $R^2 = \text{H}$) and **3.2.17h** ($R^1 = \text{Ph}$ and $R^2 = \text{H}$) afforded the desired tricycles **3.2.18d** and **3.2.18e** having four contiguous stereogenic centers in 91% and 81% yields, respectively.



a) Reaction using 2 mol% of $[\text{L3AuNCMe}]\text{SbF}_6$, b) Reaction using 1 mol % of $[\text{L4AuNCMe}]\text{SbF}_6$

Scheme 3.9 - Substrate scope for gold(I)-catalyzed carbocyclization

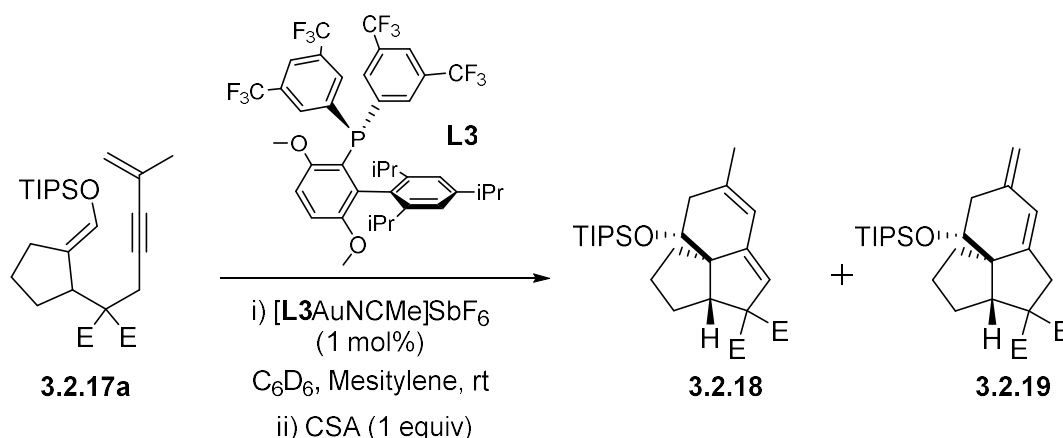
With regards to the cyclization of **3.2.17e** and **3.2.17d**, we found that the use of $[\text{L4AuNCMe}]\text{SbF}_6$ led to full conversion and the desired angular cores **3.2.18f** and **3.2.18g** were generated in 93% yield as the sole diastereomer in both cases. However, Au(I)-catalyzed DDA of **3.2.17g** containing a cyclohexenyl unit gave tetracycle **3.2.18h** in 86% yield as a 1:1 mixture of diastereomers. Cyclization of alkyne having a furyl group gave the cycloadduct **3.2.18i** in 89% yield. Interestingly, the cyclization of **3.2.17j** using $[\text{L3AuNCMe}]\text{SbF}_6$ gave the naphthalene derivative **3.2.23** in 74% yield, presumably through a cationic [1,2]-shift (*Scheme 3.10*) whereas the cyclization with $[\text{L4AuNCMe}]\text{SbF}_6$ provided the desired compound **3.2.18j** in 91% yield. Both reactions were performed without the subsequent addition of CSA.



Scheme 3.10 - Proposed mechanism for the formation of the naphthalene derivative

3.2.4 Double bond isomerization

We were interested to get more information about the kinetics of the gold(I)-catalyzed dehydro Diels-Alder reaction. Therefore, we performed a study monitoring the reaction progress using NMR spectroscopic analysis with the model substrate **3.2.17a** (Scheme 3.11). We replaced the toluene for deuterated benzene (C_6D_6) and added an equivalent of mesitylene as the internal standard. Reaction conditions are not identical but similar enough to give important information about the transformation.



Scheme 3.11 - Reaction condition for NMR experiment

Aliquots were taken at different time interval and analyzed by NMR spectroscopy to quantify the amount of **3.2.18** and **3.2.19** generated (Figure 3.4). At first glance, a significant induction period (5 minutes) was noticed for the reaction to begin. One can attribute the delay of the reaction to the dissociation of the acetonitrile ligand adorned on the gold(I) thereby liberating a coordination site on the metal. Once the reaction started we observed that the cycloadduct **3.2.18** was formed at a faster rate than the adduct **3.2.19**. Therefore, the kinetic product is the *endo*-cyclic olefin **3.2.18**, under this reaction condition. Since the starting material and the product were

undistinguishable by TLC, the reactions were always stirred for 16 hours prior to purification. In this NMR study, we quickly noticed that the transformation was completed at 60 minutes. Since no further conversion was observed after a prolonged stirring, the CSA was added at 90 minutes to allow the isomerization event to occur. After stirring for 30 minutes, all of the *exo*-cyclic olefins **3.2.19** were converted into the more thermodynamically stable tricyclic product **3.2.18** without affecting the overall yield of the transformation.

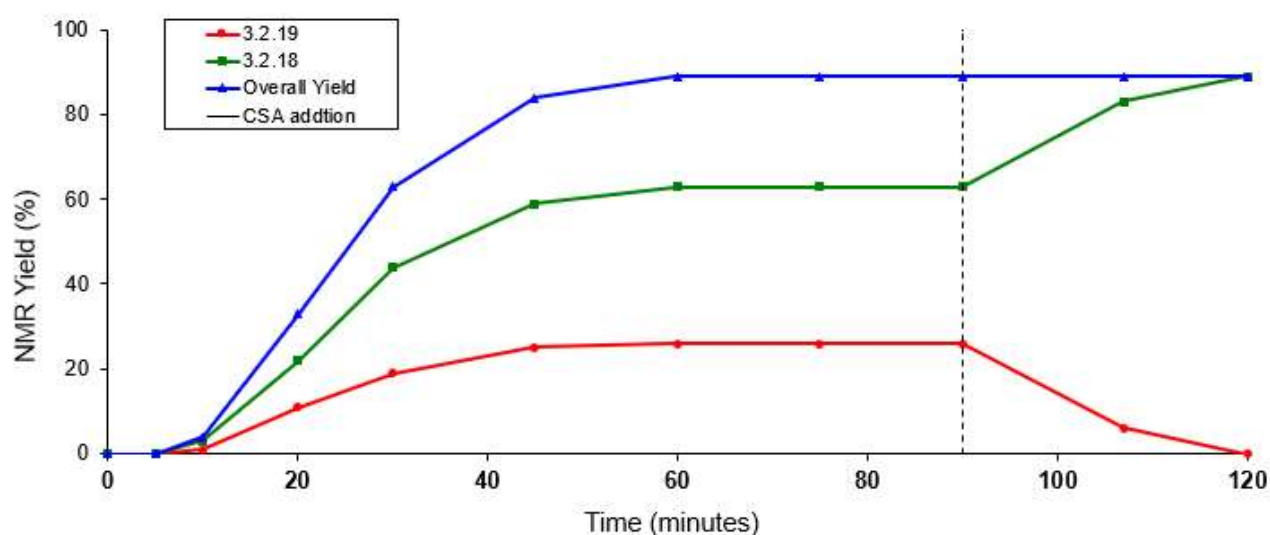


Figure 3.4 - Reaction progress quantified by NMR analysis

3.3 Magellanine and related alkaloids

Lycopodium alkaloids of the fawcettimine family such as magellanine (**3.3.1**), magellaninone (**3.3.2**), and paniculatine (**3.3.3**) were isolated in the 1970's by the group of Castillo and co-workers⁶⁴ (Figure 3.5). These three natural products possess an interesting 6-5-5-6 tetracyclic angular core and mostly differ by their oxidation state at the C-5 and C-11 position. Magellanine (**3.3.1**) was isolated in 1976 from the club moss *Lycopodium Magellanicum* and possesses 6 contiguous stereogenic centers including one quaternary at the tricyclic ring junction.

The structurally compact skeleton of **3.3.1** and its congeners have made an appealing and challenging target for the synthetic organic chemists. Seven total syntheses of magellanine have been reported and they will be discussed in the following section.

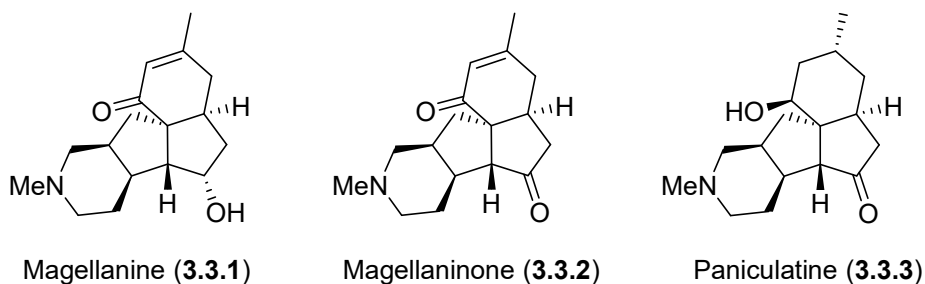
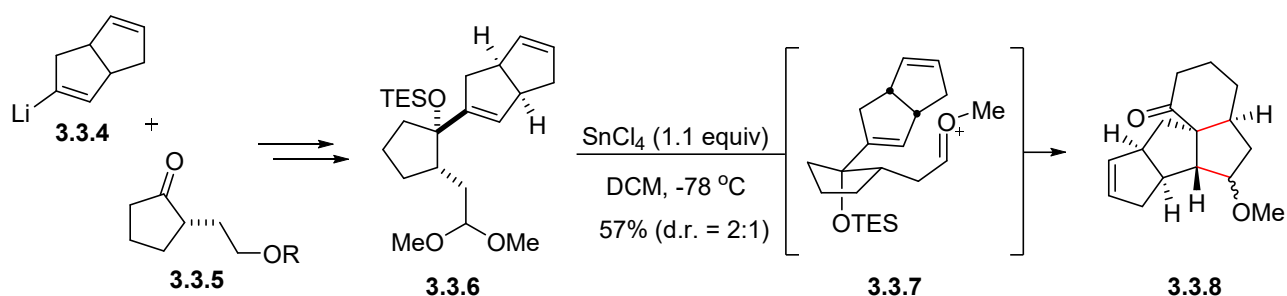


Figure 3.5 - Structures of magellanine, megallanimone and paniculatin

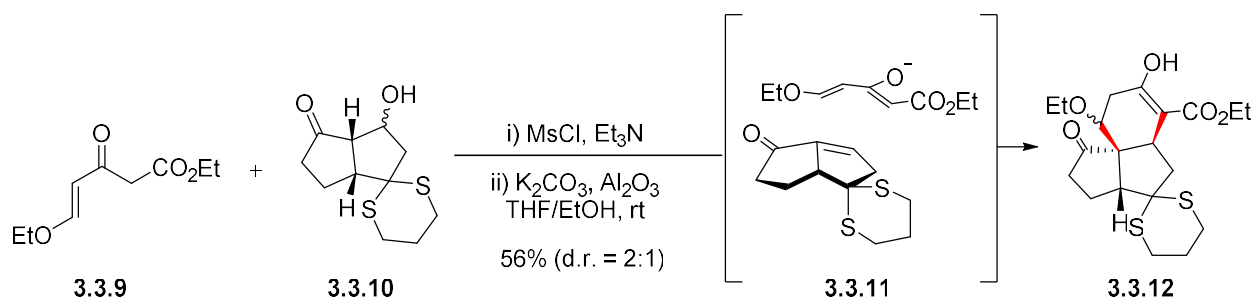
3.3.1 Previous synthetic forays of magellanine and its congeners

In 1993, Larry E. Overman reported the first enantioselective synthesis of magellanine (**3.3.1**) and magellanimone (**3.3.2**) (*Scheme 3.12*).⁶⁵ After a 1,2-addition of the vinyl lithium **3.3.4** to ketone **3.3.5**, the resulting tertiary alcohol intermediate was converted in few steps to the precursor **3.3.6**. Upon treatment with SnCl_4 the key step compound **3.3.6** underwent a domino Prins-pinacol reaction to produce the tetracyclic product **3.3.8** in 57% yield with a diastereomeric ratio of 2:1 having both the correct stereochemistry at the ring junction. Both diastereomers were carried further in the synthesis to afford magellanine (**3.3.1**) as the major product in 26 steps. The minor isomer was recuperated and converted into magellanimone (**3.3.2**) by a subsequent oxidation.



Scheme 3.12 - Prins-pinacol rearrangement by Overman

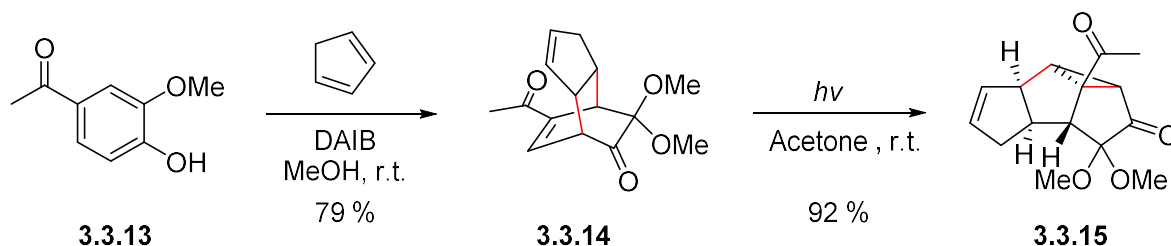
In the same year, Paquette and co-workers reported the racemic synthesis of magellanine and magellaninone.⁶⁶ After formation and elimination of the mesylate on the alcohol **3.3.10**, an enone was formed in order to react with **3.3.9**. The corresponding enolate of **3.3.9** was generated under basic condition to undergo a double Michael ring annulation with the α,β -unsaturated ketone which rapidly led to the tricyclic system **3.3.12** in 56% yield. Further functional group manipulation afforded magellanine in 31 steps.



Scheme 3.13 - Formal [4+2] cycloaddition by Paquette's and co-workers

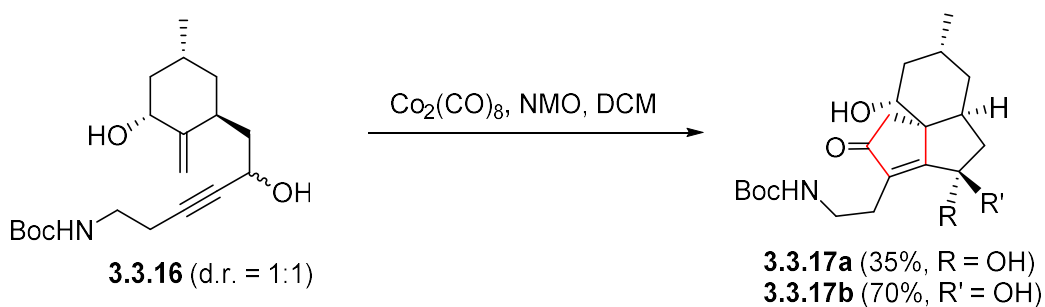
In 2002, Liao's group developed a very efficient and concise racemic synthesis of magellanine (Scheme 3.14).⁶⁷ Their work started by the use of a masked *o*-benzoquinone which is generated *in-situ* from **3.3.13** and traps smoothly with cyclopentadiene to provide **3.3.14**. The stereoselective Diels-Alder reaction generated four of the six contiguous stereocenters found on

magellanine. Upon irradiation with a fluorescent lamp, the bridged compound **3.3.14** undergoes a oxa-di- π -methane (ODMP) rearrangement to afford the tetracyclic intermediate **3.3.15** in excellent yield. The total synthesis was accomplished in only 14 steps from the acetovanillone **3.3.13**.



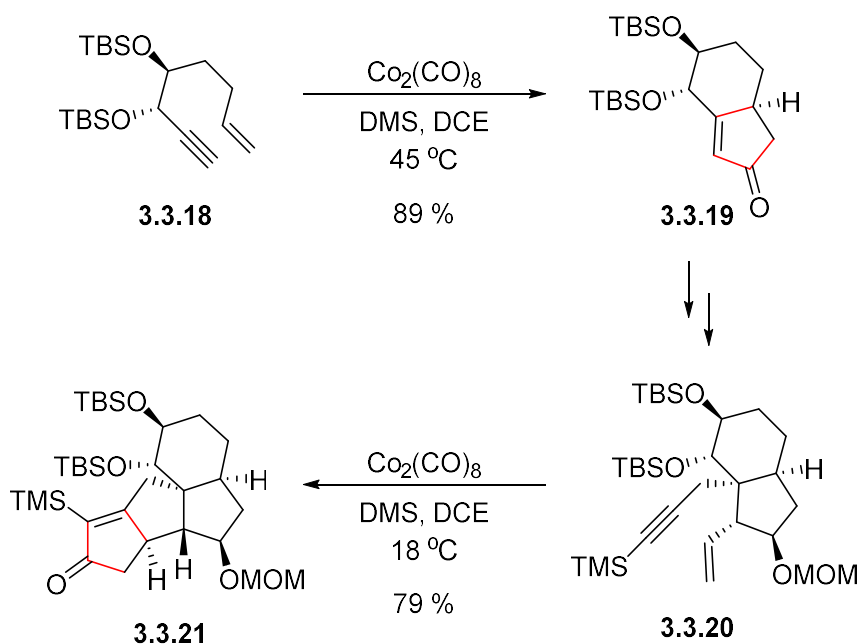
Scheme 3.14 – Key steps by Liao

Takahashi and Ishizaki accomplished a racemic formal synthesis of magellanine in 28 steps (Scheme 3.15).⁶⁸ The angular core was prepared from the monocyclic enyne **3.3.16** using a Pauson-Khand reaction. The diastereomeric mixture of **3.3.16** led to **3.3.17a** and **3.3.17b** with different isolated yields. It is believed that one diastereomer goes through a more congested transition state, leading to **3.3.17b** in lower yield. **3.3.17b** was converted into **3.3.17a** using a Mitsunobu reaction.



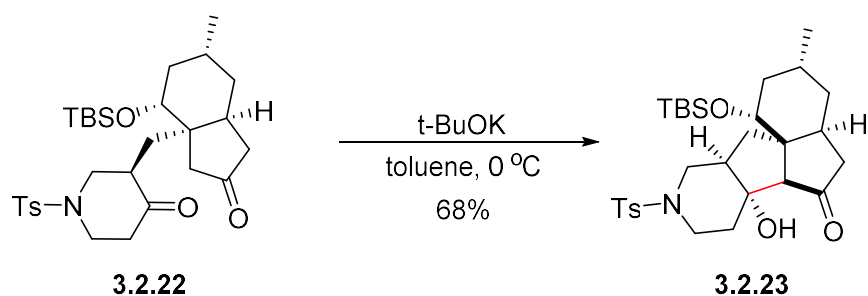
Scheme 3.15 – Pauson-Khand key step by Takahashi

Mukai reported the enantioselective total synthesis of magellanine, magellanineone and paniculatine based on two Pauson-Khand reactions (*Scheme 3.16*).⁶⁹ From the linear 1,6-enyne **3.3.18**, the bicyclic enone **3.3.19** was isolated in excellent yield. After a series of functional group manipulations, **3.3.20** was obtained in good yields. Submission of **3.3.20** under similar reaction conditions provided the tetracyclic enone **3.3.21** in 79% yield. From this route, 43 steps were required to synthesis enantiomerically pure magellanine.



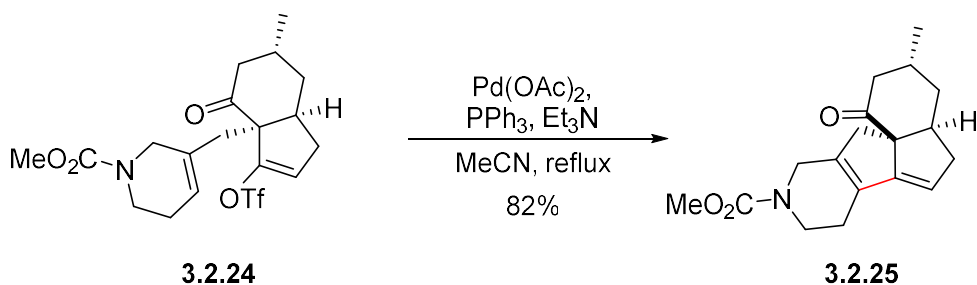
Scheme 3.16 - Pauson-Khand reaction key steps by Mukai

In 2014, the relatively short enantioselective preparation of the tetracyclic alkaloid natural products **3.3.1** was accomplished by Yang and co-workers (*Scheme 3.17*).⁷⁰ In contrast with other works, the nitrogen was installed at a much earlier stage during the synthesis. The precursor **3.2.22** was treated with *t*-BuOK in toluene and a smooth aldol cyclization occurred to yield the tetracyclic **3.2.23** with an excellent site- and stereo-selectivity. The formal synthesis of magellanine was completed in 25 steps by the interception of an intermediate prepared by Liao's group.⁶⁷



Scheme 3.17 - Site specific aldol reaction by Yang

The shortest synthesis of magellanine was reported by Yan and co-workers in 2015 (*Scheme 3.18*).⁷¹ The tetracyclic molecular framework was prepared using a Heck type coupling reaction. Upon treatment of the pseudo halide **3.2.24** with palladium, an oxidative insertion of the Pd(0) took place followed by carbopalladation and β -hydride elimination in order to generate **3.2.25** in good yield. This concise approach required only 13 steps to prepare magellanine.

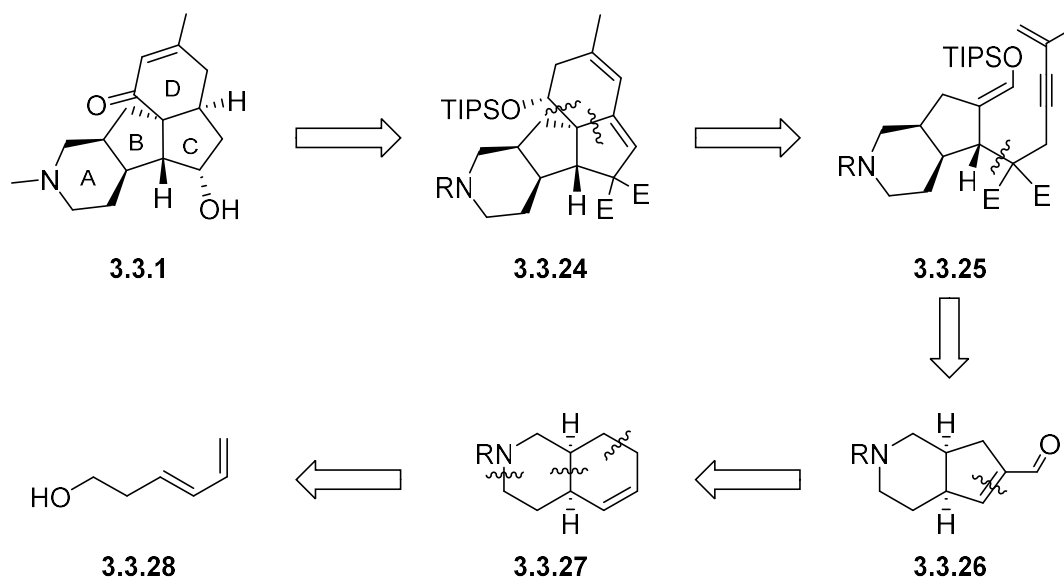


Scheme 3.18 - Palladium catalyzed olefin insertion by Yan

A specific preparation of paniculatine was reported by Sha in 1999,⁷² where many other researchers attempted to complete the synthesis of magellanine. Construction of the molecular skeleton was reported by Crimmins,⁷³ Meyers,⁷⁴ Mehta⁷⁵ and Sarpong.⁷⁶ Investigation and completion of the synthesis by few of these groups is still in progress and will not be discussed in this chapter.

3.3.2 Our retrosynthetic approach

To further demonstrate its synthetic utility, we applied the Au(I)-catalyzed dehydro Diels-Alder reaction to a concise synthesis of magellanine **3.3.1**. The key strategic disconnections made on **3.3.1** involved a carefully orchestrated C–C bond formation sequence. As such, the Au(I)-catalyzed DDA reaction of **3.3.25** would forge the C and D ring of **3.3.1** (Scheme 3.19). The cycloadduct precursor **3.3.25** could arise from a stereoselective 1,4-conjugate addition between enal **3.3.26** and a substituted malonate chain. Moreover, the enal **3.3.26** would be derived from the *cis*-decalin **3.3.27** after oxidative cleavage of the alkene followed by aldol condensation. Finally, the bicyclic fragment **3.3.27** would be assembled by a Diels-Alder reaction from **3.3.28**.

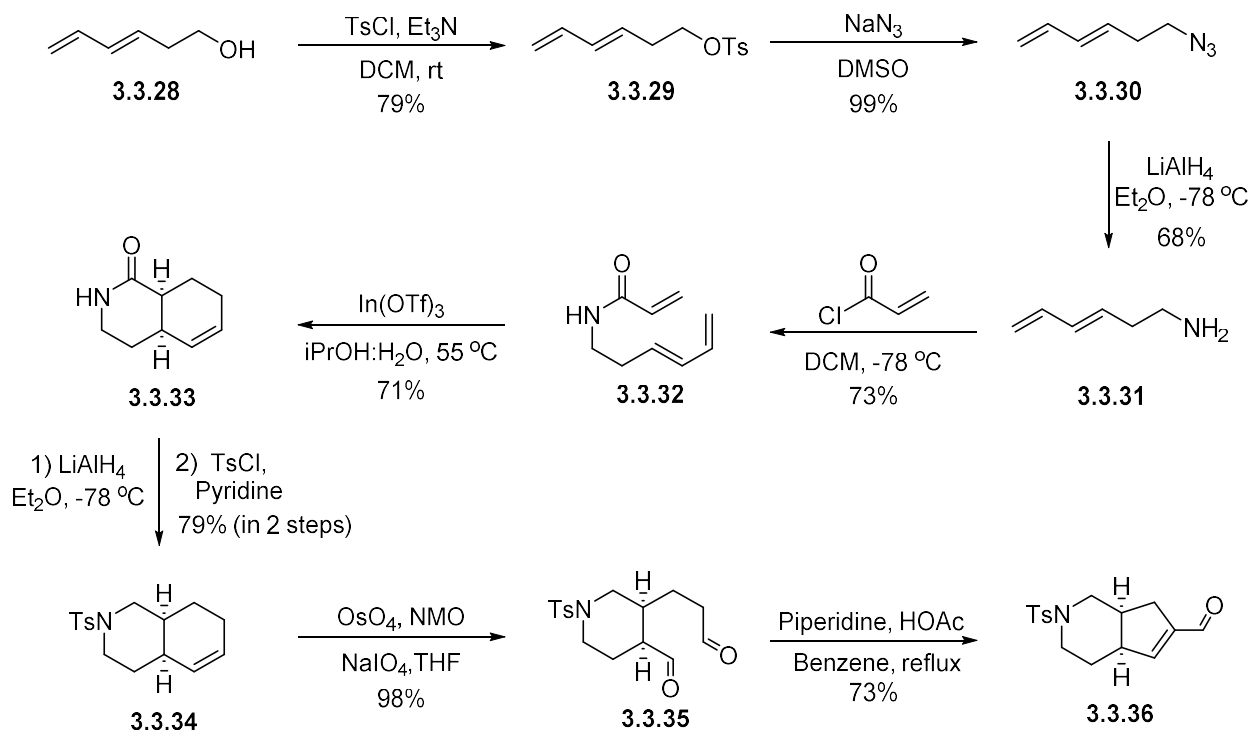


Scheme 3.19 - Retrosynthetic approach of (±)-magellanine

During the development of the shortest synthesis of magellanine, we focused primarily on efficient routes to prepare the enal **3.3.26**. The three main pathways explored will be discussed in the following sections.

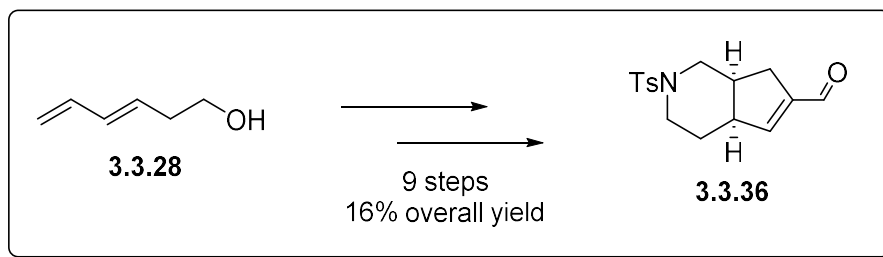
3.3.3 Route A : Enal synthesis through Lewis acid-catalyzed [4+2]

During her M.Sc. in the laboratory of Professor Louis Barriault, Geneviève Bétounay developed the first preparation of the Michael acceptor **3.3.36** (Scheme 3.20).⁶² It began with the installation of a tosyl group on the homoallylic alcohol **3.3.28** followed by a nucleophilic substitution with sodium azide to produce **3.3.30** in 78% yield over two steps. Reduction of the azide with LiAlH₄ afforded the amine in 68% yield. It is important to notice that no purification was performed until the formation of the homoallylic amine **3.3.31**, which was purified by distillation. Treatment of the amine **3.3.31** with acryloyl chloride generated the compound **3.3.32** in 73% yield. Treatment of the amine **3.3.31** with acryloyl chloride generated the compound **3.3.32** in 73% yield.



Scheme 3.20 – Geneviève Bétounay’s approach to the synthesis of enal **3.3.36**

The amide **3.3.32** was well suited for a Lewis acid-catalyzed intramolecular [4+2] cycloaddition. **3.3.32** in the presence of indium(III) triflate in water and isopropanol at 50 °C afforded the *exo*-Diels-Alder adduct **3.3.33** selectively. Notably, due to the tension during the transition state, the *endo*-adduct was not observed.⁷⁷ Unfortunately, this reaction could not be scaled up greater than 2 g of the starting amide **3.3.32** without significantly diminishing the isolated yield. The lactam was then reduced to the amine and was protected employing tosyl chloride to afford **3.3.34** in 79% yield. Under Lemieux-Johnson oxidation reaction conditions, the cleavage of the alkene **3.3.34** was observed in good yield to afford the unstable dialdehyde **3.3.35**. The crude reaction mixture was carried forth to the aldol condensation with a catalytic amount of piperidine and acetic acid under reflux using a Dean-Stark apparatus. Finally, the enal **3.3.36** was prepared in 9 steps from the alcohol **3.3.28** with an overall yield of 16% (*Scheme 3.21*). Although we obtained the desired intermediate **3.3.36**, we pursued alternative routes to reduce the number of synthetic steps.

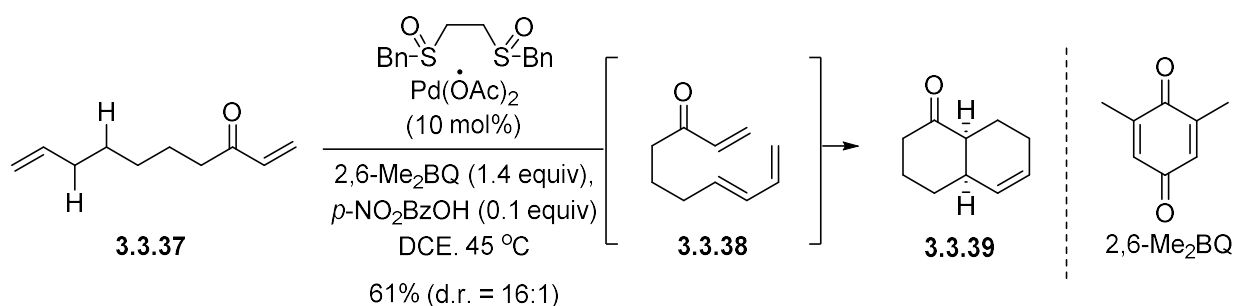


Scheme 3.21 - Overview of the route A

3.3.4 Route B : Enal synthesis through dehydrogenative Diels-Alder

In 2011, White and co-workers developed an interesting dehydrogenative Diels-Alder reaction.⁷⁸ A selected example of this methodology is highlighted in *Scheme 3.22*, which is structurally similar to **3.3.32**. They identified that a catalytic amount of Pd(II)/benzyl-sulfoxide in

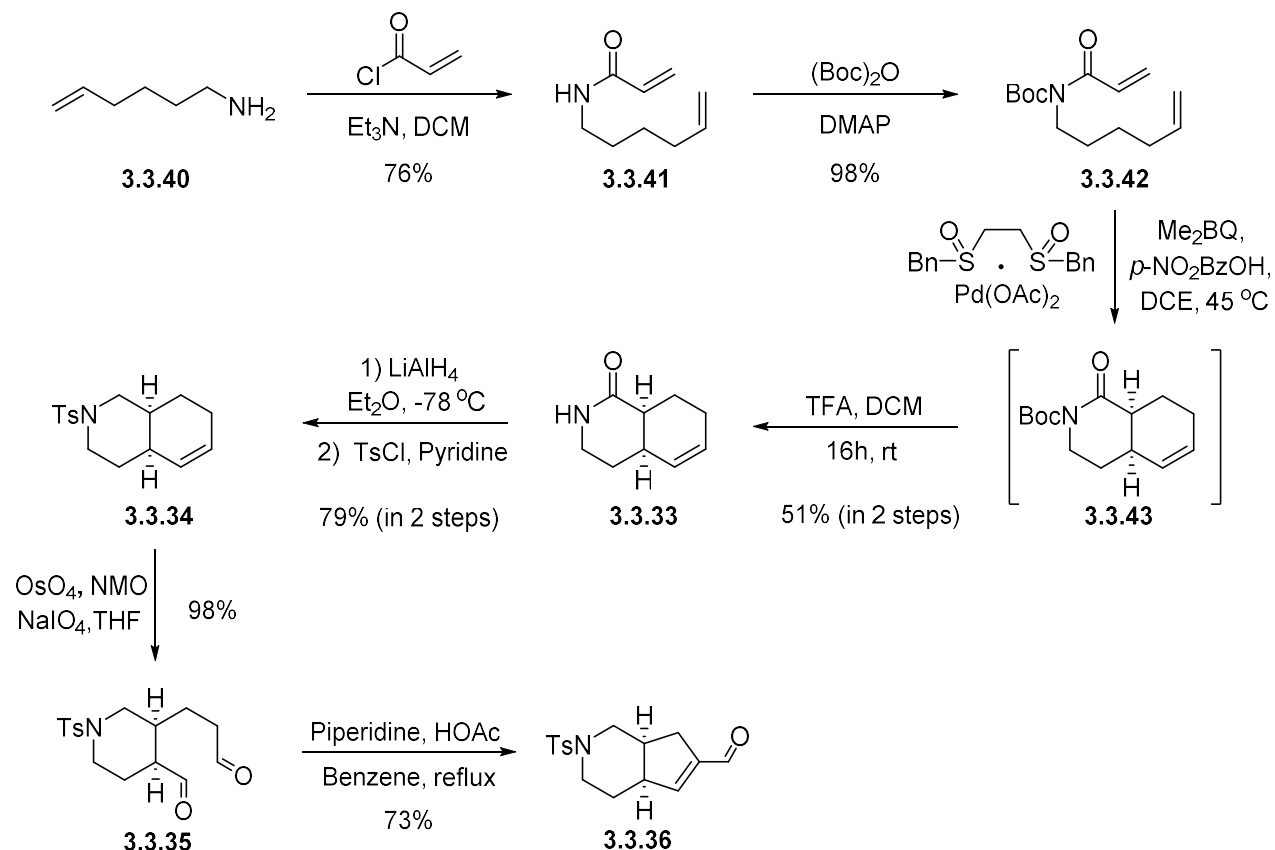
combination with *p*-NO₂BzOH was used for the formation of a π -allyl-Pd species in order to produce the diene intermediate. An internal oxidant, such as 2,6-Me₂BQ, was added to the reaction mixture to regenerate the active Pd(II) species. The bulky 2,6-dimethyl-1,4-benzoquinone was used to prevent a possible quinone Diels-Alder reaction with the diene intermediate.



Scheme 3.22 - Dehydrogenative Diels-Alder reaction by Christina White

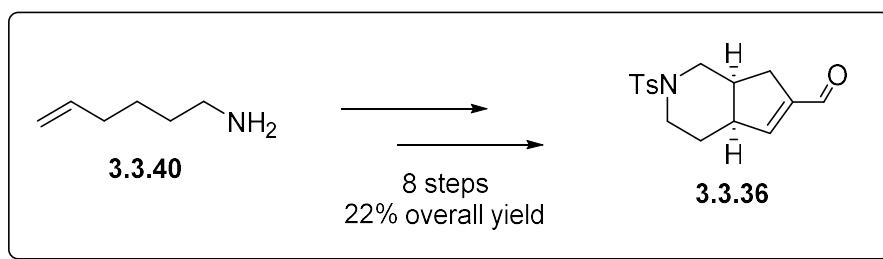
Drawing inspiration from this work, we attempted to apply this methodology for the preparation of enal **3.3.36** (*Scheme 3.23*). From the commercially available 1-amino-5-hexene **3.3.40**, the linear amide **3.3.41** was obtained after acylation with acryloyl chloride. At first glance we were disappointed to observe no conversion when **3.3.41** was submitted to the optimal condition developed for the dehydrogenative Diels-Alder reaction. Alternatively, the tosyl- and Boc- protected amides were investigated. Only the *tert*-butyloxycarbonyl-protected amide **3.3.42** led to the desired cycloadduct **3.3.43**, which could not be separated from the side products generated by the reaction. The crude reaction mixture was then treated with trifluoroacetic acid (TFA) which produced the known bicyclic lactam **3.3.33** in 51% isolated yield over 2 steps. The carbamate group was removed since it was sensitive to the reaction conditions employed later in the synthesis. Following the same procedure as previously describe in *Scheme 3.21*, the lactam **3.3.33** was reduced and protected with tosyl chloride. Oxidative cleavage of the alkene **3.3.34**

afforded the dialdehyde **3.3.35** which was submitted under aldol condensation to produce the carboxaldehyde **3.3.36**.



Scheme 3.23 - Dehydrogenative Diels-Alder reaction approach

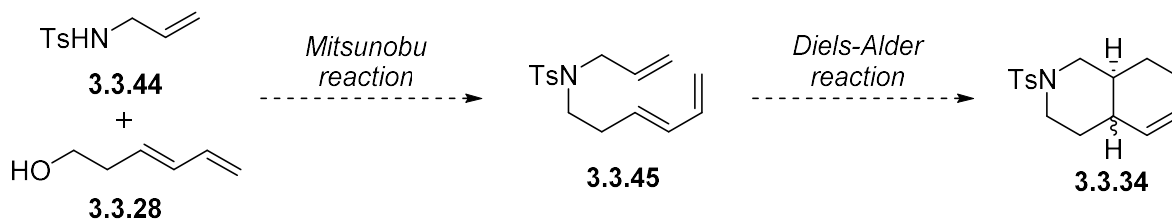
Unfortunately, because of the unexpected protection and deprotection steps of the Boc group, the Michael acceptor (**3.3.36**) was prepared in eight steps rather than six from the commercially available amine **3.3.40** (*Scheme 3.24*). This new pathway was one step shorter with a slightly better overall yield, in comparison with the previously developed *Route A*. As such, we continued to investigate shorter routes to the desired enal **3.3.36**.



Scheme 3.24 - Overview of the route B

3.3.5 Route C : Enal synthesis trough one-pot Mitsunobu/Diels-Alder reaction

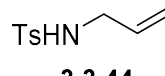
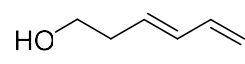
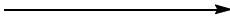
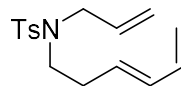

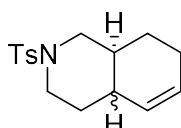
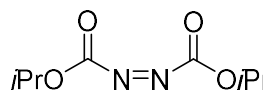
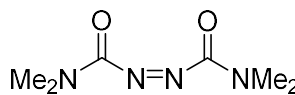
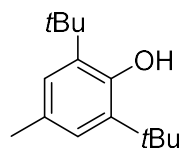
The two previous approaches (*Route A and B*) were still not able to satisfy our goal for a rapid synthesis of magellanine. Therefore, we revised and carefully analyzed the pitfalls from these pathways. In *Route A*, the homoallylic alcohol **3.3.28** had to be tosylated in order to be displaced by an azide that is further reduced with LiAlH_4 . These step-intensive transformations are not optimal for constructive bond formation. One can imagine that in a Mitsunobu reaction⁷⁹ the alcohol **3.3.28** would be *in-situ* converted into a good leaving group (*Scheme 3.25*). The nucleophile partner from that reaction would be the commercially available tosylated allylamine **3.3.44**, which would immediately form the carbon-nitrogen bond. The sulfonamide **3.3.44** possesses an acidic proton for the Mitsunobu reaction to proceed and will have the advantage of avoiding the reduction and protection of the lactam **3.3.33**. This new approach between **3.3.28** and **3.3.44** would then afford **3.3.45**. Since the carbonyl is not present on the intermediate **3.3.45**, Lewis acid-catalyzed cycloaddition will not be feasible. A thermal Diels-Alder would have to be developed. This new route would be an aggressive approach to rapidly access the isoquinoline derivative **3.3.34**.



Scheme 3.25 - Hypothetical Mitsunobu/Diels-Alder reaction sequence

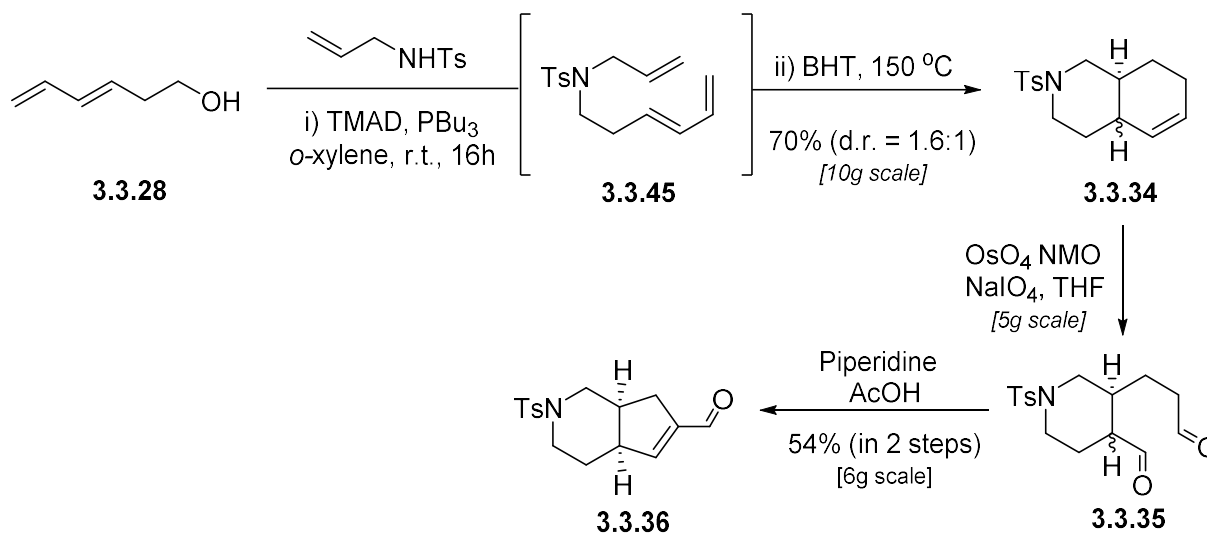
Driven by this challenge, we attempted to perform the two reactions in one step. For such a process, compatible solvents for both transformations had to be identified, thus a parallel optimization of the Mitsunobu and the Diels-Alder reaction was necessary (*Table 3.3*). We were pleased to observe the formation of **3.3.45** in 69% yield using DIAD/ PPh_3 in tetrahydrofuran (entry 1). After purification of the sulfonamide **3.3.45**, the thermal Diels-Alder reaction proceeded very slowly in refluxing toluene (72h, entry 2). Changing the toluene for higher boiling point solvent, such as *o*-xylene, led to an increment in rate of the Diels-Alder reaction with a slightly better yield (entry 3). Addition of radical inhibitors, such as BHT, during the cycloaddition transformations is known to avoid polymerization of the alkenes precursors.⁸⁰ In our case, 20 mol% of BHT had a beneficial impact on the yield of the cycloaddition, affording **3.3.34** in 95% yield (entry 4). Our efforts then focused on increasing the yield of the Mitsunobu transformation using a high boiling point solvent. Unfortunately, the Mitsunobu reaction led to very low yields in toluene (entry 5). After screening of a few reagents, we found that the use of TMAD/ PBU_3 in toluene gave the desired intermediate **3.3.45** in 72% yield (entry 6).

Table 3.3 - Optimization of the Mitsunobu and Diels-Alder reaction

<div style="display: flex; align-items: center; justify-content: center;"> <div style="text-align: center;">  <p>3.3.44</p> </div> <div style="margin: 0 10px;">+</div> <div style="text-align: center;">  <p>3.3.28</p> </div> </div> <div style="display: flex; align-items: center; justify-content: center; margin-top: 10px;"> <div style="text-align: center;"> <p>Reaction 1</p>  </div> <div style="text-align: center;">  <p>3.3.45</p> </div> <div style="text-align: center;"> <p>Reaction 2</p>  </div> <div style="text-align: center;">  <p>3.3.34</p> </div> </div>				
<div style="display: flex; justify-content: space-around; align-items: flex-end; margin-top: 20px;"> <div style="text-align: center;">  <p>Diisopropyl azodicarboxylate (DIAD)</p> </div> <div style="text-align: center;">  <p>Tetramethyl azodicarboximide (TMAD)</p> </div> <div style="text-align: center;">  <p>Butylated hydroxytoluene (BHT)</p> </div> </div>				
Entry	Reaction 1 (from 3.3.44 and 3.3.28)	Reaction 2 (from 3.3.45)	Yield of 3.3.45	Yield of 3.3.34
1	DIAD/PPh ₃ , THF	-	69%	-
2	-	Toluene, 110 °C, 72h	-	56%
3	-	<i>o</i> -xylene, 140 °C, 24h	-	68%
4	-	<i>o</i> -xylene, 140 °C, 24h ^[a]	-	95%
5	DIAD/PPh ₃ , Toluene	-	43%	-
6	TMAD/PBu ₃ , Toluene	-	72%	-

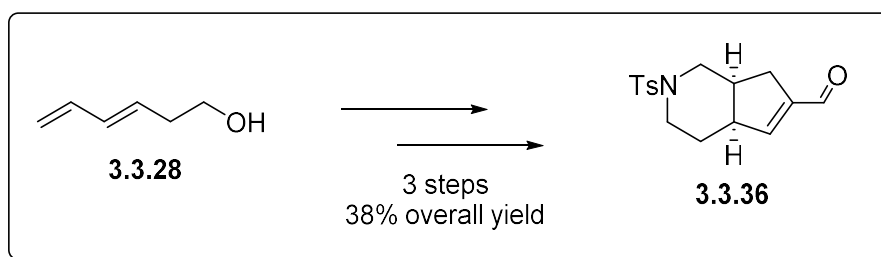
[a] = addition of 20 mol% of BHT

From this point, we were excited to try the two reactions sequentially without midway purification (*Scheme 3.26*). Therefore, the alcohol **3.3.28** was submitted under the optimized Mitsunobu reaction condition in *o*-xylene and then refluxed with 20 mol% of BHT. This reaction proceeded as expected and could be scaled up to 10 g in order to obtain **3.3.34** in 70% isolated yield with a diastereomeric ratio of 1.6:1. After Lemieux-Johnson oxidative cleavage of the decalin **3.3.34** followed by aldol condensation afforded **3.3.36**.



Scheme 3.26 - Optimized route of enal preparation

This route proves to be more efficient to the other pathways developed for the synthesis of the enal **3.3.36**. From the homoallylic alcohol **3.3.28**, it requires only three steps for the multi gram-scale preparation of the Michael acceptor in 38% overall yield (*Scheme 3.27*).

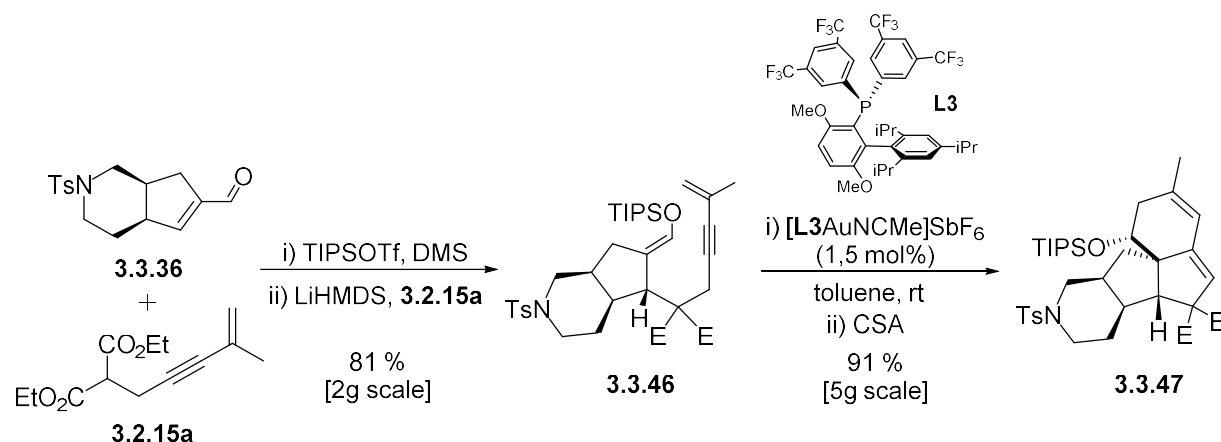


Scheme 3.27 - Overview of route C

3.3.6 End game: Total synthesis of (±)-magellanine

From the carboxaldehyde **3.3.36**, the synthesis was continued by the 1,4-addition of the substituted malonate chain **3.2.15a** to obtain the diastereomerically pure silyl enol ether **3.3.46** in

81% isolated yield. The addition of **3.2.15a** occurred on the less hindered convex face of the bicyclic enal **3.3.36**. Moreover, the *Z*-silyl enol ether was not observed which could be explained by the favored formation of the less sterically congested *E*-silyl enol ether **3.3.46**. As expected, under the optimized gold(I)-catalyzed DDA reaction conditions, the precursor **3.3.46** underwent smooth and selective formation of the tetracyclic compound **3.3.47**. It is important to emphasize the practicality of this transformation; the bench stable catalyst could be manipulated without special precautions and the reaction can be performed using unpurified solvent. The catalyst is simply added to the starting material in toluene and stirred overnight under ambient atmosphere. It is remarkable that in only five chemical transformations, all of the necessary carbon–carbon bonds of magellanine were constructed.

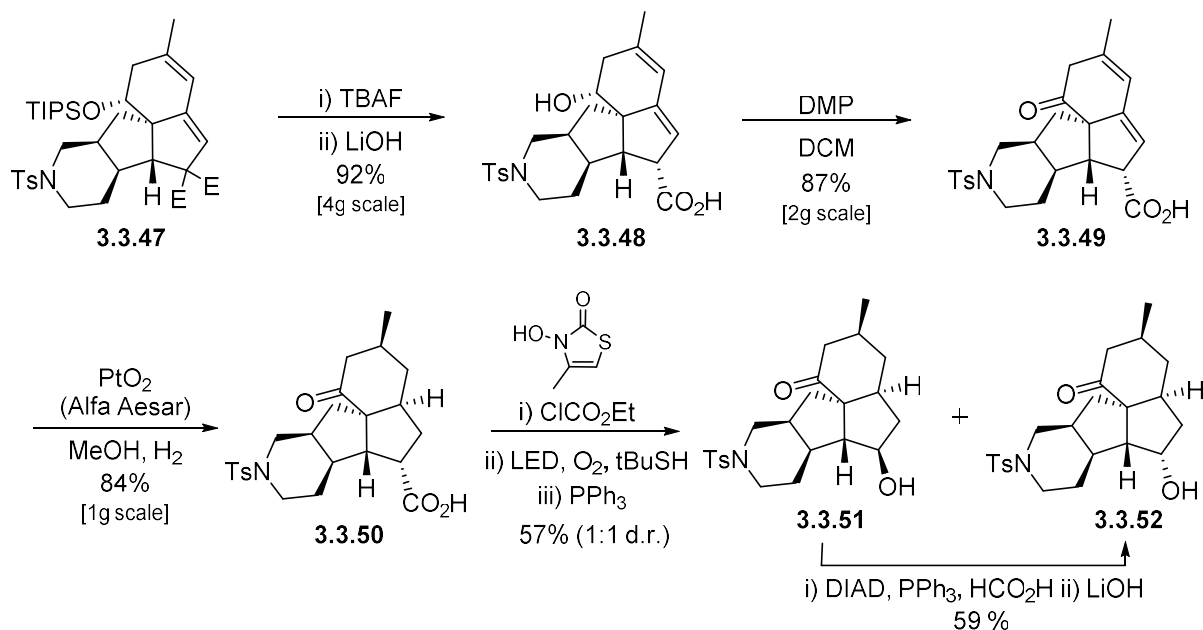


Scheme 3.28 - Key steps of the tetracyclic core formation

Next, functional group manipulation remained to generate the alcohol at the C-5 position, the enone at the C-11 position, and the tertiary amine. Removal of TIPS group on **3.3.47** with TBAF followed by the addition of LiOH and water, the mixture was heated to 140°C yielding the corresponding carboxylic acid **3.3.48** as the sole diastereomer in 92% yield over two steps (*Scheme 3.29*). Dess-Martin oxidation of the free alcohol afforded ketone **3.3.49** in 87% yield. We then

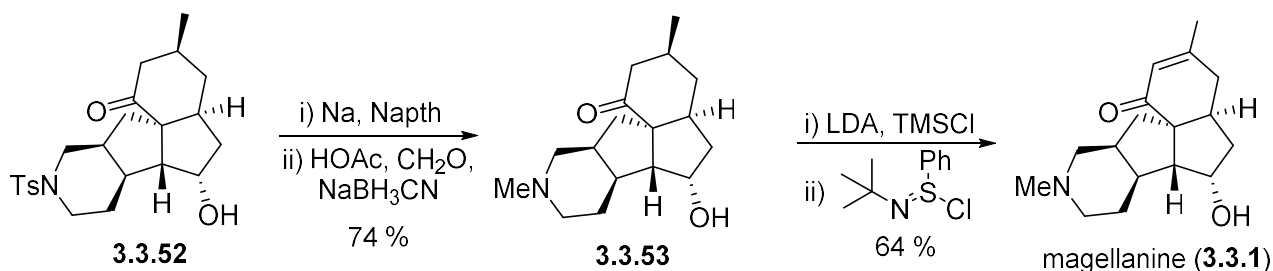
attempted to selectively reduce the alkene at the β -position of the carboxylic acid. After several unsuccessful attempts, we opted to reduce both alkenes with Adam's catalyst (PtO_2). Pleasingly, a selective hydrogenation on the convex face was accomplished affording **3.3.50** in 84% yield. It is important to note that only the platinum dioxide from Alfa Aesar company led to complete alkene reduction and reproducible results.

At this point, the carboxylic acid moiety was converted to a secondary alcohol through a Barton-McCombie oxygenative decarboxylation developed by Zard and co-workers.⁸¹ A modified 'one-pot' variant of this transformation, reported by Martin,⁸² was used to convert **3.3.50** into the alcohols **3.3.51** and **3.3.52** in 57% yield (d.r. = 1:1). A cursory inspection of the reaction mechanism reveals the formation of a secondary carbon-centered radical which is trapped with molecular oxygen to produce a peroxide. The latter was then reduced using triphenylphosphine to afford the desired alcohols **3.3.51** and **3.3.52**. The undesired diastereomer **3.3.51** was then converted to the desired **3.3.52** using a Mitsunobu protocol.⁶⁷



Scheme 3.29 – Functional group manipulation for (±)-magellanine synthesis

Analogous to the synthesis of magellanine by Yang,⁷⁰ the sulfonamide **3.3.52** was reduced with Na/naphthalene and *in-situ* submission to their described reductive amination conditions afforded the tertiary amine **3.3.53** (Scheme 3.30). The installation of the enone was achieved using Takahashi's protocol.⁶⁸ First, addition of LDA and TMSCl gave the corresponding silyl ether which upon exposure to a second equivalent of LDA and the Mukaiyama reagent⁸³ followed by an acidic work-up afforded the (±)-magellanine **3.3.1** in 64% yield. The total synthesis of (±)-magellanine was then accomplished in only 11 steps. Spectral data were identical to those reported in the literature. Using the protocol developed by Overman,⁶⁵ the final step of (±)-magellaninone could be achieved from **3.3.1** using a Jones oxidation reaction, which is the shortest formal synthesis of that natural product.



Scheme 3.30 - Last steps of (±)-magellanine synthesis

3.4 Conclusion

In summary, we have developed an innovative and operationally facile methodology for the formation of carbocycles via a gold(I)-catalyzed cycloaddition. This reaction grants access to various complex angular fused-ring systems in high diastereoselectivities. The practicality of this Au(I)-catalyzed transformation was validated in the total synthesis of (±)-magellanine which was

accomplished in only 11 steps from hexa-3,5-dien-ol; one of the shortest total syntheses known to date. Further applications of this transformation in natural product synthesis are currently ongoing and will be reported in due course.

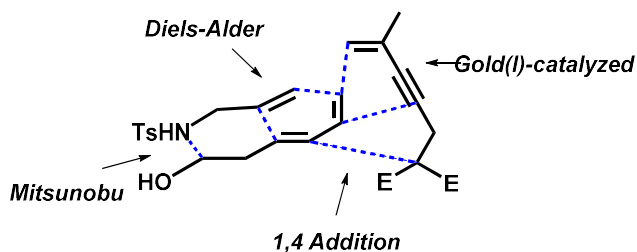


Figure 3.6 - Strategic disconnections of (±)-magellanine synthesis

3.5 References

- [52] a) K. C. Nicolaou, D. Vourloumis, N. Winssinger, P. S. Baran, *Angew. Chem. Int. Ed.* **2000**, *39*, 44-122; b) P. A. Wender, V. A. Verma, T. J. Paxton, T. H. Pillow, *Acc. Chem. Res.* **2008**, *41*, 40-49; c) T. Newhouse, P. S. Baran, R. W. Hoffmann, *Chem. Soc. Rev.* **2009**, *38*, 3010-3021; d) P. A. Wender, B. L. Miller, *Nature*, **2009**, *460*, 197-201; e) N. Z. Burns, P. S. Baran, R. W. Hoffmann, *Angew. Chem. Int. Ed.* **2009**, *48*, 2854-2867; f) I. S. Young, P. S. Baran, *Nat. Chem.* **2009**, *1*, 193-205; g) T. Gaich, P. S. Baran, *J. Org. Chem.* **2010**, *75*, 4657-4673; h) T. Newhouse, P. S. Baran, *Angew. Chem. Int. Ed.* **2011**, *50*, 3362-3374; i) W. R. Gutekunst, P. S. Baran, *Chem. Soc. Rev.* **2011**, *40*, 1976-1991; j) T. Brückl, R. D. Baxter, Y. Ishihara, P. S. Baran, *Acc. Chem. Res.* **2012**, *45*, 826-839; k) C. A. Kuttruff, M. D. Eastgate, P. S. Baran, *Nat. Prod. Rep.* **2014**, *31*, 419-432.
- [53] a) C. Aubert, L. Fensterbank, P. Garcia, M. Malacria, A. Simonneau, *Chem. Rev.* **2011**, *111*, 1954-1993; b) N. Krause, C. Winter, *Chem. Rev.* **2011**, *111*, 1994-2009; c) M. Rudolph, A. S. K. Hashmi, *Chem. Commun.* **2011**, *47*, 6536-6544; d) M. Rudolph, A. S. K. Hashmi, *Chem. Soc. Rev.* **2012**, *41*, 2448-2462; e) C. Obradors, A. M. Echavarren, *Acc. Chem. Res.* **2014**, *47*, 902-912; f) Y. Zhang, T. Luo, Z. Yang, *Nat. Prod. Rep.* **2014**, *31*, 489-503; g) L. Fensterbank, M. Malacria, *Acc. Chem. Res.* **2014**, *47*, 953-965; h) A. Fürstner, *Acc. Chem. Res.* **2014**, *47*, 925-938; i) R. Dorel, A. M. Echavarren, *Chem. Rev.* **2015**, *115*, 9028-9072.
- [54] P. Wessig, G. Müller, *Chem. Rev.*, **2008**, *108*, 2051-2063.

- [55] For Pd(0)-catalyzed DDA between enyne and yne, see: a) S. Saito, M. M. Salter, V. Gevorgyan, N. Tsuboya, K. Tando, Y. Yamamoto, *J. Am. Chem. Soc.* **1996**, *118*, 3970-3971; b) M. Rubin, A. W. Sromek, V. Gevorgian, *Synlett* **2003**, 2265-2291; with gold(I), see: c) J. Barluenga, M. A. Fernández-Rodríguez, P. García-García, E. Aguilar, *J. Am. Chem. Soc.* **2008**, *130*, 2764-2765.
- [56] a) C. Nieto-Oberhuber, S. López, A. M. Echavarren, *J. Am. Chem. Soc.* **2005**, *127*, 6178-6179; b) C. Nieto-Oberhuber, P. Pérez-Galán, E. Herrero-Gómez, T. Lauterbach, C. Rodríguez, S. López, C. Bour, A. Rosellón, D. J. Cárdenas, A. M. Echavarren, *J. Am. Chem. Soc.* **2008**, *130*, 269-279; c) N. Delpont, I. Escofet, P. Pérez-Galán, D. Spiegl, M. Raducan, C. Bour, R. Sinisi, A. Echavarren, *Catal. Sci. Technol.* **2013**, *3*, 3007-3012.
- [57] N. Mézailles, L. Ricard, F. Gagosz, *Org. Lett.*, **2005**, *19*, 4133-4136.
- [58] M.-C. P. Yeh, W.-C. Tsao, B.-J. Lee, T.-L. Lin, *Organometallics*, **2008**, *20*, 5326-5332.
- [59] C.M. Chao, M. R. Vital, P.Y. Toullec, J.-P. Genêt, V. Michelet, *Chem. Eur. J.*, **2009**, *15*, 1319-1323.
- [60] M. Morin, P. Levesque, L. Barriault, *Beilstein, J. Org. Chem.*, **2013**, *9*, 2625-2628.
- [61] a) G. Brochure, J. Polonsky, *J. Bull. Soc. Chim. Fr.*, **1960**, 963-966; b) T. Roncal, S. Corbodobés, U. Ugald, Y. He, O. Sterner, *Tetrahedron Lett.*, **2002**, *43*, 6799-6802; c) I. Kubo, F.J. Hanke, Y. Asaka, T. Matsumoto, C. H. He, J. Clarky, *Tetrahedron*, **1990**, *46*, 1515-1522, d) R. Laville, C. Castel, J.-J. Filippi, C. Delbecque, A. Audran, P.-P. Garry, L. Legendre, X. Fernandez, *J. Nat. Prod.*, **2012**, *75*, 121-126; e) A. D. Rodriguez, C. Ramirez, I. Rodriguez, C. L. Barnes, *J. Org. Chem.* **2000**, *65*, 1390-1398; f) X.-J. Wang, G.-J. Zhuang, Y. Zhang, S.-S. Yu, X.-Q. Bao, D. Zhang, Y.-H. Yuan, N.-H. Chen, S.-G. Ma, J. Qu, Y. Li, *Org. Lett.*, **2012**, *14*, 2614-2617; g) T. Amagata, M. Doi, T. Tohgo, K. Minaura, A. Numata, *Chem. Commun.*, **1999**, 1321-1322.
- [62] Genneviève Bétournay, Master thesis, *University of Ottawa*, **2012**.
- [63] a) A. Cope, D. Ambros, E. Cigamek, C. F. Howell, Z. Jacura, *J. Am. Chem. Soc.*, **1960**, *82*, 1750; b) K. Mlinaric-Majerski, M. Vinkovic, J. L. Fry, *J. Org. Chem.*, **1994**, *59*, 664-667.
- [64] a) M. Castillo, G. Morales, L. A. Loyola, *Can. J. Chem.* **1975**, *53*, 2513-2514; b) M. Castillo, G. Morales, L. A. Loyola, *Can. J. Chem.*, **1976**, *54*, 2900-2908; c) M. Castillo, L. A. Loyola, G. Morales, I. Singh, C. Calvo, H. L. Holland, D. B. MacLean, *Can. J. Chem.* **1976**, *54*, 2893-2899; d) L. A. Loyola, G. Morales, M. Castillo, *Phytochemistry*, **1979**, *18*, 1721-1723.
- [65] G. C. Hirst, T. O. Kohnson. L. E. Overman, *J. Am. Chem. Soc.*, **1993**, *115*, 2992-2993.
- [66] J. P. Williams, D. R. St. Laurent, D. Frieddrich, E. Pinard, B. A. Roden, L. A. Paquette, *J. Am. Chem. Soc.*, **1994**, *116*, 4689-4696.
- [67] C.-F. Yen, C.-C. Liao, *Angew. Chem. Int. Ed.*, **2002**, *41*, 4090-4093.

- [68] M. Ishizaki, Y. Niimi, O. Hoshino, H. Hara, T. Takahashi, *Tetrahedron*, **2005**, *61*, 4053-4065.
- [69] T. Kozaka, N. Miyakoshi, C. Mukai, *J. Org. Chem.*, **2007**, *72*, 10147-10154.
- [70] S.-Z. Jiang, T. Lei, K. Wei, Y.-R. Yang, *Org. Lett.*, **2014**, *16*, 5612-5615.
- [71] K.-W. Lin, B. Anathan, S.-F. Tseng, T.-H. Yan, *Org. Lett.*, **2015**, *17*, 3938-3940.
- [72] C.-K. Sha, F.-K. Lee, C.-J. Chang, *J. Am. Chem. Soc.* **1999**, *121*, 9875-9876.
- [73] M. T. Crimmins, P. S. Watson, *Tetrahedron Lett.*, **1993**, *34*, 199-202.
- [74] D. A. Sandgham, A. I. Meyers, *J. Chem. Soc., Chem. Commun.*, **1995**, 2511-2512.
- [75] G. Mehta, M. Sreenivasa, A. Thomas, *Tetrahedron*, **1998**, *54*, 7865-7882.
- [76] R. A. Murphy, R. Sarpong, *Org. Lett.*, **2012**, *14*, 632-635.
- [77] S. F. Martin, S. A. Williamson, R. P. Gist, K. M. Smith, *J. Org. Chem.*, **1983**, *45*, 5170-5180.
- [78] E. M. Stang, M. C. White, *J. Am. Chem. Soc.*, **2011**, *133*, 14892-14985.
- [79] T. Tsunoda, H. Kaku, S. Ito, 'New Mitsunobu reagents', *TCIMAIL*, **2005**, #123
- [80] a) T. G. Back, J. W. Payne, *Org. Lett.*, **1999**, *1*, 663-665; b) J. Barluenga, S. Lopez, J. Florez, *Angew. Chem. Int. Ed.*, **2003**, *42*, 231-233; c) A. G. Ross, X. Li, S. J. Danishefsky, *J. Am. Chem. Soc.*, **2012**, *134*, 16080-16084; d) J.-C. Han, L.-Z. Liu, Y.-Y. Chang, G.-Z. Yue, J. Guo, L.-Y. Zhou, C.-C. Li, Z. Zhang, *J. Org. Chem.*, **2013**, *78*, 5492-5504; e) D. I. Saavedra, B. D. Rencher, D.-H. Kwon, S. J. Smith, D. H. Ess, M. B. Andrus, *J. Org. Chem.*, **2018**, *82*, 2018-2026.
- [81] D. H. R. Barton, S. D. Géro, P. Holliday, B. Quiclet-Sire, S. Z. Zard, *Tetrahedron*, **1998**, *54*, 6751-6756.
- [82] S. F. Martin, C. W. Clark, J. W. Crobett, *J. Org. Chem.*, **1995**, *60*, 3236-3242.
- [83] J.-I. Matsuo, D. Iida, H. Yamanaka, T. Mukaiyama, *Tetrahedron*, **2003**, *59*, 6739-6750

CHAPTER 4

Towards the total synthesis of salvinorin A

4.1 Introduction

Salvinorin A was isolated and named in 1982 by Alfredo Ortega from the *Salvia divinorum* plant.⁸⁴ The chemical structure of the natural product was determined using a combination of spectroscopic analysis and was shown to contain a bicyclic diterpene core (*Figure 4.1*). In 1983, independent studies by Valdés reported the isolation of analogues from the same plant which were named divinorin A and divinorin B.⁸⁵ The naming was latter changed to salvinorin A and B,⁸⁶ respectively. Salvinorin C was also isolated from the same group in 2001.⁸⁷ Many other variants of these diterpenes were reported and to date, 9 different salvinorins have been identified.⁸⁸ Salvinorin A possesses a highly oxidized and condensed molecular framework. The *trans*-neoclerodane diterpenoid have seven stereogenic centers where two of them are quaternary.

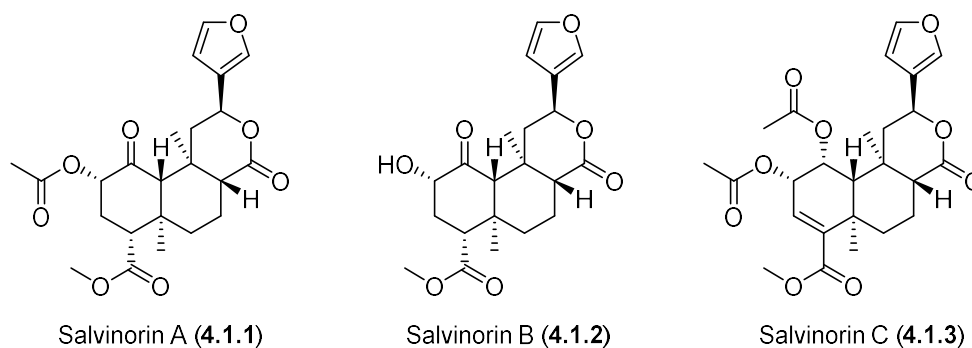
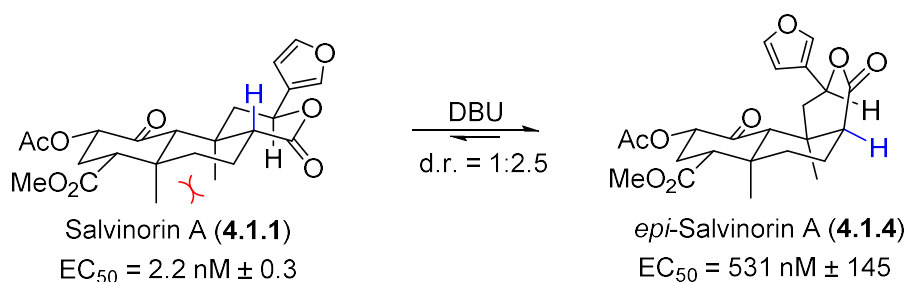


Figure 4.1 - Structure of salvinorin A-C

4.1.1 Structural features and biological properties

It was found by Bégin and co-workers that salvinorin A possesses a very sensitive epimerizable center (*Scheme 4.1*).⁸⁹ Once treated with a strong base, such as DBU, the *trans*-lactone under goes epimerization to form the more thermodynamically stable *cis*-lactone with a 2.5:1 ratio.⁹⁰ Due to the strong 1,3-diaxial repulsion between the two axial methyl groups, the *epi*-salvinorin A is favored and unfortunately, lacks biological activity. This undesirable conversion has to be taken into consideration for synthetic preparation of the active ingredient.



Scheme 4.1 - Epimerization of salvinorin A

Salvia divinorum plant was formerly used as an entheogen by indigenous Mazatec shamans in Mexico.⁹¹ Salvinorin A was found to be the active ingredient amongst all the other salvinorins biosynthesized by the plant and is responsible for the dissociative hallucinogenic side effect. At this time, it is the most potent naturally occurring hallucinogen.⁹² This *trans*-neoclerodane diterpenoid is the first non-alkaloid compound reported to be a kappa opioid receptor agonist. In contrast with morphine which acts on delta opioid receptors, kappa opioid receptors are not associated with physical dependence side effects. Salvinorin A is highly specific to kappa receptor ($EC_{50} = 2.2 \text{ nM}$) with a very low affinity for delta ($EC_{50} = >10\,000 \text{ nM}$) and mu opioid receptors ($EC_{50} = 2860 \text{ nM}$).⁹³ It is importance to note that *epi*-salvinorin A ($EC_{50} = 531 \text{ nM}$)⁸⁹ and de-

acetylated analogue salvinorin B ($EC_{50} = 371 \text{ nM}$)⁹⁴ are devoid of high affinity for the kappa opioid receptors. Therefore, deacetylation or epimerization under physiological conditions completely neutralize the biological activity of Salvinorin A, which explains the short duration of action of the ingredient (2-20 minutes).⁹⁵ Because of the latter bioactivity, salvinorin A is a promising lead for the therapeutic treatment of CNS disorders, including depression, pain, and drug addiction.⁹⁶

4.1.2 Structure-affinity relationship (SAR)

Extensive studies achieved the understanding of how salvinorin A was binding to kappa opioid receptors. A wide variety of single-point mutant and chimeric opioid receptors were prepared to evaluate and localize the ligand-binding site of this unique lipophilic KOPr agonist. Several different hypotheses based on the mutagenesis approach and molecular-modeling were reported.⁹⁷ In 2012, a more refined model for the salvinorin A binding-site interactions were proposed (*Figure 4.2*).⁹⁸ It was observed that the C315, T111 and Y313 motif are crucial to maintain high affinity to **4.1.1**. In addition, exposure of KOPr to an analogue possessing a thiocyanate group rather than a 2-acetoxy moiety produces irreversible binding of the C315.

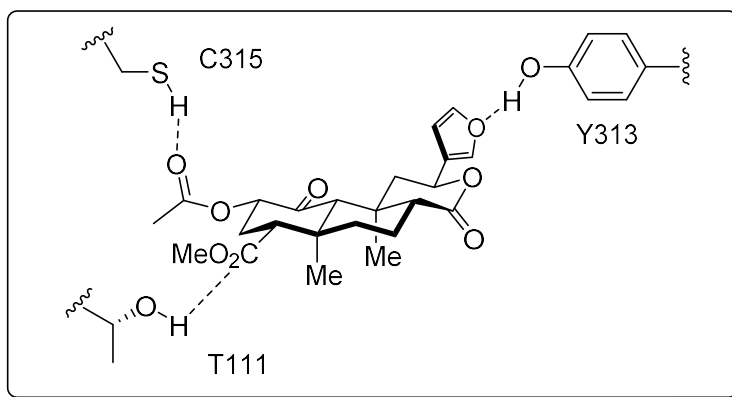


Figure 4.2 - Salvinorin A proposed binding site

Several synthetic analogues of salvinorin A were prepared using a semi-synthesis approach to further understand and optimize the biological activity.⁹⁹ Structural modifications were limited to the accessible functional groups such as the 2-position acetoxy group, the 4-position carbomethoxy group, the 17-position carbonyl and the furan ring. Although, interesting observations were made and are summarized in *Figure 4.3*.

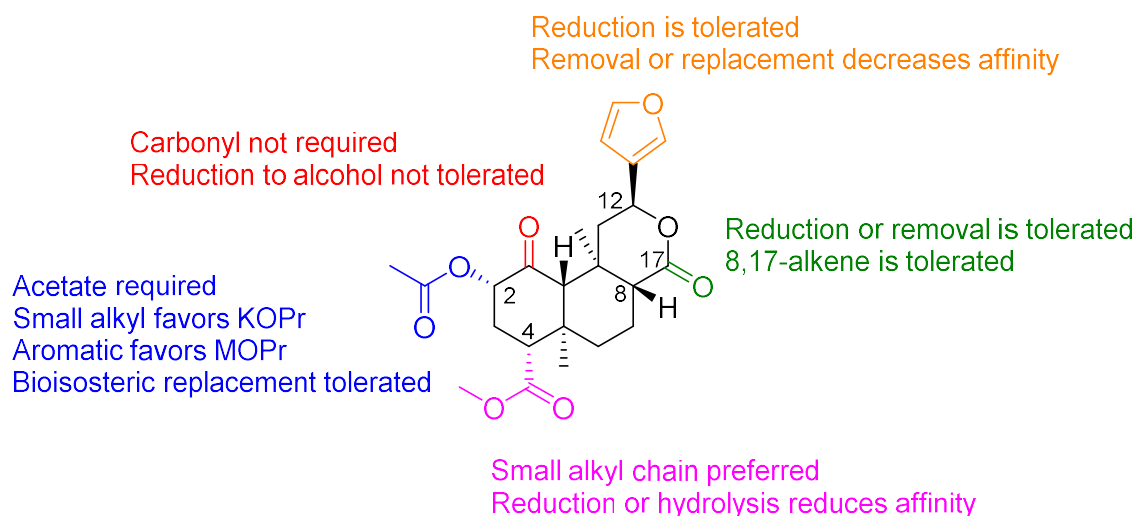


Figure 4.3 – Structural modification tolerance from the structure-activity relationship

Many efforts were made in order to identify a more potent kappa opioid receptor agonist. During these works, two other potent ingredients were identified with interesting analgesic properties (*Figure 4.4*), 2-mexothymethyl salvinorin B (**4.1.5**, MOM-Sal B) and 22-thiocyanatosalvinorin A (**4.1.6**, RB-64). MOM-sal B was identified to possess a longer lasting duration of action and to be five-fold more potent with an EC_{50} of 0.6 nM.¹⁰⁰ On the other hand, RB-64 exhibited irreversible binding to the kappa-opioid receptor.¹⁰¹

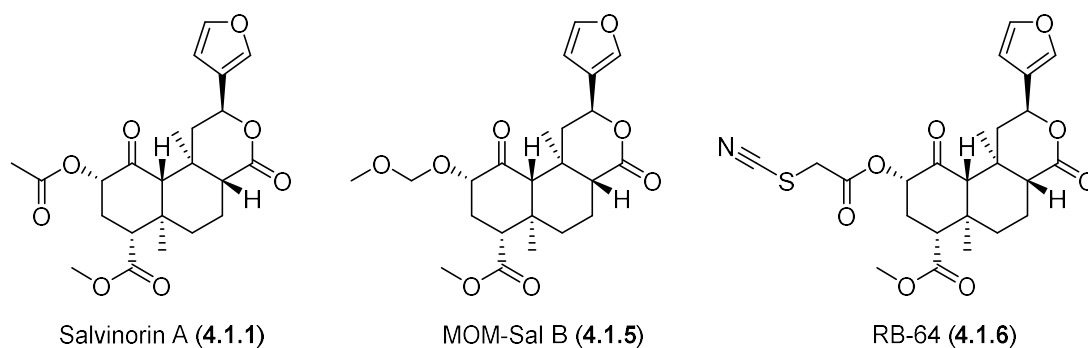
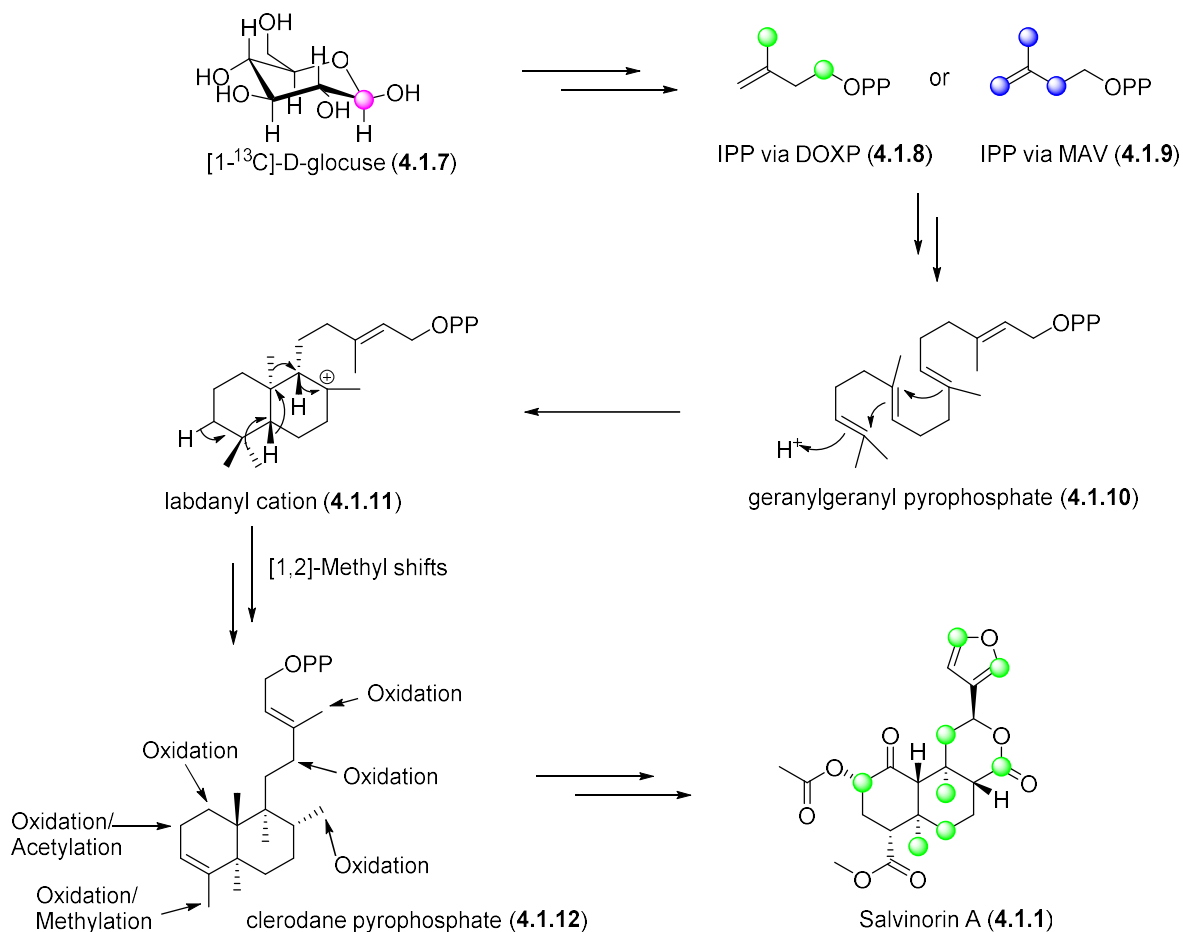


Figure 4.4 - Structure comparison of salvinorin A with MOM-Sal B and RB-64

4.1.3 Biosynthesis

NMR and mass spectroscopy analysis of the incorporated radio labelled [1- ^{13}C]-D-glucose **4.1.7** to the plant tissue revealed the biogenic origins of salvinorin A (*Scheme 4.2*).¹⁰² It was hypothesized that the biosynthesis of salvinorin A could go through two different pathways; the 1-deoxy-D-xylulose-5-phosphate pathway (DOXP) or the mevalonate pathway (MAV). In 2007, Zjamiony developed a method for the *in vitro* tissue culture of *Salvia divinorum* in order to efficiently incorporate **4.1.7**. The radio labelled isopentenyl pyrophosphate (IPP) **4.1.8** or **4.1.9** would then be generated from **4.1.7** via the DOXP (*green labelled*) or the MAV (*blue labelled*) pathway, respectively. The ^{13}C enriched IPP **4.1.8** or **4.1.9** (5 carbon unit) will produce geranylgeranyl pyrophosphate (GGPP) **4.1.10** (20 carbon unit). A diterpene synthase produces a labdanyl cation **4.1.11** from GGPP **4.1.10**, which is subsequently rearranged. A sequence of 1,2-hydride and methyl shifts from **4.1.11** forms the clerodienyl intermediate **4.1.12**. Oxygenation, acylation, and methylation reactions are then required to produce salvinorin A (**4.1.1**). NMR and mass spectroscopy analysis of the incubated leaf extract with the ^{13}C enriched glucose demonstrated the incorporation of IPP originated from the DOXP pathway rather than the classic mevalonate pathway.

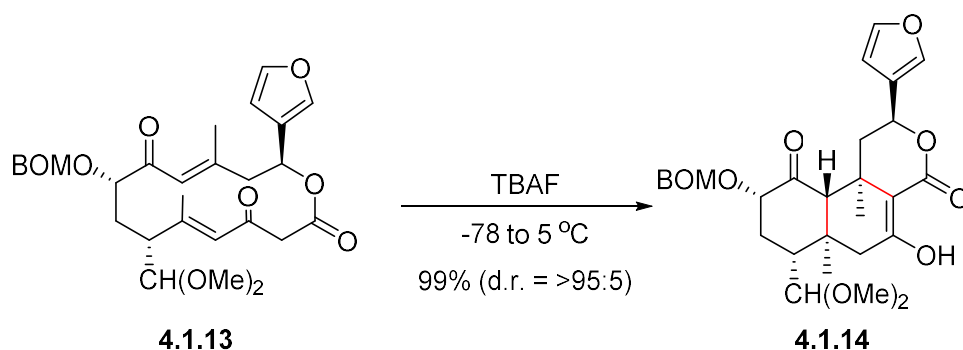


Scheme 4.2 - Simplified biosynthetic pathway for salvinorin A

4.1.4 Previous synthetic approaches

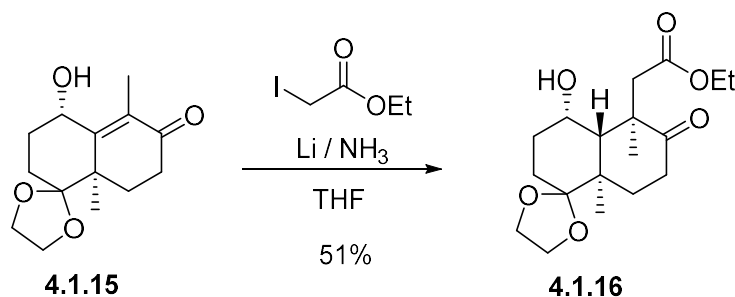
Despite the wide variety of analogues synthesized via a semi-synthetic approach, it provides a limited array of structural modification. The development of readily diversifiable synthetic routes to salvinorins are in need for the preparation of novel functionalized analogues that cannot be derived from the natural product. In 2007, Evans and co-workers accomplished the first enantioselective total synthesis of salvinorin A (*Scheme 4.3*).⁹⁰ The tricyclic core of this KOPr agonist was prepared by a transannular Michael reaction cascade of the bisenone **4.1.13**. Treatment of **4.1.13** with TBAF afforded the tricyclic scaffold **4.1.14** as a single diastereomer in quantitative

yield. Further reduction of the enol and functional group manipulation afforded 8-*epi*-salvinorin A **4.1.4** as the major adduct, which appears to be predominant under kinetic and thermodynamic control. Nonetheless, the total synthesis required 29 steps to afford enantiomerically pure salvinorin A.



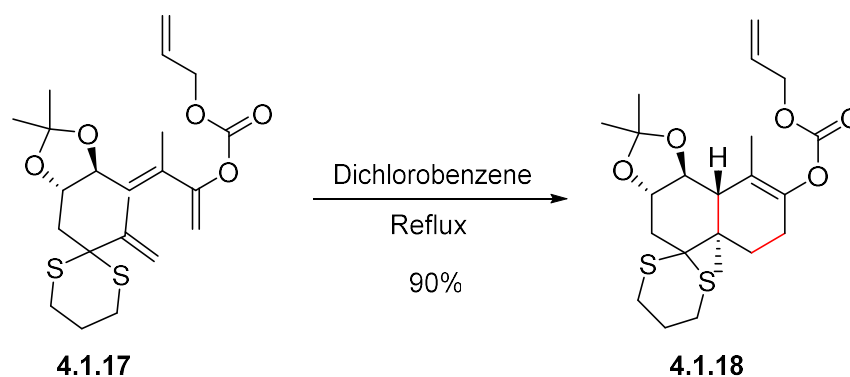
Scheme 4.3 – Synthesis of salvinorin A by Evans

From the fairly advanced Wieland-Miescher ketone derivative, Hagiwara was able to complete the total synthesis of salvinorin A.¹⁰³ A selective hydroxylation produced **4.1.15** which was carried on for the synthesis (*Scheme 4.4*). Reductive alkylation of the enone **4.1.15** in liquid ammonia afforded the substituted decalin **4.1.16**. Following by a series of other transformations involving protection and deprotection at many stages afforded salvinorin A. A revised synthetic approach was reported a year later where synthesis was accomplished in 18 steps.¹⁰⁴



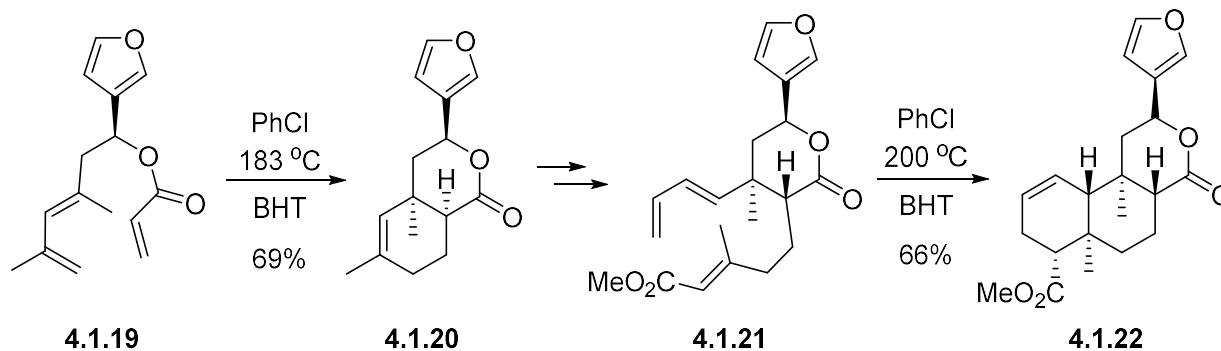
Scheme 4.4 - Synthesis of salvinorin A by Hagiwara

Forsyth and co-workers took advantage of the practical intramolecular Diels-Alder reaction (IMDA) for the construction of the 6-6 fused bicyclic system (*Scheme 4.5*).¹⁰⁵ The *exo*-selective IMDA of **4.1.17** occurred in refluxing dichlorobenzene and led to **4.1.18** in 90% isolated yield. During their synthetic investigation they also faced an epimerization issue at the C-8 position, as previously reported by Evans. However, a short racemic synthesis was achieved in 18 steps.



Scheme 4.5 - Synthesis of salvinorin A by Forsyth

More recently, Metz have used a different disconnection strategy by using two intramolecular Diels-Alder (IMDA) reactions for the construction of the tricyclic framework (*Scheme 4.6*).¹⁰⁶ The first key transformation involves the diastereoselective formation of the *endo*-cycloadduct **4.1.20** by heating **4.1.19** in chlorobenzene. The second intramolecular Diels-Alder cycloaddition of intermediate **4.1.21** took place in similar reaction conditions, affording the salvinorin-like compound **4.1.22** as the major diastereomer. The latter was converted to the natural product along with *epi*-salvinorin A **4.1.4**. Using this approach, salvinorin A was assembled in 18 steps, which constitutes one the shortest routes to the natural product.



Scheme 4.6 - Synthesis of salvinorin A by Metz

Other synthetic analogues of the salvinorins were prepared using different strategic bond disconnections and led to several compounds that maintain strong KOPr agonism.¹⁰⁷

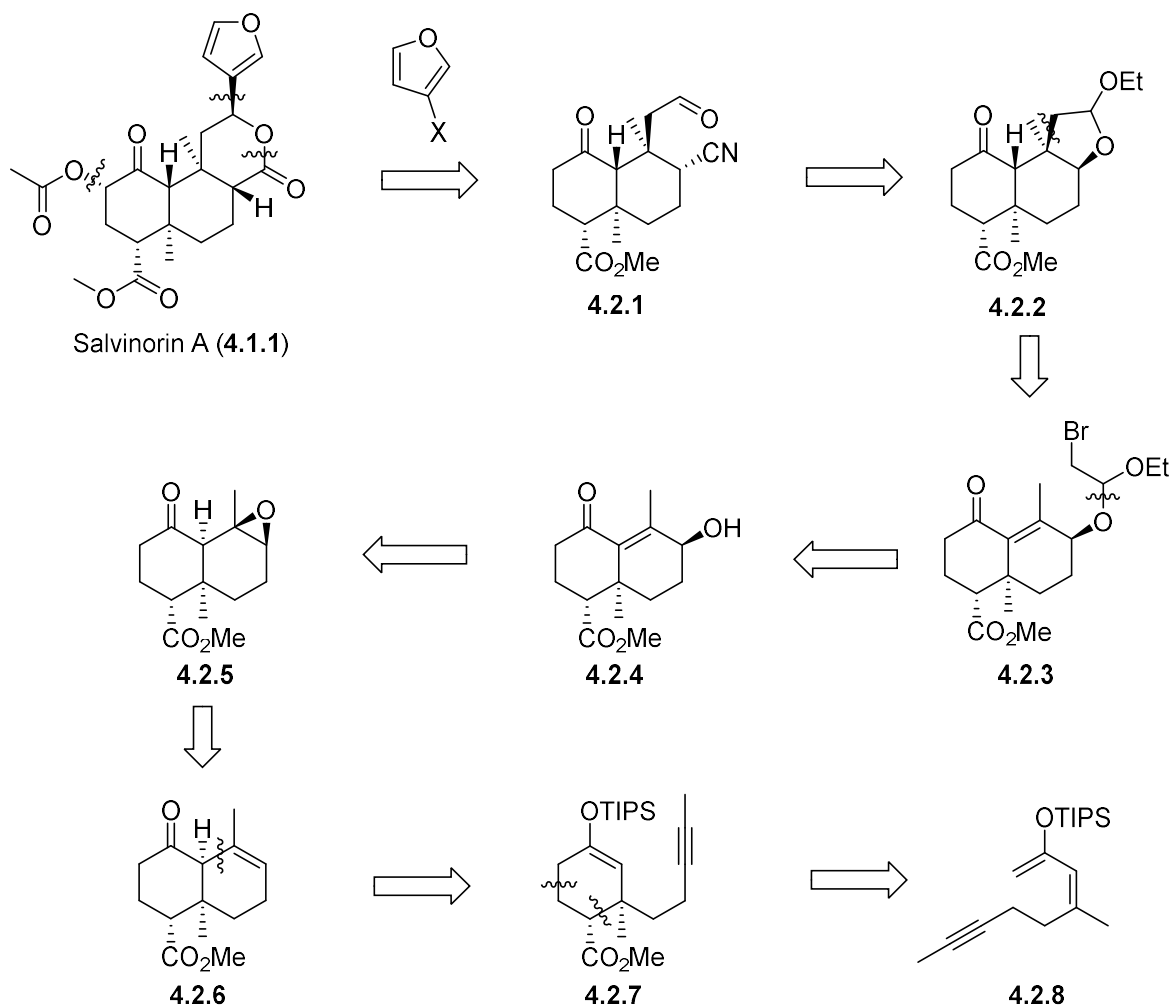
4.2 Progress towards salvinorin A

Despite the fact that many total syntheses of salvinorin A were accomplished, they all suffer from obtaining *epi*-salvinorin A as a by product of the synthesis which is a consequence of establishing the C-8 stereocenter at a late stage. We thought we could use a different approach and set the stereochemistry at a much earlier stage in the synthesis. In order to afford a new synthetic approach, we revised an existing methodology that was developed in our laboratory.

4.2.1 Retrosynthetic analysis

Owing to the facile epimerization at C-8 (*cf.* Scheme 4.1), the lactone moiety on **4.1.1** would be installed at a late stage by the cyclization of an alkoxide onto the nitrile **4.2.1** (Scheme 4.7). One can imagine that the aldehyde group on **4.2.1** would come from the opening of the lactol

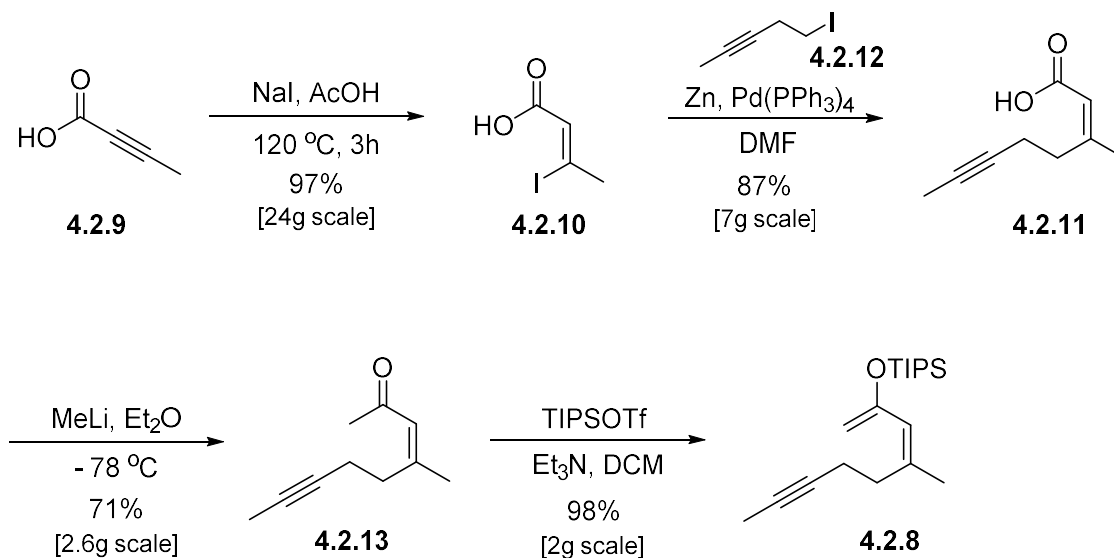
4.2.2. The latter would be obtained through a light-enabling radical cyclization using dimeric gold(I) complexes. The bromoacetal **4.2.3** would arise from acetalization of the secondary alcohol **4.2.4**, which would be the result of an epoxide opening. Using a selective *6-endo-dig* carbocyclization that we developed with a monomeric gold(I) Lewis acid catalyst, **4.2.6** would originate from the silyl enol ether **4.2.7**. Finally, cyclic silyl enol ether **4.2.7** would be the result of an intermolecular Diels-Alder reaction (IMDA) between diene **4.2.8** and methyl acrylate.



Scheme 4.7 - Retrosynthetic analysis of salvinorin A

4.2.2 Synthesis of the diene and Diels-Alder cycloaddition

The preparation of the diene **4.2.8** started with 2-butynoic acid **4.2.9** which, upon treatment with sodium iodide in acetic acid, generated the compound **4.2.10** in near quantitative yield without purification (*Scheme 4.8*).¹⁰⁸ Optimization of the Negishi-type coupling led to the substituted alkene **4.2.11** in 85% yield. The organozinc reagent from the iodo alkyne **4.2.12** was formed with zinc dust and both were used in excess in order to quench the acid proton of **4.2.10**, where the remaining zincate undergoes transmetalation with a palladium species. Exclusive formation of the *Z*-alkene was observed in dimethylformamide.¹⁰⁹ The ketone **4.2.13** was obtained from the carboxylic acid **4.2.11** with an excess amount of methyl lithium in diethyl ether. Silyl enol ether formation with triisopropyl silyl triflate was performed and afforded **4.2.8** in 98% yield. All these chemical transformations were carried out on multi-gram scale.

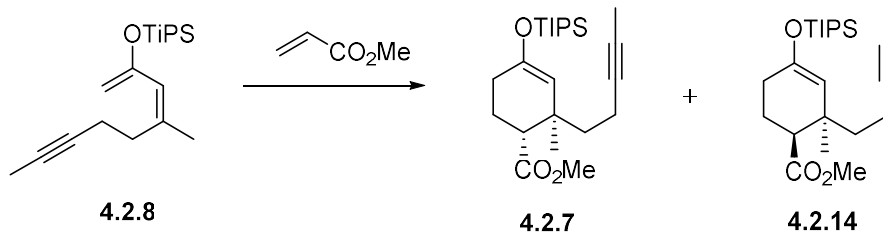


Scheme 4.8 - Synthesis of the diene 4.2.8

With the diene **4.2.8** in hand, we were ready to investigate the intermolecular Diels-Alder reaction with methyl acrylate (*Table 4.1*). At first glance no conversion was observed using

thermal conditions (*entries 1 and 2*). On the other hand, addition of ethylaluminum sesquichloride led to complete conversion and good regioselectivity, but lacked diastereoselectivity (*entries 3 and 4*). We were satisfied to observe the exclusive formation of the *endo*-cycloadduct **4.2.7** using a substoichiometric amount of diethyl aluminum chloride (*entry 5*). Increasing the equivalence of the Lewis acid had a beneficial effect on the yield of the transformation (*entry 6 and 7*). It is important to note that scaling up the reaction had a negative impact on the diastereomeric ratio of the cycloadducts and on the conversion of starting material **4.2.8**. We eventually observed that trace amounts of water was necessary for the reaction to proceed. Using non-distilled (not dry) solvent and no flame-dried glassware led to reproducible results on larger scale. However, the active catalyst species remains unknown.

Table 4.1 - Optimization of the Diels-Alder cycloaddition

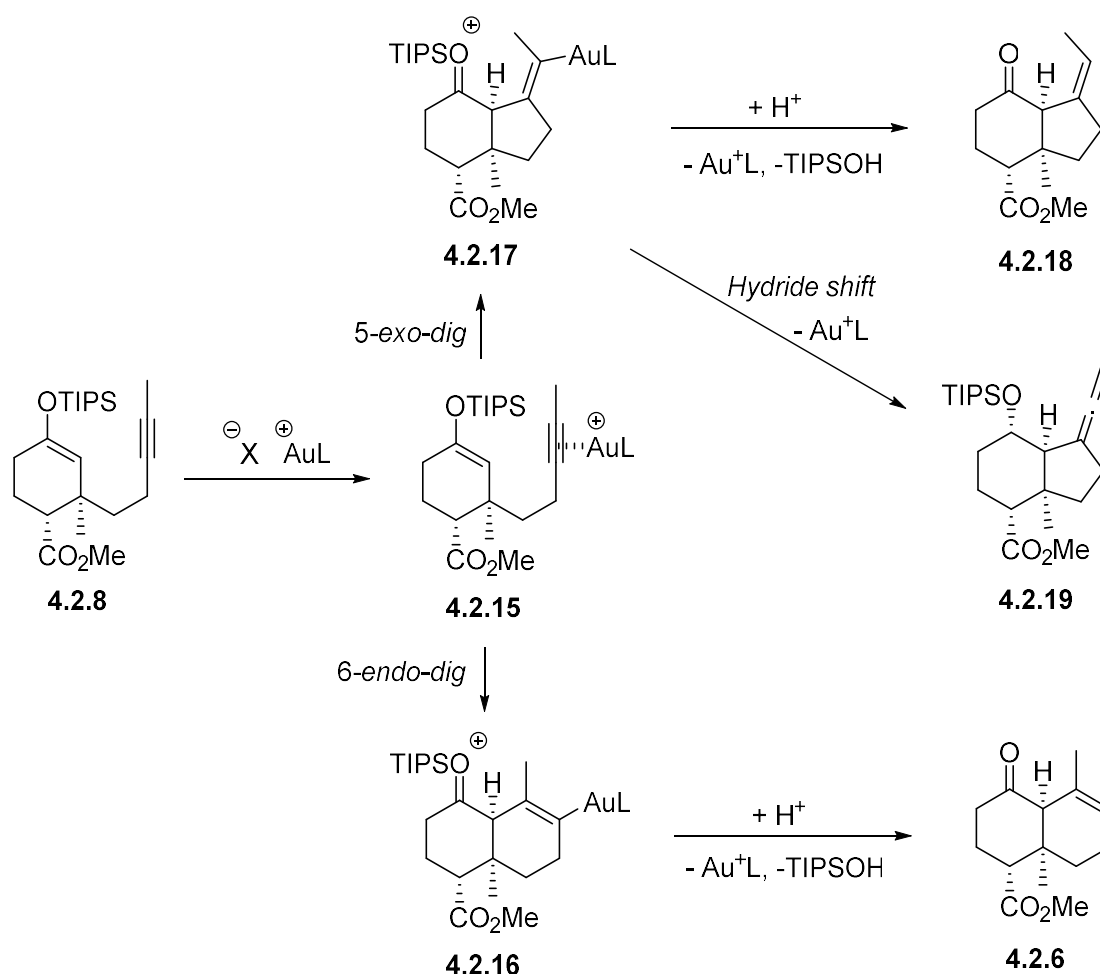


Entry	Lewis Acid	Solvent	Temperature	Conversion ^[a]	Ratio (4.2.7 : 4.2.14)
1	-	DCE	100 °C	0%	N/A
2	-	Toluene	140 °C	0%	N/A
3	Et ₂ AlCl-EtAlCl ₂ (0.2 equiv.)	DCM	-78 to 0 °C	>98%	1.1 : 1
4	Et ₂ AlCl-EtAlCl ₂ (0.2 equiv.)	DCM	-40 °C	>98%	1.1 : 1
5	Et ₂ AlCl (0.2 equiv.)	DCM	-78 to 0 °C	21%	> 20 : 1
6	Et ₂ AlCl (0.6 equiv.)	DCM	-78 to 0 °C	45%	> 20 : 1
7	Et ₂ AlCl (1.2 equiv.)	DCM	-78 to 0 °C	85% (81%) ^[b]	> 20 : 1

[a] = Mesitylene was used as the internal standard, [b] = Isolated yield of **4.2.7**

4.2.3 Decalin formation via a 6-endo-dig gold(I)-catalyzed carbocyclization

Based on previous observations and expertise with gold(I) catalysis, we were aware of some possible side products that could arise from the carbocyclization of **4.2.8** (Scheme 4.9). Ideally, the silyl enol ether would undergo the 6-endo-dig cyclization via **4.2.15** which would generate **4.2.6** after protodeauration of the intermediate **4.2.16**. Alternatively, the activated complex **4.2.15** could lead to the 5-exo-dig vinyl gold **4.2.17** which would produce **4.2.18**. Moreover, a competitive hydride shift could occur with **4.2.17** leading to the allene **4.2.19**.



Scheme 4.9 - Possible products from **4.2.8**

Using ligand **L6** adorned on the gold(I) centre, known to catalyze regioselectivity 6-*endo-dig* carbocyclization,¹¹⁰ a mixture of **4.2.19**, **4.2.18** and **4.2.6** was obtained (Table 4.2). A solvent optimization was performed and the 6-*endo* product **4.2.6** was favored in most cases. We observed that acetone and halogenated solvents provided a slightly superior selectivity for this transformation (entries 5-8). Using a mixture of DCM:acetone was even better at an optimal solvent ratio of 20:1 (entries 9-11).

Table 4.2 - Solvent optimization of the gold-catalyzed carbocyclization

Reaction scheme showing the carbocyclization of compound **4.2.8** to products **4.2.19**, **4.2.18**, and **4.2.6**. The reaction is catalyzed by **[L6AuNCMe]SbF₆** (10 mol%) in various solvents.

Structure of **4.2.8**: A cyclohexene derivative with an OTIPS group, a CO₂Me group, and an ethynyl group.

Structure of **L6**: A phosphine ligand with a central phosphorus atom bonded to two *t*Bu groups and two *i*Pr groups on a benzene ring.

Structure of **4.2.19**: A bicyclic product with a TIPS group, a CO₂Me group, and an ethynyl group.

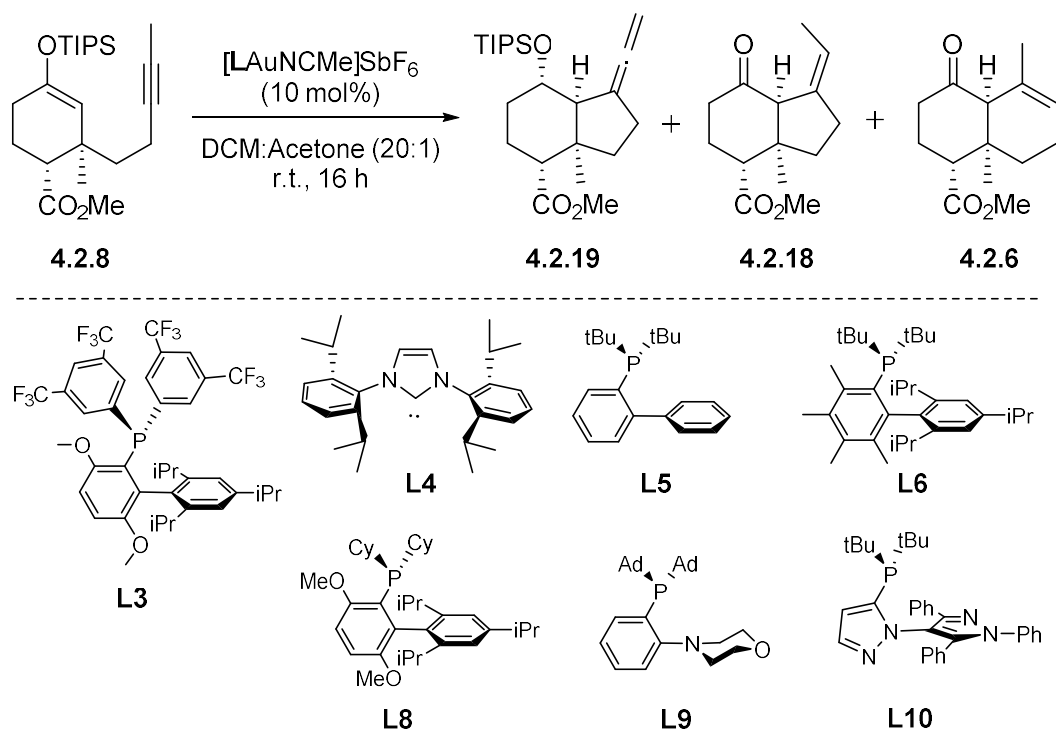
Structure of **4.2.18**: A bicyclic product with a CO₂Me group and an ethynyl group.

Structure of **4.2.6**: A bicyclic product with a CO₂Me group and an ethynyl group.

Entry	Solvent	Ratio (4.2.19 : 4.2.18 : 4.2.6)
1	Toluene	13 : 47 : 40
2	MeNO ₂	36 : 22 : 42
3	MeCN	16 : 42 : 42
4	DMF	0 : 56 : 44
5	DCE	54 : 0 : 46
6	CHCl ₃	8 : 43 : 49
7	DCM	52 : 0 : 48
8	Acetone	0 : 40 : 60
9	DCM:Acetone (50:1)	22 : 14 : 64
10	DCM:Acetone (20:1)	19 : 14 : 67
11	DCM:acetone (5:1)	11 : 31 : 58

According to our previous study, we found that **L6** was generally the best ligand to use for such regioselective reactions. In some cases, specific substrates were falling out of the trend so we decided to explore more gold(I) complexes to further increase the formation of the desired 6-*endo* adduct **4.2.6** (Table 4.3).

Table 4.3 - Ligand optimization



Entry	Ligand	Conversion ^[a]	Product Ratio (4.2.19 : 4.2.18 : 4.2.6)
1	L4	>98%	0 : 45 : 55
2	L3	79%	0 : 33 : 57
3	L8	>98%	5 : 30 : 65
4	L6	>98%	19 : 14 : 67
5	L11	>98%	5 : 27 : 68
6	L9	>98%	9 : 20 : 69
7	L10	39%	0 : 27 : 73
8	L5	>98% (76%) ^[b]	2 : 18 : 80

[a] Mesitylene was used as an internal standard. [b] Isolated yield of **4.2.6**

We rapidly noticed that **L4**, **L3** and **L8** were not optimal for the formation of **4.2.6** (*entries 1–3*). Interestingly, **L11** and **L9** gave a better ratio towards the desired decalin **4.2.6** (*entries 5 and 6*). **L10** was more selective with a ratio of 0:27:73 favoring the cycloadduct **4.2.6** but suffered from poor conversion. Surprisingly the best ligand for this transformation was **L5** which is not consistent with our previous findings (*entry 8*). We hypothesized that this transformation is more substrate specific than we would have imagined. Nonetheless, careful column purification of the reaction mixture led to the isolation of **4.2.6** in 76% yield from two grams of the silyl enol ether **4.2.8**.

4.2.4 Enone functionalization

Moving forward in the synthesis, the alkene **4.2.8** was ready to be submitted under epoxidation reaction conditions (*Table 4.4*).

Table 4.4 - Epoxidation of **4.2.8**

Entry	Reagent	Solvent	Ratio (4.2.20 : 4.2.5)
1	<i>m</i> -CPBA	EtOAc	1 : 1
2	<i>m</i> -CPBA	Et ₂ O	1 : 1.2
3	<i>m</i> -CPBA	DCM	1 : 1.8
4	<i>m</i> -CPBA, NaHCO ₃	DCM	1 : 1.9
5	Oxone, Acetone	DCM	2 : 1
6	Formic Acid, H ₂ O ₂	DCM	1 : 5 (81%) ^[a]

[a] = Isolated yield of **4.2.5** on 2.5 gram scale

The challenge of this transformation resides in the selective epoxidation of the more hindered concave face of **4.2.8**. We first observed that with *m*-CPBA reagent, the epoxide was obtained with a ~1:1 to 1:2 mixture of **4.2.20** and **4.2.5** (*entries 1-4*). This result was a complete surprise for us. Based on literature precedent and typically with *cis*-decalin substrates,¹¹¹ we had expected a better selectivity where the major product **4.2.20** would have originated from an epoxidation on the most accessible face of the molecule. Other reagents were then examined. Due to the short half-life of dimethyldioxirane (DMDO),¹¹² we opted for an *in-situ* formation of the reagent using a combination of oxone and acetone which slightly favored the formation of the epoxide **4.2.20** (*entry 5*). The best condition was a mixture of formic acid and hydrogen peroxide for the *in-situ* preparation of performic acid.¹¹³ The epoxide **4.2.5** was isolated on a gram scale with 81% yield (*entry 6*). The structure was also confirmed by x-ray crystallography. These results were surprising and did not follow the expected trend according to bulkiness of the epoxidizing reagent. Due to the peroxyacid reagents which favor the reactivity at the more hindered concave face, one can hypothesize that the carbonyl at the β -position of the alkene could act as a directing group for the epoxidation reaction (*Figure 4.5*). Therefore, we propose that the peroxyacid can add on the carbonyl of **4.2.8** to form the intermediate **4.2.21** which would lead to the desired product **4.2.5**. Alternatively, hydrogen bonding of the acid with the ketone could explain the observed selectivity, as shown by the complex **4.2.22**. This type of ketone-directed epoxidation was firstly reported by Armstrong and Wood in 1994.¹¹⁴

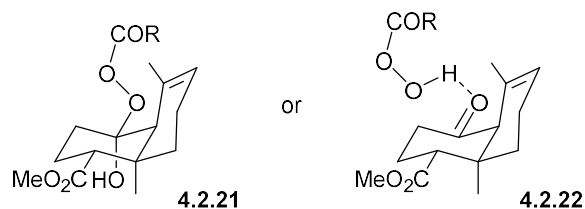
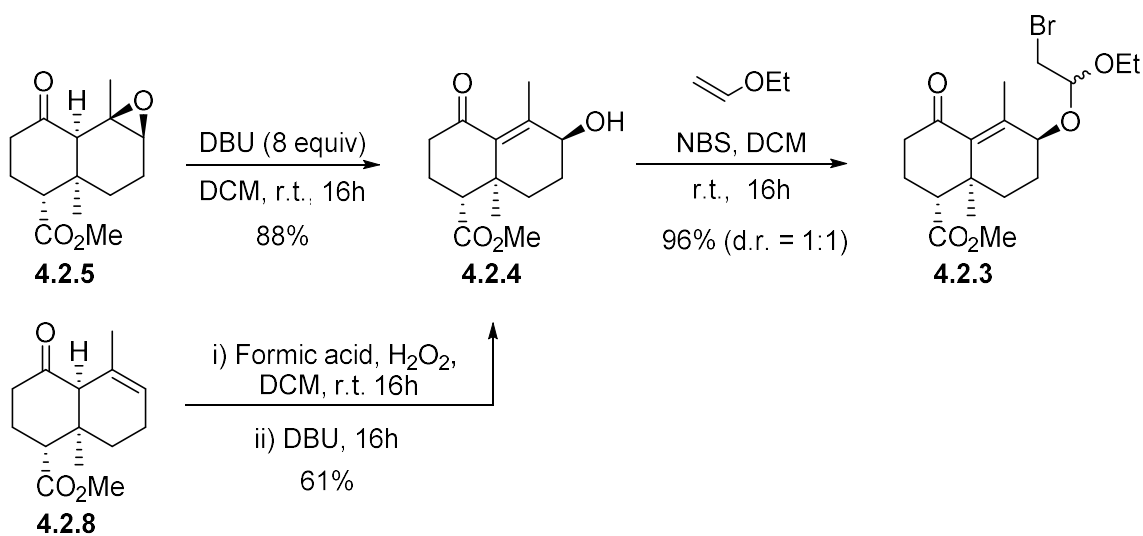


Figure 4.5 - Proposed complexes for the selective epoxidation

Taking advantage of this result, we pursued the synthesis using epoxide **4.2.5**. The latter was then opened using DBU yielding the allylic alcohol **4.2.4** in 88% (*Scheme 4.10*). The secondary alcohol could also be prepared in one step from the alkene **4.2.8** by sequential addition of formic acid/H₂O₂ and DBU. This "one pot" transformation afforded the desired enone **4.2.4** in 61% yield. Upon treatment with NBS and vinyl ethyl ether, the α -bromo acetal **4.2.3** was isolated in 96% yield as a 1:1 mixture of inseparable diastereomers.

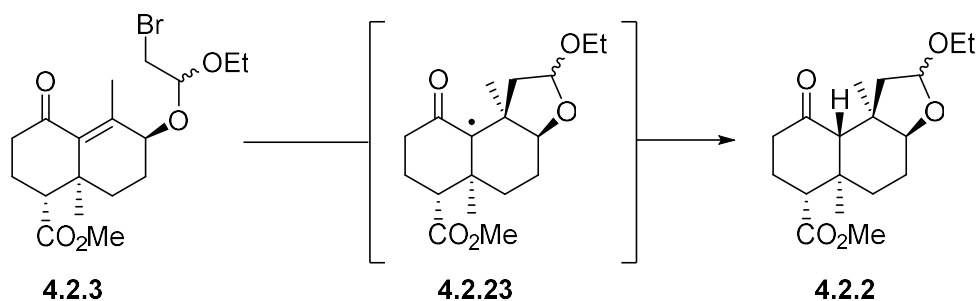


*Scheme 4.10 - Preparation of the α -bromo acetal **4.2.3***

We took advantage of the alcohol stereochemistry aimed at directing the radical cyclization of the bromo acetal on the top face of the enone **4.2.3**. This 5-*exo-trig* cyclization would set the quaternary center with the proper configuration. For this transformation, we first investigated a more conventional approach using AIBN as the radical initiator in combination with Bu₃SnH, which plays the role of hydrogen donor and enables the chain propagation reaction (*entry 1, Table 4.5*). The reaction went to full conversion and the cyclic acetal **4.2.2** was isolated in 85% yield as a 1:1 mixture of diastereomers at the acetal position. Notably, the *trans*-decalin was formed

selectively due to the thermodynamic stability of the *trans*-ring junction in combination with the hydrogen atom abstraction of **4.2.23** via the less hindered face. This transformation lacks practicality since AIBN and the Bu₃SnH had to be separately added via a syringe pump over one hour to a refluxing mixture of the starting material **4.2.3** in benzene. Moreover, the usage of stoichiometric amount of Bu₃SnH is not environmentally friendly. We decided to carry out photoredox gold(I)-catalyzed processes, recently developed in our laboratory (*cf. Chapter 1*). The reagents were simply dissolved in pre-degassed acetonitrile and the mixture was irradiated with 365 nm LEDs. The desired tricycle **4.2.2** was isolated in 87% yield using 7.5 mol% of the dimeric gold(I) catalyst (*entry 3*). In this transformation, diisopropylethylamine (DIPEA) plays the roles of hydrogen donor as well as sacrificial reductant to turnover the photoredox catalyst.

Table 4.5 - Optimization of the radical cyclization

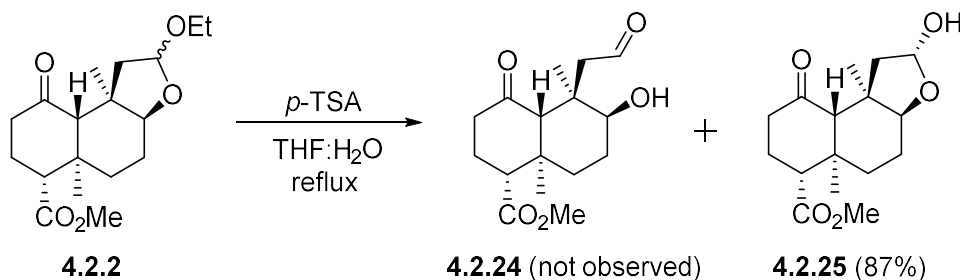


Entry	Conditions	Solvent	Activation	Conversion
1	AIBN, Bu ₃ SnH	Benzene	80 °C	100% (85%) ^[a]
2	[Au ₂ (dppm) ₂]Cl ₂ (5 mol %), DIPEA	MeCN	365 LED	95%
3	[Au ₂ (dppm) ₂]Cl ₂ (7.5 mol%), DIPEA	MeCN	365 LED	100% (87%) ^[a]

[a] = Isolated yield of **4.2.2** as a mixture of diastereomer (1:1)

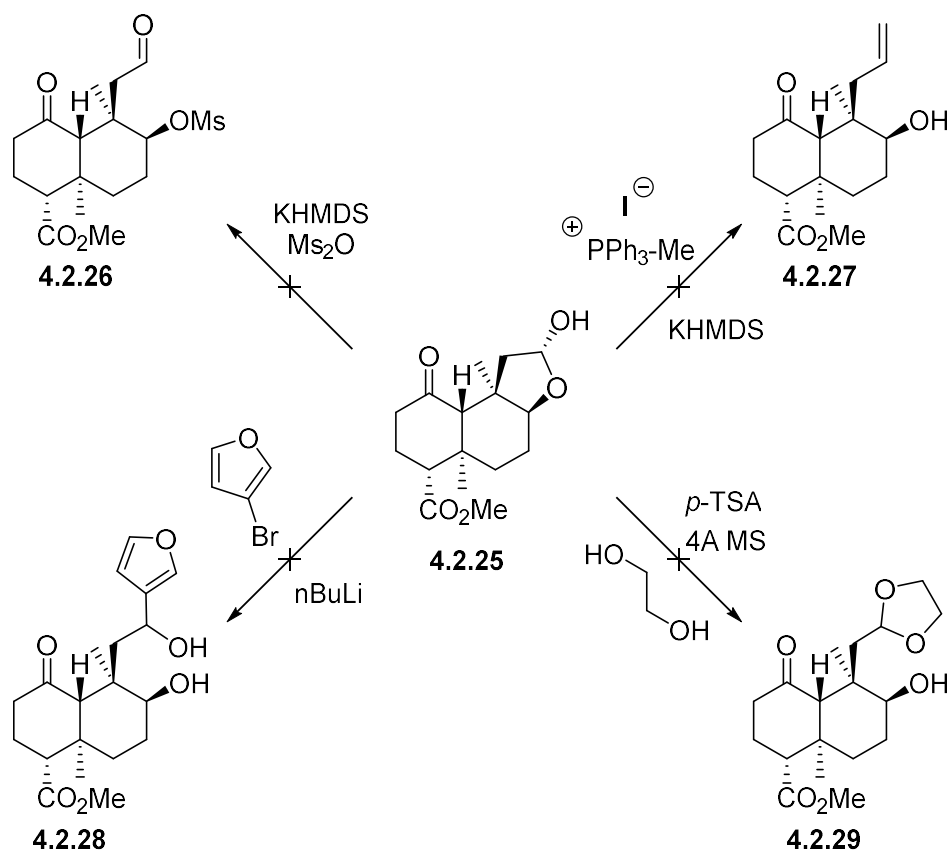
4.2.5 Exploring the reactivity of the acetal / lactol

Four stereocenters are now established on **4.2.2** but the furan and the lactone moiety remain to be installed. One can imagine that the acetal **4.2.2** in presence of water and protic acid would generate the corresponding 1,4-hydroxyaldehyde **4.2.24** (*Scheme 4.11*). Unfortunately, the desired compound **4.2.24** could not be obtained using a wide variety of acids in combination with different solvents. The lactol **4.2.25** was the major adduct from those transformations and isolated in 87% yield with no trace of the aldehyde **4.2.24** using *p*-TSA in refluxing THF:H₂O. 1,4 and 1,5-hydroxyaldehyde are known to be in equilibrium with the closed lactol form, usually favoring the more thermodynamically stable cyclic structure.¹¹⁵



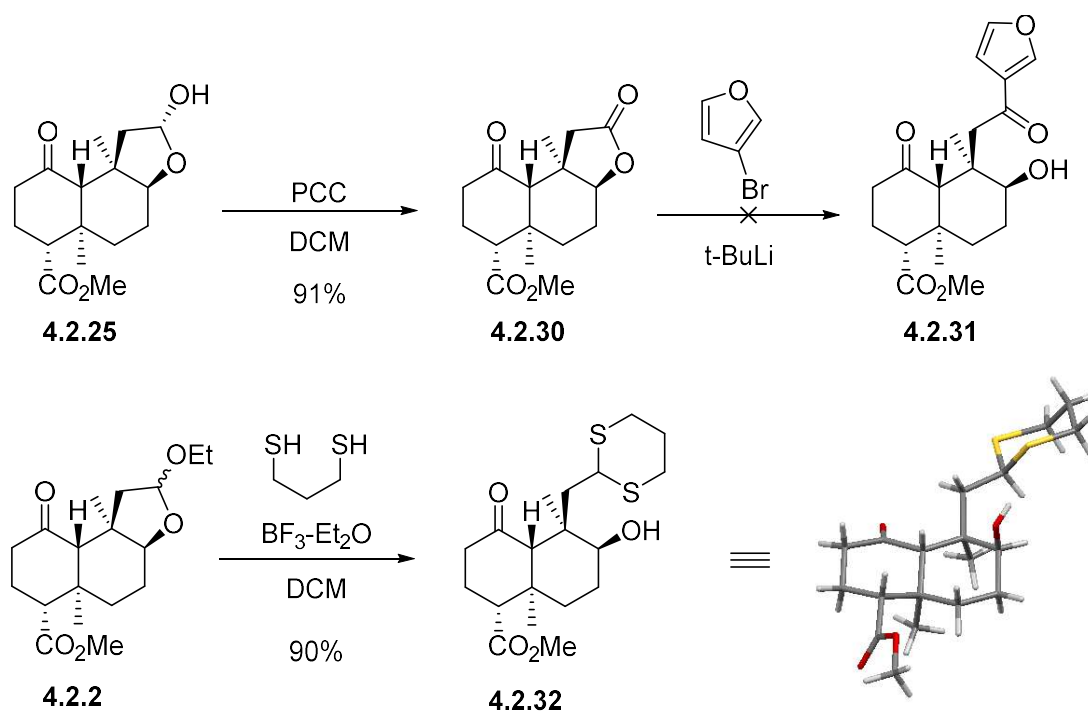
Scheme 4.11 - Lactol vs 1,4-hydroxyaldehyde

It was previously reported that in many cases, the minor 1,4-hydroxyaldehyde (in equilibrium with the lactol) can be converted to the desired product using irreversible transformations.¹¹⁶ As shown in *Scheme 4.12*, we examined a few chemical transformations to trap the aldehyde **4.2.24**. All attempts to intercept the presumably existent 1,4-hydroxyaldehyde **4.2.24** failed. Formation of a leaving group (**4.2.26**), Wittig reaction (**4.2.27**), nucleophilic addition (**4.2.28**) or trans-acetalization (**4.2.29**) were unsuccessful to afford any of the desired products.



Scheme 4.12 - Attempts to trap the opened lactol 4.2.25

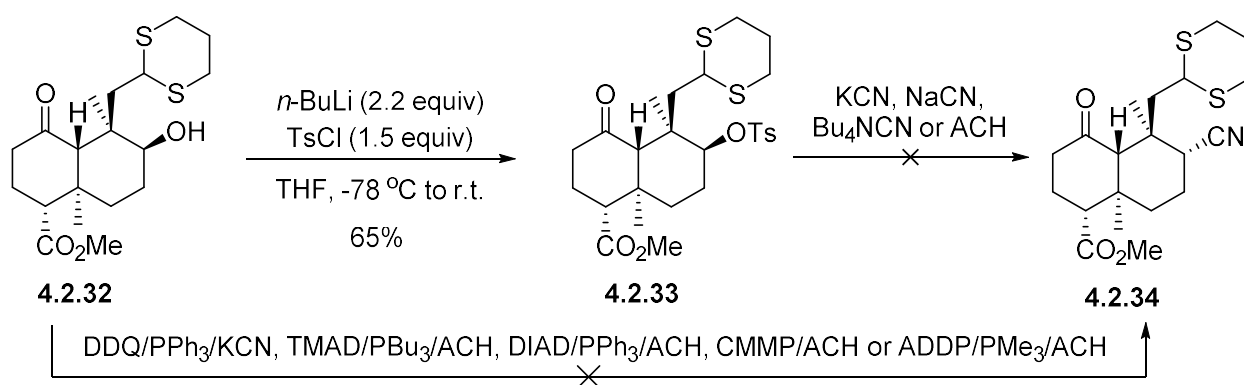
Although, we were successful in obtaining the oxidized **4.2.25** from PCC to form the lactone **4.2.30** in 91% yield (*Scheme 4.13*). We tackled a chemoselective addition of the 3-bromofuran on **4.2.30**, and being out of luck, our trials led to a complex mixture of products. We were satisfied to succeed in the formation of a dithiane **4.2.32** from the cyclic acetal **4.2.2**. With a stoichiometric amount of boron trifluoride and 1,3-propanedithiol, the secondary alcohol was finally accessible on **4.2.32**, which was isolated in 90% yield. The stereochemistry was confirmed by X-ray crystallography.



Scheme 4.13 - Successful transformations from 4.2.25 or 4.2.2

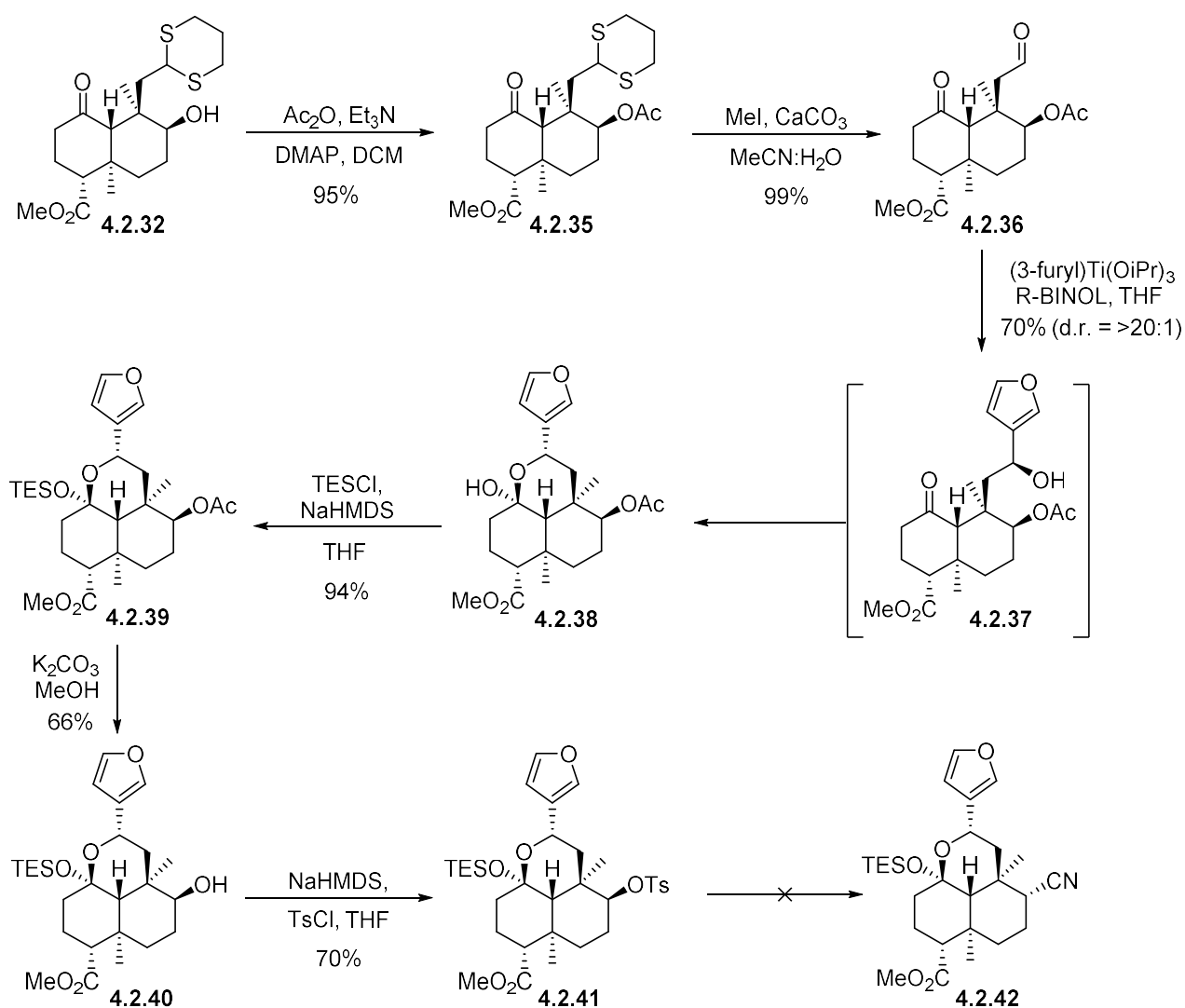
4.2.6 En route towards the synthesis of salvinorin A

We opted to continue the synthesis from the dithioacetal **4.2.32** since the secondary alcohol is now exposed for derivatization. Forming a leaving group from the alcohol was not an easy task. After screening various reagents, we identified that deprotonation with *n*-BuLi was necessary to form the tosylated compound **4.2.33** in 65% yield (*Scheme 4.14*). It is important to note that we have never been able to obtain the mesylate or triflate using classical reaction conditions. From **4.2.33**, we then tried to install the nitrile by a substitution reaction with KCN, NaCN, Bu₄N⁺CN⁻, and acetone cyanohydrin (ACH). None of these reactions led to the desired intermediate **4.2.34**. Only starting material or the elimination product was observed from those attempts. Moreover, Mitsunobu type reaction conditions¹¹⁷ were attempted to directly convert **4.2.32** into **4.2.34** but failed.



Scheme 4.14 - Attempts to form a nitrile at the C-8 position

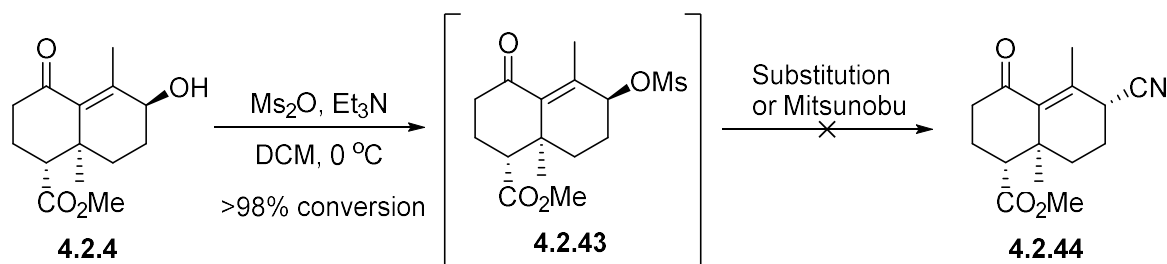
We hypothesized that the dithioacetal was interfering with the transformation by being too hindered to allow the substitution of **4.2.33**. Therefore, we investigated another route in which the dithiane would not be present during the substitution and hopefully installing the nitrile successfully. Alternatively, an acetyl group could be installed on **4.2.32** in 95% yield using acetic anhydride and triethylamine (*Scheme 4.15*). The dithiane was easily removed in quantitative yield using methyl iodide and calcium carbonate to finally reveal the aldehyde **4.2.36**. The furan moiety was installed using a protocol developed by Sibi¹¹⁸ and modified by Forsyth,¹⁰⁵ to afford the diastereomerically pure lactol **4.2.38** in 70% yield via **4.2.37**. The resulting quaternary alcohol was protected with TESCl followed by removal of the acetate group to give compound **4.2.40** in 66% isolated yield. Tosylation with NaHMDS gave the intermediate **4.2.41** which was then ready to be substituted by a nitrile source. Much to our chagrin, the nucleophilic substitution on **4.2.41** did not lead the desired product **4.2.42**; only starting material was recovered. All attempts to force the reaction under thermal conditions resulted in the elimination of the tosyl group.



Scheme 4.15 - Incorporation of the furan moiety and attempt to install the nitrile

The last few steps from **4.2.32** (Scheme 4.15) were not optimal in terms of the required amount of chemical transformations since it possesses many protection/deprotection steps. We obviously encountered the same issues of substitution on the secondary alcohol. Presumably the quaternary center next to the alcohol was problematic and makes the substitution a very challenging step.

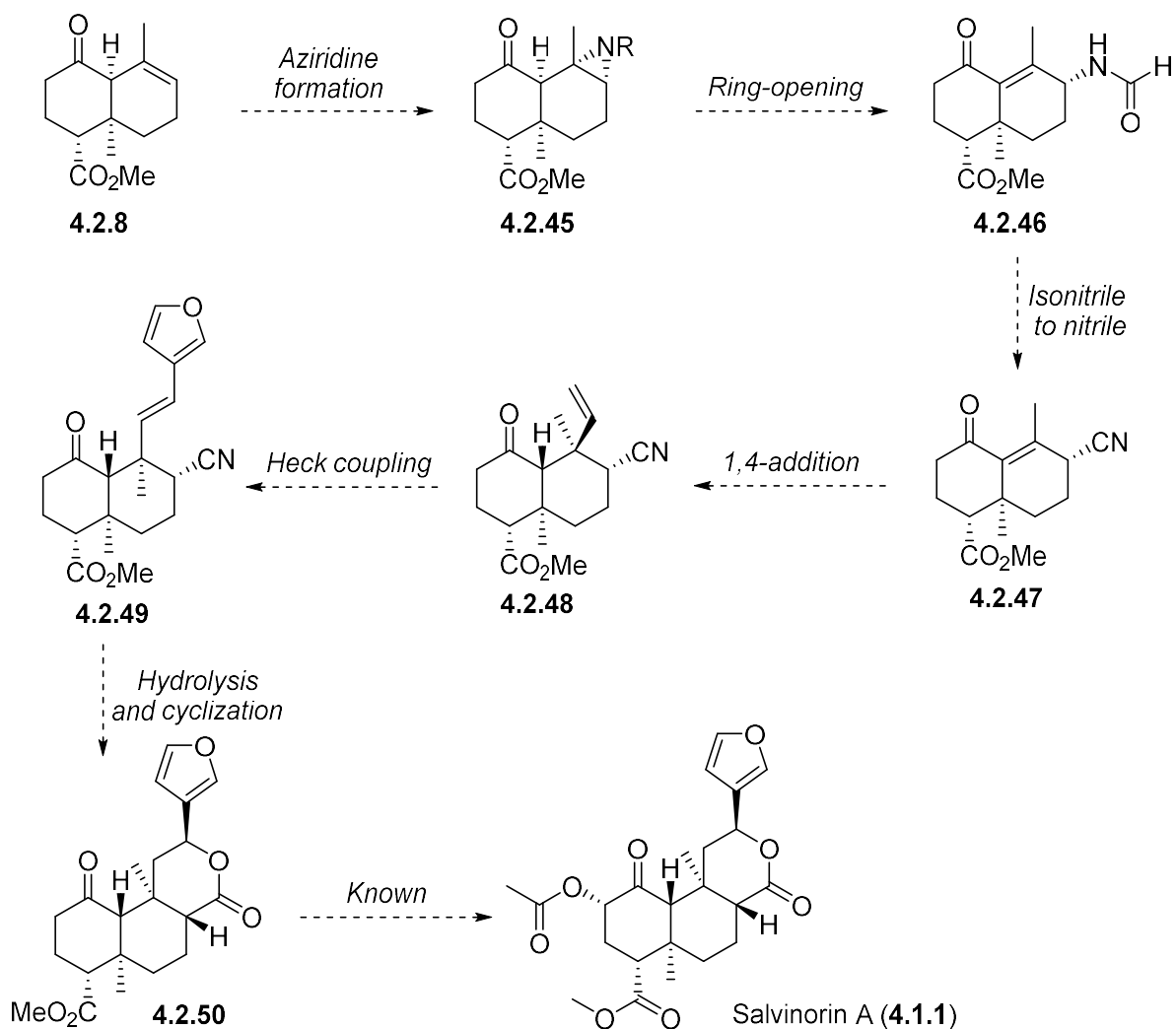
We attempted to substitute the alcohol at an earlier stage during the synthesis (*Scheme 4.16*). The enone **4.2.4** was treated with methanesulfonic anhydride and led to **4.2.43** in full conversion. The crude reaction mixture was used for the subsequent substitution reaction due to degradation on silica gel of the mesylate **4.2.43**. Unfortunately, similar problems were observed as previously described. The compound **4.2.43** was either eliminating or degrading using various reaction conditions for the substitution. We hypothesized that the elimination was favored due to the conjugated alkenes formed.



*Scheme 4.16 - Substitution from the enone **4.2.4***

4.3 Future work

The formation of the nitrile at the C-8 was problematic in all the pathways investigated. As a future work, the nitrogen will be installed at an earlier stage (*Scheme 4.17*). From the decalin **4.2.8**, aziridination¹¹⁹ of the alkene could be performed rather than epoxidation in order to generate **4.2.45**. Opening of the aziridine **4.2.45** could be accomplished similarly to the epoxide and would result in the formation of the formate **4.2.46**. From there, an isonitrile could be generated and rearranged to the nitrile **4.2.47**.¹²⁰ 1,4-Addition of a vinyl group onto the enone **4.2.47** would arise to the intermediate **4.2.48**.

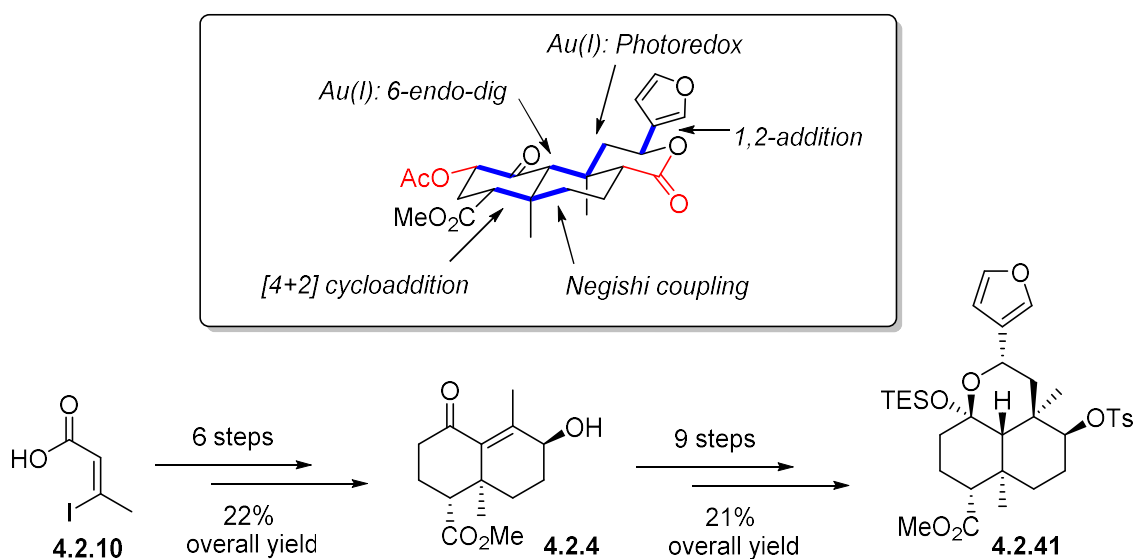


Scheme 4.17 - Alternative preparation of salvinorin A

Analogous to the work of Shenvi,^{107c} a Heck type reaction could be performed to install the furan moiety **4.2.49**. Hydrolysis of the nitrile **4.2.49** under acidic conditions could also catalyse the Markovnikov-type cyclization to produce the lactone **4.2.50**. The tricycle **4.2.50** has been prepared by Higawara¹⁰³ and elaboration of this route would be a formal synthetic approach towards salvinorin A **4.1.1**. It requires three steps to install the *O*-acetyl group but we believe it could be potentially accomplished in one step using $\text{Mn}(\text{OAc})_3$.¹²¹

4.4 Conclusion

In conclusion, we demonstrated the efficiency of Diels-Alder cycloaddition and the gold(I)-catalyzed 6-*endo-dig* carbocyclization for the formation of the decalin framework. Photoredox catalysis with gold(I) dimers was also proven to be useful for the construction of the C-9 quaternary center. Key disconnections of the salvinorin A skeleton are highlighted in *Scheme 4.18* illustrating the remaining bonds to construct in red.



Scheme 4.18 – Summary of the current approach

The decalin **4.2.4** was efficiently prepared in 22% overall yield from the commercially available (*Z*)-3-iodobut-2-enoic acid **4.2.10**. Five constructive bonds were made during these six steps. On the other hand, it required nine steps for the synthesis of the intermediate **4.2.41**, where only three constructive bonds were formed. More research is underway for the completion of the natural product. The proposed route in section 4.3 *Future work* will be investigated and could potentially result in the synthesis of salvinorin A in only 12 steps. We are enthusiastic and confident to finish this synthetic approach and to publish our work in broad readership journal.

4.5 References

- [84] A. Ortega, *J. Chem. Soc. Perkin. Trans.*, **1982**, *1*, 2505-2508.
- [85] L.J. Valdes III, *PhD thesis*, **1983**, University of Michigan.
- [86] L.J. Valdes III, W. M. Butler, G. M. Hatfield, A. G. Paul, M. Koreeda, *J. Org. Chem.*, **1984**, *49*, 4716-4720.
- [87] L.J. Valdes III, H.-M. Chang, D. C Visger, M. Koreeda, *Org. Lett.*, **2001**, *3*, 3935-3937
- [88] a) T. A. Munro, M. A. Rizzacasa, *J. Nat. Prod.*, **2003**, *66*, 703-705; b) D. Y. W. Lee, Z. Ma, L.-Y. Liu-Chen, Y. Wang, Y. Chen, W. A. Carlezon, B. Cohen, *Bioorg. Med. Chem.*, **2005**, *13*, 5635-5639; c) O. Shiota, K. Nagamuatsu, S. Sekita, *J. Nat. Prod.*, **2006**, *69*, 1782-1786; d) Z. Ma, D. Y. W. Lee, *Tetrahedron Letters*, **2007**, *48*, 5461-5464; e) L. M. Kutrzebra, D. Ferreira, J. K. Zjawiony, *J. Nat. Prod.*, **2009**, *72*, 1361-1363.
- [89] C. Bégin, M. R. Richards, J.-G. Li, Y. Wang, W. Xu, L.Y. Liu-Chen, W. A. Carlezon, B. M. Cohen, *Bioorg. Med. Chem. Lett.*, **2006**, *16*, 4679-1685.
- [90] J. R. Scheerer, J. F. Lawrence, G. C. Wangm D. A. Evans, *J. Am. Chem. Soc.*, **2007**, *129*, 8968-8969.
- [91] J. M. Watt. 'Plants in the development of modern medecin', *Harvard university press*, **1972**, *67*
- [92] B.L. Roth, K. Baner, R. Westkaeemper, D. Siebert, K.C. Rice, S. Steinberg, P Ernsberger, R.B. Rothman, *Proc. Natl. Acad. Scie. U.S.A.*, **2002**, *18*, 11934-11939.
- [93] A. Lozama, C. W. Cunningham, M. J. Caspers, J. T. Douglas, C. M. Dersch, R. B. Rothman, T. E. Prisinzano, *J. Nat. Prod.*, **2011**, *74*, 718-726.
- [94] C. Bégin, M. R. Richards, Y. Wang, Y. Chen, L.-Y. Liu-Chen, Z. Ma, D. Y. W. Lee, W. A. Carlezon, B. Cohen, *Med. Chem. Lett.*, **2005**, *15*, 2761-2765.
- [95] a) M. W. Johnson, K. A. Maclean, C. J. Reissig, T. E. Prisinzano, R. R. Griffiths, *Drug. Alcohol. Depend.*, **2011**, *115*, 150-155; b) K. A. Maclean, M. W. Johnson, C. J. Reissig, T. E. Prisinzano, R.R. Griffiths, *Psychopharmacology*, **2013**, *226*, 381-391.
- [96] a) J. O. Fajemiroye, P. R. Prabhakar, C. L. da Cunha, E. A. Costa, J. K. Zjawiony, *Eur. J. Pharmacol.*, **2017**, *800*, 96-106; b) K. Paton, N. Kumar, S. R. Crowley, J. L. Harper, T. E. Prisinzano, B. M. Kivell, *Eur. J. Pain*, **2017**, *21*, 1039-1050; c) U. Coffen, A. Canseco-

- Alba, K. Simon-Arceo, A. Almanza, F. Mercado, M. León-Olea, F. Pellicer, F. *Eur. J. Pain*, **2018**, *22*, 311-318; d) A. W. M. Ewald, P. J. Bosch, A. Culverhouse, R. S. Crowley, B. Neuenswander, T. E. Prisinzano, B. M. Kivell, *Psychopharmacology*, **2017**, *234*, 2499-2514; e) Y. Zhou, R. Crowley, T. Prisinzano, M. J. Kreek, *J. Neurosci. Lett.*, **2018**, *673*, 19-23.
- [97] a) F. Yan, P. D. Mosier, R. B. Westkaemper, J. Stewart, J. K. Zjawiony, T. A. Vorthmer, D. J. Sheffler, B. L. Roth, *Biochemistry*, **2005**, *44*, 8643-8651; b) B. E. Kane, M. J. Nieto C. R. McCurdy, D. M. Ferguson, *FEBS Journal*, **2006**, *273*, 1966-1974; c) T. A. Vorthmers, P. D. Mosier, R. B. Westkaemper, B. L. Roth, *J. Biol. Chem.*, **2007**, *282*, 3146-3156; d) B. E. Kane, C. R. McCurdy, D. E. Ferguson, *J. Med. Chem.*, **2008**, *51*, 1824-1830; e) F. Yan, R. V. Bikbulatov, V. Mocanu, N. Dicheva, C. E. Parker, W. C. Wetsel, P. D. Mosier, R. B. Westkaemper, J. A. Allen, J. K. Zjawiony, B. L. Roth, *Biochemistry*, **2009**, *48*, 6898-6908.
- [98] H. Wu, D. Wacker, M. Mileni, V. Katritch, G. W. Han, E. Vardy, W. Liu, A. A. Thompson, X.-P. Huang, F. I. Carroll, S. W. Mascarella, R. B. Westkaemper, P. D. Mosier, B. L. Roth, V. Cherezov, R. C. Stevens, *Nature*, **2012**, *485*, 327-334.
- [99] For reviews see: a) T. E. Prisinzano, R. B. Rothman, *Chem. Rev.*, **2008**, *108*, 1732-1743; b) J. J. Roach, R. A. Shenvi, *Bioorg. Med. Chem. Lett.*, **2018**, *28*, 1436-1445.
- [100] Y. Wang, Y. Chen, W. Xu, D. Y. W. Lee, Z. Ma, S. M. Rawls, A. Cowan, L.-Y. Liu-Chen, *J. Pharmacol. Exp. Ther.*, **2008**, *324*, 1073-1083.
- [101] K. L. White, J. E. Robinson, H. Zhu, J. F. DiBerto, P. R. Polepally, J. K. Zjawiony, D. E. Nichols, C. J. Malanga, B. L. Roth, *J. Pharmacol. Exp. Ther.*, **2015**, *352*, 98-109.
- [102] L. Kutrzeba, F. E. Dayan, J'L. Howell, J. Feng, J.-L. Giner, J. K. Zjawiony, *Phytochemistry*, **2007**, *68*, 1872-1881.
- [103] M. Nozawa, Y. Suka, T. Hoshi, T. Suzuki, H. Hagiwara, *Org. Lett.*, **2008**, *10*, 1365-1368.
- [104] H. Hagiwara, Y. Suka, T. Nojima, T. Suzuki, *Tetrahedron*, **2009**, *65*, 8420-4825.
- [105] N. J. Line, A. C. Burns, S. C. Butler, J. Casbohm, C. J. Forsyth, *Chem. Eur. J.*, **2016**, *22*, 17983-17986.
- [106] Y. Wang, P. Metz, *Org. Lett.*, **2018**, *20*, 3418-3421.
- [107] a) J. J. Roach, Y. Sasano, C. L. Schmid, S. Zaidi, V. Katritch, R. C. Stevens, L. M. Bohn, R. A. Shenvi, *ACS Cent. Sci.*, **2017**, *3*, 1329-1336; b) A. M. Sherwood, S. E. Williamson, R. S. Crowley, L. M. Abbott, V. W. Day, T. E. Prisinzano, *Org. Lett.*, **2017**, *19*, 5414-5417; c) S. Hirasawa, M. Cho, T. F. Brust, J. J. Roach, L. M. Bohn, R. A. Shenvi, *Bioorg. Med. Chem. Lett.*, **2018**, *28*, in press (DOI: 10.1016/j.bmcl.2018.01.055)
- [108] J. S. Blair, R. Palchuadhuri, P. J. Hergenrother, *J. Am. Chem. Soc.*, **2010**, *132*, 5469-5478.
- [109] M. Abarbri, J. Thibonnet, J.-L. Parrain, A. Duchene, *Synthesis*, **2002**, *4*, 543-551.

- [110] F. Barabé, P. Levesque, L. Barriault, *Org. Lett.*, **2011**, *13*, 5580-5583.
- [111] For examples see: a) R. P. W. Kesselman, J. B. P. A. Wijnberg, J. Minnaard, R. E. Walinga, A. de Groot, *J. Org. Chem.*, **1991**, *56*, 7237-7244; b) L.-K. Sy, N.-Y. Zhu, G. D. Brown, *Tetrahedron*, **2001**, *57*, 40, 8495-8510; c) L. A. Paquette, I. Efremov, L. Zuosheng, *J. Org. Chem.*, **2005**, *70*, 505-509; d) S. G. Pardeshi, D. E. Ward, *J. Org. Chem.*, **2008**, *73*, 1071-1076; e) H. Miyaoka, Y. Abe, N. Sekiya, H. Mitome, E. Kawashima, *Chem. Comm.*, **2012**, *48*, 901-903.
- [112] R. W. Murray, *Chem. Rev.*, **1989**, *89*, 1187-1201.
- [113] D. Swern, *Chem Rev.*, **1949**, *45*, 1-68.
- [114] a) A. Armstrong, P. A. Barsanti, P. A. Clarke, A. Wood, *Tetrahedron Lett.*, **1994**, *35*, 6155-6158; b) A. Armstrong, P. A. Barsanti, P. A. Clarke, A. Wood, *J. Chem. Soc. Perkin Trans I*, **1996**, 1373-1380.
- [115] a) C. D. Hurd, W. H. Saunders, *J. Am. Chem. Soc.*, **1952**, *74*, 5324-5329; b) K. Endo, H. Takahashi, M. Aihara, *Heterocycles*, **1996**, *42*, 589-596.
- [116] a) R. Tsang, B. Fraser-Reid, *J. Am. Chem. Soc.*, **1986**, *108*, 2116-2117; b) A. C. Cunat, D. Diez-Martin, S. V. Ley, F. J. Montgomery, *J. Chem. Soc. Perkin Trans I*, **1996**, 611-619; c) P. Manus, N. Westwood, M. Spyvee, C. Frost, P. Linnane, F. Tavares, V. Lynch, *Tetrahedron*, **1999**, *55*, 6435-6452; d) E. J Enholm, J. S. Cottone, F. Allais, *Org. Lett.*, **2001**, *3*, 145-147; e) Y.-Y. Ku, T. Grieme, P. Raje, P. Sharma, S. A. King, H. E. Monton, *J. Am. Chem. Soc.*, **2002**, *124*, 4282-4286; f) D. A. Evans, G. Borg, K. A. Scheidt, *Angew. Chem. Int. Ed.*, **2002**, *41*, 3188-3191.
- [117] a) W. S. Trahanovsky, K. E. Swenson, *J. Org. Chem.*, **1981**, *46*, 2985-2987; b) T. Tsunada, K. Uemoto, C. Nagino, M. Kawamura, H. Kaku, S. Ito, *Tetrahedron Lett.*, **1999**, *40*, 7355-7358; c) N. Iranpoor, H. Firouzabadi, B. Akhlaginia, N. Nowrouzi, *J. Org. Chem.*, **2003**, *69*, 2562-2564.
- [118] a) M. P. Sibi, L. He, *Org. Lett.*, **2004**, *6*, 1749-1752; b) S. Zhou, C.-R. Chen, H.-M. Gau, *Org. Lett.*, **2010**, *12*, 48-51; c) A. Matsuda, T. Ushimaru, Y. Kobayashi, T. Harada, *Chem. Eur. J.*, **2017**, *23*, 8605-8609.
- [119] J. L. Jat, M. P. Paydial, H. Gao, Q.-L. Xu, M. Yousufuddin, D. Devarajan, D. H. Ess, L. Kurtis, J. R. Falck, *Science*, **2014**, *343*, 61-65.
- [120] C. Ruchardt, M. Meier, K. Haaf, J. Pakusch, E. K. A. Wolber, B. Muller, *Angew. Chem. Int. Ed.*, **1991**, *30*, 893-901.
- [121] a) G. J. Williams, N. R. Hunter, *Can. J. Chem.*, **1976**, *54*, 3830-3832; b) C. Tanyeli, C. Iyigun, *Tetrahedron*, **2003**, *59*, 7135-7139.

CHAPTER 5

Conclusion

The field of homogenous gold-catalyzed transformation is relatively new and has rapidly grown since the first report of its kind in 1986. Many researchers have taken advantage of the soft π -Lewis-acidity of gold, caused by the relativistic effect, for the activation of an unsaturated moiety such as alkyne. The work described in the previous chapters focus on the construction of architecturally complex molecules using gold(I)-catalyzed transformations. With the development of these methodologies with gold salts, we were able to catalyze the regioselective carbocyclization of silyl enol ethers onto alkynes by the judicious choice of the ligand adorn on gold. Utilization of these methodologies resulted in the preparations of functionalized bridged, angular and fused polycyclic compounds.

In chapter 2, we isolated new chromatographically stable organogold complexes from a Conia-ene type reaction in the formation of bridged carbocycles. We observed that the trialkyl silyl substituent on a terminal alkyl resulted in an unexpected 1,2-silyl migration while silyl with phenyl groups undergo the standard *6-endo-dig*. Mechanistic studies led us to propose a relatively rare vinylidene intermediate during the silyl migration. Further investigation of the reactivity of these vinylgold led to the formation of $C(sp^2)-C(sp^3)$ bond using various electrophilic reagents. Synergistic dual catalysis with Au and Pd was also achieved for the construction of functionalized bridged carbocycles.

Inspired by the work of Echavarren and co-workers for the cycloisomerization of enyne, in chapter 3, we developed a creative way to generate angular framework from monocyclic silyl

enol ethers. Isomerization of the alkene was accomplished using camphor-10-sulfonic acid which led to the sole formation of the more thermodynamically stable endo-cyclic olefin. The ligand on gold(I) was also investigated for the regioselectivity, where [JackiephosAuNCMe]SbF₆ was identified to be optimal to generate the 5-*exo-dig* product. These reactions conditions were applied to a wide variety of substrates affording the desired product in good yield and diastereoselectivity. This methodology was then applied to the synthesis of (±)-magellanine, a structurally compact tetracyclic angular alkaloid. The success of this synthesis is attributed to a Mitsunobu/Diels-alder sequence and to our gold(I)-catalyzed methodology to rapidly access the angular framework. The total synthesis of (±)-magellanine was achieved in 11 steps and 5% overall yield; the shortest known to date.

In chapter 4, the total synthesis of the biologically active *trans*-neoclerodane diterpenoid (±)-salvinorin A was attempted. A [4+2] cycloaddition followed by a challenging regioselective 6-*endo-dig* carbocyclization with Au(I) rapidly forged the A and B ring of the natural product. A presumably ketone directed epoxidation afforded an homoallylic alcohol after the opening of the epoxide, which was used to direct a second carbocyclization using photoredox catalysis. Au(I) photoredox catalytic system was shown to be a good alternative to the more toxic and traditional Bu₃SnH/AIBN reagents for the formation of carbon center radical from non-activated carbon-bromide bonds. With this approach, we successfully constructed most of the carbon-carbon bonds found in (±)-salvinorin A. Completion of this natural product is currently in progress as proposed at the end of the chapter 4.

CHAPTER 6

Additional information

6.1 Claims to original research

- Synthesis, characterization and isolation of new vinylgold complexes.
- Optimization of the vinylgold formation.
- Identification and screening of the terminal silyl groups for a controlled 1,2-silyl migration.
- Additional support for a gold vinylidene formation.
- Construction of C(sp³)-C(sp²) bonds from vinylgolds using electrophilic reagents.
- Optimization of a new methodology for angular core formation including the cycloisomerization and the catalyst screening process.
- Investigation and preparation of the scope for the synthesis of an angular framework.
- Optimization and investigation of different routes for the synthesis of magellanine.
- Development of the shortest synthesis of magellanine know to date.
- Application of the gold(I)-catalyzed 6-*endo-dig* carbocyclization to the synthesis of the salvinorin A molecular core.
- Optimization and exploration of new synthetic pathways towards salvinorin A.

6.2 Publications from this work

- P. McGee, G. Bellavance, L. Korobkov, A. Tarasewicz, L. Barriault, "*Synthesis and Isolation of Organogold Complexes via a Controlled 1,2-Silyl Migration*", *Chem. Eur. J.*, **2015**, 1, 9662-9665.

- P. McGee, G. Bétournay, F. Barabé, L. Barriault, *"An 11-Step Total Synthesis of Magellanine Through a Gold(I)-Catalyzed Dehydro Diels-Alder Reaction"*, *Angew. Chem. Int. Ed.* **2017**, 56, 6280-6283.
- P. McGee, J. Brousseau, L. Barriault, *"Development of New Gold(I)-Catalyzed Carbocyclization and their Application in the Synthesis of Natural Products"*, *Isr. J. Chem.* **2017**, 57, 1-11.

6.3 Oral presentations

- 26th Quebec-Ontario Mini-Symposium on Bioorganic and Organic Chemistry (QOMSBOC), *"Synthesis of angular and fused carbocycles with Au(I) catalyst"*, **2015**.
- 98th Canadian Chemical Conference and Exhibition (CSC), *"Synthesis of angular and fused polycyclic cores with Au(I) catalyst"*, **2015**.
- 24th Quebec-Ontario Mini-Symposium on Bioorganic and Organic Chemistry (QOMSBOC), *"Synthesis of angular polycyclic molecules with Au(I) catalyst"*, **2013**.

6.4 Poster presentations

- Gordon Research Conferences: Natural product and Bioactive compound (GRC), *"Gold catalysis: synthesis of magellanine and salvinorin A"*, **2016**.
- The International Chemical Congress of Pacific Basin Societies (PacifiChem), *"Formation of angular and fused carbocycles"*, **2015**.
- 16th Symposium on the Latest Trends in Organic Synthesis (LTOS-16), *"Au(I) catalysis: formation of angular and fused carbocycles"*, **2014**.
- International Symposium on Homogeneous Catalysis (ISHCXIX), *"Au(I) catalysis: formation of angular and fused carbocycles"*, **2014**.

- Ottawa-Carleton Chemistry Symposium (OCCI), *"Au(I) catalysis: formation of angular and fused carbocycles "*, **2014**.
- 24th Quebec-Ontario Mini-Symposium on Bioorganic and Organic Chemistry (QOMSBOC), *"Development of a novel synergic dual-catalyzed reaction with Au(I) and Pd"*, **2013**.
- 96th Canadian Chemical Conference and Exhibition (CSC). *"Efforts in the total synthesis of magellanine and progress towards a synergic dual-catalysis with gold and palladium"*, **2013**.
- Ottawa-Carleton Chemistry Symposium (OCCI), *"Efforts in the total synthesis of Magellanine and progress towards a synergic dual-catalysis with gold and palladium"*, **2013**.
- Synthesis Day at University of Ottawa, *"Progress towards development of a new dual-catalysed reaction with gold and palladium using a vinyl-gold intermediate"*, **2012**.

CHAPTER 7

Experimental procedures

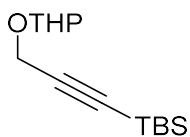
All reactions were performed under nitrogen or argon atmosphere in flame-dried glassware equipped with a magnetic stir bar and a rubber septum, unless otherwise indicated. All other commercial reagents were used without purification, unless otherwise noted. Reactions were monitored by thin layer chromatography (TLC) analysis of aliquots using glass sheets pre-coated (0.2 mm layer thickness) with silica gel 60 F254 (E. Merck). Thin layer chromatography plates were viewed under UV light and stained with phosphomolybdic acid or p-anisaldehyde staining solution. Column chromatographies were carried out with silica gel 60 (230-400 mesh, Merck). ^1H and ^{13}C NMR spectra were recorded in deuterated solvents, on Bruker AMX 300 MHz, Bruker AMX 500 MHz and Bruker AMX 400 MHz spectrometers. IR spectra were recorded with a Bomem Michelson 100 FTIR spectrometer. HRMS were obtained on a Kratos Analytical Concept instrument (University of Ottawa Mass Spectrum Centre).

7.1 Isolation and reactivity of vinylgold complexes

This section includes all characterization of *Chapter 2*.

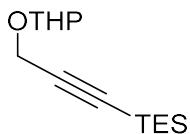
7.1.1 Silylation of the terminal alkynes for the preparation of 2.3.2

General procedure (GP1): THP-protected propargyl alcohol (71.3 mmol) in THF (25 ml) at -40 °C and was stirred for 2 hours. The corresponding silyl chloride (85.6 mmol) was added at -78 °C and the reaction mixture was stirred for 1 hour at -78 °C and then 3 hours at room temperature. The reaction mixture was then quenched with saturated NH₄Cl and the aqueous layer was extracted with Et₂O (2 x 25ml). The combined organic layer was dried over anhydrous MgSO₄, filtered and the solvent was evaporated under reduce pressure. The crude was purified by flash column chromatography on silica gel (eluted with hexane:EtOAc (97:3)) to give the desired compound as a colorless oil.



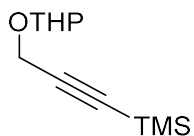
tert-butyltrimethylsilyl(3-((tetrahydro-2H-pyran-2-yl)oxy)prop-1-yn-1-yl)silane (2.3.2a)

Synthesized according to GP1 (98%). Spectroscopic data recorded were consistent with that reported previously.¹²²



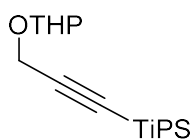
triethyltrimethylsilyl(3-((tetrahydro-2H-pyran-2-yl)oxy)prop-1-yn-1-yl)silane (2.3.2b)

Synthesized according to GP1 (97%). Spectroscopic data recorded were consistent with that reported previously.¹²²



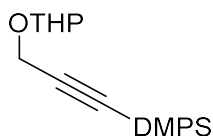
trimethyl(3-((tetrahydro-2*H*-pyran-2-yl)oxy)prop-1-yn-1-yl)silane (2.3.2c)

Synthesized according to GP1 (98%). Spectroscopic data recorded were consistent with that reported previously.¹²²



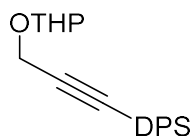
triisopropyl(3-((tetrahydro-2*H*-pyran-2-yl)oxy)prop-1-yn-1-yl)silane (2.3.2d)

Synthesized according to GP1 (98%). Spectroscopic data recorded were consistent with that reported previously.¹²²



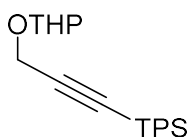
dimethyl(phenyl)(3-((tetrahydro-2*H*-pyran-2-yl)oxy)prop-1-yn-1-yl)silane (2.3.2e)

Synthesized according to GP1 (85%). Spectroscopic data recorded were consistent with that reported previously.¹²²



***tert*-butyldiphenyl(3-((tetrahydro-2*H*-pyran-2-yl)oxy)prop-1-yn-1-yl)silane (2.3.2f)**

Synthesized according to GP1 (43%). Spectroscopic data recorded were consistent with that reported previously.¹²²

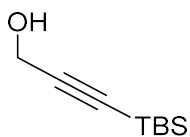


triphenyl(3-((tetrahydro-2*H*-pyran-2-yl)oxy)prop-1-yn-1-yl)silane (2.3.2g)

Synthesized according to GP1 (93%). Spectroscopic data recorded were consistent with that reported previously.¹²²

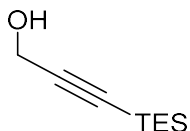
7.1.2 Removal of THP protecting groups on 2.3.2

General procedure (GP2): p-TSA (0.57 mmol) was added to the protected propargyl alcohol (57.34 mmol) in methanol (60 ml) and was refluxed overnight. The solvent was evaporated and the residue was dissolved in ethyl acetate (60 ml) and water (60 ml). The aqueous phase was extracted with EtOAc (2 x 50 ml) and the combined organic phase was dry over anhydrous MgSO₄. After filtration, the solvent was evaporated under reduce pressure and the crude product was purified by flash column chromatography on silica gel (eluted with hexane:EtOAc (95:5)) to give the desired propargyl alcohol as a colorless oil.



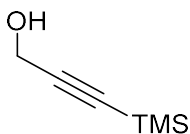
3-(tert-butyldimethylsilyl)prop-2-yn-1-ol (2.3.3a)

Synthesized according to GP2 from **2.3.2a** (96%). Spectroscopic data recorded were consistent with that reported previously.¹²²



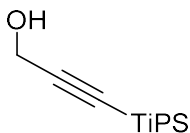
3-(triethylsilyl)prop-2-yn-1-ol (2.3.3b)

Synthesized according to GP2 from **2.3.2b** (97%). Spectroscopic data recorded were consistent with that reported previously.¹²²



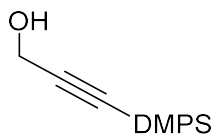
3-(trimethylsilyl)prop-2-yn-1-ol (2.3.3c)

Synthesized according to GP2 from **2.3.2c** (89%). Spectroscopic data recorded were consistent with that reported previously.¹²²



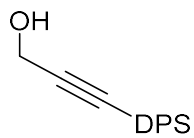
3-(triisopropylsilyl)prop-2-yn-1-ol (2.3.3d)

Synthesized according to GP2 from **2.3.2d** (77%). Spectroscopic data recorded were consistent with that reported previously.¹²²



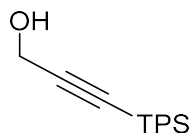
3-(dimethyl(phenyl)silyl)prop-2-yn-1-ol (2.3.3e)

Synthesized according to GP2 from **2.3.2e** (85%). Spectroscopic data recorded were consistent with that reported previously.¹²²



3-(tert-butylphenylsilyl)prop-2-yn-1-ol (2.3.3f)

Synthesized according to GP2 from **2.3.2f** (81%). Spectroscopic data recorded were consistent with that reported previously.¹²²

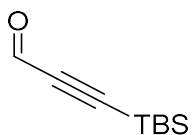


3-(triphenylsilyl)prop-2-yn-1-ol (2.3.3g)

Synthesized according to GP2 from **2.3.2g** (74%). Spectroscopic data recorded were consistent with that reported previously.¹²²

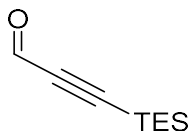
7.1.3 Oxidation of the propargylic alcohols 2.3.3

General procedure (GP3): Pyridinium chlorochromate (50.82 mmol) was added to the propargyl alcohol (33.88 mmol) with silica (11 g) and sodium acetate (5.08 mmol) in DCM (40 ml) at room temperature and the reaction mixture was stirred for 4 hours. The resulting brown solution was filtrated over cotton and the filtrate was passed on a silica plug with DCM (250 ml). Solvent was evaporated carefully and the resulting aldehyde was obtained as a colorless oil.



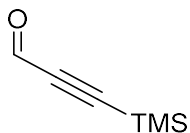
3-(tert-butyldimethylsilyl)propionaldehyde (2.3.4a)

Synthesized according to GP3 from **2.3.3a** (95%). Spectroscopic data recorded were consistent with that reported previously.¹²²



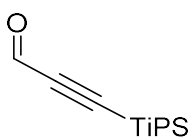
3-(triethylsilyl)propionaldehyde (2.3.4b)

Synthesized according to GP3 from **2.3.3b** (96%). Spectroscopic data recorded were consistent with that reported previously.¹²²



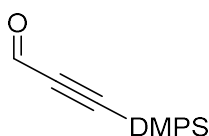
3-(trimethylsilyl)propionaldehyde (2.3.4c)

Synthesized according to GP3 from **2.3.3c** (95%). Spectroscopic data recorded were consistent with that reported previously.¹²²



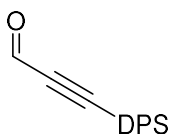
3-(triisopropylsilyl)propionaldehyde (2.3.4d)

Synthesized according to GP3 from **2.3.3d** (95%). Spectroscopic data recorded were consistent with that reported previously.¹²²



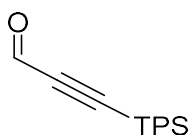
3-(dimethyl(phenyl)silyl)propionaldehyde (2.3.4e)

Synthesized according to GP3 from **2.3.3e** (99%). Spectroscopic data recorded were consistent with that reported previously.¹²²



3-(tert-butyl diphenylsilyl)propiolaldehyde (2.3.4f)

Synthesized according to GP3 from **2.3.3f** (94%). Spectroscopic data recorded were consistent with that reported previously.¹²²



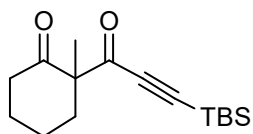
3-(triphenylsilyl)propiolaldehyde (2.3.4g)

Synthesized according to GP3 from **2.3.3g** (98%). Spectroscopic data recorded were consistent with that reported previously.¹²²

7.1.4 Aldol reaction and Dess-Martin oxidation for the formation of 2.3.5

General procedure (GP4): 2-Methylcyclohexanone (33.82 mmol) was added to LDA (30.44 mmol) in THF (165 ml) at -78 °C and the reaction was warmed to room temperature and then heated at reflux for 5 hours. Cooled down to -78 °C and then the corresponding aldehyde (**2.3.4a-f**, 38.9 mmol, diluted in 10 ml of THF) was added via a cannula. The mixture was stirred for 15 minutes and then quenched with diluted NH₄Cl. The aqueous layer was extracted with EtOAc (2 x 25ml) and then the combined organic layer was dried over anhydrous MgSO₄, filtered and the solvent was evaporated under reduce pressure. Dess-Martin periodinane (16.8 mmol) was added to the crude of alcohol (9.31 mmol) diluted in DCM (50 ml). The reaction was let stir at room temperature for 30 minutes and then 100 ml of 50 % Na₂S₂O₃ (sat.) and 50 % NaHCO₃ (5 %) was added. Stir vigorously

for 60 minutes and the aqueous phase was extracted with DCM (50 ml). The combined organic phase was dried over MgSO_4 and filtrated through cotton. The solvent was then remove under reduce pressure and the crude product was purified by flash column chromatography on silica gel (eluted with hexane:ethyl acetate (96:4)) to give the corresponding diketone.



2-[3-(tert-butyldimethylsilyl)prop-2-ynoyl]-2-methylcyclohexan-1-one (2.3.5a)

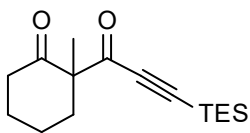
Synthesized according to GP4 from **2.3.4a** (3.8g 72 % yield).

^1H NMR (400 MHz, $\text{CHLOROFORM-}d$) δ ppm = 2.68-2.59 (m, 1 H), 2.50-2.44 (m, 2 H), 2.07-1.95 (m, 1 H), 1.78-1.58 (m, 3 H), 1.58-1.47 (m, 1 H), 1.30 (s, 3 H), 0.96 (s, 9 H), 0.18 (s, 6 H).

^{13}C NMR (101 MHz, $\text{CHLOROFORM-}d$) δ ppm = 208.44 (C), 188.20 (C), 100.40 (C), 99.92 (C), 63.82 (C), 41.32 (CH_2), 37.64 (CH_2), 27.52 (CH_2), 25.93 ($3\times\text{CH}_3$), 22.59 (CH_2), 20.80 (CH_3), 16.57 (C), -5.30 ($2\times\text{CH}_3$).

HRMS (EI) m/z calcd for $\text{C}_{16}\text{H}_{26}\text{O}_2\text{Si}$ [$(\text{M}-\text{C}_4\text{H}_9)^+$] 221.0992, found 221.0998.

FTIR (Neat, cm^{-1}): ν = 2931 (s), 2364 (m), 1720 (s), 1666 (s).



2-methyl-2-[3-(triethylsilyl)prop-2-ynoyl]cyclohexan-1-one (2.3.5b)

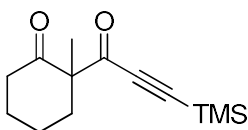
Synthesized according to GP4 from **2.3.4b** (3.6g 21 % yield).

¹H NMR (400 MHz, CHLOROFORM-*d*) δ ppm = 2.66-2.58 (m, 1 H), 2.50-2.39 (m, 2 H), 2.05-1.94 (m 1 H), 1.76-1.57 (m, 3 H), 1.56-1.41 (m, 1 H), 1.28 (s, 3 H), 0.98 (t, J = 7.90 Hz, 9 H), 0.64 (q, J = 7.82 Hz, 6 H).

¹³C NMR (101 MHz, CHLOROFORM-*d*) δ ppm = 208.55 (C), 188.31 (C), 100.45 (C), 99.89 (C), 63.87 (C), 41.22 (CH₂), 37.60 (CH₂), 27.54 (CH₂), 22.43 (CH₂), 20.78 (CH₃), 7.35 (3x CH₃), 3.80 (3x CH₂).

HRMS (EI) m/z calcd for C₁₆H₂₆O₂Si [(M-C₂H₅)⁺] 249.1305, found 249,1314.

FTIR (Neat, cm⁻¹): ν = 2936 (s), 2357 (m), 1737(s), 1678 (s).



2-methyl-2-[3-(trimethylsilyl)prop-2-ynoyl]cyclohexan-1-one (2.3.5c)

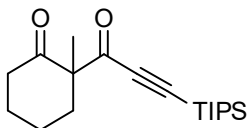
Synthesized according to GP4 from **2.3.4c** (1.3g, 21 % yield).

¹H NMR (400 MHz, CHLOROFORM-*d*) δ ppm = 2.61-2.53 (m, 1 H), 2.46-2.36 (m, 2 H), 2.03-1.91 (m, 1 H), 1.75-1.57 (m, 3 H), 1.54-1.44 (m, 1 H), 1.24 (s, 3 H), 0.20 (s, 9 H).

¹³C NMR (101 MHz, CHLOROFORM-*d*) δ ppm = 208.32 (C), 188.72 (C), 102.35 (C), 99.44 (C), 63.51 (CH₂), 41.38 (CH₂), 37.74 (CH₂), 27.95 (CH₂), 22.86 (CH₂), 21.05 (CH₃), -0.36 (3xCH₃).

HRMS (EI) m/z calcd for $C_{13}H_{20}O_2Si$ 236.1233, found 236.1228.

FTIR (Neat, cm^{-1}): ν = 2938 (s), 2149 (m), 1722 (s), 1667 (s), 1551 (m).



2-methyl-2-{3-[tris(propan-2-yl)silyl]prop-2-ynoyl}cyclohexan-1-one (2.3.5d)

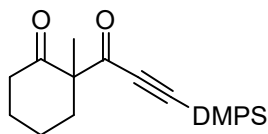
Synthesized according to GP4 from **2.3.4d** (1.6g, 50 % yield).

1H NMR (400 MHz, CHLOROFORM-*d*) δ ppm = 2.67-2.60 (m, 1 H), 2.47-2.39 (m, 2 H), 2.03-1.95 (m, 1 H), 1.75-1.58 (m, 3 H), 1.55-1.46 (m, 1 H), 1.27 (s, 3 H), 1.15-1.02 (m, 21 H).

^{13}C NMR (101 MHz, CHLOROFORM-*d*) δ ppm = 208.32 (C), 188.11 (C), 101.98 (C), 99.44 (C), 64.24 (C), 42.10 (CH_2), 38.11 (CH_2), 26.86 (CH_2), 22.86 (CH_2), 20.73 (CH_3), 18.51 (6x CH_3), 11.25 (3xCH).

HRMS (EI) m/z calcd for $C_{19}H_{32}O_2Si$ [(M- C_4H_9) $^+$] 277.1618, found 277.1639.

FTIR (Neat, cm^{-1}): ν = 2941 (s), 2357 (m), 1733 (s), 1666 (s).



2-{3-[dimethyl(phenyl)silyl]prop-2-ynoyl}-2-methylcyclohexan-1-one (2.3.5e)

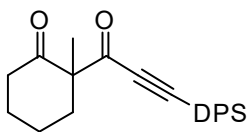
Synthesized according to GP4 from **2.3.4e** (600mg, 18 % yield)

¹H NMR (400 MHz, CHLOROFORM-*d*) δ ppm = 7.61-7.57 (m, 2 H), 7.44-7.37 (m, 3 H), 2.67-2.59 (m, 1 H), 2.50-2.43 (m, 2 H), 2.06-1.96 (m, 1 H), 1.78-1.61 (m, 3 H), 1.58-1.49 (m, 1 H), 1.31 (s, 3 H), 0.50 (s, 6 H).

¹³C NMR (101 MHz, CHLOROFORM-*d*) δ ppm = 208.50 (C), 188.17 (C), 134.46 (C), 133.72 (2xCH), 130.11 (CH), 128.20 (2xCH), 100.39 (C), 99.47 (C), 63.97 (C), 42.23 (CH₂), 37.62 (CH₂), 27.52 (CH₂), 22.31 (CH₂), 20.72 (CH₃), -1.69 (2xCH₃).

HRMS (EI) m/z calcd for C₁₈H₂₂O₂Si is 298.1389, found 298.1403.

FTIR (Neat, cm⁻¹): ν = 2937 (m), 2361 (m), 1720 (s), 1667 (s).



2-[3-(tert-butyldiphenylsilyl)prop-2-ynoyl]-2-methylcyclohexan-1-one (2.3.5f)

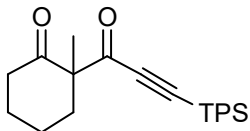
Synthesized according to GP4 from **2.3.4f** (2.1 g, 26 % yield).

¹H NMR (400 MHz, CHLOROFORM-*d*) δ ppm = 7.78-7.72 (m, 4 H), 7.48-7.38 (m, 6 H), 2.77-2.70 (m, 1 H), 2.55-2.49 (m, 2 H), 2.08-2.00 (m, 1 H), 1.81-1.65 (m, 3 H), 1.64-1.56 (m, 1 H), 1.40 (s, 3 H), 1.13 (s, 9 H).

¹³C NMR (101 MHz, CHLOROFORM-*d*) δ ppm = 208.34 (C), 187.96 (C), 135.52 (4xCH), 131.19 (2xC), 130.18 (2xCH), 128.08 (4xCH), 102.67 (C), 96.91 (C), 64.04 (C), 41.27 (CH₂), 37.50 (CH₂), 27.52 (CH₂), 26.99 (3xCH₃), 22.44 (CH₂), 20.78 (CH₃), 18.88 (C).

HRMS (EI) m/z calcd for C₂₆H₃₀O₂Si [(M-C₄H₉)⁺] 345.1305, found 245.1332.

FTIR (Neat, cm⁻¹): ν = 2934 (m), 2357 (m), 1700 (s), 1653 (s).



2-methyl-2-[3-(triphenylsilyl)prop-2-ynoyl]cyclohexan-1-one (2.3.5g)

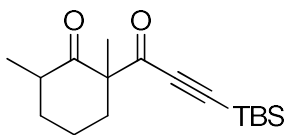
Synthesized according to GP4 from **2.3.5g** (1.5g, 66 % yield).

¹H NMR (400 MHz, CHLOROFORM-*d*) δ ppm = 7.68-1.64 (m, 6 H), 7.52-7.41 (m, 9 H), 2.76-2.68 (m, 1 H), 2.53-2.47 (m, 2 H), 2.07-1.97 (m, 1 H), 1.80-1.65 (m, 3 H), 1.64-1.55 (m, 1 H), 1.40 (s, 3 H).

¹³C NMR (101 MHz, CHLOROFORM-*d*) δ ppm = 208.36 (C), 188.14 (C), 135.61 (6xCH), 131.32 (3xC), 130.64 (3xCH), 128.33 (6xCH), 102.53 (C), 96.30 (C), 64.02 (C), 41.20 (CH₂), 37.56 (CH₂), 27.47 (CH₂), 20.77 (CH₃), 20.43 (CH₂).

HRMS (EI) m/z calcd for C₂₈H₂₆O₂Si is 422.1702, found 422.1714.

FTIR (Neat, cm⁻¹): ν = 2935 (m), 1716 (s), 1662 (s).



2-[3-(tert-butyldimethylsilyl)prop-2-ynoyl]-2,6-dimethylcyclohexan-1-one (2.3.5h)

Synthesized according to GP4 from **2.3.4a** (410mg, 59 %).

¹H NMR (400 MHz, CHLOROFORM-*d*) δ ppm = 2.62 (dq, J =14.0, 2.9 Hz, 1 H), 2.52 (q, J =6.6 Hz 1 H), 2.05-1.97 (m, 1 H), 1.77-1.62 (m, 2 H), 1.45 (td, J =13.7, 4.6 Hz, 1 H), 1.33 (td, J =12.9, 4.4 Hz, 1 H), 1.26 (s, 3 H), 1.02 (d, J =6.6 Hz, 3 H), 0.93 (m, 9 H), 0.15 (s, 3 H), 0.14 (s, 3 H).

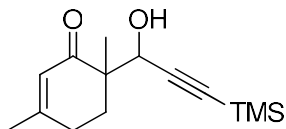
¹³C NMR (101 MHz, CHLOROFORM-*d*) δ ppm = 209.52 (C), 188.08 (C), 100.41 (C), 100.07 (C), 64.21 (C), 45.20 (CH), 37.98 (CH₂), 36.78 (CH₂), 25.96 (3xCH₃), 22.61 (CH₂), 21.05 (CH₃), 16.55 (C), 14.80 (CH₃), -5.27 (2xCH₃).

HRMS (EI) m/z calcd for C₁₇H₂₈O₂Si [(M-C₄H₉)⁺] 235.1149, found 235.1136.

FTIR (Neat, cm⁻¹): ν = 2931 (s), 2149 (w), 1720 (s), 1667 (s), 1451 (m).

7.1.5 Aldol reaction for the formation of 2.3.8

General procedure (GP5): 2.5M n-Butyllithium (3.52 mL, 8.46 mmol) was added to a of diisopropylamine (0.87 g, 8.86 mmol) in THF (30 mL) at -78 °C. The reaction was stirred for 30 minutes and then 3,6-dimethylcyclohex-2-enone (1.00 g, 8.05 mmol) was added. The solution was stirred for 30 minutes at -78 °C, **C1-C7** (9.66 mmol) was added to the mixture and then brought to room temperature for 1 hour. A saturated solution of NH₄Cl (30 mL) was then added. The aqueous layer was extracted with ethyl acetate and the combined organic phase was dried with MgSO₄. The organic phase was then purified by flash chromatography on silica gel with ethyl acetate to hexanes (20:80) to give the desired compound.



2-[1-hydroxy-3-(trimethylsilyl)prop-2-yn-1-yl]-2,5,5-trimethylcyclohexan-1-one (2.3.8a'')

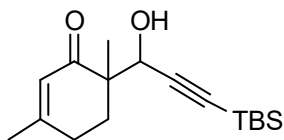
Synthesized according to GP5 from **2.3.4c** (0.85g, 64 % yield), major diastereoisomer:

¹H NMR (400 MHz, CHLOROFORM-*d*) δ ppm = 5.78 (s, 1 H), 4.58 (s, 1 H), 2.52-2.39 (m, 1 H), 2.37-2.23 (m, 1 H), 1.97 (s, 3 H), 1.98-1.96 (m, 1 H), 1.86-1.74 (m, 1 H), 1.24 (s, 3 H), 0.16 (s, 9 H).

¹³C NMR (101 MHz, CHLOROFORM-*d*) δ ppm = 205.68 (C), 162.97 (C), 125.03 (CH), 102.76 (C), 90.62 (C), 68.45 (CH), 46.19 (C), 31.13 (CH₂), 28.09 (CH₂), 24.06 (CH₃), 15.05 (CH₃), -0.13 (3xCH₃).

HRMS (EI) m/z calcd for C₁₄H₂₂O₂Si is 250.1389, found 250.1349.

FTIR (Neat, cm⁻¹): ν = 3415 (w), 2970 (w), 2366 (w), 1634 (s), 838 (s).



2-[3-(tert-butyldimethylsilyl)-1-hydroxyprop-2-yn-1-yl]-2,5,5-trimethylcyclohexan-1-one (2.3.8b'')

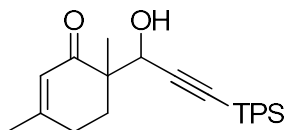
Synthesized according to GP5 from **2.3.4a** (0.93g, 81 % yield), major diastereomer:

¹H NMR (400 MHz, CHLOROFORM-*d*) δ ppm = 5.79 (s, 1 H), 4.61 (s, 1 H), 2.53-2.40 (m, 1 H), 2.36-2.24 (m, 1 H), 2.02-1.97 (m, 1 H), 1.97 (s, 3 H), 1.89-1.73 (m, 1 H), 1.26 (s, 3 H), 0.93 (s, 9 H), 0.11 (s, 6 H).

¹³C NMR (101 MHz, CHLOROFORM-*d*) δ ppm = 205.55 (C), 162.89 (C), 125.07 (CH), 103.49 (C), 88.88 (C), 68.47 (CH), 46.32 (C), 31.19 (CH₂), 28.08 (CH₂), 26.12 (3xCH₃), 24.06 (CH₃), 16.54 (C), 15.18 (CH₃), -4.64 (CH₃), -4.68 (CH₃).

HRMS (EI) m/z calcd for C₁₇H₂₈O₂Si [(M-C₄H₉)⁺] 235.1149, found 235.1139.

FTIR (Neat, cm⁻¹): ν = 3458 (m), 2948 (m), 1647 (s) .



**2-[1-hydroxy-3-(triphenylsilyl)prop-2-yn-1-yl]-2,5,5-trimethylcyclohexan-1-one
(2.3.8c'')**

Synthesized according to GP5 from **2.3.4g** (0.76g, 51 % yield), major diastereomer:

¹H NMR (400 MHz, CHLOROFORM-*d*) δ ppm = 7.67-7.61 (m, 6 H), 7.46-7.34 (m, 9 H), 5.82 (s, 1 H), 4.77 (d, J =2.2 Hz, 1 H), 4.31 (d, J =2.5, 1 H), 2.51-2.37 (m, 1 H), 2.34-2.23 (m, 1 H), 2.05-1.88 (m, 2 H), 1.97 (s, 3 H), 1.33 (s, 3 H) .

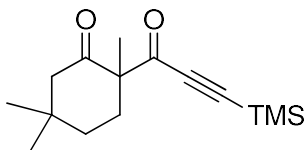
¹³C NMR (101 MHz, CHLOROFORM-*d*) δ ppm = 205.20 (C), 163.03 (C), 135.56 (6xCH), 133.27 (3xC), 129.98 (3xCH), 127.99 (6xCH), 125.06 (CH), 107.91 (C), 85.87 (C), 68.73 (CH), 46.65 (C), 31.04 (CH₂), 28.05 (CH₂), 24.10 (CH₃), 15.60 (CH₃).

HRMS (EI) m/z calcd for C₂₉H₂₈O₂Si is 436.1859, found 436.1828.

FTIR (Neat, cm⁻¹): ν = 3397 (m), 2954 (m), 1635 (s), 696 (s).

7.1.6 Conjugated addition and oxidation to produce 2.3.8

General procedure (GP6): Copper iodide (1.302 g, 6.84 mmol) was added to a round bottom flask and THF (25 mL) was added afterwards. Starting material (1.00 g, 3.42 mmol) and dimethylsulfide (2.5 mL) was added to the solution and was stirred until all copper iodide was dissolved. The solution then was cooled to 0 °C. 3M Methylmagnesium bromide (4.79 mL, 14.36 mmol) was added slowly over 90 minutes. Once the addition had completed, the reaction mixture was stirred for 5 hours. A saturated solution of NH₄Cl (50 mL) was then added. The aqueous layer was extracted with ethyl acetate and ether. The combined organic phase was dried with MgSO₄, passed through a celite plug and the solvent was evaporated. To the crude oil was added Dess-Martin Periodinane (1.65 g, 3.89 mmol) and DCM (7 mL). The reaction mixture was stirred for 1 hour. A 50:50 mixture of 5% NaHCO₃ (3.5 mL) and Na₂O₃S₂ (3.5 mL) was added and stirred for 30 min. The aqueous layer was extracted with DCM and the combined organic phase was dried with MgSO₄. The organic phase was then purified by flash chromatography on silica gel with ethyl acetate to hexanes (4:96) to give the desired compound.



2,5,5-trimethyl-2-[3-(trimethylsilyl)prop-2-ynoyl]cyclohexan-1-one (2.3.8a)

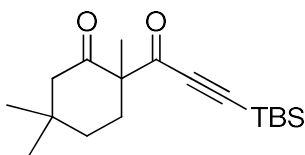
Synthesized according to GP6 from **2.3.8a''** (0.62g, 65 % yield).

¹H NMR (400 MHz, CHLOROFORM-*d*) δ ppm = 2.59 - 2.51 (m, 1 H), 2.33 (d, J = 13.4 Hz, 1 H), 2.18 (dd, J = 13.5, 2.1 Hz, 1 H), 1.68 – 1.61 (m, 2 H), 1.52 - 1.45 (m, 1 H), 1.28 (s, 3 H), 1.01 (s, 3 H), 0.88 (s, 3 H), 0.23 (s, 9 H).

¹³C NMR (101 MHz, CHLOROFORM-*d*) δ ppm = 208.31 (C), 187.98 (C), 101.51 (C), 99.28 (C), 62.57 (C), 53.9 (CH₂), 36.67 (C), 35.38 (CH₂), 32.88 (CH₂), 30.84 (CH₃), 26.09 (CH₃), 20.39 (CH₃), -0.84 (3x CH₃).

HRMS (EI) m/z calcd for C₁₅H₂₄O₂Si [(M-CH₃)⁺] 249.1305, found 249.1299.

FTIR (Neat, cm⁻¹): ν = 2923 (s), 1722 (s), 1674 (s), 1046 (m).



2-[3-(tert-butyldimethylsilyl)prop-2-ynoyl]-2,5,5-trimethylcyclohexan-1-one (2.3.8b)

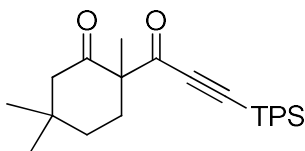
Synthesized according to GP6 from **2.3.8b''** (0.81g, 82 % yield).

¹H NMR (400 MHz, CHLOROFORM-*d*) δ ppm = 2.59-2.52 (m, 1 H), 2.35 (d, J = 13.5 Hz, 1 H), 2.19 (dd, J = 13.5, 2.2 Hz, 1 H), 1.69 - 1.63 (m, 2 H), 1.52 - 1.44 (m, 1 H), 1.29 (s, 3 H), 1.02 (s, 3 H), 0.95 (s, 9 H), 0.88 (s, 3 H), 0.18 (s, 3 H), 0.17 (s, 3 H).

¹³C NMR (101 MHz, CHLOROFORM-*d*) δ ppm = 208.12 (C), 187.84 (C), 100.46 (C), 100.03 (C), 62.67 (C), 54.02 (CH₂), 36.77 (C), 35.43 (CH₂), 32.88 (CH₂), 31.08 (CH₃), 25.93 (3xCH₃), 25.87 (CH₃), 20.48 (CH₃), 16.63 (C), -5.28 (2xCH₃).

HRMS (EI) m/z calcd for $C_{18}H_{30}O_2Si [(M-CH_3)^+]$ 291.1775, found 217.1742.

FTIR (Neat, cm^{-1}): ν = 2933 (s), 1722 (s), 1666 (s), 1045 (m).



2,5,5-trimethyl-2-[3-(triphenylsilyl)prop-2-ynoyl]cyclohexan-1-one (2.3.8c)

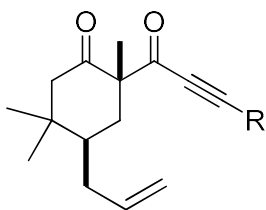
Synthesized according to GP6 from **2.3.8c''** (0.52g, 82 % yield).

1H NMR (400 MHz, $CHCl_3-d$) δ ppm = 7.65-7.60 (m, 6 H), 7.51 - 7.40 (m, 9 H), 2.63 (dd, J = 12.5, 4.0 Hz, 1 H), 2.37 (d, J = 13.6 Hz, 1 H), 2.22 (dd, J = 13.6, 2.1 Hz, 1 H), 1.73 (d, J = 12.3 Hz, 1 H), 1.68 (d, J = 12.3 Hz, 1H) 1.53-1.48 (m, 1 H), 1.37 (s, 3 H), 0.99 (s, 3 H), 0.91 (s, 3 H).

^{13}C NMR (101 MHz, $CHCl_3-d$) δ ppm = 208.08 (C), 187.73 (C), 135.60 (6xCH), 131.31 (3xC), 130.58 (3xCH), 128.29 (6xCH), 102.57 (C), 96.25 (C), 62.80 (C), 53.99 (CH_2), 36.76 (C), 35.41 (CH_2), 32.91 (CH_2), 30.84 (CH_3), 26.15 (CH_3), 20.45 (CH_3)

HRMS (EI) m/z calcd for $C_{30}H_{30}O_2Si$ is 450.2015, found 450.2062.

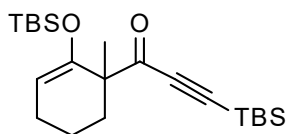
FTIR (Neat, cm^{-1}): ν = 2964 (s), 1716 (s), 1676(s), 1429 (m), 1118 (s).



(**2.3.9d**, R = TMS and **2.3.8e**, R = TBS) Synthesized according to following literature.¹²³

7.1.7 Silyl enol ether formation

General procedure (GP7): *t*-butyldimethylsilyl triflate (10.24 mmol) was added to the corresponding diketone (5.12 mmol) and Et₃N (15.36 mmol) in DCM (30 ml) at room temperature. The mixture was heated at reflux overnight and then a solution of saturated NaHCO₃ (25 ml) was added. The aqueous layer was extracted with DCM (2 x 25ml). The combined organic layer was dried over anhydrous MgSO₄, filtered and the solvent was evaporated under reduce pressure. The crude product was purified by flash column chromatography on silica gel (eluted with benzen:hexane (30:70)) to give the desired silyl enol ether.



3-(tert-butyldimethylsilyl)-1-{2-[(tert-butyldimethylsilyl)oxy]-1-methylcyclohex-2-en-1-yl}prop-2-yn-1-one (2.3.6a**)**

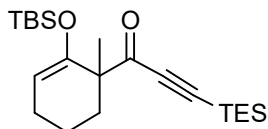
Synthesized according to GP7 from **2.2.5a** (4.5g, 93 % yield).

¹H NMR (400 MHz, CHLOROFORM-*d*) δ ppm = 4.87 (dd, *J* = 4.9, 3.3 Hz, 1 H), 2.17-2.03 (m, 3 H), 1.74-1.67 (m, 1 H), 1.58-1.48 (m, 2 H), 1.29 (s, 3 H), 0.96 (s, 9 H), 0.86 (s, 9 H), 0.17 (s, 3 H), 0.16 (s, 3 H), 0.15 (s, 3 H), 0.12 (s, 3 H).

¹³C NMR (101 MHz, CHLOROFORM-*d*) δ ppm = 191.24 (C), 151.07 (C), 103.19 (CH), 101.67 (C), 96.36 (C), 54.14 (C), 33.90 (CH₂), 25.98 (3xCH₃), 25.59 (3xCH₃), 24.07 (CH₂), 20.06 (CH₃), 18.80 (C), 18.15 (CH₂), 16.71 (C), -4.36 (CH₃), -4.95 (CH₃), -5.16 (CH₃), -5.22 (CH₃).

HRMS (EI) m/z calcd for C₂₂H₄₀O₂Si₂ is 392.2567, found 392.2531.

FTIR (Neat, cm⁻¹): ν = 2927 (m), 2357 (m), 1660 (s), 1244 (m).



1-{2-[(tert-butyldimethylsilyl)oxy]-1-methylcyclohex-2-en-1-yl}-3-(triethylsilyl)prop-2-yn-1-one (2.3.6b)

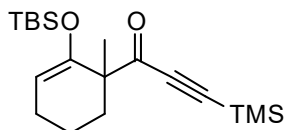
Synthesized according to GP7 from **2.3.5b** (0.24g, 87 % yield).

¹H NMR (400 MHz, CHLOROFORM-*d*) δ ppm = 4.85 (dd, *J* = 4.6, 3.4 Hz, 1 H), 2.18-2.00 (m, 3 H), 1.73-1.64 (m, 1 H), 1.57-1.46 (m, 2 H), 1.28 (s, 3 H), 0.98 (t, *J* = 8.0 Hz, 9 H), 0.84 (s, 9 H), 0.63 (q, *J* = 8.0 Hz, 6 H), 0.14 (s, 3H), 0.10 (s, 3 H).

¹³C NMR (101 MHz, CHLOROFORM-*d*) δ ppm = 191.31 (C), 151.14 (C), 103.17 (CH), 102.16 (C), 95.79 (C), 54.11 (C), 34.00 (CH₂), 25.56 (3xCH₃), 24.13 (CH₂), 20.17 (CH₃), 18.83 (CH₂), 18.07 (C), 7.34 (3xCH₂), 3.90 (3xCH₂), -4.58 (CH₃), -4.84 (CH₃).

HRMS (EI) m/z calcd for C₂₂H₄₀O₂Si₂ is 392.2567, found 392.2550.

FTIR (Neat, cm⁻¹): ν = 2934 (w), 2357 (m), 1703 (s), 1646 (s).



1-{2-[(tert-butyldimethylsilyl)oxy]-1-methylcyclohex-2-en-1-yl}-3-(trimethylsilyl)prop-2-yn-1-one (2.3.6c)

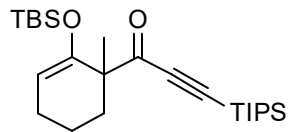
Synthesized according to GP7 from **2.3.5c** (1.4g, 71 % yield).

¹H NMR (400 MHz, CHLOROFORM-*d*) δ ppm = 4.86 (dd, J = 4.8, 3.4 Hz, 1 H), 2.15-2.02 (m, 3 H), 1.73-1.64 (m, 1 H), 1.57-1.46 (m, 2 H), 1.29 (s, 3 H), 0.86 (s, 9 H), 0.21 (s, 9 H), 0.16 (s, 3H), 0.13 (s, 3 H).

¹³C NMR (101 MHz, CHLOROFORM-*d*) δ ppm = 191.39 (C), 151.07 (C), 103.15 (CH), 101.19 (C), 97.99 (C), 53.98 (C), 34.03 (CH₂), 25.65 (3xCH₃), 24.23 (CH₂), 20.49 (CH₃), 19.06 (C), 18.17 (CH₂), -0.53 (3xCH₃), -4.63 (2xCH₃)

HRMS (EI) m/z calcd for C₁₉H₃₄O₂Si₂ is 350.2097, found 350.2103.

FTIR (Neat, cm⁻¹): ν = 2934 (m), 2364 (m), 1686 (s), 1646 (s), 1250 (m).



1-{2-[(tert-butyldimethylsilyl)oxy]-1-methylcyclohex-2-en-1-yl}-3-[tris(propan-2-yl)silyl]prop-2-yn-1-one (2.3.6d)

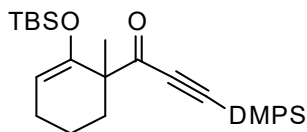
Synthesized according to GP7 from **2.3.5d** (1.9g, 86 % yield).

¹H NMR (400 MHz, CHLOROFORM-*d*) δ ppm = 4.86 (t, J = 3.8 Hz, 1 H), 2.23-2.01 (m, 3 H), 1.74-1.65 (m, 1 H), 1.58-1.46 (m, 2 H), 1.28 (s, 3 H), 1.12-1.04 (m, 21 H), 0.84 (s, 9 H), 0.15 (s, 3 H), 0.10 (s, 3 H).

¹³C NMR (101 MHz, CHLOROFORM-*d*) δ ppm = 191.01 (C), 151.19 (C), 103.27 (CH), 102.99 (C), 94.90 (C), 54.33 (C), 33.87 (CH₂), 25.56 (3x CH₃), 24.15 (CH₂), 20.14 (CH₃), 18.78 (CH₂), 18.51 (6 x CH₃), 18.02 (C), 11.13 (3 x CH), -4.19 (CH₃), -5.10 (CH₃)

HRMS (EI) m/z calcd for C₂₅H₄₆O₂Si₂ [(M-C₄H₉)⁺] 377.2327, found 377.2358.

FTIR (Neat, cm⁻¹): ν = 2927 (m), 2357 (m), 1653 (s), 1250 (m).



1-{2-[(tert-butyldimethylsilyl)oxy]-1-methylcyclohex-2-en-1-yl}-3-[dimethyl(phenyl)silyl]prop-2-yn-1-one (2.3.6e)

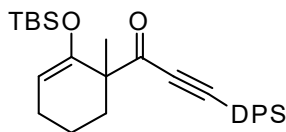
Synthesized according to GP7 from **2.3.5e** (0.69g, 82 % yield).

¹H NMR (400 MHz, CHLOROFORM-*d*) δ ppm = 7.65-7.62 (m, 2 H), 7.42-7.36 (m, 3 H), 4.90 (dd, J = 4.8, 3.3 Hz, 1 H), 2.20-2.04 (m, 3 H), 1.76-1.67 (m, 1 H), 1.60-1.49 (m, 2 H), 1.33 (s, 3 H), 0.86 (s, 9 H), 0.48 (s, 3 H), 0.47 (s, 3 H), 0.14 (s, 3 H), 0.13 (s, 3 H).

¹³C NMR (101 MHz, CHLOROFORM-*d*) δ ppm = 191.23 (C), 151.05 (C), 135.25 (C), 133.82 (2xCH), 129.84 (CH), 128.01 (2xCH), 103.14 (CH), 102.40 (C), 95.43 (C), 54.22 (C), 33.91 (CH₂), 25.60 (3xCH₃), 24.08 (CH₂), 20.12 (CH₃), 18.86 (CH₂), 18.11 (C), -1.38 (CH₃), -1.51 (CH₃), -4.61 (CH₃), -4.72 (CH₃).

HRMS (EI) m/z calcd for $C_{24}H_{36}O_2Si_2$ is 412.2254, found 412.2282.

FTIR (Neat, cm^{-1}): ν = 2927 (m), 2357 (m), 1680 (s), 1244 (m).



1-{2-[(tert-butyldimethylsilyl)oxy]-1-methylcyclohex-2-en-1-yl}-3-(tert-butyldiphenylsilyl)prop-2-yn-1-one (2.3.6f)

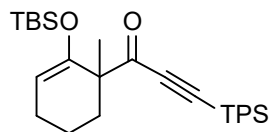
Synthesized according to GP7 from **2.3.5f** (2.2g, 82 % yield).

1H NMR (400 MHz, CHLOROFORM-*d*) δ ppm = 7.80-7.76 (m, 4 H), 7.44-7.35 (m, 6 H), 4.95 (dd, J = 5.1, 3.0 Hz, 1 H), 2.31-2.07 (m, 3 H), 1.80-1.71 (m, 1 H), 1.62-1.53 (m, 2 H), 1.34 (s, 3 H), 1.10 (s, 9 H), 0.85 (s, 9 H), 0.10 (s, 3 H), 0.07 (s, 3 H).

^{13}C NMR (101 MHz, CHLOROFORM-*d*) δ ppm = 190.84 (C), 151.12 (C), 135.64 (4xCH), 131.86 (C), 131.82 (C), 129.89 (2xCH), 127.86 (4xCH), 104.56 (C), 103.42 (CH), 92.53 (C), 54.50 (C), 33.78 (CH₂), 27.02 (3xCH₃), 25.60 (3xCH₃), 24.10 (CH₂), 19.95 (CH₃), 18.89 (C), 18.74 (CH₂), 18.05 (C), -4.08 (CH₃), -5.24 (CH₃).

HRMS (EI) m/z calcd for $C_{32}H_{44}O_2Si_2$ is 516.2880, found 516.2873.

FTIR (Neat, cm^{-1}): ν = 2927 (m), 2357 (m), 1660 (s), 1244 (m).



1-{2-[(tert-butyldimethylsilyl)oxy]-1-methylcyclohex-2-en-1-yl}-3-(triphenylsilyl)prop-2-yn-1-one (2.3.6g)

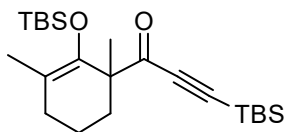
Synthesized according to GP7 from **2.3.5g** (1.5g, 92 % yield).

¹H NMR (400 MHz, CHLOROFORM-*d*) δ ppm = 7.69-7.66 (m, 6 H), 7.49-7.44 (m, 3 H), 7.42-7.38 (m, 6 H), 4.94 (dd, J = 4.9, 3.2 Hz, 1 H), 2.29-2.09 (m, 3 H), 1.79-1.70 (m, 1 H), 1.63-1.52 (m, 2 H), 1.36 (s, 3 H), 0.83 (s, 9 H), 0.11 (s, 3 H), 0.00 (s, 3 H).

¹³C NMR (101 MHz, CHLOROFORM-*d*) δ ppm = 191.01 (C), 151.10 (C), 135.69 (6xCH), 131.98 (3xC), 130.35 (3xCH), 128.11 (6xCH), 104.50 (C), 103.21 (CH), 92.00 (C), 54.49 (C), 33.77 (CH₂), 25.57 (3xCH₃), 24.09 (CH₂), 19.97 (CH₃), 18.76 (CH₂), 18.02 (C), -4.51 (CH₃), -4.97 (CH₃).

HRMS (EI) m/z calcd for C₃₄H₄₀O₂Si₂ is 536.2567, found 536.2568.

FTIR (Neat, cm⁻¹): ν = 2927 (m), 2360 (m), 1658 (s), 1245 (m).



3-(tert-butyldimethylsilyl)-1-{2-[(tert-butyldimethylsilyl)oxy]-1,3-dimethylcyclohex-2-en-1-yl}prop-2-yn-1-one (2.3.6h)

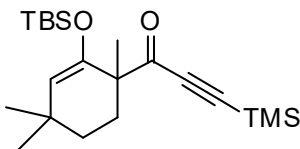
Synthesized according to GP7 (refluxed in DCE) from **2.3.5h** (0.41g, 75 % yield).

¹H NMR (400 MHz, CHLOROFORM-*d*) δ ppm = 2.12-1.95 (m, 3 H), 1.59 (s, 3 H), 1.58-1.44 (m, 3 H), 1.31 (s, 3 H), 0.94 (s, 9 H), 0.89 (s, 9 H), 0.14 (s, 3 H), 0.13 (s, 3 H), 0.12 (s, 3 H), 0.06 (s, 3 H).

¹³C NMR (101 MHz, CHLOROFORM-*d*) δ ppm = 192.00 (C), 143.29 (C), 113.44 (C), 102.13 (C), 97.10 (C), 54.05 (C), 35.67 (CH₂), 31.17 (CH₂), 26.12 (3x CH₃), 25.69 (3x CH₃), 20.83 (CH₃), 18.86 (CH₂), 18.54 (CH₃), 17.60 (C), 16.65 (C), -3.08 (CH₃), -3.71 (CH₃), -5.20 (2x CH₃).

HRMS (EI) m/z calcd for C₂₃H₄₂O₂Si₂ [(M-C₄H₉)⁺] 349.2014, found 349.2032.

FTIR (Neat, cm⁻¹): ν = 2927 (m), 2357 (m), 1653 (s).



1-{2-[(tert-butyldimethylsilyl)oxy]-1,4,4-trimethylcyclohex-2-en-1-yl}-3-(trimethylsilyl)prop-2-yn-1-one (2.3.9a)

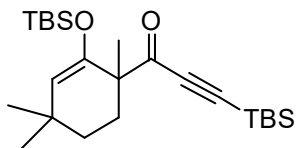
Synthesized according to GP7 from **2.3.8a** (0.63g, 49 % yield).

¹H NMR (400 MHz, CHLOROFORM-*d*) δ ppm = 4.63 (s, 1 H), 2.29 (td, J =12.4, 2.4 Hz, 1 H), 1.53 - 1.38 (m, 3 H), 1.26 (s, 3 H), 1.07 (s, 3 H), 1.01 (s, 3 H), 0.86 (s, 9 H), 0.21 (s, 9 H), 0.17 (s, 3 H), 0.14 (s, 3 H).

¹³C NMR (101 MHz, CHLOROFORM-*d*) δ ppm = 191.21 (C), 149.51 (C), 114.20 (CH), 100.95 (C), 97.20 (C), 54.09 (C), 33.28 (CH₂), 32.33 (C), 31.31 (CH₃), 30.59 (CH₂), 29.21 (CH₃), 25.58 (3x CH₃), 19.51 (CH₃), 18.10 (C), -0.74 (3xCH₃), -4.72 (CH₃), -4.77 (CH₃)

HRMS (EI) m/z calcd for C₂₁H₃₈O₂Si₂ is 378.2410, found 378.2408.

FTIR (Neat, cm⁻¹): ν = 2954 (m), 2366 (m), 1677 (s), 1654 (s).



3-(tert-butyldimethylsilyl)-1-{2-[(tert-butyldimethylsilyl)oxy]-1,4,4-trimethylcyclohex-2-en-1-yl}prop-2-yn-1-one (2.3.9b)

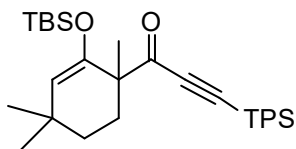
Synthesized according to GP7 from **2.3.8b** (0.23g, 72 % yield).

¹H NMR (400 MHz, CHLOROFORM-*d*) δ ppm = 4.62 (s, 1 H), 2.33-2.24 (m, 1 H), 1.50-1.39 (m, 3 H), 1.26 (s, 3 H), 1.07 (s, 3 H), 1.01 (s, 3 H), 0.95 (s, 9 H), 0.86 (s, 9 H), 0.17 (s, 3 H), 0.15 (s, 6 H), 0.12 (s, 3 H).

¹³C NMR (101 MHz, CHLOROFORM-*d*) δ ppm = 190.98 (C), 149.54 (C), 114.40 (CH), 101.77 (C), 95.95 (C), 54.08 (C), 33.25 (CH₂), 32.33 (C), 31.39 (CH₃), 30.64 (CH₂), 29.34 (CH₃), 26.05 (3x CH₃), 25.59 (3xCH₃), 19.59 (CH₃), 18.08 (C), 16.66 (C), -4.28 (CH₃), -5.10 (2xCH₃), -5.12 (CH₃).

HRMS (EI) m/z calcd for C₂₄H₄₄O₂Si₂ is 420.2880 found 420.2788.

FTIR (Neat, cm⁻¹): ν = 2939 (m), 1681 (s), 1652 (s).



1-{2-[(tert-butyldimethylsilyl)oxy]-1,4,4-trimethylcyclohex-2-en-1-yl}-3-(triphenylsilyl)prop-2-yn-1-one (2.3.9c)

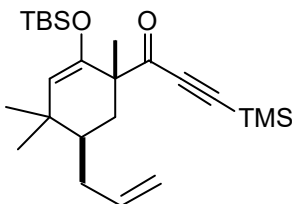
Synthesized according to GP7 from **2.3.8c** (0.41g, 72 %).

¹H NMR (400 MHz, CHLOROFORM-*d*) δ ppm = 7.66-7.62 (m, 6 H), 7.47 - 7.35 (m, 9 H), 4.66 (s, 1 H), 2.38-2.29 (m, 1 H), 1.48-1.42 (m, 3 H), 1.31 (s, 3 H), 0.99 (s, 3 H), 0.90 (s, 3 H), 0.82 (s, 9 H), 0.09 (s, 3 H), 0.06 (s, 3 H).

¹³C NMR (101 MHz, CHLOROFORM-*d*) δ ppm = 190.75 (C), 149.30 (C), 135.68 (6xCH), 131.91 (3xC), 130.28 (3xCH), 128.08 (6xCH), 114.65 (CH), 104.05 (C), 91.77 (C), 54.21 (C), 33.20 (CH₂), 32.31 (C), 31.41 (CH₃), 30.58 (CH₂), 29.27 (CH₃), 25.57 (3xCH₃), 19.62 (CH₃), 18.05 (C), -4.31 (CH₃), -5.14 (CH₃).

HRMS (EI) m/z calcd for C₃₆H₄₄O₂Si₂ is 564.2880 found 564.2895.

FTIR (Neat, cm⁻¹): ν = 2927 (m), 1681 (s), 1654 (s).



1-{2-[(tert-butyldimethylsilyl)oxy]-1,4,4-trimethyl-5-(prop-2-en-1-yl)cyclohex-2-en-1-yl}-3-(trimethylsilyl)prop-2-yn-1-one (2.3.9d)

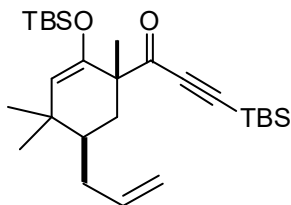
Synthesized according to GP7 from **2.3.8d** (0.45g, 90 % yield).

¹H NMR (400 MHz, CHLOROFORM-*d*) δ ppm = 5.76-5.66 (m, 1 H), 5.04-4.97 (m, 2 H), 4.65 (s, 1 H), 2.32-2.25 (m, 1 H), 2.05 (dd, J =14.0, 2.2 Hz, 1 H), 1.64-1.55 (m, 3 H), 1.30 (s, 3 H), 1.04 (s, 3 H), 0.87 (s, 9 H), 0.83 (s, 3 H), 0.23 (s, 9 H), 0.18 (s, 3 H), 0.17 (s, 3 H).

¹³C NMR (101 MHz, CHLOROFORM-*d*) δ ppm = 191.13 (C), 148.78 (C), 137.92 (CH), 117.39 (CH), 115.88 (CH₂), 101.15 (C), 98.98 (C), 53.77 (C), 39.91 (CH), 36.65 (CH₂), 35.06 (C), 34.19 (CH₂), 29.29 (CH₃), 25.72 (3xCH₃), 23.18 (CH₃), 22.34 (CH₃), 18.18 (C), -0.75 (3xCH₃), -4.21 (CH₃), -4.95 (CH₃).

HRMS (EI) m/z calcd for C₂₄H₄₂O₂Si₂ [(M-C₄H₉)⁺] 361.2014, found 361.2039.

FTIR (Neat, cm⁻¹): ν = 2957 (m), 2354 (m), 1650 (s), 827 (s).



3-(tert-butyldimethylsilyl)-1-{2-[(tert-butyldimethylsilyl)oxy]-1,4,4-trimethyl-5-(prop-2-en-1-yl)cyclohex-2-en-1-yl}prop-2-yn-1-one (2.2.8)

Synthesized according to GP7 from **2.3.8e** (0.31g, 88 % yield).

¹H NMR (400 MHz, CHLOROFORM-*d*) δ ppm = 5.75-5.66 (m, 1 H), 5.03-4.96 (m, 2 H), 4.65 (s, 1 H), 2.30-2.25 (m, 1 H), 2.07 (dd, J = 14.2, 2.6 Hz, 1 H), 1.64-1.50 (m, 2 H), 1.37-1.29 (m, 1 H), 1.32 (s, 3 H), 1.02 (s, 3 H), 0.96 (s, 9 H), 0.87 (s, 9 H), 0.82 (s, 3 H), 0.18 (s, 3 H), 0.17 (s, 9 H).

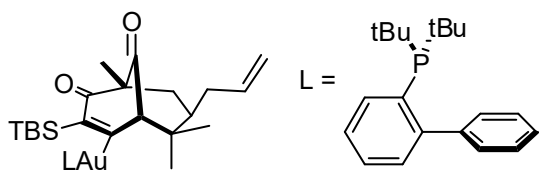
¹³C NMR (101 MHz, CHLOROFORM-*d*) δ ppm = 190.72 (C), 148.66 (C), 137.86 (CH), 117.55 (CH), 115.99 (CH₂), 101.72 (C), 97.59 (C), 53.83 (C), 39.99 (CH), 36.56 (CH₂), 35.04 (C), 34.13 (CH₂), 29.27 (CH₃), 26.07 (3xCH₃), 25.76 (3xCH₃), 23.21 (CH₃), 22.48 (CH₃), 18.18 (C), 16.64 (C), -4.27 (CH₃), -4.84 (CH₃), -5.12 (2xCH₃).

HRMS (EI) m/z calcd for $C_{27}H_{48}O_2Si_2$ is 460.3193, found 460.3235.

FTIR (Neat, cm^{-1}): ν = 2929 (m), 2358 (w), 1672 (s), 823 (s) .

7.1.8 Vinylgold formation

General procedure (GP8): Add LAu(I) (0.2 mmol) to the silyl enol ether (0.61 mmol) diluted in freshly distilled DCM (4 ml) at room temperature and stirred for 30 minutes. Evaporate the solvent under reduce pressure and the crude product was purified by flash column chromatography on silica gel (eluted with hexane:ethyl acetate (90:10)) to give the desired vinyl gold species as a white solid.



[3-(tert-butyldimethylsilyl)-5,8,8-trimethyl-4,9-dioxo-7-(prop-2-en-1-yl)bicyclo[3.3.1]non-2-en-2-yl]gold[di-tert-butyl(2-phenylphenyl)phosphine] (2.2.10)

Synthesized according to GP8 from **2.2.8** (59 mg, 50 % yield).

1H NMR (400 MHz, $CHCl_3-d$) δ ppm = 7.89 (t, J = 6.9 Hz, 1H), 7.48-7.38 (m, 3 H), 7.22-7.12 (m, 3H), 7.03 (d, J = 7.5 Hz, 1H), 6.92 (7, J = 7.4 Hz, 1H), 5.61-5.50 (m, 1 H), 4.93-4.88 (m, 2 H), 3.37 (d, J = 7.5 Hz, 1H), 2.17-2.12 (m, 1 H), 1.89 (dd, J = 13.4,

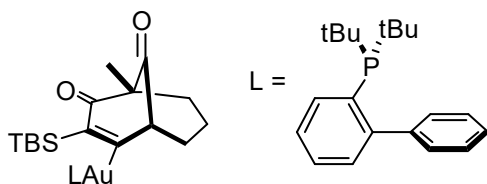
4.2 Hz, 1 H), 1.66-1.35 (m, 2 H), 1.47 (d, $J = 14.2$ Hz, 9 H), 1.39 (d, $J = 14.5$ Hz, 9 H), 1.20 (s, 3 H), 1.19 (s, 3 H), 0.84 (s, 12 H), 0.36 (s, 3 H), 0.22 (s, 3 H).

^{13}C NMR (101 MHz, CHLOROFORM-*d*) δ ppm = 220.65 (d, $J = 111.9$ Hz, C), 210.65 (d, $J = 3.3$ Hz, C), 204.83 (d, $J = 13.2$ Hz, C), 150.18 (d, $J = 15.5$ Hz, C), 147.09 (d, $J = 4.7$ Hz, C), 142.28 (d, $J = 5.2$ Hz, C), 137.36 (CH), 134.65 (CH), 133.21 (d, $J = 7.5$ Hz, CH), 130.04 (d, $J = 2.3$ Hz, CH), 129.17 (CH), 129.12 (CH), 129.04 (CH), 128.43 (CH), 127.89 (d, $J = 33.4$ Hz, C), 127.58 (CH), 126.28 (d, $J = 5.2$ Hz, CH), 115.97 (CH₂), 75.57 (CH), 61.31 (C), 42.88 (CH₂), 41.74 (C), 37.68 (CH), 36.84 (d, $J = 11.8$ Hz, C), 36.66 (d, $J = 9.9$ Hz, C), 33.80 (CH₂), 30.77 (d, $J = 7.0$ Hz, 3xCH₃), 30.54 (d, $J = 7.1$ Hz, 3xCH₃), 28.81 (CH₃), 27.96 (3xCH₃), 21.73 (CH₃), 17.99 (C), 15.84 (CH₃), 1.39 (CH₃), -2.34 (CH₃)

HRMS (ESI) m/z calcd for C₄₁H₆₀O₂PSiAu [(M+Na⁺) 863.3652, found 863.3663.

FTIR (Neat, cm⁻¹): $\nu = 2960$ (m) 1704 (s), 1631 (s), 904 (s), 731 (s).

M.p. (Dec. 231 °C).



[3-(tert-butyldimethylsilyl)-5-methyl-4,9-dioxobicyclo[3.3.1]non-2-en-2-yl]gold[di-tert-butyl(2-phenylphenyl)phosphine] (2.4.1a)

Synthesized according to GP8 from **2.3.6a** (215 mg, 84 % yield).

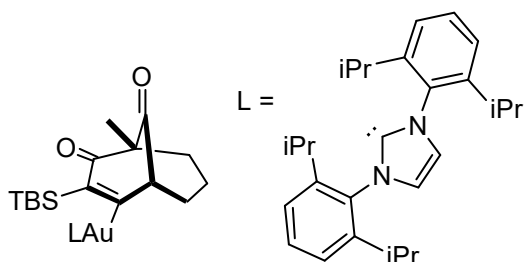
¹H NMR (400 MHz, CHLOROFORM-*d*) δ ppm = 7.92-7.87 (m, 1 H), 7.52-7.42 (m, 3 H), 7.24-7.20 (m, 3 H), 7.13-7.07 (m, 2 H), 3.55-3.52 (m, 1 H), 2.02-1.96 (m, 1 H), 1.87-1.78 (m, 2 H), 1.54-1.46 (m, 2 H), 1.44 (d, J = 1.5 Hz, 9 H), 1.40 (d, J = 1.5 Hz, 9 H), 1.38-1.28 (m, 1 H), 1.17 (s, 3 H), 0.86 (s, 9 H), 0.34 (s, 3 H), 0.21 (s, 3 H).

¹³C NMR (101 MHz, CHLOROFORM-*d*) δ ppm = 219.56 (d, J = 109.8 Hz, C), 213.52 (d, J = 3.3 Hz, C), 205.26 (d, J = 12.7 Hz, C), 150.08 (d, J = 15.9 Hz, C), 145.07 (d, J = 5.1 Hz, C), 142.52 (d, J = 5.2 Hz, C), 134.57 (CH), 133.42 (d, J = 7.6 Hz, CH), 130.07 (d, J = 2.0 Hz, CH), 129.23 (CH), 129.21 (CH), 128.96 (CH), 128.62 (CH), 127.78 (d, J = 33.9 Hz, C), 127.48 (CH), 126.41 (d, J = 5.1 Hz, CH), 62.13 (CH), 61.96 (C), 42.04 (CH₂), 37.55 (d, J = 20.3 Hz, C), 36.70 (d, J = 17.9 Hz, C), 30.76 (d, J = 6.2 Hz, 3xCH₃), 30.70 (d, J = 6.4 Hz, 3xCH₃), 30.38 (CH₂), 28.12 (3xCH₃), 18.02 (CH₂), 17.72 (C), 16.00 (CH₃), 0.35 (CH₃), -2.17 (CH₃).

HRMS (EI) m/z calcd for C₃₆H₅₂O₂P₁Si₁Au₁ [(M-C₄H₉)⁺] is 715.2424, found 715.2472.

FTIR (Neat, cm⁻¹): ν = 2927 (m), 1703 (s), 1086 (s).

M.p. (Dec. 215 °C).



[3-(tert-butyldimethylsilyl)-5,8,8-trimethyl-4,9-dioxobicyclo[3.3.1]non-2-en-2-yl]gold[1,3-bis(2,6-diisopropylphenyl)imidazol-2-ylidene] (2.4.1b)

Synthesized according to GP8 from **2.3.6a** (22 mg, 63 % yield).

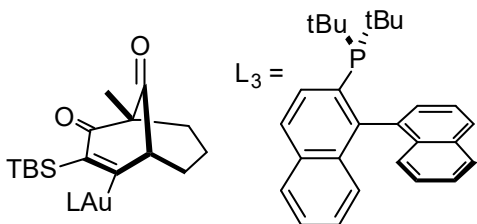
¹H NMR (400 MHz, CHLOROFORM-*d*) δ ppm = 7.49 (t, *J* = 7.8 Hz, 2 H), 7.32-7.27 (m, 4 H), 7.19 (s, 2 H), 3.17-3.14 (m, 1 H), 2.66-2.57 (m, 4 H), 1.74-1.68 (m, 1 H), 1.62-1.58 (m, 1 H), 1.34 (d, *J* = 6.8 Hz, 6 H), 1.30 (d, *J* = 6.8 Hz, 6 H), 1.21 (d, *J* = 6.8 Hz, 6 H), 1.18 (d, *J* = 6.8 Hz, 6 H), 1.15-1.08 (m, 2 H), 1.00 (s, 3 H), 0.91-0.80 (m, 2 H), 0.65 (s, 9 H), -0.09 (s, 3 H), -0.24 (s, 3 H).

¹³C NMR (101 MHz, CHLOROFORM-*d*) δ ppm = 216.5 (C), 214.4 (C), 204.5 (C), 194.3 (C), 146.5 (C), 145.6 (2xC), 145.5 (2xC), 134.7 (2xC), 130.4 (2xCH), 124.2 (2xCH), 124.1 (2xCH), 123.3 (2xCH), 62.3 (CH), 62.2 (C), 41.9 (CH₂), 30.4 (CH₂), 28.8 (2xCH), 28.7 (2xCH), 28.0 (3xCH₃), 24.5 (2xCH₃), 24.5 (2xCH₃), 23.9 (2xCH₃), 23.8 (2xCH₃), 17.9 (CH₂), 17.2 (C), 16.1 (CH₃), -1.0 (CH₃), -2.4 (CH₃).

HRMS (ESI) *m/z* calcd for C₄₃H₆₁O₂N₂SiAu is 862.4168, found 862.4193.

FTIR (Neat, cm⁻¹): ν = 2962 (m), 2927 (m), 1708 (s), 1635 (s), 1458 (s).

M.p. (Dec. 254 °C) .



[5,8,8-trimethyl-4,9-dioxo-2-(tri-tert-butylsilyl)bicyclo[3.3.1]non-2-en-3-yl]gold[

di-tert-butyl[1-(naphthalen-1-yl)naphthalen-2-yl]phosphine] (2.4.1c)

Synthesized according to GP8 from **2.3.6a** (69 mg, 70 % yield), mixture of diastereomer (1:1).

Diastereomer 1:

¹H NMR (400 MHz, CHLOROFORM-*d*) δ ppm = 8.10-7.09 (m, 11 H), 6.87 (d, J =9.4 Hz, 1 H), 6.73 (d, J =9.2 Hz, 1 H), 3.65 (s, 1 H), 1.96-1.26 (m, 6 H), 1.48 (d, J =14.9 Hz, 9 H), 1.42 (d, J =14.4 Hz, 9 H), 1.21 (s, 3 H), 0.71 (s, 9 H), 0.04 (s, 3 H), -0.79 (s, 3 H).

¹³C NMR (101 MHz, CHLOROFORM-*d*) δ ppm = 219.55 (d, J = 110.1 Hz, C), 213.60 (d, J = 3.4 Hz, C), 205.27 (d, J = 13.1 Hz, C), 147.43 (d, J = 15.9 Hz, C), 144.96 (d, J = 5.6 Hz, C), 136.52 (d, J = 7.1 Hz, C), 134.40 (d, J = 8.4 Hz, C), 133.94 (C), 133.69 (d, J = 1.7 Hz, C), 133.32 (C), 129.88 (CH), 129.28 (CH), 128.90 (CH), 128.74 (CH), 128.30 (d, J = 1.2 Hz, CH), 127.80 (CH), 127.39 (CH), 127.17 (d, J = 34.0 Hz, C), 127.14 (d, J = 5.1 Hz, CH), 126.75 (CH), 126.42 (CH), 126.24 (CH), 125.94 (CH), 125.88 (CH), 62.29 (CH), 62.19 (C), 42.15 (CH₂), 37.94 (d, J = 20.2 Hz, C), 36.58 (d, J = 17.5 Hz, C), 31.28 (d, J = 7.5 Hz, 3xCH₃), 30.87 (d, J = 6.7 Hz, 3xCH₃), 30.35 (CH₂), 27.94 (3xCH₃), 17.97 (CH₂), 17.66 (C), 16.07 (CH₃), -1.27 (CH₃), -2.72 (CH₃).

Diastereomer 2:

¹H NMR (400 MHz, CHLOROFORM-*d*) δ ppm = 8.10-7.09 (m, 11 H), 6.89 (d, J =8.9 Hz, 1 H), 6.70 (d, J =8.7 Hz, 1 H), 2.18 (s, 1 H), 1.96-1.26 (m, 6 H), 1.49 (d, J =14.4 Hz, 9 H), 1.39 (d, J =14.4 Hz, 9 H), 1.12 (s, 3 H), 0.82 (s, 9 H), 0.40 (s, 3 H), 0.08 (s, 3 H).

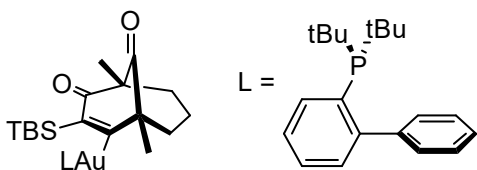
¹³C NMR (101 MHz, CHLOROFORM-*d*) δ ppm = 218.93 (d, J = 110.6 Hz, C), 213.50 (d, J = 3.8 Hz, C), 205.24 (d, J = 13.2 Hz, C), 147.37 (d, J = 15.5 Hz, C), 145.31 (d, J = 5.1 Hz, C), 136.42 (d, J = 6.6 Hz, C), 134.35 (d, J = 9.0 Hz, C), 133.65 (2xC), 133.40

(C), 130.08 (CH), 129.95 (CH), 128.72 (CH), 128.59 (CH), 128.23 (d, $J = 1.2$ Hz, CH), 127.78 (CH), 127.39 (CH), 127.08 (d, $J = 5.9$ Hz, CH), 126.94 (d, $J = 33.0$ Hz, C), 126.73 (CH), 126.10 (CH), 126.00 (CH), 125.97 (CH), 125.88 (CH), 61.94 (C), 60.23 (CH), 41.89 (CH₂), 37.45 (d, $J = 17.9$ Hz, C), 37.29 (d, $J = 17.0$ Hz, C), 31.36 (d, $J = 7.1$ Hz, 3xCH₃), 30.94 (d, $J = 7.10$ Hz, 3xCH₃), 30.27 (CH₂), 28.31 (3xCH₃), 17.87 (CH₂), 17.60 (C), 16.13 (CH₃), 0.14 (CH₃), -1.9 (CH₃).

HRMS (EI) m/z calcd for C₄₄H₅₆O₂PSiAu is 872.3453, found 872.3431.

FTIR (Neat, cm⁻¹): $\nu = 2927$ (m), 1708 (s), 1635 (s), 1458 (s).

M.p. (Dec. 256 °C).



[3-(tert-butyldimethylsilyl)-1,5-dimethyl-4,9-dioxobicyclo[3.3.1]non-2-en-2-yl]gold[di-tert-butyl(2-phenylphenyl)phosphine] (2.4.1d)

Synthesized according to GP8 from **2.3.6h** (52 mg, 55 % yield).

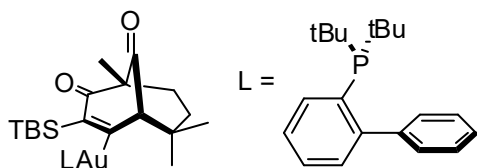
¹H NMR (400 MHz, CHLOROFORM-*d*) δ ppm = 7.93-7.89 (m, 1 H), 7.49-7.42 (m, 2 H), 7.33-7.17 (m, 6 H), 1.86-1.82 (m, 1 H), 1.76-1.72 (m, 1 H), 1.54-1.49 (m, 3 H), 1.47 (d, $J = 4.8$ Hz, 9 H), 1.43 (d, $J = 4.9$ Hz, 9 H), 1.35 (s, 3 H), 1.27-1.24 (m, 1 H), 1.14 (s, 3 H), 0.82 (s, 9 H), 0.38 (s, 3 H), 0.31 (s, 3 H).

^{13}C NMR (101 MHz, CHLOROFORM-*d*) δ ppm = 223.10 (d, J = 107.6 Hz, C), 214.72 (d, J = 4.3 Hz, C), 205.68 (d, J = 12.3 Hz, C), 149.80 (d, J = 15.6 Hz, C), 145.98 (d, J = 4.2 Hz, C), 142.10 (d, J = 5.2 Hz, C), 134.91 (CH), 133.66 (d, J = 7.5 Hz, CH), 130.04 (d, J = 2.4 Hz, CH), 129.80 (br.s, 2xCH), 128.60 (br.s, 2xCH), 127.84 (d, J = 30.4 Hz, C), 127.31 (CH), 127.80 (C), 126.34 (d, J = 5.2 Hz, CH), 60.95 (C), 58.41 (d, J = 1.4 Hz, C), 41.27 (CH₂), 39.09 (CH₂), 37.74 (d, J = 15.2 Hz, C), 37.27 (d, J = 18.4 Hz, C), 30.86 (d, J = 6.6 Hz, 3xCH₃), 30.79 (d, J = 7.4 Hz, 3xCH₃), 28.42 (3xCH₃), 19.07 (CH₂), 17.76 (C), 16.68 (CH₃), 0.61 (CH₃), -0.44 (CH₃).

HRMS (ESI) m/z calcd for C₃₇H₅₄O₂PSiAu is 786.3296, found 786.3263.

FTIR (Neat, cm⁻¹): ν = 2997 (m), 1686 (s), 1089 (s).

M.p. 183-185 °C.



[3-(tert-butyldimethylsilyl)-5,8,8-trimethyl-4,9-dioxobicyclo[3.3.1]non-2-en-2-yl]gold[di-tert-butyl(2-phenylphenyl)phosphine] (2.4.1e)

Synthesized according to GP8 from **2.3.9b** (27 mg, 35 % yield).

^1H NMR (400 MHz, CHLOROFORM-*d*) δ ppm = 7.90 (t, J = 7.0 Hz, 1 H), 7.49-7.41 (m 3 H), 7.24-7.13 (m, 3 H), 7.05-7.02 (m, 1 H), 6.95 (t, J = 7.4 Hz, 1 H), 3.38 (d, J = 2.4 Hz, 1 H), 1.80-1.76 (m, 1 H), 1.62-1.56 (m, 2 H), 1.47 (d, J = 14.3 Hz, 9 H), 1.39 (d, J =

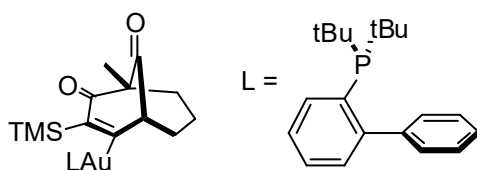
14.5 Hz, 9 H), 1.20 (s, 3 H), 1.13 (s, 3 H), 1.05-1.00 (m, 1 H), 0.97 (s, 3 H), 0.85 (s, 9 H), 0.35 (s, 3 H), 0.19 (s, 3 H).

¹³C NMR (101 MHz, CHLOROFORM-*d*) δ ppm = 221.4 (d, J = 111.1 Hz, C), 211.39 (d, J = 3.3 Hz, C), 205.17 (d, J = 13.3 Hz, C), 150.21 (d, J = 16.3 Hz, C), 146.59 (d, J = 4.7 Hz, C), 142.25 (d, J = 5.2 Hz, C), 134.64 (CH), 133.64 (d, J = 7.6 Hz, CH), 130.02 (d, J = 2.2 Hz, CH), 129.25 (CH), 129.12 (CH), 129.02 (CH), 128.43 (CH), 127.88 (d, J = 33.4 Hz, C), 127.57 (C), 126.25 (d, J = 5.7 Hz, C), 73.92 (CH), 60.00 (C), 39.95 (C), 37.37 (CH₂), 36.86 (d, J = 20.2 Hz, C), 36.68 (d, J = 17.8 Hz, C), 31.63 (CH₂), 30.75 (d, J = 7.1 Hz, 3xCH₃), 30.63 (CH₃), 30.58 (d, J = 7.1 Hz, 3xCH₃), 28.02 (3xCH₃), 26.93 (CH₃), 17.97 (C), 15.88 (CH₃), 1.32 (CH₃), -2.43 (CH₃).

HRMS (EI) m/z calcd for C₃₈H₅₆O₂PSiAu is 800.3453, found 800.3469.

FTIR (Neat, cm⁻¹): ν = 2923 (m), 1708 (s), 1635 (s), 1465 (s).

M.p. (Dec. 186 °C).



[5-methyl-4,9-dioxo-3-(trimethylsilyl)bicyclo[3.3.1]non-2-en-2-yl]gold[di-tert-butyl(2-phenylphenyl)phosphine] (2.4.1f)

Synthesized according to GP8 from **2.3.6c** (21 mg, 77 % yield).

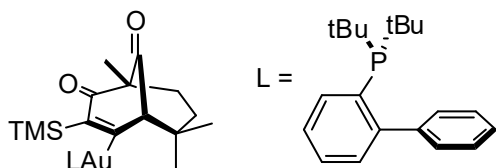
¹H NMR (400 MHz, CHLOROFORM-*d*) δ ppm = 7.89 (t, *J* = 7.2 Hz, 1 H), 7.50-7.40 (m, 3 H), 7.25-7.17 (m, 3 H), 7.13-7.07 (m, 2 H), 3.50-3.48 (m, 1 H), 1.99-1.93 (m, 1 H), 1.86-1.76 (m, 2 H), 1.50-1.45 (m, 2 H), 1.43 (d, *J* = 4.0 Hz, 9 H), 1.39 (d, *J* = 4.2 Hz, 9 H), 1.34-1.28 (m, 1 H), 1.17 (s, 3 H), 0.25 (s, 9 H).

¹³C NMR (101 MHz, CHLOROFORM-*d*) δ ppm = 217.34 (d, *J* = 109.6 Hz, C), 213.78 (d, *J* = 3.7 Hz, C), 205.33 (d, *J* = 12.9 Hz, C), 150.16 (d, *J* = 16.6 Hz, C), 147.40 (d, *J* = 5.1 Hz, C), 142.69 (d, *J* = 5.5 Hz, C), 134.69 (CH), 133.14 (d, *J* = 7.7 Hz, CH), 130.19 (d, *J* = 1.9 Hz, CH), 129.34 (CH), 129.11 (CH), 129.01 (CH), 128.77 (CH), 127.94 (d, *J* = 33.7 Hz, C), 127.62 (CH), 126.57 (d, *J* = 5.2 Hz, CH), 62.22 (C), 61.94 (CH), 41.90 (CH₂), 37.56 (d, *J* = 19.7 Hz, C), 36.97 (d, *J* = 18.3 Hz, C), 30.90 (d, *J* = 4.4 Hz, 3xCH₃), 30.83 (d, *J* = 4.4 Hz, 3xCH₃), 30.25 (CH₂), 18.03 (CH₂), 16.03 (CH₃), 1.92 (3x CH₃).

HRMS (ESI) *m/z* calcd for C₃₃H₄₆O₂PSiAu is 730.2670, found 730.2657.

FTIR (Neat, cm⁻¹): ν = 2943 (m), 1699 (s), 1633 (s), 1085 (m).

M.p. (Dec. 219 °C).



[5,8,8-trimethyl-4,9-dioxo-3-(trimethylsilyl)bicyclo[3.3.1]non-2-en-2-yl]gold[di-tert-butyl(2-phenylphenyl)phosphine] (2.4.1g)

Synthesized according to GP8 from **2.3.9a** (34 mg, 74 % yield).

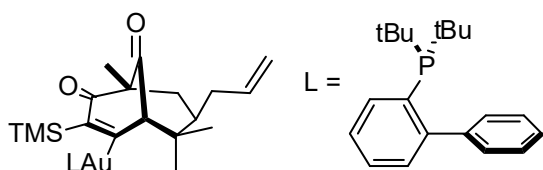
¹H NMR (400 MHz, CHLOROFORM-*d*) δ ppm = 7.91-7.87 (m, 1 H), 7.49-7.42 (m, 2 H), 7.39 (t, *J* = 7.7 Hz, 1 H), 7.23-7.15 (m, 3 H), 7.02 (d, *J* = 7.7 Hz, 1 H), 6.95 (t, *J* = 7.5 Hz, 1 H), 3.30 (d, *J* = 2.5 Hz, 1 H), 1.78-1.72 (m, 1 H), 1.65-1.50 (m, 3 H), 1.46 (d, *J* = 14.4 Hz, 1 H), 1.39 (d, *J* = 14.5 Hz, 9 H), 1.20 (s, 3 H), 1.09 (s, 3 H), 0.96 (s, 3 H), 0.24 (s, 9 H).

¹³C NMR (101 MHz, CHLOROFORM-*d*) δ ppm = 219.36 (d, *J* = 111.7 Hz, C), 211.2 (d, *J* = 3.3 Hz, C), 204.7 (d, *J* = 13.1 Hz, C), 150.18 (d, *J* = 16.0 Hz, C), 149.02 (d, *J* = 4.8 Hz, C), 142.32 (d, *J* = 5.6 Hz, C), 134.64 (CH), 133.11 (d, *J* = 7.5 Hz, CH), 130.02 (d, *J* = 1.9 Hz, CH), 129.09 (CH), 129.03 (CH), 128.76 (CH), 128.62 (CH), 127.81 (d, *J* = 33.3 Hz, C), 127.64 (CH), 126.28 (CH), 73.36 (CH), 60.45 (C), 39.56 (C), 36.88 (d, *J* = 19.2 Hz, C), 36.78 (CH₂), 36.70 (d, *J* = 16. Hz, C), 31.47 (CH₂), 30.7 (d, *J* = 7.1 Hz, 3xCH₃), 30.61 (CH₃), 30.60 (d, *J* = 7.2 Hz, 3xCH₃), 26.77 (CH₃), 15.89 (CH₃), 2.28 (3x CH₃)

HRMS (ESI) *m/z* calcd for C₃₅H₅₀O₂PSiAu is 58.2983, found 758.2966.

FTIR (Neat, cm⁻¹): ν = 2923 (m), 1704 (s), 1627 (s), 1454 (m).

M.p. (Dec. 185 °C).



[5,8,8-trimethyl-4,9-dioxo-7-(prop-2-en-1-yl)-3-(trimethylsilyl)bicyclo[3.3.1]non-2-en-2-yl]gold[di-tert-butyl(2-phenylphenyl)phosphine] (2.4.1h)

Synthesized according to GP8 from **2.3.9d** (20 mg, 69 % yield).

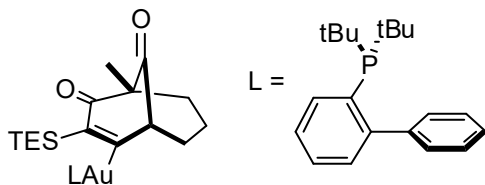
¹H NMR (400 MHz, CHLOROFORM-*d*) δ ppm = 7.91-7.87 (m, 1H), 7.48-7.42 (m, 2 H), 7.37 (t, *J* = 7.5 Hz, 1H), 7.23-7.15 (m, 3H), 7.02 (d, *J* = 7.7 Hz, 1H), 6.94 (d, *J* = 7.5 Hz, 1H), 5.62-5.53 (m, 1 H), 4.95-4.89 (m, 2 H), 3.29 (d, *J* = 2.7 Hz, 1H), 2.15-2.11 (m, 1 H), 1.86 (dd, *J* = 13.0, 2.5 Hz, 1 H), 1.58-1.51 (m, 2 H), 1.46 (d, *J* = 14.3 Hz, 9 H), 1.39 (d, *J* = 14.5 Hz, 9 H), 1.20 (s, 3 H), 1.16 (s, 3 H), 0.91-0.85 (m, 1 H), 0.83 (s, 3 H), 0.24 (s, 9 H).

¹³C NMR (101 MHz, CHLOROFORM-*d*) δ ppm = 218.42 (d, *J* = 112.7 Hz, C), 210.70 (d, *J* = 3.4 Hz, C), 204.38 (d, *J* = 13.2 Hz, C), 150.30 (d, *J* = 16.6 Hz, C), 149.89 (d, *J* = 4.8 Hz, C), 142.45 (d, *J* = 5.3 Hz, C), 137.56 (CH), 134.76 (CH), 133.27 (d, *J* = 7.4 Hz, CH), 130.14 (d, *J* = 2.2 Hz, CH), 129.18 (CH), 129.12 (CH), 128.95 (CH), 128.77 (CH), 127.91 (d, *J* = 33.6 Hz, C), 127.76 (CH), 126.38 (d, *J* = 5.1 Hz, CH), 115.79 (CH₂), 75.09 (CH), 61.86 (C), 42.53 (CH₂), 41.59 (C), 37.48 (CH), 36.99 (d, *J* = 13.2 Hz, C), 36.80 (d, *J* = 11.3 Hz, C), 33.77 (CH₂), 30.90 (d, *J* = 7.2 Hz, 3xCH₃), 30.7 (d, *J* = 7.0 Hz, 3xCH₃), 28.91 (CH₃), 21.83 (CH₃), 15.95 (CH₃), 2.35 (3xCH₃).

HRMS (ESI) *m/z* calcd for C₃₈H₅₄O₂PSiAu is 798.3296, found 798.3286.

FTIR (Neat, cm⁻¹): ν = 2923 (s), 1701 (s), 1627 (s), 1461 (m).

M.p. (Dec. 222 °C).



[5-methyl-4,9-dioxo-3-(triethylsilyl)bicyclo[3.3.1]non-2-en-2-yl]gold[di-tert-butyl(2-phenylphenyl)phosphine] (2.4.1i)

Synthesized according to GP8 from **2.3.6b** (64 mg, 83 % yield).

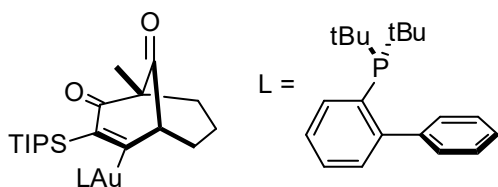
¹H NMR (400 MHz, CHLOROFORM-*d*) δ ppm = 7.90-7.86 (m, 1 H), 7.51-7.41 (m, 3 H), 7.25-7.17 (m, 3 H), 7.13-7.05 (m, 2 H), 3.48-3.46 (m, 1H), 1.99-1.93 (m, 1 H), 1.84-1.75 (m, 2 H), 1.48-1.43 (m, 2 H), 1.43 (d, J = 2.6 Hz, 9 H), 1.38 (d, J = 2.4 Hz, 9 H), 1.32-1.27 (m, 1 H), 1.14 (s, 3 H), 0.90-0.83 (m, 12 H), 0.76-0.68 (m, 3 H).

¹³C NMR (101 MHz, CHLOROFORM-*d*) δ ppm = 218.73 (d, J = 109.7 Hz, C), 213.75 (d, J = 3.1 Hz, C), 205.29 (d, J = 13.2 Hz, C), 150.09 (d, J = 16.5 Hz, C), 144.53 (d, J = 5.2 Hz, C), 142.42 (d, J = 5.7 Hz, C), 134.62 (CH), 133.08 (d, J = 7.5 Hz, CH), 130.07 (d, J = 1.9 Hz, CH), 129.12 (2xCH), 128.87 (CH), 128.66 (CH), 127.67 (d, J = 33.5 Hz, C), 127.61 (CH), 127.43 (CH), 61.98 (CH), 61.87 (C), 41.83 (CH₂), 37.56 (d, J = 20.3 Hz, C), 36.76 (d, J = 18.4 Hz, C), 30.75 (d, J = 6.6 Hz, 3xCH₃), 30.48 (CH₂), 30.43 (d, J = 7.0 Hz, 3xCH₃), 17.99 (CH₂), 16.00 (CH₃), 7.82 (3xCH₃), 5.07 (3xCH₂).

HRMS (ESI) m/z calcd for C₃₆H₅₂O₂PSiAu is 772.3140, found 772.3169.

FTIR (Neat, cm⁻¹): ν = 2941 (m), 1703 (s), 1093 (s).

M.p. (Dec. 204 °C).



[5-methyl-4,9-dioxo-3-[tris(propan-2-yl)silyl]bicyclo[3.3.1]non-2-en-2-yl]gold[di-tert-butyl(2-phenylphenyl)phosphine] (2.4.1j)

Synthesized according to GP8 from **2.3.6d** (34 mg, 30 % yield).

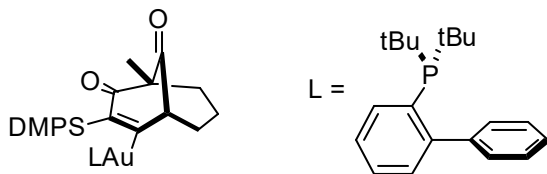
¹H NMR (400 MHz, CHLOROFORM-*d*) δ ppm = 7.94-7.90 (m, 1 H), 7.67-7.62 (m, 1 H), 7.50-7.43 (m, 2 H), 7.29-7.19 (m, 4 H), 7.10-7.07 (m, 1 H), 3.58-3.56 (m, 1 H), 2.04-1.98 (m, 1 H), 1.89-1.83 (m, 2 H), 1.77 (sept, J = 7.5 Hz, 3 H), 1.50-1.47 (m, 1 H), 1.42 (d, J = 11.4 Hz, 9 H), 1.39 (d, J = 11.7 Hz, 9 H), 1.15 (s, 3 H), 1.06-1.04 (m, 2 H), 1.00 (d, J = 7.5 Hz, 9 H), 0.99 (d, J = 7.5 Hz, 9 H).

¹³C NMR (101 MHz, CHLOROFORM-*d*) δ ppm = 218.07 (d, J = 109.8 Hz, C), 213.69 (d, J = 3.3 Hz, C), 206.00 (d, J = 13.3 Hz, C), 150.26 (d, J = 15.6 Hz, C), 143.78 (d, J = 5.8 Hz, C), 142.28 (d, J = 5.3 Hz, C), 134.95 (CH), 133.59 (d, J = 7.3 Hz, CH), 130.19 (d, J = 2.2 Hz, CH), 129.53 (CH), 129.25 (CH), 129.12 (CH), 128.85 (CH), 127.96 (CH), 127.36 (d, J = 32.7 Hz, C), 126.38 (d, J = 5.1 Hz, CH), 61.93 (C), 61.62 (CH), 41.12 (CH₂), 38.04 (d, J = 19.8 Hz, C), 36.82 (d, J = 18.0 Hz, C), 31.07 (d, J = 6.5 Hz, 3xCH₃), 30.17 (d, J = 6.95 Hz, 3xCH₃), 29.72 (CH₂), 19.52 (3xCH₃), 19.31 (3xCH₃), 18.08 (CH₂), 16.22 (CH₃), 12.66 (3xCH₃).

HRMS (ESI) m/z calcd for C₃₉H₅₈O₂PSiAu is 814.3609, found 814.3639.

FTIR (Neat, cm⁻¹): ν = 2931 (m), 1696 (s), 1089 (s).

M.p. (Dec. 180 °C).



[3-[dimethyl(phenyl)silyl]-5-methyl-4,9-dioxobicyclo[3.3.1]non-2-en-2-yl]gold[di-tert-butyl(2-phenylphenyl)phosphine] (2.4.1k)

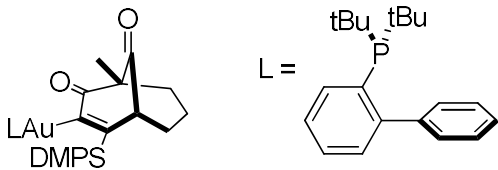
Synthesized according to GP8 from **2.3.6e** (20 % yield).

¹H NMR (400 MHz, CHLOROFORM-*d*) δ ppm = 7.87-7.83 (m, 1 H), 7.54-7.52 (m, 2 H), 7.47-7.40 (m, 3 H), 7.27-7.11 (m, 7 H), 7.06-7.04 (m, 1 H), 3.53-3.51 (m, 1 H), 2.05-1.98 (m, 1 H), 1.87-1.77 (m, 2 H), 1.72-1.43 (m, 3H), 1.39 (d, J = 14.3 Hz, 9 H), 1.29 (d, J = 14.8 Hz, 9 H), 1.12 (s, 3 H), 0.54 (s, 3 H), 0.50 (s, 3 H).

¹³C NMR (101 MHz, CHLOROFORM-*d*) δ ppm 219.27 (d, J = 108.8 Hz, C), 213.55 (d, J = 3.3 Hz, C), 204.79 (d, J = 12.7 Hz, C), 150.01 (d, J = 16.0 Hz, C), 145.24 (d, J = 4.7 Hz, C), 142.55 (d, J = 5.2 Hz, C), 141.60 (C), 134.58 (CH), 133.83 (2xCH), 133.06 (d, J = 7.6 Hz, CH), 130.10 (d, J = 1.9 Hz, CH), 129.21 (CH), 129.06 (CH), 128.95 (CH), 128.70 (CH), 127.79 (CH), 127.70 (d, J = 35.9 Hz, C), 127.63 (CH), 127.11 (2xCH), 126.49 (d, J = 5.2 Hz, CH), 61.99 (C), 61.89 (CH), 41.79 (CH₂), 37.46 (d, J = 20.4 Hz, C), 36.77 (d, J = 18.4 Hz, C), 30.74 (d, J = 7.1 Hz, 3xCH₃), 30.61 (d, J = 7.1 Hz, 3xCH₃), 30.37 (CH₂), 18.04 (CH₂), 15.88 (CH₃), 2.24 (CH₃), 0.76 (CH₃).

HRMS (ESI) m/z calcd for C₃₈H₄₈O₂PSiAu is 792.2827, found 792.2801.

FTIR (Neat, cm⁻¹): ν = 2993 (w), 1693 (s), 1669 (s), 1086 (s).



[2-[dimethyl(phenyl)silyl]-5-methyl-4,9-dioxobicyclo[3.3.1]non-2-en-3-yl]gold[di-tert-butyl(2-phenylphenyl)phosphine] (2.4.2a)

Synthesized according to GP8 from **2.3.6e** (14 mg, 27 % yield).

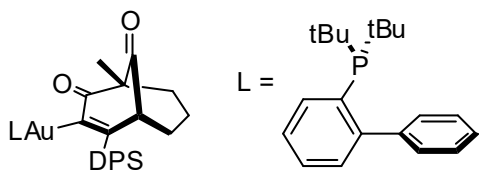
¹H NMR (400 MHz, CHLOROFORM-*d*) δ ppm = 7.89-7.84 (m, 1 H), 7.59-7.35 (m, 6 H), 7.23-7.05 (m, 7 H), 3.44-3.42 (m, 1 H), 1.99-1.91 (m, 1 H), 1.87-1.75 (m, 2 H), 1.65-1.45 (m, 3 H), 1.42-1.36 (m, 18 H), 1.15-1.14 (m, 3 H), 0.41-0.39 (m, 3 H), 0.34-0.32 (m, 3 H).

¹³C NMR (101 MHz, CHLOROFORM-*d*) δ ppm 215.60 (C), 213.79 (C), 204.84 (d, J = 57.6 Hz, C), 150.11 (d, J = 5.8 Hz, C), 143.41 (C), 142.85 (C), 142.51 (C), 134.57 (2xCH), 132.98 (d, J = 8.0 Hz, CH), 132.88 (d, J = 8.0 Hz, CH), 130.03 (d, J = 6.6 Hz, CH), 129.23 (d, J = 7.1 Hz, CH), 129.07 (CH), 128.91 (CH), 128.67 (2xCH), 128.30 (d, J = 25.7 Hz, C), 127.59 (CH), 127.29 (CH), 126.45 (CH), 62.01 (d, J = 38.2 Hz, C), 61.62 (d, J = 7.0 Hz, CH), 41.95 (CH₂), 41.49 (CH₂), 37.51-36.68 (m, 2xC), 30.81-20.32 (m, 6xCH₃), 29.73 (CH₂), 29.57 (C), 15.75 (d, J = 28.1 Hz, CH₃), 12.85 (CH₃), 4.74 (d, J = 12.1 Hz, CH₃).

HRMS (ESI) m/z calcd for C₃₈H₄₈O₂PSiAu is [(M+Na⁺)] 815.2821, found 815.2725.

FTIR (Neat, cm⁻¹) : ν = 2993 (w), 1693 (s), 1669 (s), 1086 (s).

M.p. 50-53 °C.



[2-(tert-butyldiphenylsilyl)-5-methyl-4,9-dioxobicyclo[3.3.1]non-2-en-3-yl]gold[di-tert-butyl(2-phenylphenyl)phosphine] (2.4.2b)

Synthesized according to GP8 from **2.3.6e** (13 mg, 25 % yield).

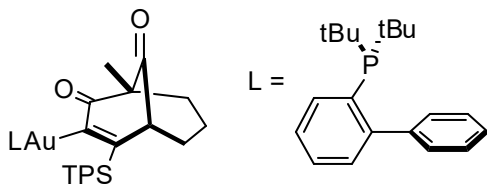
¹H NMR (400 MHz, CHLOROFORM-*d*) δ ppm = 7.82-7.78 (m, 1H), 7.65-7.63 (m, 2H), 7.40-7.32 (m, 4H), 7.27-7.22 (m, 6H), 7.21-7.17 (m, 3H), 7.15-7.09 (m, 3H), 3.54-3.52 (m, 1H), 2.04-1.99 (m, 1H), 1.70-1.57 (m, 2H), 1.52-1.49 (m, 2H), 1.47-1.44 (m, 1H), 1.34 (s, 3H), 1.32-1.28 (m, 9H), 1.26 (s, 9H), 0.91-0.78 (m, 9H).

¹³C NMR (101 MHz, CHLOROFORM-*d*) δ ppm = 213.36 (C), 209.26 (C), 189.1 (d, J = 104.6 Hz, C), 158.90 (C), 150.00 (d, J = 15.0 Hz, C), 142.46 (C), 137.21 (CH), 136.70 (2xCH), 136.62 (d, J = 41.7 Hz, C), 134.50 (CH), 133.11 (CH), 129.66 (CH), 129.50 (CH), 129.06 (C), 128.59 (d, J = 9.3 Hz, CH), 128.33 (C), 128.08 (CH), 127.35 (4xCH), 127.15 (4xCH), 126.27 (CH), 125.94 (CH), 62.82 (C), 55.26 (CH), 42.52 (CH₂), 37.90 (C), 36.18 (C), 30.84 (3xCH₃), 30.21 (3xCH₃), 30.05 (3xCH₃), 29.75 (CH₂), 19.33 (C), 17.95 (CH₂), 17.03 (CH₃).

HRMS (ESI) m/z calcd for C₄₆H₅₆O₂PSiAu is 896.3453, found 896.3432.

FTIR (Neat, cm⁻¹): ν = 3072 (w) 2927 (m) 1669 (s) 1653 (s) 1086 (s).

M.p. (Dec. 267 °C).



[5-methyl-4,9-dioxo-2-(triphenylsilyl)bicyclo[3.3.1]non-2-en-3-yl]gold[di-tert-butyl(2-phenylphenyl)phosphine (2.4.2c)

Synthesized according to GP8 from **2.3.6g** (290 mg, 98 % yield).

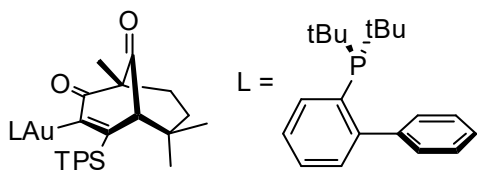
¹H NMR (400 MHz, CHLOROFORM-*d*) δ ppm = 7.72-7.68 (m, 1H), 7.61-7.58 (m, 6H), 7.44-7.01 (m, 17H), 3.02-3.00 (m, 1H), 2.11-2.05 (m, 1H), 1.87-1.74 (m, 1H), 1.52-1.39 (m, 4H), 1.35 (s, 3H), 1.19-1.00 (m, 9H), 0.79-0.63 (m, 9H).

¹³C NMR (101 MHz, CHLOROFORM-*d*) δ ppm = 213.46 (C), 208.18 (C), 191.72 (d, J = 103.7 Hz, C), 156.91 (d, J = 4.1 Hz, C), 150.11 (d, J = 15.7 Hz, C), 142.82 (d, J = 5.5 Hz, C), 136.91 (6xCH), 136.01 (3xC), 134.76 (CH), 133.21 (d, J = 5.5 Hz, CH), 129.65 (CH), 129.62 (d, J = 2.2 Hz, CH), 129.43 (CH), 129.10 (3xCH), 128.66 (CH), 128.25 (CH), 128.20 (d, J = 32.3 Hz, C), 127.39 (6xCH), 126.14 (CH), 126.05 (CH), 63.41 (C), 54.69 (d, J = 7.3 Hz, CH), 42.49 (CH₂), 37.32 (d, J = 20.3 Hz, C), 36.53 (d, J = 18.3 Hz, C), 30.50 (d, J = 7.0 Hz, 3xCH₃), 30.24 (d, J = 7.5 Hz, 3xCH₃), 30.20 (CH₂), 18.04 (CH₂), 17.10 (CH₃).

HRMS (ESI) m/z calcd for C₄₈H₅₂O₂PSiAu is 916.3140, found 916.3127.

FTIR (Neat, cm⁻¹): ν = 1716 (s), 1643 (s), 1427 (s).

M.p. (Dec. 258 °C).



[5,8,8-trimethyl-4,9-dioxo-2-(triphenylsilyl)bicyclo[3.3.1]non-2-en-3-yl]gold[di-tert-butyl(2-phenylphenyl)phosphine] (2.4.2d)

Synthesized according to GP8 from **2.3.9c** (29 mg, 40 % yield).

¹H NMR (400 MHz, CHLOROFORM-*d*) δ ppm = 7.26 (t, J = 6.9 Hz, 1H), 7.63-7.14 (m, 22H), 7.10-7.06 (m, 1H), 3.00 (s, 1H), 1.99-1.86 (m, 2H), 1.76-1.66 (m, 1H), 1.47-1.41 (m, 1H), 1.32 (s, 3H), 1.09-0.85 (m, 9H), 0.80-0.49 (m, 9 H), 0.63 (s, 3H), 0.55 (s, 3H).

¹³C NMR (101 MHz, CHLOROFORM-*d*) δ ppm = 211.55 (C), 207.93 (C), 193.51 (d, J = 103.0 Hz, C), 157.85 (C), 149.94 (d, J = 15.6 Hz, C), 142.60 (d, J = 5.2 Hz, C), 137.28 (6xCH), 136.4 (3xC), 134.69 (CH), 133.28 (d, J = 7.5 Hz, CH), 130.13 (CH), 129.56 (d, J = 1.9 Hz, CH), 129.37 (CH), 128.74 (3xCH), 128.47 (CH), 127.93 (d, J = 31.5 Hz, C), 127.78 (CH), 127.17 (6xCH), 126.55 (CH), 125.92 (d, J = 5.3 Hz, CH), 64.71 (d, J = 7.2 Hz, CH), 61.71 (C), 38.62 (C), 37.35-37.16 (m, C), 36.82 (CH₂), 36.50-36.26 (m, C), 31.70 (CH₂), 30.47 (d, J = 6.7 Hz, 3xCH₃), 30.09 (d, J = 6.7 Hz, 3xCH₃), 29.19 (CH₃), 25.93 (CH₃), 17.11 (CH₃).

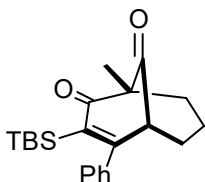
HRMS (ESI) m/z calcd for C₅₀H₅₆O₂PSiAu is 944.3453, found 944.3487.

FTIR (Neat, cm⁻¹): ν = 1716 (s) 1643 (s) 1427 (s).

M.p. (Dec. 228 °C).

7.1.9 Transmetalation of vinylgold with palladium

General procedure (GP9): In a sealed cap vial, **10L₁** (1 mmol) was added to Pd(OAc)₂ (0.05 mmol), PCy₃ (0.1 mmol), PhBr (1.5 mmol) in PhCF₃ (10 ml) at room temperature and the solution was degassed with argon for 10 minutes. The reaction mixture was allowed to be heat at 100 °C for 24 hours and then solvent was evaporated under reduce pressure. The crude product was purified by flash column chromatography on silica gel (eluted with hexane:EtOAc (95:5)) to give the desired product.



3-(tert-butyldimethylsilyl)-1-methyl-4-phenylbicyclo[3.3.1]non-3-ene-2,9-dione (2.6.1a)

Synthesized according to GP9 from **2.4.1a** (11 mg, 83 % yield).

¹H NMR (400 MHz, CHLOROFORM-*d*) δ ppm = 7.39-7.35 (m, 3 H), 7.18-7.13 (m, 2 H), 3.39 (dd, J = 3.8, 3.2 Hz, 1 H), 2.11-2.05 (m, 1 H), 1.99-1.60 (m, 5 H), 1.24 (s, 3 H), 0.89 (s, 9 H), -0.20 (s, 3 H), -0.58 (s, 3 H).

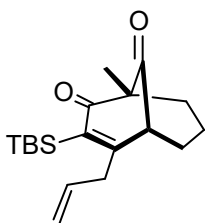
¹³C NMR (101 MHz, CHLOROFORM-*d*) δ ppm = 211.17 (C), 205.03 (C), 168.58 (C), 141.13 (C), 140.96 (C), 128.45 (CH), 128.18 (2xCH), 127.11 (2xCH), 58.67 (CH), 61.61 (C), 42.35 (CH₂), 29.70 (CH₂), 28.56 (3xCH₃), 18.33 (CH₂), 17.73 (C), 16.01 (CH₃), -2.29 (CH₃), -2.66 (CH₃).

HRMS (EI) m/z calcd for $C_{22}H_{30}O_2Si_1 [(M-CH_3)^+]$ is 339.1775, found 339.178.

FTIR (Neat, cm^{-1}): ν = 2927 (m), 2357 (m), 1660 (s).

7.1.10 Alkylation of vinylgold

General procedure (GP10): In a sealed cap vial, compound **10L₁** or **14j** (20 mg) was diluted with $PhCF_3$ (0.2 ml), 5 equivalents of the alkylating agent was added and the reaction mixture was heated at 100 °C for 24h or until no more starting material was seen by TLC analysis. The solvent was evaporated under reduce pressure and the crude mixture was purified by flash column chromatography on silica gel (eluted with hexane:EtOAc (~90:10)) to give the desired alkylated product.



3-(tert-butyldimethylsilyl)-1-methyl-4-(prop-2-en-1-yl)bicyclo[3.3.1]non-3-ene-2,9-dione (2.6.1b)

Synthesized according to GP10 from **2.4.1a** (9 mg, 75 % yield)

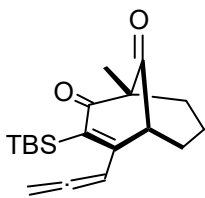
¹H NMR (400 MHz, CHLOROFORM-*d*) δ ppm = 5.72 (dddd, J =17.3, 10.0, 7.5, 4.9 Hz, 1 H), 5.21 (dd, J =10.1, 1.1 Hz, 1 H), 5.10 (dd, J =17.2, 1.2 Hz, 1 H), 3.41-3.33 (m, 2 H),

2.98 (dd $J=14.8$, 7.5 Hz, 1 H), 2.02-1.90 (m, 3 H), 1.62-1.49 (m, 3 H), 1.17 (s, 3 H), 0.94 (s, 9 H), 0.24 (s, 3 H), 0.20 (s, 3 H).

^{13}C NMR (101 MHz, CHLOROFORM-*d*) δ ppm = 210.8 (C), 205.1 (C), 167.9 (C), 140.1 (C), 133.1 (CH), 119.2 (CH₂), 60.9 (C), 54.0 (CH), 42.1 (CH₂), 40.6 (CH₂), 30.9 (CH₂), 27.6 (3xCH₃), 18.6 (CH₂), 18.2 (C), 15.9 (CH₃), -0.9 (CH₃), -0.16 (CH₃).

HRMS (EI) m/z calcd for C₁₉H₃₀O₂Si is 318.2015, found 354.2007.

FTIR (Neat, cm⁻¹): ν = 2935 (m), 1728 (s), 1659 (s), 1086 (s).



3-(tert-butyldimethylsilyl)-1-methyl-4-(propa-1,2-dien-1-yl)bicyclo[3.3.1]non-3-ene-2,9-dione (2.6.1c)

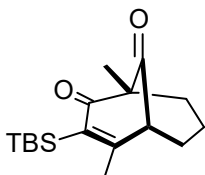
Synthesized according to GP10 from **2.4.1a** (13 mg, 63 % yield)

^1H NMR (400 MHz, CHLOROFORM-*d*) δ ppm = 6.56 (t, J = 6.5 Hz, 1 H), 5.22 (dd, J = 6.6, 14.8 Hz, 1 H), 5.18 (dd, J = 6.6, 14.8 Hz, 1 H), 3.66-3.64 (m, 1 H), 2.02-1.91 (m, 3 H), 1.62-1.54 (m, 3 H), 1.18 (s, 3 H), 0.94 (s, 9 H), 0.27 (s, 3 H), 0.22 (s, 3 H).

^{13}C NMR (101 MHz, CHLOROFORM-*d*) δ ppm = 212.70 (C), 211.23 (C), 204.15 (C), 159.99 (C), 139.75 (C), 95.26 (CH), 79.43 (CH₂), 61.51 (C), 52.03 (CH), 41.94 (CH₂), 32.10 (CH₂), 27.51 (3xCH₃), 18.81 (CH₂), 18.40 (C), 16.04 (CH₃), -0.42 (CH₃), -1.48 (CH₃)

HRMS (EI) m/z calcd for $C_{19}H_{28}O_2Si$ is 316.1859, found 316.1866.

FTIR (Neat, cm^{-1}): ν = 2927 (m), 2854(m), 1731 (s), 1654 (s).



3-(tert-butyldimethylsilyl)-1,4-dimethylbicyclo[3.3.1]non-3-ene-2,9-dione (2.6.1d)

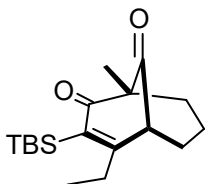
Synthesized according to GP10 from **12.4.1a** (11 mg, 98 % yield)

1H NMR (400 MHz, $CHCl_3-d$) δ ppm = 3.15 (t, $J=3.5$ Hz, 1 H), 2.12 (s, 3 H), 2.04-1.93 (m, 3 H), 1.61-1.48 (m, 3 H), 1.17 (s, 3 H), 0.94 (s, 9 H), 0.24 (s, 3 H), 0.19 (s, 3 H).

^{13}C NMR (101 MHz, $CHCl_3-d$) δ ppm = 211.1 (C), 204.3 (C), 167.5 (C), 139.2 (C), 60.9 (C), 57.6 (CH), 41.9 (CH₂), 30.6 (CH₂), 27.5 (3xCH₃), 24.2 (CH₃), 18.6 (CH₂), 18.4 (C), 16.0 (CH₃), -0.8 (CH₃), -1.8 (CH₃).

HRMS (EI) m/z calcd for $C_{17}H_{28}O_2Si [(M-CH_3)^+]$ is 277.1618, found 277.1620.

FTIR (Neat, cm^{-1}): ν = 2935 (m), 2854 (m), 1728 (s), 1654 (s).



3-(tert-butyldimethylsilyl)-4-ethyl-1-methylbicyclo[3.3.1]non-3-ene-2,9-dione (2.6.1e)

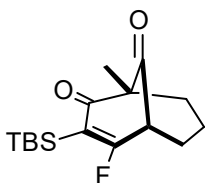
Synthesized according to GP10 from **2.4.1a** (12 mg, 92 % yield)

¹H NMR (400 MHz, CHLOROFORM-*d*) δ ppm = 3.32 (t, J = 3.4 Hz, 1 H), 2.63 (qd, J =13.2, 7.4 Hz, 1 H), 2.22 (qd, J =13.2, 7.5 Hz, 1 H), 2.02-1.95 (m, 3 H), 1.62-1.52 (m, 3 H), 1.17 (s, 3 H), 1.13 (t, J =7.5 Hz, 3 H), 0.93 (s, 9 H), 0.24 (s, 3 H), 0.19 (s, 3 H).

¹³C NMR (101 MHz, CHLOROFORM-*d*) δ ppm = 211.0 (C), 205.3 (C), 172.4 (C), 138.5 (C), 60.8 (C), 53.9 (CH), 42.0 (CH₂), 31.2 (CH₂), 29.5 (CH₂), 27.6 (3xCH₃), 18.5 (CH₂), 18.2 (C), 15.9 (CH₃), 12.8 (CH₃), -0.9 (CH₃), -1.6 (CH₃).

HRMS (EI) m/z calcd for C₁₈H₃₀O₂Si [(M-C₄H₉)⁺] is 249.1305, found 249.1337.

FTIR (Neat, cm⁻¹): ν = 2933 (m), 1726 (s), 1658 (s), 1461(m).



**3-(tert-butyldimethylsilyl)-4-fluoro-1-methylbicyclo[3.3.1]non-3-ene-2,9-dione
(2.6.1f)**

Synthesized according to GP10 from **2.4.1a** (6 mg, 33 % yield)

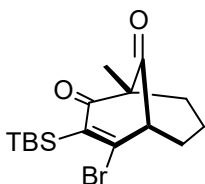
¹H NMR (400 MHz, CHLOROFORM-*d*) δ ppm = 3.43 (dt, J =13.3, 3.4 Hz, 1 H), 2.24-2.17 (m, 1 H), 2.06-1.95 (m, 2 H), 1.77-1.69 (m, 2 H), 1.65-1.57 (m, 1 H), 1.20 (s, 3 H), 0.91 (s, 9 H), 0.23 (s, 6 H).

¹³C NMR (101 MHz, CHLOROFORM-*d*) δ ppm = 208.3 (J =12.6 Hz, C), 201.0 (J =25.7 Hz, C), 181.0 (J =292 Hz, C), 121.3 (J =21.5 Hz, C), 61.1 (J =4.3 Hz, C), 52.2 (J =27.7 Hz,

CH), 41.9 (CH₂), 30.1 (*J*=3.7 Hz, CH₂), 26.8 (3xCH₃), 18.5 (CH₂), 17.6 (C), 16.0 (CH₃), -3.7 (*J*=5.9 Hz, CH₃), -4.0 (*J*=2.8 Hz, CH₃).

HRMS (EI) *m/z* calcd for C₁₆H₂₅O₂SiF [(M-C₄H₉)⁺] is 239.0898, found 239.0900.

FTIR (Neat, cm⁻¹): *ν* = 2927 (m), 1739 (s), 1670 (s), 1612 (s).



4-bromo-3-(tert-butyldimethylsilyl)-1-methylbicyclo[3.3.1]non-3-ene-2,9-dione

(2.6.1g)

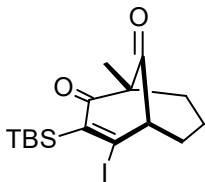
Synthesized according to GP10 from **2.4.1a** (9 mg, 98 % yield)

¹H NMR (400 MHz, CHLOROFORM-*d*) *δ* ppm = 3.69 (t, *J* = 3.7 Hz, 1 H), 2.31-2.23 (m, 1 H), 2.04-1.89 (m, 2 H), 1.69-1.55 (m, 3 H), 1.18 (s, 3 H), 0.97 (s, 9 H), 0.36 (s, 3 H), 0.25 (s, 3 H).

¹³C NMR (101 MHz, CHLOROFORM-*d*) *δ* ppm = 208.2 (C), 201.0 (C), 156.6 (C), 145.1 (C), 63.4 (CH), 61.4 (C), 42.3 (CH₂), 30.9 (CH₂), 27.7 (3x CH₃), 18.8 (C), 18.3 (CH₂), 16.0 (CH₃), -0.5 (CH₃), -1.6 (CH₃).

HRMS (EI) *m/z* calcd for C₁₆H₂₅O₂SiBr [(M-C₄H₉)⁺] is 299.0097, found 299.0119.

FTIR (Neat, cm⁻¹): *ν* = 2939 (m), 1737 (s), 1666 (s), 1542 (s).



3-(tert-butyldimethylsilyl)-4-iodo-1-methylbicyclo[3.3.1]non-3-ene-2,9-dione (2.6.1h)

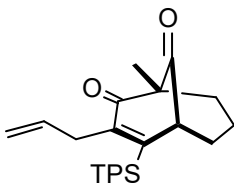
Synthesized according GP10 from **2.4.1a** (11 mg, 98 % yield)

¹H NMR (400 MHz, CHLOROFORM-*d*) δ ppm = 3.91 (dd, J = 4.1, 3.1 Hz, 1 H), 2.28-2.21 (m, 1 H), 2.05-1.98 (m, 1 H), 1.88-1.78 (m, 1 H), 1.67-1.51 (m, 3 H), 1.18 (s, 3 H), 0.99 (s, 9 H), 0.40 (s, 3 H), 0.25 (s, 3 H).

¹³C NMR (101 MHz, CHLOROFORM-*d*) δ ppm = 208.1 (C), 200.6 (C), 152.5 (C), 136.6 (C), 68.8 (CH), 61.9 (C), 42.2 (CH₂), 31.05 (CH₂), 28.2 (3xCH₃), 19.1 (C), 18.2 (CH₂), 16.0 (CH₃), 0.37 (CH₃), -1.0 (CH₃).

HRMS (EI) m/z calcd for C₁₆H₂₅O₂Si [(M-C₄H₉)⁺] is 346.9959, found 3346.9893.

FTIR (Neat, cm⁻¹): ν = 2927 (m), 1737 (s), 1666 (s), 1108 (s).



1-methyl-3-(prop-2-en-1-yl)-4-(triphenylsilyl)bicyclo[3.3.1]non-3-ene-2,9-dione (2.6.2b)

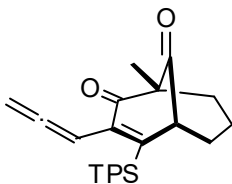
Synthesized according to GP10 from **2.4.2c** (13 mg, 65 % yield)

¹H NMR (400 MHz, CHLOROFORM-*d*) δ ppm = 7.55-7.52 (m, 6 H), 7.48-7.43 (m, 3 H), 7.41-7.37 (m, 6 H), 5.19 (ddt, J = 17.1, 10.3, 6.4 Hz, 1 H), 4.59 (dd, J = 10.2, 1.6 Hz, 1 H), 4.31 (dd, J = 17.4, 1.6 Hz, 1 H), 3.39-3.36 (m, 1 H), 3.12 (ddt, J = 14.4, 6.4, 1.5 Hz, 1 H), 3.05 (dd, J = 14.4, 6.4 Hz, 1 H), 2.08-2.03 (m, 1 H), 1.82-1.54 (m, 5H), 1.24 (s, 3 H).

¹³C NMR (101 MHz, CHLOROFORM-*d*) δ ppm = 210.32 (C), 201.16 (C), 151.42 (C), 150.99 (C), 136.16 (6xCH), 133.51 (CH), 132.38 (3xC), 130.25 (3xCH), 128.30 (6xCH), 116.55 (CH₂), 62.34 (C), 52.59 (CH), 42.27 (CH₂), 36.67 (CH₂), 30.04 (CH₂), 17.48 (CH₂), 15.97 (CH₃).

HRMS (EI) m/z calcd for C₃₁H₃₀O₂Si is 462.2015, found 462.2041.

FTIR (Neat, cm⁻¹): ν = 2935 (m), 1724 (s), 1666 (s), 1427 (s).



**1-methyl-3-(propa-1,2-dien-1-yl)-4-(triphenylsilyl)bicyclo[3.3.1]non-3-ene-2,9-dione
(2.6.2c)**

Synthesized according to GP10 from **2.4.2c** (9 mg, 33 %), inseparable mixture with the protodeaurated product.

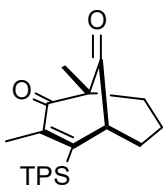
¹H NMR (400 MHz, CHLOROFORM-*d*) δ ppm = 7.53-7.51 (m, 6 H), 7.49-7.47 (m, 3 bvcH), 7.41-7.36 (m, 6 H), 5.82 (t, J = 6.8 Hz, 1 H), 4.73 (dd, J = 13.0, 6.8 Hz, 1 H), 4.68

(dd, $J = 13.1, 6.8$ Hz, 1 H), 3.42 (t, $J = 3.2$ Hz, 1 H), 2.02-1.97 (m, 2 H), 1.67-1.61 (m, 4 H), (s, 3 H).

^{13}C NMR (101 MHz, CHLOROFORM-*d*) δ ppm = 212.64 (C), 209.64 (C), 199.64 (C), 151.45 (C), 144.85 (C), 136.16 (6xCH), 132.11 (3xC), 130.95 (3xCH), 128.31 (6xCH), 88.90 (CH), 75.34 (CH₂), 62.51 (C), 53.00 (CH), 42.72 (CH₂), 30.53 (CH₂), 17.73 (CH₂), 16.19 (CH₃).

HRMS (EI) m/z calcd for C₃₁H₂₈O₂Si is 460.1859, found 460.1857.

FTIR (Neat, cm⁻¹): $\nu = 2948$ (w), 1726 (s), 1670 (s), 908 (s), 729 (s).



1,3-dimethyl-4-(triphenylsilyl)bicyclo[3.3.1]non-3-ene-2,9-dione (2.6.2d)

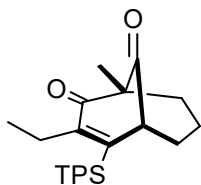
Synthesized according to GP10 from **2.4.2c** (17 mg, 98 % yield)

^1H NMR (400 MHz, CHLOROFORM-*d*) δ ppm = 7.54-7.50 (m, 6 H), 7.48-7.43 (m, 3 H), 7.42-7.37 (m, 6 H), 3.35-7.32 (m, 1 H), 2.08-2.02 (m, 1 H), 1.75 (s, 3 H), 1.66-1.54 (m, 5 H), 1.27 (s, 3 H).

^{13}C NMR (101 MHz, CHLOROFORM-*d*) δ ppm = 210.37 (C), 201.79 (C), 150.56 (C), 148.88 (C), 135.93 (6xCH), 132.47 (3xC), 130.17 (3xCH), 128.32 (6xCH), 62.24 (C), 52.44 (CH), 42.36 (CH₂), 29.97 (CH₂), 18.55 (CH₃), 17.58 (CH₂), 16.09 (CH₃)

HRMS (EI) m/z calcd for C₂₉H₂₈O₂Si is 436.1859, found 436.1860.

FTIR (Neat, cm⁻¹): ν = 2939 (m) 1724 (s) 1666 (s) 1427 (s).



3-ethyl-1-methyl-4-(triphenylsilyl)bicyclo[3.3.1]non-3-ene-2,9-dione (2.6.2e)

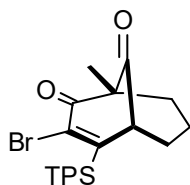
Synthesized according to GP10 from **2.4.2c** (10 mg, 97 % yield)

¹H NMR (400 MHz, CHLOROFORM-*d*) δ ppm = 7.56-7.52 (m, 6 H), 7.48-7.42 (m, 3 H), 7.41-7.37 (m, 6 H), 3.34 (t, J = 3.5 Hz, 1 H), 2.34 (qd, J = 13.7, 7.2 Hz, 1 H), 2.24 (dd, J = 13.6, 7.1 Hz, 1 H), 2.07-2.00 (m, 1 H), 1.81-1.54 (m, 5 H), 1.24 (s, 3 H), 0.37 (t, J = 7.2 Hz, 3 H).

¹³C NMR (101 MHz, CHLOROFORM-*d*) δ ppm = 210.5 (C), 201.3 (C), 154.5 (C), 150.0 (C), 136.1 (6xCH), 132.6 (3xC), 130.1 (3xCH), 128.2 (6xCH), 62.4 (C), 52.3 (CH), 42.3 (CH₂), 30.0 (CH₂), 26.3 (CH₂), 17.4 (CH₂), 16.0 (CH₃), 11.7 (CH₃).

HRMS (EI) m/z calcd for C₃₀H₃₀O₂Si is 450.2015, found 450.2031.

FTIR (Neat, cm⁻¹): ν = 2933 (m), 1724 (s), 1666 (s), 1429 (s).



3-bromo-1-methyl-4-(triphenylsilyl)bicyclo[3.3.1]non-3-ene-2,9-dione (2.6.2g)

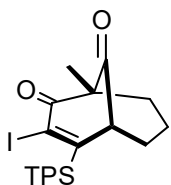
Synthesized according to GP10 from **2.4.2c** (11 mg, 98 % yield)

¹H NMR (400 MHz, CHLOROFORM-*d*) δ ppm = 7.59-7.56 (m, 6 H), 7.49-7.44 (m, 3 H), 7.42-7.38 (m, 6 H), 3.42 (t, *J* = 3.3 Hz, 1 H), 2.15-2.09 (m, 1 H), 1.89-1.78 (m, 1 H), 1.77-1.61 (m, 4 H), 1.32 (s, 3 H).

¹³C NMR (101 MHz, CHLOROFORM-*d*) δ ppm = 208.0 (C), 193.9 (C), 156.8 (C), 137.5 (C), 136.1 (6xCH), 131.3 (3xC), 130.3 (3xCH), 128.3 (6xCH), 62.8 (C), 54.9 (CH), 42.4 (CH₂), 29.7 (CH₂), 17.5 (CH₂), 16.5 (CH₃).

HRMS (EI) *m/z* calcd for C₂₈H₂₅O₂SiBr is 500.0807, found 500.0772.

FTIR (Neat, cm⁻¹): ν = 2927 (m), 1731 (s), 1683 (s), 1431 (s).



3-iodo-1-methyl-4-(triphenylsilyl)bicyclo[3.3.1]non-3-ene-2,9-dione (2.6.2h)

Synthesized according to GP10 from **2.4.2c** (12 mg, 98 % yield)

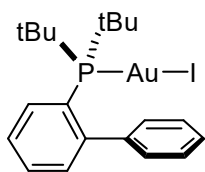
¹H NMR (400 MHz, CHLOROFORM-*d*) δ ppm = 7.61-7.57 (m, 6 H), 7.50-7.45 (m, 3 H), 7.43-7.38 (m, 6 H), 3.43 (dd, *J* = 4.2, 2.7 Hz, 1 H), 2.13-2.07 (m, 1 H), 1.84-1.53 (m, 5 H), 1.33 (s, 3 H).

¹³C NMR (101 MHz, CHLOROFORM-*d*) δ ppm = 208.7 (C), 195.3 (C), 163.7 (C), 136.3 (6xCH), 131.3 (3xC), 130.3 (3xCH), 128.3 (6xCH), 122.2 (C), 62.0 (C), 56.1 (CH), 42.6 (CH₂), 29.7 (CH₂), 17.7 (CH₂), 16.9 (CH₃).

HRMS (EI) m/z calcd for $C_{28}H_{25}O_2SiI$ is 548.0668, found 548.0676.

FTIR (Neat, cm^{-1}): ν = 2366 (m), 1731 (s), 1681 (s), 1108 (s), 689 (s).

7.1.11 Other side products



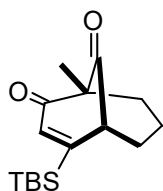
Side product from GP9

1H NMR (400 MHz, CHLOROFORM-*d*) δ ppm = 7.87 (t, J = 7.6 Hz, 1 H) 7.57-7.50 (m, 3 H) 7.46 (t, J = 7.64 Hz, 2 H) 7.30-7.27 (m, 1 H) 7.10 (d, J = 7.4 Hz, 2 H) 1.44 (s, 9 H), 1.40 (s, 9 H).

^{13}C NMR (101 MHz, CHLOROFORM-*d*) δ ppm = 150.13 (J = 40.7 Hz, 2xC) 142.28 (J = 7.00 Hz, C) 133.97 (J = 1.8 Hz, 2xCH) 133.31 (J = 7.4 Hz, CH) 130.53 (J = 2.2 Hz, 2xCH) 129.20 (J = 4.4 Hz, CH) 128.41 (CH) 126.75 (J = 6.3 Hz, CH) 126.32 (C) 38.26 (d, J = 20.7 Hz, 2xC) 30.92 (d, J = 7.0 Hz, 6xCH₃).

HRMS (EI) m/z calcd for $C_{22}H_{31}PAuI$ is 622.0560, found 622.0605.

FTIR (Neat, cm^{-1}): ν = 2961 (w), 670 (m), 606 (m).



Compound 2.7.10

Side product from dual-catalysis

¹H NMR (400 MHz, CHLOROFORM-*d*) δ ppm = 6.65 (s, 1H), 3.48 (dd, *J* = 4.4, 2.7 Hz, 1H), 2.00 (tt, *J* = 9.0, 3.7 Hz, 2H), 1.92 – 1.79 (m, 1H), 1.69 – 1.52 (m, 3H), 1.21 (s, 3H), 0.90 (s, 9H), 0.19 (s, 6H).

¹³C NMR (101 MHz, CHLOROFORM-*d*) δ ppm = δ 209.91 (C), 201.38 (C), 162.61 (C), 140.11 (CH), 62.44 (C), 52.20 (CH), 41.59 (CH₂), 30.00 (CH₂), 26.66 (3xCH₃), 17.50 (C), 17.23 (CH₂), 15.46 (CH₃), -6.24 (CH₃), -6.49 (CH₃).

HRMS (EI) *m/z* calcd for C₁₆H₂₆O₂Si is 278.1702, found 278.1719.

FTIR (Neat, cm⁻¹): ν = 2927 (m), 2357 (m), 1660 (s).

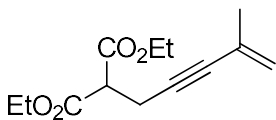
7.2 Gold(I)-catalyzed [4+2] and its application to the synthesis of magellanine

This section includes all characterization of *Chapter 3*.

7.2.1 Sonogashira coupling for the formation of 3.2.15

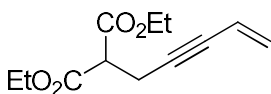
General procedure (GP11): Copper iodide (215 mg, 1.13 mmol) and Pd(PPh₃)₄ (653 mg, 0.6 mmol) was added to diethyl propargyl malonate (5.6 g, 28.2 mmol) in THF (94 ml, 0.3 M). DIPEA (15.8 ml, 113 mmol) and vinyl halide (42.2 mmol) was then added and the reaction mixture was heated at 50 °C for 2 hours. A dry pack was performed and then

the crude product was purified by flash column chromatography on silica gel (eluted with hexanes:EtOAc (98:2 to 95:5)) to give the desired enyne.



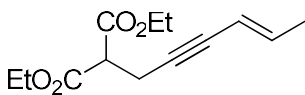
Diethyl (4-methylpent-4-en-2-yn-1-yl)propanedioate (3.2.15a)

Synthesized according to GP11 from 2-bromopropen (5.2 g, 87%). Spectroscopic data recorded were consistent with that reported previously.¹²⁴



Diethyl pent-4-en-2-yn-1-ylpropanedioate (3.2.15b)

Synthesized according to GP11 from vinyl bromide (0.96 g, 85%). Spectroscopic data recorded were consistent with that reported previously.¹²⁵



Diethyl (4E)-hex-4-en-2-yn-1-ylpropanedioate (3.2.15c)

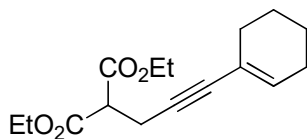
Synthesized according to GP11 using *trans*-bromopropene (0.79 g, 74%).

¹H NMR (400 MHz, CHLOROFORM-*d*) δ ppm = 6.05 (dq, J = 15.8, 6.8 Hz, 1 H), 5.41 (dq, J = 15.8, 1.9 Hz, 1 H), 4.21 (dq, J = 7.1, 0.53 Hz, 4 H), 3.53 (t, J = 7.8 Hz, 1 H), 2.86 (dd, J = 7.7, 2.0 Hz, 2 H), 1.73 (dd, J = 6.8, 1.8 Hz, 3 H), 1.27 (t, J = 7.1 Hz, 6 H).

¹³C NMR (101 MHz, CHLOROFORM-*d*) δ ppm = 168.1 (2xC), 139.2 (CH), 110.6 (CH), 83.4 (C), 81.0 (C), 61.7 (2xCH₂), 51.6 (CH), 19.4 (CH₂), 18.5 (CH₃), 14.1 (2xCH₃).

HRMS (EI) m/z calcd for C₁₃H₁₈O₄ [M⁺]: 238.1205; found: 238.1206.

FTIR (neat, cm⁻¹): ν = 2961 (m), 2358 (w), 1729 (s), 1145 (s).



Diethyl [3-(cyclohex-1-en-1-yl)prop-2-yn-1-yl]propanedioate (3.2.15d)

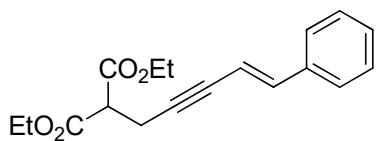
Synthesized according to GP11 using 1-bromocyclohexene (0.86 g, 54%).

¹H NMR (400 MHz, CHLOROFORM-*d*) δ ppm = 6.00-5.97 (m, 1 H), 4.21 (dd, J = 7.1, 1.1 Hz, 4 H), 3.53 (t, J = 7.8 Hz, 1 H), 2.87 (d, J = 7.8 Hz, 2 H), 2.06-2.01 (m, 4 H), 1.61-1.51 (m, 4 H), 1.27 (t, J = 7.1 Hz, 6 H).

¹³C NMR (101 MHz, CHLOROFORM-*d*) δ ppm = 168.1 (2xC), 134.2 (CH), 120.5 (C), 84.3 (C), 82.4 (C), 61.6 (2xCH₂), 51.7 (CH), 29.3 (CH₂), 25.5 (CH₂), 22.3 (CH₂), 21.5 (CH₂), 19.4 (CH₂), 14.1 (2xCH₃).

HRMS (EI) m/z calcd for C₁₆H₂₂O₄ [M⁺]: 278.1518; found: 278.1521.

FTIR (neat, cm⁻¹): ν = 2965 (m), 2368 (w), 1728 (s), 1163 (m).



Diethyl [(4*E*)-5-phenylpent-4-en-2-yn-1-yl]propanedioate (3.2.15e)

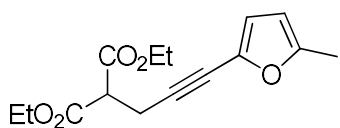
Synthesized according to GP11 using *trans*-bromostyrene (1.39 g, 93%).

¹H NMR (400 MHz, CHLOROFORM-*d*) δ ppm = 7.36-7.24 (m, 5 H), 6.87 (d, J = 16.2 Hz, 1 H), 6.10 (dt, J = 16.2, 2.2 Hz, 1 H), 4.24 (q, J = 7.1 Hz, 4 H), 3.60 (t, J = 7.7 Hz, 1 H), 2.96 (dd, J = 7.7, 2.1 Hz, 2 H), 1.29 (t, J = 7.1 Hz, 6 H).

¹³C NMR (101 MHz, CHLOROFORM-*d*) δ ppm = 168.1 (2xC), 141.0 (CH), 136.3 (C), 128.7 (2xCH), 128.5 (CH), 126.2 (2xCH), 108.1 (CH), 87.7 (C), 81.6 (C), 61.8 (2xCH₂), 51.5 (CH), 19.7 (CH₂), 14.1 (2xCH₃).

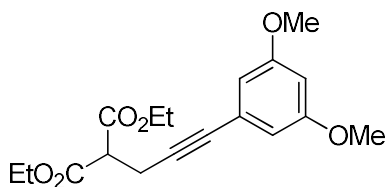
HRMS (EI) m/z calcd for C₁₈H₂₀O₄ [M^+]: 300.1361; found: 300.1349.

FTIR (neat, cm⁻¹): ν = 2938 (m), 2364 (w), 1731 (s), 750 (m).



Diethyl [3-(5-methylfuran-2-yl)prop-2-yn-1-yl]propanedioate (3.2.15f)

Synthesized according to GP11 using 2-iodo-4-methylfuran (0.44 g, 80%). Spectroscopic data recorded were consistent with that reported previously.¹²⁵



Diethyl [3-(3,5-dimethoxyphenyl)prop-2-yn-1-yl]propanedioate (3.2.15g)

Synthesized according to GP11 using dimethoxyiodobenzene (1.49 g, 89%).

¹H NMR (400 MHz, CHLOROFORM-*d*) δ ppm = 6.61 (d, J = 2.3 Hz, 2 H), 6.40 (d, J = 2.3 Hz, 1 H), 4.24 (dq, J = 7.1, 0.8 Hz, 4 H), 3.75 (s, 6 H), 3.64 (t, J = 7.8 Hz, 1 H), 2.99 (d, J = 7.8 Hz, 2 H), 1.28 (t, J = 7.2 Hz, 6 H).

¹³C NMR (101 MHz, CHLOROFORM-*d*) δ ppm = 168.1 (2xC), 160.5 (2xC), 124.5 (C), 109.5 (2xCH), 101.5 (CH), 85.1 (C), 82.4 (C), 61.8 (2xCH₂), 55.4 (2xCH₃), 51.4 (CH), 19.4 (CH₂), 14.1 (2xCH₃).

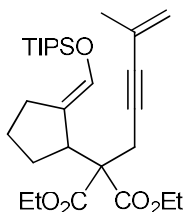
HRMS (EI) m/z calcd for C₁₈H₂₂O₆ [M^+]: 334.1416; found: 334.1451.

FTIR (neat, cm⁻¹): ν = 2948 (m), 2360 (w), 1731 (s), 1585 (s), 1153 (s).

7.2.2 Preparation of 3.2.17 via conjugated 1,4 addition

General procedure (GP12): To a solution of carboxaldehyde D (2.1 mmol) in THF (14 mL) at -78 °C was added TIPSOTf (3.3 mmol) dropwise. After stirring for 30 minutes, dimethyl sulfide (4.2 mmol) was added dropwise along the side of the flask. The reaction mixture was stirred at -78 °C for 60 minutes. In another flask, the desired malonate chain C or 17 (4.2 mmol) in THF (3 mL) was added to LiHMDS (4.6 mmol in 4 mL of THF) at 0

°C. This solution was cooled to -78 °C and then added dropwise along the side of the flask to the reaction mixture containing aldehyde C at -78 °C. The reaction mixture was warmed up to room temperature and stirred overnight. An aqueous saturated solution of NaHCO₃ was then added and the mixture was extracted with diethyl ether (3X) and the combined organic layers were dried over MgSO₄, filtered and concentrated. The residue was purified by flash chromatography (2% ethyl acetate in hexanes) to afford the desired product (815 mg, 1.7 mmol) as a colorless oil.



Compound 3.2.17a

Synthesized according to GP12 from **3.2.15a** and 1-cyclopentene-1-carboxaldehyde (3.61g, 71%).

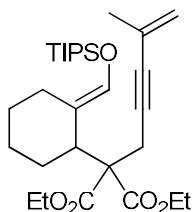
¹H NMR (400 MHz, CHLOROFORM-*d*) δ ppm = 6.49-6.48 (m, 1H), 5.17-5.16 (m, 1H), 5.13-5.12 (m, 1H), 4.26-4.11 (m, 4H), 3.44-3.40 (m, 1H), 3.06 (d, J = 17.1 Hz, 1H), 2.88 (d, J = 17.1 Hz, 1H), 2.57-2.48 (m, 1H), 2.06-1.94 (m, 3H), 1.82 (t, J = 1.2 Hz, 3H), 1.61-1.46 (m, 2H), 1.25 (t, J = 7.1 Hz, 6H), 1.17-1.05 (m, 21H).

¹³C NMR (101 MHz, CHLOROFORM-*d*) δ ppm = 170.4 (C), 170.3 (C), 135.6 (CH), 126.8 (C), 122.5 (C), 120.9 (CH₂), 84.7 (C), 84.7 (C), 61.3 (CH₂), 61.2 (CH₂), 60.6 (C),

43.8 (CH), 29.6 (CH₂), 27.5 (CH₂), 25.0 (CH₂), 23.9 (CH₂), 23.5 (CH₃), 17.8 (3xCH₃), 17.8 (3xCH₃), 14.0 (CH₃), 14.0 (CH₃), 12.0 (3xCH).

HRMS (EI) *m/z* calcd for C₂₈H₄₆O₅Si [M⁺]: 490.3115; found: 490.3084.

FTIR (neat, cm⁻¹): ν = 2966 (m), 2337 (w), 1726 (s), 1182 (s).



Compound 3.2.17b

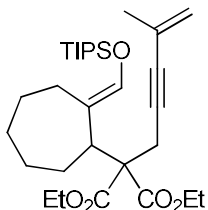
Synthesized according to GP12 from **3.2.15a** and 1-cyclohexene-1-carboxaldehyde (0.43 g, 94%).

¹H NMR (400 MHz, CHLOROFORM-*d*) δ ppm = 6.41 (s, 1H), 5.13-5.11 (m, 1H), 5.10-5.09 (m, 1H), 4.27-4.06 (m, 4H), 3.01-2.99 (m, 1 H), 2.96 (d, *J* = 16.8 Hz, 1H), 2.87 (d, *J* = 16.8 Hz, 1H), 2.52 (dt, *J* = 13.7, 3.88 Hz, 1H), 2.12-2.06 (m, 1H), 1.81-1.71 (m, 2H), 1.79-1.78 (m, 3H), 1.57-1.45 (m, 2H), 1.24 (t, *J* = 7.2 Hz, 3H), 1.23 (t, *J* = 7.2 Hz, 3H), 1.15-1.03 (m, 21H).

¹³C NMR (101 MHz, CHLOROFORM-*d*) δ ppm = 171.7 (C), 170.5 (C), 136.1 (CH), 126.8 (C), 120.7 (CH₂), 118.1 (C), 85.0 (C), 84.6 (C), 61.4 (CH₂), 61.2 (CH₂), 59.6 (C), 40.9 (CH), 29.2 (CH₂), 29.5 (CH₂), 25.7 (CH₂), 23.6 (CH₂), 23.5 (CH₃), 22.7 (CH₂), 17.8 (6xCH₃), 14.0 (CH₃), 13.9 (CH₃), 12.0 (3xCH).

HRMS (EI) *m/z* calcd for C₂₉H₄₈O₅Si [M⁺]: 504.3271; found 504.3288.

FTIR (neat, cm⁻¹): ν = 2919 (m), 2332 (w), 1426 (s), 1164 (s).



Compound 3.2.17c

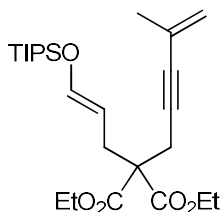
Synthesized according to GP12 from **3.2.15a** and 1-cycloheptene-1-carboxaldehyde (0.18 g, 42%).

¹H NMR (400 MHz, CHLOROFORM-*d*) δ ppm = 6.41 (s, 1H), 5.15-5.14 (m, 1H), 5.12-5.10 (m, 1H), 4.24-4.08 (m, 4H), 2.97-2.92 (m, 1H), 2.93 (d, J = 17.0 Hz, 1H), 2.86 (d, J = 17.0 Hz, 1H), 2.57 (dd, J = 4.4, 11.0 Hz, 1H), 2.22 (quint, J = 7.1 Hz, 1H), 1.81 (t, J = 1.3 Hz, 3H), 1.80-1.56 (m, 4H), 1.25 (t, J = 7.1 Hz, 3H), 1.23 (t, J = 7.1 Hz, 3H), 1.20-1.08 (m, 3H), 1.08-1.04 (m, 20 H).

¹³C NMR (101 MHz, CHLOROFORM-*d*) δ ppm = 170.1 (C), 170.1 (C), 139.7 (CH), 126.9 (C), 120.8 (CH₂), 118.8 (C), 84.9 (C), 84.7 (C), 61.1 (CH₂), 61.1 (CH₂), 60.8 (C), 45.0 (CH), 31.9 (CH₂), 29.3 (CH₂), 28.1 (CH₂), 26.1 (CH₂), 25.8 (CH₂), 24.8 (CH₂), 23.6 (CH₃), 17.8 (3xCH₃), 17.8 (3xCH₃), 14.0 (CH₃), 14.0 (CH₃), 12.0 (3xCH).

HRMS (EI) m/z calcd for C₃₀H₅₀O₅Si [M^+]: 518.3428; found: 518.3409.

FTIR (neat, cm⁻¹): ν = 2919 (m), 2384 (w), 1729 (s), 1182 (s).



Compound 3.2.17d

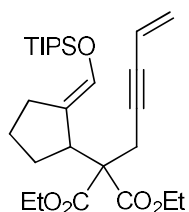
Synthesized according to GP12 from **3.2.15a** and acrolein (0.71 g, 65%).

¹H NMR (400 MHz, CHLOROFORM-*d*) δ ppm = 6.42 (dt, J = 11.8, 1.1 Hz, 1H), 5.18-5.16 (m, 1H), 5.14-5.12 (m, 1H), 4.77 (dt, J = 11.8, 8.0 Hz, 1 H), 4.22-4.14 (m, 4H), 2.88 (s, 2 H), 2.64 (dd, J = 8.1, 1.1 Hz, 2H), 1.83 (dd, J = 1.5, 1.0 Hz, 3 H), 1.24 (t, J = 7.2 Hz, 6H), 1.16-1.08 (m, 3H), 1.07-1.04 (m, 18H).

¹³C NMR (101 MHz, CHLOROFORM-*d*) δ ppm = 170.0 (2xC), 144.2 (CH), 126.8 (C), 121.0 (CH₂), 103.2 (CH₂), 84.6 (C), 83.7 (C), 61.4 (2xCH₂), 57.4 (C), 30.4 (CH₂), 23.6 (CH₃), 23.1 (CH₂), 17.7 (6xCH₃), 14.1 (2xCH₃), 12.0 (3xCH).

HRMS (EI) m/z calcd for C₂₅H₄₂O₅Si [M^+]: 450.2802: found: 450.2687.

FTIR (neat, cm⁻¹): ν = 2961 (m), 2311 (w), 1737 (s), 1180 (s).



Compound 3.2.17

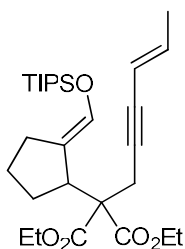
Synthesized according to GP12 from **3.2.15c** and 1-cyclopentene-1-carboxaldehyde (0.38 g, 77%).

¹H NMR (400 MHz, CHLOROFORM-*d*) δ ppm = 6.47-6.46 (m, 1H), 5.67 (ddt, J = 17.6, 11.6, 2.1 Hz, 1H), 5.49 (dd, J = 17.5, 2.3 Hz, 1H), 5.36 (dd, J = 11.1, 2.3 Hz, 1H), 4.22-4.09 (m, 4H), 3.42-3.39 (m, 1H), 3.03 (dd, J = 17.3, 2.1 Hz, 1H), 2.87 (dd, J = 17.2, 2.2 Hz, 1H), 2.54-2.47 (m, 1H), 2.03-1.90 (m, 3H), 1.59-1.44 (m, 2H), 1.23 (t, J = 7.2 Hz, 3H), 1.23 (t, J = 17.1 Hz, 3H), 1.14-1.03 (m, 21H).

¹³C NMR (101 MHz, CHLOROFORM-*d*) δ ppm = 170.4 (C), 170.3 (C), 135.6 (CH), 126.2 (C), 122.4 (CH₂), 117.2 (CH), 86.3 (C), 82.2 (C), 61.3 (CH₂), 61.2 (CH₂), 60.6 (C), 43.9 (CH), 29.6 (CH₂), 27.6 (CH₂), 25.1 (CH₂), 23.9 (CH₂), 17.8 (3xCH₃), 17.8 (3xCH₃), 14.0 (CH₃), 14.0 (CH₃), 12.0 (3xCH).

HRMS (EI) m/z calcd for C₂₇H₄₄O₅Si [M⁺]: 476.2958; found: 476.3000.

FTIR (neat, cm⁻¹): ν = 2995 (m), 2332 (w), 1729 (s), 1172 (s).



Compound 3.2.17f

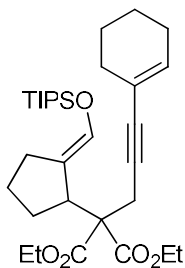
Synthesized according to GP12 from **3.2.15c** and 1-cyclopentene-1-carboxaldehyde (0.27 g, 52%).

¹H NMR (400 MHz, CHLOROFORM-*d*) δ ppm = 6.48-6.46 (m, 1H), 6.00 (dq, J = 15.8, 6.8 Hz, 1H), 5.39 (dq, J = 15.8, 1.9 Hz, 1H), 4.22-4.08 (m, 4H), 3.42-3.38 (m, 1H), 3.00 (dd, J = 17.0, 1.9 Hz, 1H), 2.85 (dd, J = 17.0, 1.9 Hz, 1H), 2.54-2.47 (m, 1H), 2.03-1.90 (m, 3H), 1.71 (dd, J = 6.9, 1.7 Hz, 3H), 1.71-1.58 (m, 2H), 1.23 (t, J = 7.2 Hz, 6H), 1.14-1.03 (m, 21H).

¹³C NMR (101 MHz, CHLOROFORM-*d*) δ ppm = 170.4 (C), 170.4 (C), 138.7 (CH), 135.6 (CH), 122.4 (C), 110.8 (CH), 83.6 (C), 82.1 (C), 61.3 (CH₂), 61.2 (CH₂), 60.7 (C), 43.8 (CH), 29.6 (CH₂), 27.6 (CH₂), 25.1 (CH₂), 23.9 (CH₂), 18.4 (CH₃), 17.8 (3xCH₃), 17.8 (3xCH₃), 14.1 (CH₂), 14.0 (CH₂), 12.0 (3xCH).

HRMS (EI) m/z calcd for C₂₈H₄₆O₅Si [M⁺]: 490.3115; found: 490.3074.

FTIR (neat, cm⁻¹): ν = 2940 (m), 2342 (w), 1724 (s), 1185 (s).



Compound 3.2.17g

Synthesized according to GP12 using **3.2.15d** and 1-cyclopentene-1-carboxaldehyde (0.34 g, 78%).

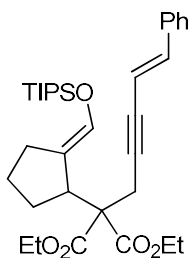
¹H NMR (400 MHz, CHLOROFORM-*d*) δ ppm = 6.49-6.47 (m, 1H), 5.96-5.93 (m, 1H), 4.23-4.10 (m, 4H), 3.43-3.39 (m, 1H), 3.03 (d, J = 17.1 Hz, 1H), 2.85 (d, J = 17.1 Hz, 1H),

2.54-2.46 (m, 1H), 2.04-1.93 (m, 7H), 1.60-1.46 (m, 6 H), 1.23 (t, $J = 7.1$ Hz, 6H), 1.15-1.03 (m, 21H).

^{13}C NMR (101 MHz, CHLOROFORM-*d*) δ ppm = 170.5 (2xC), 135.6 (CH), 133.7 (CH), 122.5 (C), 120.7 (C), 85.4 (C), 82.5 (C), 61.3 (CH₂), 61.1 (CH₂), 60.7 (C), 43.7 (CH), 29.6 (CH₂), 29.3 (CH₂), 27.5 (CH₂), 25.5 (CH₂), 25.1 (CH₂), 23.9 (CH₂), 22.3 (CH₂), 21.5 (CH₂), 17.8 (3xCH₃), 17.8 (3xCH₃), 14.1 (CH₃), 14.0 (CH₃), 12.0 (3xCH).

HRMS (EI) m/z calcd for C₃₁H₅₀O₅Si [M^+]: 530.3428: found 530.3390.

FTIR (neat, cm⁻¹): ν = 2945 (m), 2358 (w), 1729 (s), 1177 (s).



Compound 3.2.17h

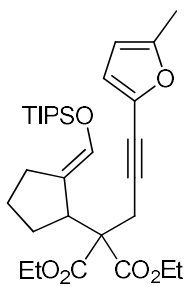
Synthesized according to GP12 from **3.2.15e** and 1-cyclopentene-1-carboxaldehyde (0.50 g, 87%).

^1H NMR (400 MHz, CHLOROFORM-*d*) δ ppm = 7.33-7.20 (m, 5H), 6.81 (d, $J = 16.3$ Hz, 1H), 6.51-6.50 (m, 1H), 6.08 (dt, $J = 16.2, 2.1$ Hz, 1H), 4.25-4.12 (m, 4H), 3.47-3.43 (m, 1H), 3.11 (dd, $J = 17.3, 2.2$ Hz, 1H), 2.94 (dd, $J = 17.3, 2.2$ Hz, 1H), 2.57-2.49 (m, 1H), 2.07-1.93 (m, 3H), 1.62-1.45 (m, 2H), 1.25 (t, $J = 7.1$ Hz, 6H), 1.14-1.03 (m, 21H).

¹³C NMR (101 MHz, CHLOROFORM-*d*) δ ppm = 170.4 (C), 170.3 (C), 140.7 (CH), 136.4 (C), 135.7 (CH), 128.7 (2xCH), 128.4 (CH), 126.1 (2xCH), 122.4 (C), 108.4 (CH), 82.6 (C), 80.0 (C), 61.4 (CH₂), 61.3 (CH₂), 60.7 (C), 43.4 (CH), 29.6 (CH₂), 27.6 (CH₂), 25.4 (CH₂), 23.9 (CH₂), 17.8 (3xCH₃), 17.8 (3xCH₃), 14.1 (CH₃), 14.0 (CH₃), 12.0 (3xCH).

HRMS (EI) m/z calcd for C₃₃H₄₈O₅Si [M⁺]: 552.3271; found: 552.3291.

FTIR (neat, cm⁻¹): ν = 2950 (m), 2368 (w), 1724 (s), 1193 (s).



Compound 3.2.17i

Synthesized according to GP12 from **3.2.15f** and 1-cyclopentene-1-carboxaldehyde (0.39 g, 93%).

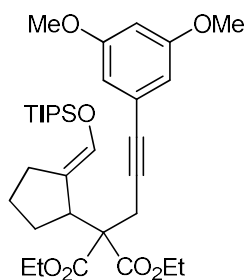
¹H NMR (400 MHz, CHLOROFORM-*d*) δ ppm = 6.50-6.49 (m, 1H), 6.31 (d, J = 3.2 Hz, 1H), 5.89-5.87 (m, 1H), 4.24-4.11 (m, 4H), 3.47-3.43 (m, 1H), 3.15 (d, J = 17.2 Hz, 1H), 2.99 (d, J = 17.3 Hz, 1H), 2.56-2.49 (m, 1H), 2.23 (s, 3H), 2.07-1.93 (m, 3H), 1.63-1.45 (m, 2H), 1.24 (t, J = 7.2 Hz, 6H), 1.14-1.03 (m, 21H).

¹³C NMR (101 MHz, CHLOROFORM-*d*) δ ppm = 170.3 (C), 170.2 (C), 152.9 (C), 135.7 (CH), 135.4 (C), 122.3 (C), 115.4 (CH), 106.6 (CH), 89.6 (C), 74.2 (C), 61.5 (CH₂), 61.3

(CH₂), 60.6 (C), 43.9 (CH), 29.6 (CH₂), 27.6 (CH₂), 25.2 (CH₂), 23.9 (CH₂), 17.8 (3xCH₃), 17.7 (3xCH₃), 14.0 (CH₃), 14.0 (CH₃), 13.7 (CH₃), 12.0 (3xCH).

HRMS (EI) m/z calcd for C₃₀H₄₆O₆Si [M⁺]: 530.3064; found: 530.3072.

FTIR (neat, cm⁻¹): ν = 2955 (m), 2337 (w), 1731 (s), 1180 (s).



Compound 3.2.17j

Synthesized according to GP12 from **3.2.15g** and 1-cyclopentene-1-carboxaldehyde (0.57 g, 94%).

¹H NMR (400 MHz, CHLOROFORM-*d*) δ ppm = 6.51-6.50 (m, 1H), 6.58 (d, *J* = 2.4 Hz, 2H), 6.37 (t, *J* = 2.3 Hz, 1H), 4.27-4.11 (m, 4H), 3.74 (s, 6H), 3.50-3.45 (m, 1H), 3.13 (d, *J* = 17.2 Hz, 1H), 2.96 (d, *J* = 17.1 Hz, 1H), 2.57-2.49 (m, 1H), 2.08-1.95 (m, 3H), 1.63-1.46 (m, 2H), 1.25 (t, *J* = 7.1 Hz, 3 H), 1.24 (t, *J* = 7.1 Hz, 3H), 1.15-1.03 (m, 21H).

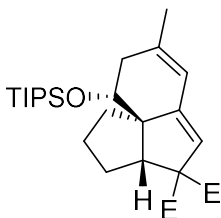
¹³C NMR (101 MHz, CHLOROFORM-*d*) δ ppm = 170.4 (C), 170.3 (C), 160.4 (2xC), 135.6 (CH), 124.8 (C), 122.5 (C), 109.5 (2xCH), 101.2 (CH), 85.4 (C), 83.4 (C), 61.4 (CH₂), 61.3 (CH₂), 60.7 (C), 55.4 (2xCH₃), 43.9 (CH), 29.7 (CH₂), 27.6 (CH₂), 25.0 (CH₂), 23.9 (CH₂), 17.8 (3xCH₃), 17.8 (3xCH₃), 14.1 (CH₃), 14.0 (CH₃), 12.0 (3xCH).

HRMS (EI) m/z calcd for C₃₃H₅₀O₇Si [M⁺]: 586.3326; found: 586.3278.

FTIR (neat, cm⁻¹): ν = 2940 (m), 2337 (w), 1729 (s), 1151 (s).

7.2.3 Gold(I)-catalyzed [4+2] cycloaddition

General procedure (GP13): To a solution of the silyl enol ether in toluene (0.05 M) was added [LAuNCMe][SbF₆] (1 mol%). After stirring at room temperature for 16 hours, CSA (1 equivalent) was added to the reaction mixture and stirred for 1 hour. The solvent was evaporated under reduce pressure and the crude mixture was purified by flash chromatography (3% ethyl acetate in hexanes) to provide the desired product.



Compound 3.2.18a

Synthesized according to GP13 using **3.2.17a** (47 mg, 96%).

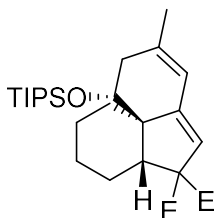
¹H NMR (400 MHz, CHLOROFORM-*d*) δ ppm = 5.92 (s, 1H), 5.27 (s, 1H), 4.28-4.02 (m, 5H), 3.54 (d, J = 8.2 Hz, 1H), 2.18 (d, J = 7.3 Hz, 1H), 1.94-1.86 (m, 1 H), 1.73 (s, 3H), 1.72-1.64 (m, 1H), 1.59-1.50 (m, 3H), 1.45-1.34 (m, 2H), 1.25 (t, J = 7.2 Hz, 3H), 1.20 (t, J = 7.1 Hz, 3H), 1.10-1.05 (m, 21H).

¹³C NMR (101 MHz, CHLOROFORM-*d*) δ ppm = 171.2 (C), 171.1 (C), 149.7 (C), 139.9 (C), 118.9 (CH), 118.8 (CH), 73.1 (CH), 71.3 (C), 64.5 (C), 61.4 (CH₂), 61.0 (CH₂), 48.7

(CH), 40.1 (CH₂), 31.4 (CH₂), 29.5 (CH₂), 25.1 (CH₂), 23.2 (CH₃), 18.3 (3XCH₃), 18.3 (3XCH₃), 14.2 (CH₃), 14.1 (CH₃), 13.0 (3XCH).

HRMS (EI) *m/z* calcd for C₂₈H₄₆O₅Si [M⁺]: 490.3115; found: 490.3127.

FTIR (neat, cm⁻¹): ν = 2945 (m), 1731 (s), 1096 (s).



Compound 3.2.18b

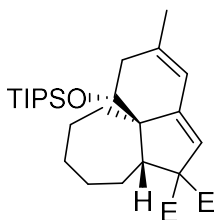
Synthesized according to GP13 using **3.2.17b** (39.5 mg, 79%).

¹H NMR (400 MHz, CHLOROFORM-*d*) δ ppm = 5.94 (s, 1H), 5.31 (s, 1H), 4.26-4.10 (m, 4H), 4.00(dd, *J* = 5.9, 10.0 Hz, 1H), 3.10 (d, *J* = 6.2 Hz, 1H), 2.41 (dd, *J* = 10.2, 17.5 Hz, 1H), 2.23 (dd, *J* = 5.4, 17.8 Hz, 1H), 2.14-1.80 (m, 5H), 1.76 (s, 3H), 1.53-1.46 (m, 1H), 1.42-1.37 (m, 1H), 1.28-1.22 (m, 6H), 1.14-1.08 (m, 21H).

¹³C NMR (101 MHz, CHLOROFORM-*d*) δ ppm = 172.2 (C), 171.2 (C), 153.0 (C), 139.4 (C), 119.9 (CH), 118.4 (CH), 79.4 (CH), 67.9 (C), 61.4 (CH₂), 61.3 (CH₂), 50.2 (C), 48.4 (CH), 39.1 (CH₂), 27.9 (CH₂), 23.5 (CH₂), 23.1 (CH₃), 21.5 (2xCH₂), 18.4 (3xCH₃), 18.3 (3xCH₃), 14.1 (CH₃), 13.9 (CH₃), 13.3 (3xCH).

HRMS (EI) *m/z* calcd for C₂₆H₄₁O₅Si [M⁺ - C₃H₇]: 461.2717; found 461.2768.

FTIR (neat, cm⁻¹): ν = 2950 (m), 1726 (s), 1091 (s).



Compound 3.2.18c

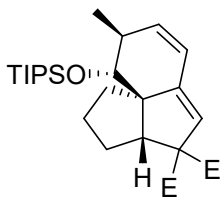
Synthesized according to GP13 using **3.2.17c** (30.5 mg, 61%).

¹H NMR (400 MHz, CHLOROFORM-*d*) δ ppm = 5.90 (s, 1H), 5.30 (s, 1H), 4.27-4.08 (m, 4H), 3.91 (dd, J = 5.4, 1.4 Hz, 1H), 3.43 (dd, J = 5.6, 10.6 Hz, 1H), 2.39 (dd, J = 10.4, 10.7 Hz, 1H), 2.21 (dd, J = 5.3, 17.8 Hz, 1H), 2.14-2.05 (m, 2H), 1.91-1.84 (m, 2H), 1.76 (s, 3H), 1.66-1.57 (m, 2H), 1.54-1.38 (m, 4H), 1.26 (t, J = 7.2 Hz, 3H), 1.23 (t, J = 7.1 Hz, 3H), 1.14-1.09 (m, 21H).

¹³C NMR (101 MHz, CHLOROFORM-*d*) δ ppm = 172.0 (C), 171.4 (C), 152.3 (C), 139.1 (C), 119.1 (CH), 118.5 (CH), 79.2 (CH), 71.0 (C), 61.3 (CH₂), 61.1 (CH₂), 57.9 (C), 50.7 (CH), 39.8 (CH₂), 32.2 (CH₂), 30.4 (CH₂), 29.8 (CH₂), 25.1 (CH₂), 24.1 (CH₂), 22.9 (CH₃), 18.3 (3xCH₃), 18.2 (3xCH₃), 14.1 (CH₃), 14.1 (CH₃), 13.2 (3xCH).

HRMS (EI) m/z calcd for C₃₀H₅₀O₅Si [M^+]: 518.3428; found 518.3415.

FTIR (neat, cm⁻¹): ν = 2924 (m), 1726 (s), 1052 (s).



Compound 3.2.18d

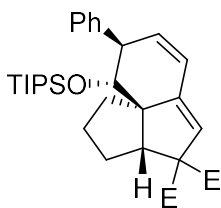
Synthesized according to GP13 using **3.2.17f** (45.5 mg, 91%).

¹H NMR (400 MHz, CHLOROFORM-*d*) δ ppm = 6.11 (dd, J = 2.7, 9.5 Hz, 1H), 5.56 (dd, J = 2.5, 9.6 Hz, 1H), 5.41 (s, 1H), 4.50-4.06 (m, 4H), 3.76 (d, J = 8.3 Hz, 1H), 3.52 (d, J = 8.4 Hz, 1H), 2.37-2.30 (m, 1H), 2.02-1.93 (m, 1H), 1.76-1.66 (m, 1H), 1.60-1.35 (m, 4H), 1.27 (t, J = 7.1 Hz, 3H), 1.22 (t, J = 7.1 Hz, 3H), 1.16-1.10 (m, 24 H).

¹³C NMR (101 MHz, CHLOROFORM-*d*) δ ppm = 171.0 (C), 170.7 (C), 149.2 (C), 137.8 (CH), 121.5 (CH), 121.0 (CH), 80.2 (CH), 71.7 (C), 65.6 (C), 31.4 (CH₂), 61.1 (CH₂), 48.8 (CH), 39.5 (CH), 31.3 (CH₂), 29.9 (CH₂), 24.8 (CH₂), 18.9 (CH₃), 18.6 (3XCH₃), 18.6 (3XCH₃), 14.2 (3XCH), 14.2 (CH₃), 14.1 (CH₃).

HRMS (EI) m/z calcd for C₂₈H₄₆O₅Si [M⁺]: 490.3115; found: 490.3080.

FTIR (neat, cm⁻¹): ν = 2950 (m), 1737 (s), 1099 (s).



Compound 3.2.18e

Synthesized according to GP13 using **3.2.17h** (40.5 mg, 81%).

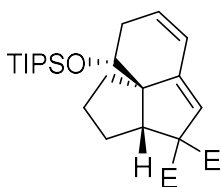
¹H NMR (400 MHz, CHLOROFORM-*d*) δ ppm = 7.27-7.16 (m, 5H), 6.20 (dd, J = 2.7, 9.7 Hz, 1H), 5.57 (dd, J = 2.3, 9.6 Hz, 1H), 5.50 (s, 1H), 4.31-4.08 (m, 5H), 3.52 (d, J = 8.4 Hz, 1H), 3.41 (dt, J = 2.5, 8.5 Hz, 1H), 2.18-2.10 (m, 1H), 1.79-1.68 (m, 1H), 1.65-

1.40 (m, 4H), 1.27 (t, $J = 7.2$ Hz, 3H), 1.24 (t, $J = 7.1$ Hz, 3H), 0.93 (d, $J = 7.5$ Hz, 9H), 0.91 (d, $J = 7.6$ Hz, 9H), 0.53 (septet, $J = 7.6$ Hz, 3H).

^{13}C NMR (101 MHz, CHLOROFORM-*d*) δ ppm = 170.9 (C), 170.7 (C), 148.9 (C), 142.9 (C), 136.4 (CH), 129.5 (2xCH), 128.2 (2xCH), 126.9 (CH), 121.7 (CH), 121.5 (CH), 80.0 (C), 71.7 (C), 66.2 (C), 61.5 (CH₂), 61.1 (CH₂), 52.8 (CH), 49.0 (CH), 31.4 (CH₂), 30.1 (CH₂), 24.9 (CH₂), 18.7 (3xCH₃), 18.4 (3xCH₃), 14.2 (CH₃), 14.1 (CH₃), 14.0 (3xCH).

HRMS (EI) m/z calcd for C₃₃H₄₈O₅Si [M⁺]: 552.3271; found: 552.3254.

FTIR (neat, cm⁻¹): $\nu = 2924$ (m), 1734 (s), 1096 (s).



Compound 3.2.18f

Synthesized according to GP13 using **3.2.17e** (46.5 mg, 93%).

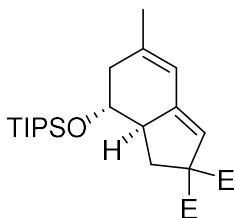
^1H NMR (400 MHz, CHLOROFORM-*d*) δ ppm = 6.17 (dd, $J = 2.4, 9.6$ Hz, 1H), 5.73 (ddd, $J = 2.4, 5.4, 9.6$ Hz), 5.41 (s, 1H), 4.30-4.05 (m, 5H), 3.59 (s, $J = 8.2$ Hz, 1H), 2.38 (ddt, $J = 1.0, 5.7, 18.0$ Hz, 1H), 2.20 (ddt, $J = 2.4, 9.7, 18.0$ Hz, 1H), 1.97-1.89 (m, 1H), 1.77-1.68 (m, 1H), 1.62-1.53 (m, 2H), 1.46-1.41 (m, 2H), 1.27 (t, $J = 7.1$ Hz, 3H), 1.22 (t, $J = 7.1$ Hz, 3H), 1.13-1.04 (m, 21H).

^{13}C NMR (101 MHz, CHLOROFORM-*d*) δ ppm = 171.0 (C), 170.8 (C), 149.2 (C), 130.6 (CH), 123.1 (CH), 121.1 (CH), 73.2 (CH), 71.2 (C), 64.9 (C), 61.4 (CH₂), 61.1 (CH₂), 48.9

(CH), 35.1 (CH₂), 31.0 (CH₂), 29.3 (CH₂), 25.0 (CH₂), 18.3 (3xCH₃), 18.2 (3xCH₃), 14.2 (CH₃), 14.1 (CH₃), 13.0 (3xCH).

HRMS (EI) *m/z* calcd for C₂₄H₃₇O₅Si [M⁺-C₃H₇]: 433.6736; found: 433.2394.

FTIR (neat, cm⁻¹): ν = 2945 (m), 1724 (s), 1096 (s).



Compound 3.2.18g

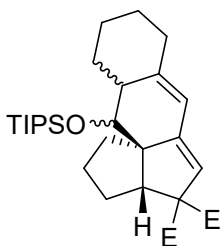
Synthesized according to GP13 using **3.2.17d** (46.5 mg, 93%).

¹H NMR (400 MHz, CHLOROFORM-*d*) δ ppm = 6.00 (s, 1H), 5.47 (d, *J* = 2.0 Hz, 1H), 4.23-4.12 (m, 4H), 3.75 (ddd, *J* = 6.0, 10.3, 15.1 Hz, 1H), 2.92 (d, *J* = 7.0 Hz, 12.7 Hz, 1H), 2.87-2.91 (m, 1H), 2.30-2.23 (m, 2H), 2.00 (d, *J* = 8.9 Hz, 12.8 Hz, 1H), 1.78 (s, 3H), 1.26-1.21 (m, 6H), 1.07 (s, 21H).

¹³C NMR (101 MHz, CHLOROFORM-*d*) δ ppm = 171.8 (C), 170.9 (C), 146.8 (C), 141.5 (C), 119.1 (CH), 119.0 (CH), 74.0 (CH), 65.8 (C), 61.4 (CH₂), 61.3 (CH₂), 50.7 (CH), 41.8 (CH₂), 38.0 (CH₂), 25.6 (CH₃), 18.2 (3xCH₃), 18.2 (3xCH₃), 14.1 (2xCH₃), 12.7 (3xCH).

HRMS (EI) *m/z* calcd for C₂₂H₃₅O₅Si [M⁺-C₃H₇]: 407.2248; found: 407.2263.

FTIR (neat, cm⁻¹): ν = 2935 (m), 1731 (s), 1104 (s).



Compound 3.2.18h

Synthesized according to GP13 from **3.2.17g** (43 mg, 86%).

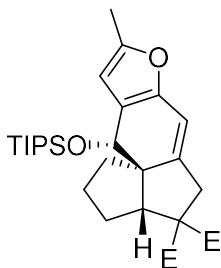
Mixture of diastereomers (1:1:1):

¹H NMR (400 MHz, CHLOROFORM-*d*) δ ppm = 5.89 (s, 2H), 5.64 (s, 1H), 5.40 (s, 1H), 5.32 (s, 1H), 5.32 (s, 1H), 4.28-4.01 (m, 12H), 3.87 (d, J = 10.5 Hz, 1H), 3.77 (d, J = 7.9 Hz, 1H), 3.51 (d, J = 7.1 Hz, 1H), 3.46 (d, J = 8.1 Hz, 1H), 3.22 (dd, J = 4.2, 8.2 Hz, 1H), 3.15 (d, J = 14.6 Hz, 1H), 2.57 (d, J = 2.36 Hz, 1H), 2.36-1.35 (series of m, 45H), 1.26-1.15 (m, 18H), 1.15-1.10 (m, 63H).

¹³C NMR (101 MHz, CHLOROFORM-*d*) δ ppm = 171.4 (C), 171.3 (C), 171.2 (C), 171.0 (C), 170.9 (C), 170.4 (C), 149.4 (C), 148.9 (C), 148.4 (C), 147.1 (C), 143.9 (C), 137.1 (C), 123.9 (CH), 121.0 (CH), 119.8 (CH), 119.6 (CH), 116.1 (CH), 114.8 (CH), 80.0 (CH), 79.5 (CH), 75.1 (CH), 65.1 (C), 64.5 (C), 63.5 (C), 61.3 (CH₂), 61.3 (CH₂), 61.1 (CH₂), 61.2 (CH₂), 61.0 (2xCH₂), 59.3 (C), 51.2 (CH), 50.0 (CH), 48.6 (CH), 47.3 (CH), 46.9 (CH), 41.3 (CH), 40.5 (CH₂), 36.1 (CH₂), 35.3 (CH₂), 35.0 (CH₂), 32.7 (CH₂), 31.8 (CH₂), 31.5 (CH₂), 31.3 (CH₂), 31.0 (CH₂), 29.9 (CH₂), 29.3 (CH₂), 28.8 (CH₂), 27.4 (CH₂), 27.3 (CH₂), 27.2 (CH₂), 26.9 (CH₂), 26.1 (CH₂), 25.7 (CH₂), 25.7 (CH₂), 25.0 (CH₂), 22.7 (CH₂), 18.6 (3xCH₃), 18.6 (3xCH₃), 18.6 (3xCH₃), 18.6 (3xCH₃), 18.4 (3xCH₃), 18.3 (3xCH₃), 14.4 (3xCH), 14.2 (3xCH), 14.1 (2xCH₃), 14.1 (2xCH₃), 13.7 (2xCH₃), 13.2 (3xCH).

HRMS (EI) m/z calcd for $C_{28}H_{43}O_5Si$ [$M^+ - C_3H_7$]: 487.2874; found: 487.2880.

FTIR (neat, cm^{-1}): ν = 2929 (m), 1731 (s), 1456 (m), 1211 (s).



Compound 3.2.18i

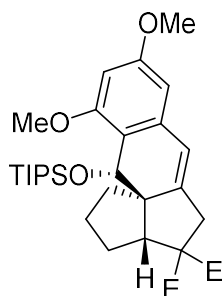
Synthesized according to GP13 from **3.2.17i** (44.5 mg, 89%).

1H NMR (400 MHz, CHLOROFORM-*d*) δ ppm = 5.99 (s, 1H), 5.91 (d, J = 2.6 Hz, 1H), 5.56 (s, 1H), 4.24-4.13 (m, 4H), 3.21-3.14 (m, 2H), 2.74-2.67 (m, 2H), 2.26 (s, 3H), 1.88-1.80 (m, 1H), 1.73-1.65 (m, 1H), 1.61-1.55 (m, 1H), 1.29-1.18 (m, 3H), 1.26 (t, J = 7.1 Hz, 3H), 1.20 (t, J = 7.1 Hz, 3H), 1.17-1.12 (m, 18H).

^{13}C NMR (101 MHz, CHLOROFORM-*d*) δ ppm = 171.3 (C), 170.0 (C), 149.9 (C), 147.8 (C), 146.5 (C), 122.6 (C), 109.1 (CH), 106.3 (CH), 75.9 (CH), 64.9 (C), 63.5 (C), 61.4 (CH₂), 61.2 (CH₂), 49.7 (CH), 37.4 (CH₂), 32.7 (CH₂), 31.2 (CH₂), 27.5 (CH₂), 18.4 (3xCH₃), 18.3 (3xCH₃), 14.1 (CH₂), 14.1 (CH₂), 13.9 (CH₃), 13.3 (3xCH).

HRMS (EI) m/z calcd for $C_{28}H_{41}O_6Si$ [$M^+ - C_2H_5$]: 501.2678; found: 500.9783.

FTIR (neat, cm^{-1}): ν = 2955 (m), 1726 (s), 1050 (s).



Compound 3.2.18j

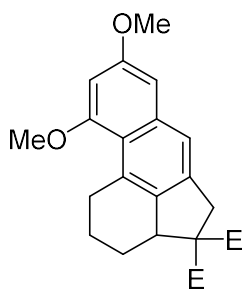
Synthesized according to GP13 from **3.2.17j** (45.5 mg, 91%).

¹H NMR (400 MHz, CHLOROFORM-*d*) δ ppm = 6.30 (d, J = 2.4 Hz, 1H), 6.12 (d, J = 2.4 Hz, 1H), 5.96 (d, J = 2.5 Hz, 1H), 5.47 (s, 1H), 4.26-4.12 (m, 4H), 3.76 (s, 3H), 3.70 (s, 3H), 3.34 (t, J = 8.6 Hz, 1H), 3.20 (dd, J = 2.6, 15.6 Hz, 1H), 2.72 (d, J = 15.6 Hz, 1H), 2.47-2.41 (m, 1H), 1.94-1.86 (m, 1H), 1.82-1.71 (m, 1H), 1.59-1.50 (m, 2H), 1.39-1.30 (m, 3H), 1.27 (t, J = 7.1 Hz, 3H), 1.21 (t, J = 7.1 Hz, 3H), 1.16 (d, J = 7.6 Hz, 9H), 1.13 (d, J = 7.6 Hz, 9H).

¹³C NMR (101 MHz, CHLOROFORM-*d*) δ ppm = 171.2 (C), 170.2 (C), 159.1 (C), 158.9 (C), 150.1 (C), 137.8 (C), 118.6 (C), 118.5 (CH), 103.4 (CH), 98.2 (CH), 78.1 (CH), 64.4 (C), 61.3 (CH₂), 61.1 (CH₂), 60.4 (C), 55.2 (CH₃), 55.1 (CH₃), 48.9 (CH), 38.1 (CH₂), 32.00 (CH₂), 31.8 (CH₂), 27.1 (CH₂), 18.9 (3xCH₃), 18.5 (3xCH₃), 14.2 (2xCH₃), 14.1 (3xCH).

HRMS (EI) m/z calcd for C₃₀H₄₃O₇Si (-C₃H₇): 586.3326; found: 586.3293.

FTIR (neat, cm⁻¹): ν = 2945 (m), 1729 (s), 1141 (s).



Compound 3.2.23

Synthesized according to GP13 from **3.2.17j** (26.5 mg, 76%).

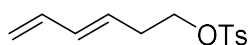
¹H NMR (400 MHz, CHLOROFORM-*d*) δ ppm = 7.33 (s, 1H), 6.66 (d, J = 204 Hz, 1H), 6.40 (d, J = 2.4 Hz, 1H), 4.35-4.22 (m, 2H), 4.14-4.01 (m, 2H), 3.87 (s, 3H), 3.84 (s, 3H), 3.84-3.79 (m, 1H), 3.65 (dd, J = 6.2, 18.8 Hz, 1H), 3.55 (d, J = 16.1 Hz, 1H), 3.27 (dd, J = 16.0, 1.2 Hz, 1H), 3.14-3.04 (m, 1H), 2.31-2.25 (m, 1H), 2.22-2.16 (m, 1H), 1.89-1.80 (m, 1H), 1.31 (t, J = 7.1 Hz, 3H), 1.30-1.26 (m, 1H), 1.16 (t, J = 7.1 Hz, 3H).

¹³C NMR (101 MHz, CHLOROFORM-*d*) δ ppm = 171.6 (C), 170.3 (C), 159.5 (C), 157.0 (C), 139.1 (C), 137.2 (C), 136.1 (C), 131.2 (C), 119.7 (C), 119.2 (CH), 99.7 (CH), 97.8 (CH), 64.9 (C), 61.3 (CH₂), 60.9 (CH₂), 55.2 (CH₃), 55.2 (CH₃), 48.6 (CH), 39.7 (CH₂), 28.3 (CH₂), 25.2 (CH₂), 24.6 (CH₂), 14.1 (CH₃), 14.1 (CH₃).

HRMS (EI) m/z calcd for C₂₄H₂₈O₆ [M⁺]: 412.1886; found 412.1807.

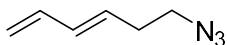
FTIR (neat, cm⁻¹): ν = 2937 (m), 1728 (s), 1241 (s), 1157 (s).

7.2.4 Synthesis of magellanine: Route A



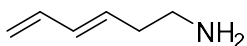
(E)-Hexa-3,5-dienyl 4-methylbenzenesulfonate (3.3.29)

To a flask containing alcohol **3.3.28** ¹²⁶ (12.8 g, 0.130 mol) in triethylamine (73 mL) was added TsCl (27.6, 0.145 mol) at 0 °C in portions over 15 minutes. The mixture was left to stir at room temperature overnight then was poured into water and extracted three times with ether. The combined organic extracts were washed twice with 1M HCl, once with sat. aqu. NaHCO₃ and once with brine, then dried over MgSO₄ and concentrated to yield the tosylated alcohol **3.10** (26.1 g, 79%) as an orange oil. The crude product was used without further purification. Spectroscopic data recorded were consistent with that reported previously.¹²⁷



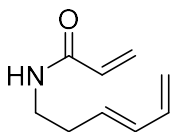
(E)-6-Azidohexa-1,3-diene (3.3.30)

Sodium azide (3.94 g, 60.6 mmol) was added to a solution of tosylate **3.3.29** (10.2 g, 40.4 mmol) in DMSO (48.0 mL). The mixture was stirred at room temperature overnight and was then diluted with water at 0 °C and extracted three times with ether. The combined ethereal layers were washed with water and with brine, dried with MgSO₄ and concentrated to give azide **3.11** (4.95 g, 99%) as an orange oil. The crude product was used in the following step without further purification. Spectroscopic data recorded were consistent with that reported previously.¹²⁸



(E)-Hexa-3,5-dien-1-amine (3.3.31)

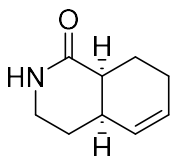
LiAlH₄ (4.33 g, 0.108 mol) was added to ether (1.0 L) in a flask which was then brought to 0 °C. Azide **3.3.30** (12.7 g, 0.103 mol) was added slowly and the mixture was left to stir at room temperature for 4 hours. The reaction mixture was quenched with aqueous sodium L-tartrate (25 g/L) at 0 °C and was left to stir at room temperature for 1.5 hours. The phases were separated and the aqueous layer was extracted 3 times with ether. The combined organic layers were washed with brine, dried with MgSO₄ and concentrated, affording the crude amine **3.3.31** as a yellow oil. The crude product was distilled (heat gun, ≤ 2 Torr) to a colourless oil (6.82 g, 68%). Caution should be exercised during the distillation as overheating of this product can result in polymerization. Spectroscopic data recorded were consistent with that reported previously.¹²⁸



(E)-N-(Hexa-3,5-dienyl)acrylamide (3.3.32)

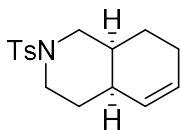
Triethylamine (1.5 mL, 10.6 mmol) was added to a flask containing amine **3.3.31** (940 mg, 9.67 mmol) in DCM (22 mL) at room temperature. This mixture was then added slowly and along the side of the flask to a solution of acryloyl chloride (0.79 mL, 9.67 mmol) in DCM (22 mL) at -78 °C. This transparent yellow reaction mixture was then left to warm to room temperature and stirred for 4 hours, then sat. aqu. NaHCO₃ was added and the mixture was extracted 3 times with ethyl acetate. The combined organic layers were washed with brine, dried with MgSO₄ and concentrated under reduced pressure. Flash chromatography (40% ethyl acetate in hexanes) gave amide **3.3.32** (1.07 g, 73%) as a colourless oil. Polymerization of this compound was observed with a sample of lesser

purity stored in the fridge. Spectroscopic data recorded were consistent with that reported previously.¹²⁹



(±)-(4aR,8aS)-2,3,4,4a,8,8a-Hexahydroisoquinolin-1(7H)-one (3.3.33)

This experiment was performed with glassware which was not flame dried and was not kept under an argon atmosphere. In(OTf)₃ (375 mg, 0.668 mmol) was added to a flask containing amide **3.3.33** (505 mg, 3.34 mmol) in a mixture of distilled water (40 mL) and isopropanol (6.5 mL). The mixture was brought to 50 °C and stirred overnight. The reaction mixture was then brought to room temperature and extracted three times with ethyl acetate. The combined organic layers were washed with brine and dried with MgSO₄ and concentrated in vacuo to give lactam **3.3.33** as a pale-yellow solid (360.1 mg, 71%). Recrystallization from THF and Et₂O gave **3.3.33** as white crystals. Attempts at scaling up this transformation to more than 2 g of amide **3.3.32** resulted in significantly decreased yields. Spectroscopic data recorded were consistent with that reported previously.¹²⁹



(±)-(4aR,8aS)-2-Tosyl-1,2,3,4,4a,7,8,8a-octahydroisoquinoline (3.3.34)

LiAlH₄ (1.06 g, 2.66 mmol) was added to THF (67 mL) in a flask which was then brought to 0 °C. Lactam **3.3.33** (1.83 g, 12.1 mmol) in THF (93 mL) was added slowly and the

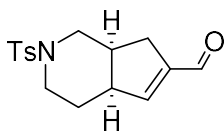
mixture was left to stir at room temperature overnight. The reaction mixture was quenched with aqueous sodium L-tartrate (25 g/L) at 0 °C and was left to stir at room temperature for 1 hour and 30 minutes. The phases were separated and the aqueous layer was extracted 3 times with ethyl acetate. The combined organic layers were washed with brine, dried with MgSO₄ and concentrated. The crude was carried on without further purification. To a flask containing the amine in pyridine (6.8 mL) was added TsCl (2.54 g, 13.3 mmol) at 0 °C in portions over 15 minutes. The mixture was left to stir at room temperature overnight, and then poured into water and extracted three times with ethyl acetate. The combined organic extracts were washed twice with 2M HCl, once with sat. aqu. NaHCO₃ and once with brine, then dried over MgSO₄ and concentrated. Flash chromatography (15% Et₂O in hexanes) yielded the tosylated amine **3.3.34** (2.77 g, 79% over 2 steps) as a white crystalline solid.

¹H NMR (400 MHz, CHLOROFORM-*d*) δ ppm = 7.60 (d, *J* = 8.2 Hz, 2H), 7.28 (d, *J* = 8.1 Hz, 2H), 5.62-5.58 (m, 1 H), 5.43 (ddt, *J* = 10.0, 3.8, 1.9 Hz, 1H), 3.19-3.07 (m, 2H), 2.79 (dd, *J* = 11.4, 3.8 Hz, 1H), 2.66-2.61 (m, 1H), 2.40 (s, 3H), 2.11-2.03 (m, 1H), 2.02-1.89 (m, 3H), 1.85-1.66 (m, 2H), 1.64-1.43 (m, 2H).

¹³C NMR (101 MHz, CHLOROFORM-*d*) δ ppm = 143.3 (C), 133.5 (C), 129.6 (CH), 129.6 (2xCH), 127.7 (2xCH), 127.5 (CH), 49.5 (CH₂), 45.0 (CH₂), 33.3 (CH), 32.9 (CH), 29.4 (CH₂), 24.0 (CH₂), 23.2 (CH₂), 21.5 (CH₃).

HRMS (EI) *m/z* calcd for C₁₆H₂₁NO₂S [M⁺]: 291.1293; found 291.1276.

FTIR (neat, cm⁻¹): ν = 3017 (m), 2925 (m), 2838 (m), 1489 (s).



(±)-3-(3-oxopropyl)-1-Tosylpiperidine-4-carbaldehyde (3.3.36)

To a flask containing quinoline **3.3.34** (5 g, 17.16 mmol) in a solvent mixture of THF (160 mL) and water (54 mL) was added a solution of osmium tetroxide (4% wt in water, 5.45 mL, 0.85 mmol). After stirring for 5 minutes at room temperature, NMO (60% in water, 8.04 g, 34.3 mmol) was added. Once all starting material was judged consumed by TLC, NaIO₄ (11 g, 51.5 mmol) was added to the reaction mixture. The reaction mixture was monitored by TLC and upon completion, an aqueous solution of 20% Na₂S₂O₃ was added. The aqueous layer was extracted 3 times with diethyl ether and the combined organic layers were washed with 20% Na₂S₂O₃, brine, dried over MgSO₄ and concentrated *in vacuo* (rotary evaporator water bath temperatures ≤ 40 °C) to give the crude dialdehyde. The latter was dissolved in benzene (500 mL) and piperidine acetic acid salt was added (250 mg, 1.7 mmol). The flask was equipped with a Dean-Stark and a reflux condenser, and the solution was heated to reflux for about 1 hour or until all starting material was consumed by TLC. The resulting orange solution was washed twice with each 2N HCl, sat. aq. NaHCO₃ and brine. The organic layer was dried MgSO₄, filtered and concentrated. Purification by flash chromatography (30% to 50% ethyl acetate in hexanes) afforded the enal **3.3.36** (3.83 g, 73%) as viscous oil.

¹H NMR (400 MHz, CHLOROFORM-*d*) δ ppm = 9.70 (s, 1H), 7.61 (d, *J* = 8.2 Hz, 2H), 7.31 (d, *J* = 8.2 Hz, 2H), 6.66 (s, 1H), 3.23-3.16 (m, 1H), 3.14-3.08 (m, 1H), 2.95-2.90 (m,

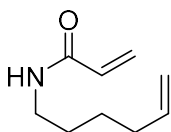
1H), 2.81 (ddd, $J = 3.6, 8.9, 12.1$ Hz, 1H), 2.64-2.55 (m, 3H), 2.42 (s, 3H), 2.32-2.26 (m, 1H), 2.06-1.98 (m, 1H), 1.77-1.69 (m, 1H).

^{13}C NMR (101 MHz, CHLOROFORM-*d*) δ ppm = 189.58 (CH), 154.01 (CH), 147.00 (C), 143.58 (C), 133.48 (C), 129.75 (2xCH), 127.58 (2xCH), 46.87 (CH₂), 44.01 (CH₂), 42.66 (CH), 37.04 (CH), 31.71 (CH₂), 26.44 (CH₂) 21.54 (CH₃).

HRMS (EI) m/z calcd for C₁₆H₁₉NO₃S [M⁺]: 305.1086; found 305.1067.

FTIR (neat, cm⁻¹): 2930 (m), 2857 (w), 1678 (s).

7.2.5 Synthesis of magellanine: Route B



***N*-(hex-5-en-1-yl)acrylamide (3.3.41)**

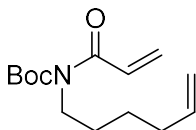
Triethylamine (3.54 mL, 25.4 mmol) was added to a flask containing amine **3.3.40** (2.1 g, 21 mmol) in DCM (50 mL) at room temperature. This mixture was then added slowly and along the side of the flask to a solution of acryloyl chloride (1.9 mL, 23.3 mmol) in DCM (50 mL) at -78 °C. The reaction mixture was then left to warm to room temperature and stirred for 4 hours, then sat. aqueous NaHCO₃ was added and the mixture was extracted 3 times with dichloromethane. The combined organic layers were washed with brine, dried with MgSO₄ and concentrated under reduced pressure. Flash chromatography (40% ethyl acetate in hexanes) gave amide **3.3.41** (2.46 g, 76%) as a colourless oil.

¹H NMR (400 MHz, CHLOROFORM-*d*) δ ppm = 6.25 (dd, J = 17.0, 1.6 Hz, 1H), 6.09 (dd, J = 17.0, 10.2 Hz, 1H), 5.91 (br.s, 1H), 5.77 (ddt, J = 16.9, 10.2, 6.7 Hz, 1H), 5.60 (dd, J = 10.2, 1.6 Hz, 1H), 4.99 (dq, J = 17.2, 1.7 Hz, 1H), 4.94 (ddt, J = 10.1, 2.2, 1.2 Hz, 1H), 3.31 (q, J = 7.1, 5.8 Hz, 2H), 2.16 – 1.91 (m, 2H), 1.61 – 1.48 (m, 2H), 1.48 – 1.26 (m, 2H).

¹³C NMR (101 MHz, CHLOROFORM-*d*) δ ppm = 165.61 (C), 138.37 (CH), 130.97 (CH), 126.16 (CH₂), 114.82 (CH₂), 39.46 (CH₂), 33.33 (CH₂), 28.99 (CH₂), 26.16 (CH₂).

HRMS (EI) m/z calcd for C₉H₁₅NO₁ [M⁺]: 153.1154; found 154.1272.

FTIR (neat, cm⁻¹): 3278 (s), 3075 (m), 2930 (s), 1654 (s), 1544 (s).



***tert*-butyl acryloyl(hex-5-en-1-yl)carbamate (3.3.42)**

Boc₂O (2.85 g, 13 mmol) was added to the amide **3.3.41** (1g, 6.5 mmol) and DMAP (80 mg, 0.7 mmol) and stirred overnight. The reaction mixture was quenched with sat. aqueous NaHCO₃ and extracted three times with dichloromethane. The combined organic layers were washed with brine, dried with MgSO₄ and concentrated under reduced pressure. Flash chromatography (8% ethyl acetate in hexanes) gave the carbamate **3.3.42** (1.64 g, 98%) as a colourless oil.

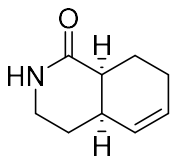
¹H NMR (400 MHz, CHLOROFORM-*d*) δ ppm = 6.98 (dd, J = 16.9, 10.4 Hz, 1H), 6.28 (dd, J = 16.9, 1.8 Hz, 1H), 5.79 (ddt, J = 16.9, 10.2, 6.6 Hz, 1H), 5.66 (dd, J = 10.4, 1.8

Hz, 1H), 5.00 (dq, $J = 17.1, 1.7$ Hz, 1H), 4.94 (ddt, $J = 10.2, 2.3, 1.3$ Hz, 1H), 3.71 – 3.59 (m, 2H), 2.25 – 1.94 (m, 2H), 1.63 – 1.54 (m, 2H), 1.52 (d, $J = 1.3$ Hz, 9H), 1.44 – 1.30 (m, 2H).

^{13}C NMR (101 MHz, CHLOROFORM-*d*) δ ppm = 168.61 (C), 146.75 (C), 138.51 (CH), 131.68 (CH), 127.33 (CH₂), 114.67 (CH₂), 85.18 (C), 44.66 (CH₂), 33.38 (CH₂), 28.21 (CH₂), 27.42 (3xCH₃), 26.17 (CH₂).

HRMS (EI) m/z calcd for C₁₄H₂₃NO₃ [$\text{M}^+ - \text{C}_4\text{H}_9$]: 196.0979; found 196.0941.

FTIR (neat, cm⁻¹): 3076 (w), 2978 (w), 1727 (s), 1682 (s), 1138 (s).

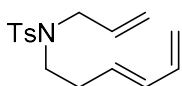


(±)-(4aR,8aS)-3,4,4a,7,8,8a-hexahydroisoquinolin-1(2H)-one (3.3.33)

The amide **3.3.42** (1 g, 3.95 mmol), Pd[1,2-bis(benzylsulfinyl)ethane](OAc)₂ (210 mg, 0.4 mmol), 2,6-Me₂BQ (1.34 g, 9.9 mmol) and p-nitrobenzoic acid (66 mg, 0.03 mmol) were dissolved in DCE (3 ml) and heated in an oil bath at 45°C for 48 hr. Upon completion, the dark red reaction mixture was filtered through a short silica plug, eluting with ~5 mL EtOAc and concentrated in vacuo a crude oil. The crude reaction mixture was dissolved in DCM (10 ml) and TFA (0.84 ml 11 mmol) was added. The reaction mixture was stirred overnight and quenched with sat. aqueous NaHCO₃. The aqueous layer was extracted three times with DCM. The combined organic layers were washed with brine, dried with MgSO₄ and concentrated under reduced pressure. Purification by flash chromatography (20%

EtOAc/hexanes) produced the cis-decalin **3.3.33** as a clear oil (305 mg, 2.0 mmol, 51% yield). Spectroscopic data recorded were consistent with that reported previously.¹²⁹

7.2.6 Synthesis of magellanine: Route C



(E)-N-allyl-N-(hexa-3,5-dien-1-yl)-4-methylbenzenesulfonamide (**3.3.45**)

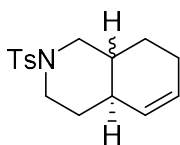
Tributylphosphine (1.17 mL, 4.72 mmol) was added to a solution of tetramethylazodicarboxamide (0.813 g, 4.72 mmol) in toluene (15 mL) at room temperature. After stirring for 30 minutes, *N*-allyl-4-methylbenzenesulfonamide (1 g, 4.72 mmol) was added in portion and stirred for 10 minutes. Alcohol **3.3.28** (0.42 mg, 4.3 mmol) was then added and the reaction mixture was stirred overnight. The reaction mixture was filtrated and the solvent was evaporated under reduced pressure. The crude residue was purified by flash chromatography (20% to 25% diethyl ether in hexanes) to afford compound **3.3.45** (0.894 g, 76%).

¹H NMR (400 MHz, CHLOROFORM-*d*) δ ppm = 7.69 (d, J = 8.3 Hz, 2H), 7.29 (d, J = 8.0 Hz, 2H), 6.24 (dt, J = 16.9, 10.3 Hz, 1H), 6.03 (dd, J = 15.3, 10.4 Hz, 1H), 5.77 – 5.45 (m, 2H), 5.26 – 4.89 (m, 4H), 3.81 (d, J = 6.4 Hz, 2H), 3.26 – 3.01 (m, 2H), 2.42 (s, 3H), 2.31 (qd, J = 7.3, 1.3 Hz, 2H).

¹³C NMR (101 MHz, CHLOROFORM-*d*) δ ppm = 143.20 (C), 137.16 (C), 136.77 (CH), 133.24 (CH), 133.16 (CH), 130.49 (CH), 129.68 (2xCH), 127.18 (2xCH), 118.81 (CH₂), 115.98 (CH₂), 50.76 (CH₂), 46.75 (CH₂), 31.76 (CH₂), 21.50 (CH₃).

HRMS (EI) m/z calcd for $C_{16}H_{21}NO_2S$ [$M^+ - C_9H_{14}N$]: 155.0167; found 155.0166.

FTIR (neat, cm⁻¹): 2975 (w), 1598 (w), 1340 (s), 1153 (s), 659 (s).



(±)-2-Tosyl-1,2,3,4,4a,7,8,8a-octahydroisoquinoline (3.3.34)

Tributylphosphine (28.9 mL, 117 mmol) was added to a solution of tetramethylazodicarboxamide (19.3 g, 112 mmol) in *o*-xylene (340 mL) at room temperature. After stirring for 30 minutes, *N*-allyl-4-methylbenzenesulfonamide (28g, 132 mmol) was added in portion and stirred for 10 minutes. Alcohol **3.3.28**⁵ (10 g, 101 mmol) was then added and the reaction mixture was stirred overnight. BHT (4.45 mg, 20 mmol) was added and the reaction mixture was heated at reflux for 16 hours. The resulting mixture was filtrated and the solvent removed under reduced pressure. The crude residue was purified by flash chromatography (20% to 25% diethyl ether in hexanes) to afford quinoline **3.3.34** (20.7 g, 70%) as a white solid containing a mixture of 2 diastereomers (1.6:1).

Major:

¹H NMR (400 MHz, CHLOROFORM-*d*) δ ppm = 7.60 (d, J = 8.2 Hz, 2H), 7.28 (d, J = 8.1 Hz, 2H), 5.62-5.58 (m, 1 H), 5.43 (ddt, J = 10.0, 3.8, 1.9 Hz, 1H), 3.19-3.07 (m, 2H), 2.79 (dd, J = 11.4, 3.8 Hz, 1H), 2.66-2.61 (m, 1H), 2.40 (s, 3H), 2.11-2.03 (m, 1H), 2.02-1.89 (m, 3H), 1.85-1.66 (m, 2H), 1.64-1.43 (m, 2H).

¹³C NMR (101 MHz, CHLOROFORM-*d*) δ ppm = 143.3 (C), 133.5 (C), 129.6 (CH), 129.6 (2xCH), 127.7 (2xCH), 127.5 (CH), 49.5 (CH₂), 45.0 (CH₂), 33.3 (CH), 32.9 (CH), 29.4 (CH₂), 24.0 (CH₂), 23.2 (CH₂), 21.5 (CH₃).

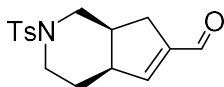
Minor:

¹H NMR (400 MHz, CHLOROFORM-*d*) δ ppm = 7.62 (d, *J* = 8.2 Hz, 2H), 7.29 (d, *J* = 8.1 Hz, 2H), 5.62-5.58 (m, 1 H), 5.39 (dq, *J* = 9.8, 1.8 Hz, 1H), 3.85 (dq, *J* = 11.5, 2.0 Hz, 1H), 3.71 (ddd, *J* = 10.8, 3.3, 1.6 Hz, 1H), 2.40 (s, 3H), 2.24 (td, *J* = 12.1, 2.7 Hz, 1H), 2.11-2.03 (m, 2H), 2.02-1.89 (m, 1H), 1.85-1.66 (m, 1H), 1.64-1.43 (m, 3H), 1.38 (dq, *J* = 12.3, 4.3 Hz, 1H), 1.23-1.12 (m, 1 H).

¹³C NMR (101 MHz, CHLOROFORM-*d*) δ ppm = 143.2 (C), 133.5 (C), 129.6 (3xCH), 127.6 (2xCH), 127.4 (CH), 51.8 (CH₂), 46.9 (CH₂), 39.9 (CH), 38.8 (CH), 31.3 (CH₂), 26.1 (CH₂), 25.3 (CH₂), 21.5 (CH₃).

HRMS (EI) *m/z* calcd for C₁₆H₂₁NO₂S [M⁺]: 291.1293; found 291.1276.

FTIR (neat, cm⁻¹): ν = 3017 (m), 2925 (m), 2838 (m), 1489 (s).



(±)-3-(3-oxopropyl)-1-Tosylpiperidine-4-carbaldehyde (3.3.36)

To a flask containing quinoline 21 (5 g, 17.16 mmol) in a solvent mixture of THF (160 mL) and water (54 mL) was added a solution of osmium tetroxide (4% wt in water, 5.45 mL, 0.85 mmol). After stirring for 5 minutes at room temperature, NMO (60% in water,

8.04 g, 34.3 mmol) was added. Once all starting material was judged consumed by TLC, NaIO₄ (11 g, 51.5 mmol) was added to the reaction mixture. The reaction mixture was monitored by TLC and upon completion, an aqueous solution of 20% Na₂S₂O₃ was added. The aqueous layer was extracted 3 times with diethyl ether and the combined organic layers were washed with 20% Na₂S₂O₃, brine, dried over MgSO₄ and concentrated *in vacuo* (rotary evaporator water bath temperatures ≤ 40 °C) to give the crude dialdehyde. The latter was dissolved in toluene (500 mL) and piperidine acetic acid salt was added (250 mg, 1.7 mmol). The flask was equipped with a Dean-Stark and a reflux condenser, and the solution was heated to reflux for about 1 hour or until all starting material was consumed by TLC. The resulting orange solution was washed twice with each 2N HCl, sat. aq. NaHCO₃ and brine. The organic layer was dried MgSO₄, filtered and concentrated. Purification by flash chromatography (30% to 50% ethyl acetate in hexanes) afforded the enal **3.3.36** (2.84 g, 54%) as viscous oil.

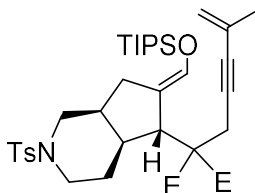
¹H NMR (400 MHz, CHLOROFORM-*d*) δ ppm = 9.70 (s, 1H), 7.61 (d, *J* = 8.2 Hz, 2H), 7.31 (d, *J* = 8.2 Hz, 2H), 6.66 (s, 1H), 3.23-3.16 (m, 1H), 3.14-3.08 (m, 1H), 2.95-2.90 (m, 1H), 2.81 (ddd, *J* = 3.6, 8.9, 12.1 Hz, 1H), 2.64-2.55 (m, 3H), 2.42 (s, 3H), 2.32-2.26 (m, 1H), 2.06-1.98 (m, 1H), 1.77-1.69 (m, 1H).

¹³C NMR (101 MHz, CHLOROFORM-*d*) δ ppm = 189.58 (CH), 154.01 (CH), 147.00 (C), 143.58 (C), 133.48 (C), 129.75 (2xCH), 127.58 (2xCH), 46.87 (CH₂), 44.01 (CH₂), 42.66 (CH), 37.04 (CH), 31.71 (CH₂), 26.44 (CH₂) 21.54 (CH₃).

HRMS (EI) *m/z* calcd for C₁₆H₁₉NO₃S [*M*⁺]: 305.1086; found 305.1067.

FTIR (neat, cm⁻¹): 2930 (m), 2857 (w), 1678 (s).

7.2.7 End game: Total synthesis of (±)-magellanine



Compound 3.3.46

A first solution was prepared as follows: To a solution of enal **3.3.36** (2.06 g, 6.75 mmol) in THF (45 mL) at -78 °C was added TIPSOTf (2.72 mL, 10.3 mmol). After stirring for 30 minutes, dimethyl sulfide (1 mL, 13.5 mmol) was added dropwise along the side of the flask. This solution was stirred at -78 °C for 60 minutes, then the second solution was added. This second solution was prepared by adding a solution of the malonate **3.3.15a** (3.22 g, 13.5 mmol) in THF (20 mL) to a suspension of LiHMDS (2.49 g, 14.85 mmol) in THF (20 mL) at -78 °C. The second solution was stirred at 0 °C for 10 minutes, and then added to the first solution at -78 °C, dropwise and along the side of the flask. The reaction mixture was warmed over night, starting from -78 °C and left to warm, then was quenched with sat. aq. NaHCO₃. The mixture was extracted with ethyl acetate (3X), and the combined organic layers were dried over MgSO₄, filtered and concentrated. Purification by flash chromatography (5%, 10% and 15% ethyl acetate in hexanes) afforded the desired product **3.3.46** (3.82 g, 81%) as a sticky oil.

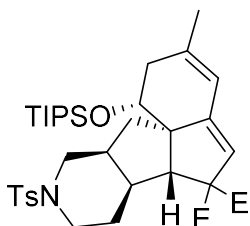
¹H NMR (400 MHz, CHLOROFORM-*d*) δ ppm = 7.61 (d, *J* = 8.3 Hz, 2H), 7.29 (d, *J* = 8.2 Hz, 2H), 6.57 (s, 1H), 5.12-5.11 (m, 2H), 4.24-4.04 (m, 4H), 3.60 (d, *J* = 11.4 Hz, 1H), 3.47 (d, *J* = 11.8 Hz, 1H), 3.05 (d, *J* = 17.3 Hz, 1H), 3.02 (s, 1H), 2.84 (d, *J* = 17.2 Hz, 1H), 2.50 (ddd, *J* = 2.5, 10.3, 17.4 Hz, 1H), 2.44-2.40 (m, 1H), 2.42 (s, 3H), 2.32-2.13 (m,

3H), 2.01-1.93 (m, 1H), 1.86-1.80 (m, 1H), 1.78 (s, 3H), 1.52 (ddd, $J = 4.0, 11.9, 13.4$ Hz, 1H), 1.23 (t, $J = 7.1$ Hz, 3H), 1.20 (t, $J = 7.2$ Hz, 3H), 1.17-1.10 (m, 3H), 1.10-1.06 (m, 18H).

^{13}C NMR (101 MHz, CHLOROFORM-*d*) δ ppm = 170.4 (C), 170.3 (C), 143.3 (C), 138.5 (CH), 133.2 (C), 129.5 (2xCH), 127.7 (2xCH), 126.5 (C), 121.3 (CH₂), 118.9 (C), 85.2 (C), 84.0 (C), 61.4 (CH₂), 61.4 (CH₂), 60.1 (C), 50.3 (CH), 47.0 (CH₂), 45.7 (CH₂), 39.8 (CH), 35.2 (CH), 29.0 (CH₂), 28.0 (CH₂), 24.7 (CH₂), 23.5 (CH₃), 21.5 (CH₃), 17.8 (3xCH₃), 17.8 (3xCH₃), 14.0 (CH₃), 13.9 (CH₃), 12.3 (3xCH).

HRMS (EI) m/z calcd for C₃₅H₅₀NO₇SSi [M⁺ - C₃H₇]: 656.3072; found 656.3089

FTIR (neat, cm⁻¹): $\nu = 2943$ (w), 2867 (m), 2219 (m), 1729 (s), 1668 (s), 1484 (m).



Compound 3.3.47

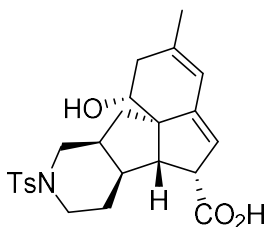
Synthesized according to GP13 from **3.3.46** (5 g, 91%).

^1H NMR (400 MHz, CHLOROFORM-*d*) δ ppm = 7.60 (d, $J = 8.2$ Hz, 2H), 7.29 (d, $J = 8.1$ Hz, 2H), 5.91 (s, 1H), 5.29 (s, 1H), 4.26-4.00 (m, 5H), 3.73-3.70 (m, 1H), 3.26 (d, $J = 11.9$ Hz, 1H), 3.26 (s, 1H), 2.42 (s, 3H), 2.40-2.20 (m, 5H), 2.12-1.98 (m, 2H), 1.75 (s, 3H), 1.48-1.36 (m, 3H), 1.19 (t, $J = 7.1$ Hz, 3H), 1.19 (t, $J = 7.1$ Hz, 3H), 1.16-1.13 (m, 21H).

^{13}C NMR (101 MHz, CHLOROFORM-*d*) δ ppm = 171.0 (C), 170.5 (C), 149.7 (C), 143.1 (C), 140.3 (C), 133.5 (C), 129.5 (2xCH), 127.7 (2xCH), 119.0 (CH), 118.5 (CH), 72.4 (CH), 71.5 (C), 64.9 (C), 61.5 (CH₂), 61.0 (CH₂), 53.2 (CH), 46.5 (CH₂), 46.1 (CH₂), 40.9 (CH), 40.3 (CH₂), 35.5 (CH), 28.9 (CH₂), 26.2 (CH₂), 23.0 (CH₃), 21.5 (CH₃), 18.3 (3xCH₃), 18.2 (3xCH₃), 14.1 (CH₃), 14.1 (CH₃), 13.4 (3xCH).

HRMS (EI) m/z calcd for C₃₅H₅₀NO₇SSi [M⁺ -C₃H₇]: 656.3072; found 656.3438.

FTIR (neat, cm⁻¹): ν = 2955 (m), 1726 (s), 1154 (s), 1093 (s).



Compound 3.3.48

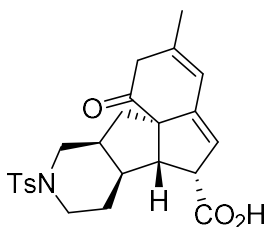
TBAF (13.13 mL, 13.13 mmol, 1M in THF) was added to a solution of **3.3.47** (6.13 g, 8.75 mmol) in THF (4 mL) at room temperature and the reaction mixture was heated at 60 °C for 3 hours. The mixture was added to a solution of LiOH (5.51 g, 131 mmol) in THF:H₂O (1:1, 175 mL) in a sealed tube and the mixture was heated to 140 °C. After stirring for overnight, the mixture was acidified with HCl 2N and extracted with ethyl acetate (3X). The combined organic layers were dried over MgSO₄, filtered and concentrated. The residue was purified by flash chromatography (60% to 80% ethyl acetate in hexanes) afforded the diastereomerically pure alcohol **3.3.48** (3.57 g, 92%) as a sticky oil.

¹H NMR (400 MHz, CHLOROFORM-*d*) δ ppm = 7.61 (d, J = 8.3 Hz, 2H), 7.31 (d, J = 8.1 Hz, 2H), 5.89 (s, 1H), 5.23 (d, J = 2.0 Hz, 1H), 3.84 (dd, J = 5.8, 10.1 Hz, 1H), 3.75-3.71 (m, 1H), 3.67 (d, J = 11.9 Hz, 1H), 3.24 (s, 1H), 2.55 (d, J = 4.2 Hz, 1H), 2.45-2.41 (m, 1H), 2.42 (s, 3H), 2.27-2.08 (m, 6H), 1.75 (s, 3H), 1.67-1.61 (m, 1H), 1.55-1.50 (m, 1H), 1.35 (dd, J = 5.5, 11.3 Hz, 1H).

¹³C NMR (101 MHz, CHLOROFORM-*d*) δ ppm = 179.5 (C), 149.2 (C), 143.3 (C), 139.3 (C), 133.4 (C), 129.6 (2xCH), 127.6 (2xCH), 118.6 (CH), 117.8 (CH), 72.0 (CH), 63.5 (C), 58.9 (CH), 53.3 (CH), 46.8 (CH₂), 46.1 (CH₂), 44.8 (CH), 39.1 (CH₂), 35.4 (CH), 28.9 (CH₂), 25.6 (CH₂), 22.9 (CH₃), 21.5 (CH₃).

HRMS (EI) m/z calcd for C₂₄H₂₉NO₅S [M⁺]: 443.1766; found 443.1811.

FTIR (neat, cm⁻¹): ν = 3166 (m), 2368 (s), 1599 (m), 1151 (s), 1043 (s).



Compound 3.3.49

Dess-Martin periodinane (3.1 g, 7.2 mmol) was added to a solution of alcohol **3.3.48** (2.67 g, 6.03 mmol) in DCM (12 mL). The mixture was stirred 40 minutes and then quenched with an aqueous solution of Na₂S₂O₃:NaHCO₃ 5% (1:1, 60 mL). The mixture was stirred for 1 hour and then extracted with DCM (3x). The combined organic layers were dried over MgSO₄, filtered and concentrated. The residue was purified by flash chromatography

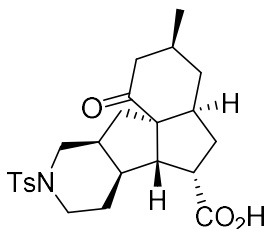
(40% to 50% ethyl acetate in hexanes with 1% AcOH) to provide the desired product **3.3.49** (2.4 g, 91%) as a sticky oil.

¹H NMR (400 MHz, CHLOROFORM-*d*) δ ppm = 7.59 (d, *J* = 8.3 Hz, 2H), 7.30 (d, *J* = 8.2 Hz, 2H), 6.11 (s, 1H), 5.30 (d, *J* = 1.6 Hz, 1H), 3.72 (d, *J* = 11.4 Hz, 1H), 3.63 (d, *J* = 12.0 Hz, 1H), 3.29-3.21 (m, 2H), 3.18 (d, *J* = 5.5 Hz, 1H), 2.71 (d, *J* = 21.0 Hz, 1H), 2.45-2.41 (m, 1H), 2.42 (s, 3H), 2.26-2.18 (m, 1H), 2.12-1.91 (m, 3H), 1.84 (s, 3H), 1.82-1.77 (m, 1H), 1.73-1.67 (m, 1H), 1.61 (dq, *J* = 4.3, 12.5 Hz, 1H).

¹³C NMR (101 MHz, CHLOROFORM-*d*) δ ppm = 205.8 (C), 179.3 (C), 146.6 (C), 143.5 (C), 138.4 (C), 133.2 (C), 129.6 (2xCH), 127.6 (2xCH), 119.2 (CH), 119.0 (CH), 70.4 (C), 56.7 (CH), 49.3 (CH), 46.3 (CH₂), 45.8 (CH₂), 44.0 (CH₂), 43.98 (CH), 37.5 (CH₂), 36.0 (CH), 25.9 (CH₂), 22.7 (CH₃), 21.5 (CH₃).

HRMS (EI) *m/z* calcd for C₂₄H₂₇NO₅S [*M*⁺]: 441.1610; found 441.1554.

FTIR (neat, cm⁻¹): ν = 2954 (m), 1704 (s), 1697 (s), 1159 (s), 1091 (m).



Compound 3.3.50

Platinum oxide (*Alfa Aesar*, 467 mg, 2.06 mmol) was added to a solution of diene **3.3.49** (910 mg, 2.06 mmol) in EtOAc : EtOH (5 mL : 20 mL) and was stirred overnight under 1 atm of H₂. The reaction mixture was then purged with argon, filtrated over cotton to remove

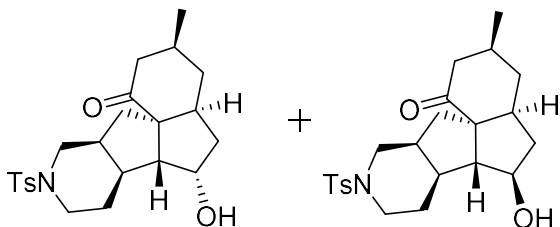
the platinum oxide and evaporated under vacuo. Purification of the crude material by flash chromatography (10% to 30% acetone in toluene) gave the desired product (782 mg, 85%) as a white solid.

^1H NMR (400 MHz, CHLOROFORM-*d*) δ ppm = 7.60 (d, J = 8.2 Hz, 2H), 7.30 (d, J = 8.1 Hz, 2H), 3.68-3.59 (m, 2H), 2.96 (d, J = 10.0 Hz, 1H), 2.72 (ddd, J = 1.8, 6.4, 18.0. Hz, 1H), 2.47 (dd, J = 3.6, 11.9 Hz, 1H), 2.36 (s, 3H), 2.36-2.00 (m, 8H), 1.75-1.65 (m, 3H), 1.50-1.32 (m, 3H), 1.31-1.22 (m, 2H), 0.98 (d, J = 6.6 Hz, 3H), 0.91-0.83 (m, 2H).

^{13}C NMR (101 MHz, CHLOROFORM-*d*) δ ppm = 213.4 (C), 180.3 (C), 143.2 (C), 133.2 (C), 129.6 (2xCH), 127.6 (2xCH), 63.9 (C), 53.1 (CH), 49.1 (CH), 48.9 (CH), 46.3 (CH), 45.8 (CH₂), 45.7 (CH₂), 41.5 (CH), 39.6 (CH), 38.0 (CH₂), 37.4 (CH₂), 36.3 (CH₂), 28.3 (CH), 25.7 (CH₂), 21.9 (CH₃), 21.5 (CH₃).

HRMS (EI) m/z calcd for C₂₄H₃₁NO₅S [M^+]: 445.1923; found 445.1971.

FTIR (neat, cm⁻¹): ν = 2987 (m), 1695 (s), 1336 (s), 1151 (s).



Compound 3.3.51 and 3.3.52

To a suspension of the acid **3.3.50** (100 mg, 0.22 mmol) in dry THF (1 mL) and toluene (5 mL) at 0 °C was added ethylchloroformate (0.024 mL, 0.25 mmol) and N-methylmorpholine (0.025 mL, 0.22 mmol). The cooling bath was removed, and the mixture

was stirred 15 minutes at room temperature. The reaction mixture was recooled to 0 °C before addition of 2-Mercapto-4-methylthiazole 3-oxide (36 mg, 0.25 mmol) and triethylamine (0.034 mL, 0.25 mmol). The mixture was stirred at 0 °C for 5 min, *tert*-dodecylmercaptan (0.21 mL, 0.9 mmol) was added, and the solution was irradiated with a 365 nm LED for 30 minutes while bubbling oxygen. Triphenylphosphine (68 mg, 3.4 mmol) was then added and the solution was stirred for 30 minutes. The solution was concentrated under reduced pressure. Purification by flash chromatography (30% to 60% ethyl acetate in hexane) afforded **3.3.51** (23.5 mg, 26%) and alcohol **3.3.52** (26.9 mg, 29%).

Compound 3.3.51:

¹H NMR (400 MHz, CHLOROFORM-*d*) δ ppm = 7.59 (d, J = 8.2 Hz, 2H), 7.30 (d, J = 8.1 Hz, 2H), 3.75-3.69 (m, 1H), 3.62-3.58 (m, 1H), 3.54 (d, J = 11.9 Hz, 1H), 2.71 (ddd, J = 201, 6.6, 17.8 Hz, 1H), 2.52-2.48 (m, 2H), 2.42 (s, 3H), 2.26-1.95 (m, 7H), 1.87-1.73 (m, 3 H), 1.63-1.46 (m, 2H), 1.14-1.05 (m, 1H), 0.97 (d, J = 6.6 Hz, 3H), 0.95-0.87 (m, 1H).

¹³C NMR (101 MHz, CHLOROFORM-*d*) δ ppm = 214.0 (C), 143.4 (C), 133.3 (C), 129.6 (2xCH), 127.6 (2xCH), 77.5 (CH), 63.0 (C), 58.0 (CH), 46.3 (CH₂), 46.1 (CH), 45.8 (CH₂), 45.7 (CH₂), 43.3 (CH₂), 40.4 (CH), 39.6 (CH₂), 37.7 (CH₂), 37.2 (CH), 28.6 (CH), 26.2 (CH₂), 22.1 (CH₃), 21.5 (CH₃).

HRMS (EI) m/z calcd for C₂₃H₃₁NO₄S [M⁺]: 417.1974; found 417.1854.

FTIR (neat, cm⁻¹): ν = 2952 (m), 1697 (s), 1332 (m), 1161 (s).

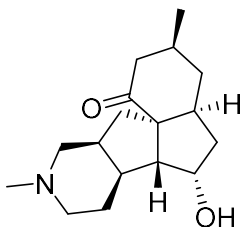
Compound 3.3.52:

¹H NMR (400 MHz, CHLOROFORM-*d*) δ ppm = 7.60 (d, *J* = 8.2 Hz, 2H), 7.29 (d, *J* = 8.0 Hz, 2H), 4.22-4.19 (m, 1H), 3.65-3.61 (m, 1H), 3.51 (d, *J* = 11.6 Hz, 1H), 2.75-2.69 (m, 2H), 2.49-2.42 (m, 2H), 2.42 (s, 3H), 2.33-2.23 (m, 1H), 2.13 (dt, *J* = 4.0, 11.3 Hz, 1H), 2.06-1.77 (m, 6H), 1.61-1.52 (m, 2H), 1.25-1.16 (m, 2H), 0.97 (d, *J* = 6.5 Hz, 3H), 0.87-0.76 (m, 1H).

¹³C NMR (101 MHz, CHLOROFORM-*d*) δ ppm = 214.4 (C), 143.3 (C), 133.2 (C), 129.5 (2xCH), 127.6 (2xCH), 73.3 (CH), 64.4 (C), 54.1 (CH), 46.4 (CH₂), 46.1 (CH₂), 46.1 (CH₂), 46.0 (CH₂), 44.8 (CH₂), 38.8 (CH), 38.8 (CH₂), 37.5 (CH₂), 36.9 (CH), 28.7 (C), 26.3 (CH₂), 22.1 (CH₃), 21.5 (CH₃).

HRMS (EI) *m/z* calcd for C₂₃H₃₁NO₄S [M⁺]: 417.1974; found 417.1976.

FTIR (neat, cm⁻¹): ν = 3471 (m), 2925 (m), 1733 (s), 1154 (s).



Compound 3.3.53

A solution of compound **3.3.52** (49 mg, 0.12 mmol) in 1, 2-dimethoxyethane (3 mL) was cooled at -78 °C and a solution of sodium naphthalene (0.48 mL, 0.24 mmol, 0.5 M in DME) (previously prepared from naphthalene (516 mg, 4.0 mmol) and sodium (71 mg, 3.0 mmol)) was added until the complete consumption of the starting material (monitored by TLC). Immediately thereafter, the reaction mixture was poured into a solution of

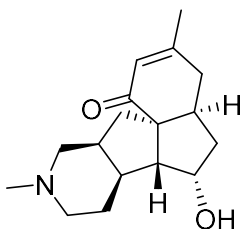
acetonitrile/acetic acid (1.2 mL, V:V=10:1) and allowed to warm-up to rt (2 min). A solution of formaldehyde (0.5 mL, 35% wt. solution in water) was then added and the mixture was stirred for 2 hours followed by NaBH₃CN (37 mg, 0.58 mmol). After stirring for 18h at rt, NaOH (2M) was added and the mixture was extracted with CHCl₃ (20 mL, x3). The combined organic layers were washed with brine, dried and concentrated under vacuo. The residue was purified by silica gel column chromatography (5% to 10% CHCl₃ in MeOH with 1% NH₂OH) to afford the amine **3.3.53** (24 mg, 74%).

¹H NMR (400 MHz, CHLOROFORM-*d*) δ ppm = 4.29-4.26 (m, 1H), 2.84-2.68 (m, 4H), 2.58-2.51 (m, 1H), 2.47-2.40 (m, 2H), 2.38 (s, 3H), 2.30-2.10 (m, 4H), 2.00-1.66 (m, 7H), 1.34-1.25 (m, 1H), 0.96 (d, *J* = 6.6 Hz, 3H), 0.86-0.76 (m, 1H).

¹³C NMR (101 MHz, CHLOROFORM-*d*) δ ppm = 214.8 (C), 73.0 (CH), 64.5 (C), 55.5 (CH₂), 54.1 (CH₂), 53.0 (CH), 46.2 (CH₃), 46.0 (CH₂), 45.8 (CH), 43.9 (CH₂), 40.2 (CH₂), 39.5 (CH), 37.7 (CH), 36.2 (CH), 29.0 (CH), 26.0 (CH₂), 22.2 (CH₃).

HRMS (EI) *m/z* calcd for C₁₇H₂₇NO₂ [M⁺]: 277.2042; found 277.2058.

FTIR (neat, cm⁻¹): ν = 3317 (m), 2941 (m), 1691 (s), 1020 (s).



Magellanine (3.3.1)

A freshly prepared solution of LDA (0.06 mL, 1M in THF) was added to a solution of **3.3.53** (8 mg, 0.075 mmol) in THF (0.4 ml) at 0 °C. The reaction mixture was stirred for 10 minutes and TMSCl (0.005 ml, 0.003 mmol) was added. After stirring for 1 hour at 0 °C, a second addition of LDA (0.06 mL, 1M in THF at -78 °C) was added followed by the addition of the Mukaiyama salt **30** (12 mg, 0.06 mmol). The mixture was stirred for 6 h and then the reaction mixture was quenched by the addition of HCl 2N. After stirring for 30 minutes, a solution of NaOH 2N was added until pH>7 and the aqueous phase was extracted with DCM (3x). The combined organic layers were dried over MgSO₄, filtered and concentrated under reduced pressure. The residue was purified by silica gel column chromatography (5% to 10% CHCl₃ in MeOH with 1% NH₂OH) to afford (±)-magellanine (**3.3.1**) (5 mg, 64%).

¹H NMR (400 MHz, CHLOROFORM-*d*) δ ppm = 5.87 (s, 1H), 4.21 (dd, *J* = 3.8, 6.2 Hz, 1H) 2.77-2.62 (m, 4H), 2.51 (ddd, *J* = 6.4, 6.4 12.7 Hz, 1H), 2.32-1.87 (m, 7H), 2.21 (s, 3H), 1.92 (s, 3H), 1.70-1.53 (m, 4H).

¹³C NMR (101 MHz, CHLOROFORM-*d*) δ ppm = 203.3 (C), 158.1 (C), 125.7 (CH), 72.0 (CH), 61.0 (C), 59.4 (CH), 56.4 (CH₂), 55.2 (CH₂), 46.7 (CH₃), 41.9 (CH₂), 41.3 (CH), 40.3 (CH), 37.3 (CH₂), 36.9 (CH), 30.4 (CH₂), 26.8 (CH₂), 24.5 (CH₃).

HRMS (EI) *m/z* calcd for C₁₇H₂₅NO₂ [M⁺]: 275.1885; found 275.1872.

FTIR (neat, cm⁻¹): ν = 2914 (m), 1637 (s), 1436 (m), 1230 (m), 727 (s).

Magellanine ¹H Comparison:

300 MHz (Paquette)	500 MHz (Mukai)	600 MHz (Yang)	400 MHz (Yan)	400 MHz (This Work)
5.86 (br s, 1H)	5.87 (s, 1H)	5.86 (s, 1H)	5.85 (s, 1H)	5.87 (s, 1H)
4.23-4.18 (m, 1H)	4.23-4.19 (m, 1H)	4.21 (dd, J = 6.5, 4.4 Hz, 1H)	4.20-4.17 (m, 1H)	4.21 (dd, J = 6.2, 3.8 Hz, 1H)
2.80-2.57 (m, 5H)	2.77-2.60 (m, 4H)	2.86-2.71 (m, 2H)	2.73-2.45 (m, 5H)	2.77-2.62 (m, 4H)
		2.71-2.59 (m, 2H)		
2.51 (ddd, J = 12, 7, 7 Hz, 1H)	2.51 (ddd, J = 12.7, 6.3, 6.3 Hz, 1H)	2.56-2.46 (m, 1H)	2.73-2.45 (m, 5H)	2.51 (ddd, J = 12.7, 6.4, 6.4 Hz, 1H)
2.30-1.50 (series of m, 10 H)	2.32-1.88 (m, 7H)	2.40-2.29 (m, 2H)	2.23-1.85 (m, 5H)	2.62-1.87 (m, 7H)
2.20 (br s, 3H)	2.20 (s, 3H)	2.30-2.19 (m, 6H)	2.17 (s, 3H)	2.21 (s, 3H)
		2.18-1.98 (m, 5H)		
1.92 (br s, 3H)	1.93 (s, 3H)	1.93 (s, 3H)	1.90 (s, 3H)	1.92 (s, 3H)
		1.90-1.79 (m, 1H)		
	1.71-1.52 (m, 4H)	1.75-1.56 (m, 4H)	1.70-1.45 (m, 7H)	1.70-1.53 (m, 4H)

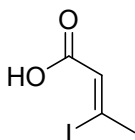
Magellanine ¹³C Comparison:

62.5 MHz (Paquette)	125.7 MHz (Mukai)	150 MHz (Yang)	101 MHz (Yan)	101 MHz (This Work)
203.2	203.3	203.3	203.5	203.3
158.0	158.0	158.3	158.2	158.1
125.7	125.7	125.6	125.5	125.7
72.1	72.0	71.8	71.6	72.0
61.0	61.0	61.0	60.9	61.0
59.6	59.6	59.0	59.7	59.4
56.5	56.5	56.1	56.5	56.4
55.4	55.4	54.8	55.4	55.2
46.9	46.9	46.5	46.8	46.7
41.9	41.9	42.0	41.8	41.9
41.4	41.4	41.1	41.2	41.3
40.2	40.3	40.4	40.1	40.3
37.3	37.3	37.3	37.2	37.3
37.0	37.0	36.7	36.8	36.9
30.4	30.4	30.3	30.4	30.4
27.0	27.0	26.5	26.9	26.8
24.5	24.5	24.5	24.4	24.5

7.3 Towards the total synthesis of salvinorin A

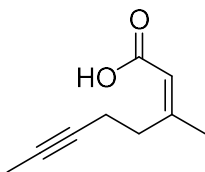
This section includes all characterization of *Chapter 4*.

7.3.1 Synthesis of the diene and Diels-Alder cycloaddition



(Z)-3-iodobut-2-enoic acid (4.2.10)

2-butyric acid (23.7 g, 281 mmol) was added to sodium iodide (67.6 g, 457 mmol) in acetic acid (103 ml) and heated at 120 °C for 3 hours. The reaction mixture was cooled down and H₂O (500ml) and Et₂O (500ml) was added. Sodium sulfite monobasic was added until the mixture turned pale yellow and the aqueous layer was extracted 3 times with ether. The combined organic layers were then dried over MgSO₄, filtered and concentrated under reduced pressure to afford pure **4.2.10** as a white solid (57 g, 97 %). Spectra match values reported in the literature.¹³⁰



(Z)-3-methylhept-2-en-5-ynoic acid (4.2.11)

1,2-dibromoethane (0.56 ml, 6.5 mmol) was added to zinc dust (12.7 g, 193 mmol) in THF (16 ml) and heated at 70 °C for 2 minutes. TMSCl (0.45 ml, 4.8 mmol) was slowly added

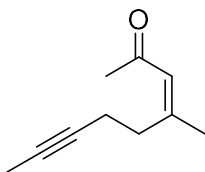
to the mixture at room temperature and stirred for 15 minutes. A solution of 5-iodopent-2-yne ¹³¹ (**4.2.12**, 18.8g, 97 mmol) in THF (16 ml) was then added slowly and the temperature was controlled with a water bath at room temperature (exothermic reaction). The mixture was heated at 40 °C for 16 hours and settle down for 1 hour without stirring. The surfactant was then transferred to a solution of **4.2.10** (6.8 g, 32 mmol) in DMF (32 ml) follow by the addition of Pd(PPh₃)₄ (1.85 g, 1.6 mmol). The reaction mixture was stirred over night and quenched with HCl (1M) follow by the addition of diethyl ether. The organic layer was extracted with NaOH 1M (3x) and the insoluble zinc residue was filtrated over cotton. The mixture was then acidified with concentrated HCl and extracted with EtOAc (3x). The combined organic layers were then dried over MgSO₄, filtered and concentrated under reduced pressure to afford **4.2.11** as a white off solid (4.25 g, 87 %).

¹H NMR (400 MHz, CHLOROFORM-*d*) δ ppm = 5.78 – 5.55 (m, 1H), 2.79 (t, *J* = 7.4 Hz, 2H), 2.33 (tq, *J* = 7.5, 2.6 Hz, 2H), 1.98 (d, *J* = 1.4 Hz, 3H), 1.76 (t, *J* = 2.6 Hz, 3H).

¹³C NMR (101 MHz, CHLOROFORM-*d*) δ ppm = 171.66 (C), 161.86 (C), 116.58 (CH), 78.22 (C), 76.37 (C), 32.77 (CH₃), 25.92 (CH₂), 17.67 (CH₃), 3.42 (CH₂).

HRMS (EI) *m/z* calcd for C₉H₁₂O₂ [M⁺]: 152.0837; found 152.0860.

FTIR (neat, cm⁻¹): ν = 2922 (s), 2854 (m), 1686 (s), 1637 (s).



(*Z*)-4-methyloct-3-en-6-yn-2-one (4.2.13)

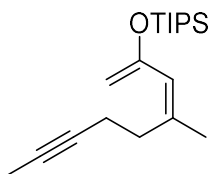
4.2.11 (2.6 g 17.1 mmol) was added to MeLi (29.7 ml, 1.38 M, 41 mmol) in THF (170 ml) at – 78 °C and brought to room temperature for 2 hours. The reaction mixture was quenched with sat. NH₄Cl and extracted with Et₂O (3x). The combined organic layers were then dried over MgSO₄, filtered and concentrated under reduced pressure. The residue was purified by silica gel column chromatography (5% to 7% EtOAc in hexane) to afford the ketone **4.2.13** (1.82 g, 71%).

¹H NMR (400 MHz, CHLOROFORM-*d*) δ ppm = 6.09 (s, 1H), 2.71 (t, *J* = 7.3 Hz, 2H), 2.30 (ddt, *J* = 7.4, 4.9, 2.6 Hz, 2H), 2.15 (s, 3H), 1.92 (d, *J* = 1.4 Hz, 3H), 1.74 (t, *J* = 2.6 Hz, 3H).

¹³C NMR (101 MHz, CHLOROFORM-*d*) δ ppm = 198.09 (C), 157.42 (C), 124.76 (CH), 78.50 (C), 76.06 (C), 32.90 (CH₂), 31.67 (CH₃), 25.91 (CH₃), 17.60 (CH₂), 3.44 (CH₃).

HRMS (EI) *m/z* calcd for C₁₀H₁₄O [*M*⁺]: 150.1045; found 150.1055.

FTIR (neat, cm⁻¹): ν = 2919 (w), 2987 (w), 1686 (s), 1614 (s), 1173 (s).



(*Z*)-triisopropyl((4-methylocta-1,3-dien-6-yn-2-yl)oxy)silane (4.2.8)

Triisopropylsilyl triflate (6.48 ml, 24.09 mmol) was added to **4.2.13** (1.81 g, 12.05 mmol) and Et₃N (5 ml, 36 mmol) in DCM (60 ml) at room temperature. The mixture was stirred overnight and then a solution of saturated NaHCO₃ (25 ml) was added. The aqueous layer was extracted with DCM (3x). The combined organic layer was dried over anhydrous

MgSO₄, filtered and the solvent was evaporated under reduce pressure. The crude was purified by flash column chromatography on basified silica gel (1% Et₃N in hexane) to give the desired silyl enol ether **4.2.8** (3.6 g, 98%).

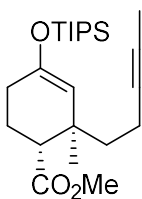
¹H NMR (400 MHz, CHLOROFORM-*d*) δ ppm = 5.61 (s, 1H), 4.27 (s, 1H), 4.19 (s, 1H), 2.60 (dd, J = 8.3, 7.4 Hz, 2H), 2.24 (ddt, J = 11.3, 7.5, 2.5 Hz, 2H), 1.77 (d, J = 1.5 Hz, 3H), 1.76 (t, J = 2.5 Hz, 3H), 1.29 – 1.17 (m, 3H), 1.15 – 1.05 (m, 18H).

¹³C NMR (101 MHz, CHLOROFORM-*d*) δ ppm = 155.50 (C), 138.60 (C), 124.31 (CH), 94.10 (CH₂), 78.91 (C), 75.71 (C), 32.29 (CH₂), 24.25 (CH₃), 18.02 (6xCH₃), 17.93 (CH₂), 12.91 (3xCH), 3.45 (CH₃).

HRMS (EI) m/z calcd for C₁₉H₃₄OSi [M⁺]: 306.2379; found 306.2401.

FTIR (neat, cm⁻¹): ν = 2944 (m), 2866 (s), 1014 (s), 679 (s).

7.3.2 Preparation of allylic alcohol 4.2.4



Compound 4.2.7

Et₂AlCl (1M) was added to **4.2.8** (1.6 g, 5.3 mmol) and methyl acrylate (0.71 ml, 7.9 mmol) in DCM (25 ml) at -78 °C. The reaction mixture was slowly warmed up to -30 °C and quenched with Et₃N:H₂O (20 ml) once the reaction mixture was completed by TLC. The aqueous layer was extracted with DCM (3x). The combined organic layer was dried over

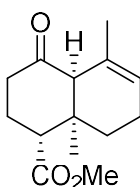
anhydrous MgSO_4 , filtered and the solvent was evaporated under reduce pressure. The crude was purified by flash column chromatography on silica gel (1% to 3% EtOAc in hexane) to give the desired silyl enol ether **4.2.7** (1.69 g, 81%).

^1H NMR (400 MHz, CHLOROFORM-*d*) δ ppm = 4.54 (d, J = 1.8 Hz, 1H), 3.68 (s, 3H), 2.39 (dd, J = 12.2, 3.1 Hz, 1H), 2.30 – 1.86 (m, 6H), 1.82 (ddd, J = 7.0, 5.6, 3.7 Hz, 1H), 1.77 (t, J = 2.5 Hz, 3H), 1.51 (ddd, J = 13.6, 11.8, 4.4 Hz, 1H), 1.19 – 1.11 (m, 3H), 1.09 – 1.07 (m, 18H), 0.93 (s, 3H).

^{13}C NMR (101 MHz, CHLOROFORM-*d*) δ ppm = 174.72 (C), 150.23 (C), 111.66 (CH), 79.54 (C), 75.19 (C), 51.27 (CH_3), 45.49 (CH), 41.42 (CH_2), 37.50 (C), 28.95 (CH_2), 24.87 (CH_3), 22.25 (CH_2), 17.97 ($6\times\text{CH}_3$), 13.94 (CH_2), 12.60 ($3\times\text{CH}$), 3.52 (CH_3).

HRMS (EI) m/z calcd for $\text{C}_{23}\text{H}_{40}\text{O}_3\text{Si}$ [M^+]: 392.2747; found 392.2743.

FTIR (neat, cm^{-1}): ν = 2932 (s), 2866 (s), 1735 (s), 1195 (s).



Compound 4.2.6

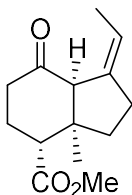
[**L5Au**NCMe] SbF_6 (167 mg, 0.22 mmol) was added to **4.2.7** (1.69 g, 4.33 mmol) in DCM:acetone (20:1, 20 ml) and stirred overnight. The solvent was evaporated under reduced pressure and the residue was purified by flash column chromatography on silica gel (5% to 8% EtOAc in hexane) to give the desired decalin **4.2.6** (969 mg, 76%).

¹H NMR (400 MHz, CHLOROFORM-*d*) δ ppm = 5.80 – 5.46 (m, 1H), 3.70 (s, 3H), 2.92 (dd, J = 10.6, 4.3 Hz, 1H), 2.81 – 2.69 (m, 1H), 2.53 – 2.21 (m, 3H), 2.20 – 1.95 (m, 3H), 1.63 (ddd, J = 13.6, 5.9, 3.9 Hz, 1H), 1.58 – 1.54 (m, 3H), 1.28 (ddd, J = 13.6, 9.6, 6.2 Hz, 1H), 0.99 (s, 3H).

¹³C NMR (101 MHz, CHLOROFORM-*d*) δ ppm = 212.38 (C), 174.27 (C), 128.89 (C), 123.32 (CH), 62.35 (CH₃), 51.51 (CH), 44.36 (CH), 38.80 (C), 38.15 (CH₂), 32.74 (CH₂), 24.65 (CH₂), 22.56 (CH₃), 22.34 (CH₂), 21.73 (CH₃).

HRMS (EI) m/z calcd for C₁₄H₂₀O₃ [M⁺]: 236.1412; found 236.1418.

FTIR (neat, cm⁻¹): ν = 2953 (m), 2255 (w), 1709 (s), 1705 (s), 729 (s).



Compound 4.2.18

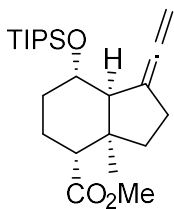
Side product during the formation of 4.2.6

¹H NMR (400 MHz, CHLOROFORM-*d*) δ ppm = 5.48 (qq, J = 6.9, 2.2 Hz, 1H), 3.65 (s, 3H), 3.02 (s, 1H), 2.64 (dd, J = 7.8, 5.9 Hz, 1H), 2.56 – 2.28 (m, 5H), 2.13 – 1.95 (m, 2H), 1.83 (ddd, J = 12.8, 8.8, 5.4 Hz, 1H), 1.44 (dq, J = 7.0, 2.0 Hz, 3H), 0.97 (s, 3H).

¹³C NMR (101 MHz, CHLOROFORM-*d*) δ ppm = 211.14 (C), 174.13 (C), 138.59 (C), 120.88 (CH), 63.28 (CH₃), 51.50 (CH), 49.98 (C), 45.96 (C), 37.79 (CH₂), 36.48 (CH₂), 29.77 (CH₂), 25.24 (CH₂), 22.16 (CH₃), 14.38 (CH₃).

HRMS (EI) m/z calcd for C₁₄H₂₀O₃ [M⁺]: 236.1412; found 236.1373.

FTIR (neat, cm⁻¹): ν = 2950 (m), 2251 (w), 1732 (s), 17007 (s), 1154 (s).



Compound 4.2.19

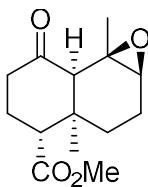
Side product during the formation of **4.2.6**

¹H NMR (400 MHz, CHLOROFORM-*d*) δ ppm = 4.86 – 4.56 (m, 2H), 4.24 – 4.03 (m, 1H), 3.66 (s, 3H), 2.58 – 2.39 (m, 2H), 2.32 (dd, J = 12.8, 2.9 Hz, 1H), 2.25 – 2.00 (m, 2H), 1.70 – 1.41 (m, 3H), 1.41 – 1.23 (m, 2H), 1.20 (s, 3H), 1.10 – 0.99 (m, 21H).

¹³C NMR (101 MHz, CHLOROFORM-*d*) δ ppm = 202.19 (C), 175.23 (C), 104.20 (C), 77.16 (CH₂), 67.94 (CH₃), 55.62 (CH), 51.15 (CH), 44.99 (C), 43.61 (CH), 37.16 (CH₂), 28.96 (CH₂), 26.75 (CH₂), 22.79 (CH₃), 18.93 (CH₂), 18.18 (6xCH₃), 12.28 (3xCH).

HRMS (EI) m/z calcd for C₂₃H₄₀O₃Si [M^+]: 392.2747; found 392.2755.

FTIR (neat, cm⁻¹): ν = 2943 (s), 2865 (s), 1736 (s), 1045 (s).



Compound 4.2.5

30% H₂O₂ (5.4 ml, 42 mmol) was added *via* a syringe pump to a solution of **4.2.6** (2.46 g, 10.4 mmol) and formic acid (1.74 ml, 62 mmol) in DCM (100 ml) over 5 hours. The

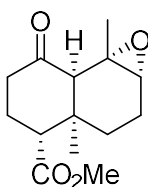
mixture was then stirred overnight at room temperature and water (100 ml) was added. The aqueous layer was extracted with DCM (3x). The combined organic layer was dried over anhydrous MgSO_4 , filtered and the solvent was evaporated under reduce pressure. The crude was purified by flash column chromatography on silica gel (10% to 20% EtOAc in hexane) to give the pure desired epoxide **4.2.5** (2.11 g, 81%).

^1H NMR (400 MHz, CHLOROFORM-*d*) δ ppm = 3.65 (s, 3H), 3.55 – 3.38 (m, 1H), 3.07 (d, J = 5.6 Hz, 1H), 2.64 – 2.49 (m, 1H), 2.39 (ddt, J = 14.0, 4.0, 1.6 Hz, 1H), 2.35 – 2.17 (m, 2H), 2.09 – 1.92 (m, 3H), 1.68 – 1.57 (m, 1H), 1.21 (s, 3H), 1.11 – 0.98 (m, 1H), 0.89 (s, 3H).

^{13}C NMR (101 MHz, CHLOROFORM-*d*) δ ppm = 210.95 (C), 174.02 (C), 61.34 (CH), 59.08 (CH_3), 57.93 (C), 51.40 (CH), 42.66 (CH), 39.23 (CH_2), 38.35 (C), 32.65 (CH_2), 24.27 (CH_2), 24.01 (CH_3), 22.23 (CH_3), 20.73 (CH_2).

HRMS (EI) m/z calcd for $\text{C}_{14}\text{H}_{20}\text{O}_4$ [$\text{M}^+ + \text{Na}^+$]: 275.1262; found 275.1238.

FTIR (neat, cm^{-1}): ν = 2941 (m), 1731 (s), 1702 (s), 1209 (s).



Compound 4.2.20

Side product during the formation of **4.2.5**

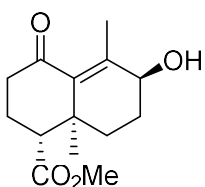
^1H NMR (400 MHz, CHLOROFORM-*d*) δ ppm = 3.67 (s, 3H), 3.04 (t, J = 1.9 Hz, 1H), 2.87 (dd, J = 12.5, 3.9 Hz, 1H), 2.54 – 2.42 (m, 2H), 2.40 – 2.19 (m, 2H), 2.08 (ddt, J =

13.5, 12.7, 4.8 Hz, 1H), 2.02 – 1.93 (m, 2H), 1.34 – 1.20 (m, 2H), 1.19 (s, 3H), 0.89 (s, 3H).

¹³C NMR (101 MHz, CHLOROFORM-*d*) δ ppm = 209.46 (C), 173.51 (C), 62.67 (CH), 59.24 (CH₃), 55.08 (C), 51.65 (CH), 43.73 (CH), 39.65 (CH₂), 36.51 (C), 28.77 (CH₂), 24.09 (CH₂), 22.81 (CH₃), 21.64 (CH₃), 20.72 (CH₂).

HRMS (EI) m/z calcd for C₁₄H₂₀O₄ [M⁺]: 252.1362; found 252.1346.

FTIR (neat, cm⁻¹): ν = 2934 (m), 2331 (w), 1732 (s), 1711 (s), 1210 (m).



Compound 4.2.4

Method A: DBU (10 ml, 67 mmol) was added to **4.2.5** (2.1 g, 8.3 mmol) in DCM (40 ml) and stirred for 16 hours. A saturated solution of NH₄Cl was added and the aqueous layer was extracted with DCM (3x). The combined organic layer was dried over anhydrous MgSO₄, filtered and the solvent was evaporated under reduce pressure. The crude was purified by flash column chromatography on silica gel (40% to 60% EtOAc in hexane) to give the desired alcohol **4.2.4** (1.85 g, 88%).

Method B: 30% H₂O₂ (0.11 ml, 0.76 mmol) was added *via* a syringe pump to a solution of **4.2.6** (45 mg, 0.19 mmol) and formic acid (0.032 ml, 1.14 mmol) in DCM (1.9 ml) over 3 hours. The reaction mixture was stirred for 16 hours and DBU (0.29 ml, 1.9 mmol) was added. 16 hours later a saturated solution of NH₄Cl was added and the aqueous layer was

extracted with DCM (3x). The combined organic layer was dried over anhydrous MgSO_4 , filtered and the solvent was evaporated under reduce pressure. The crude was purified by flash column chromatography on silica gel (40% to 60% EtOAc in hexane) to give the desired alcohol **4.2.4** (29 mg, 61%).

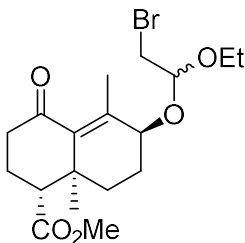
^1H NMR (400 MHz, CHLOROFORM-*d*) δ ppm = 3.99 (t, J = 3.2 Hz, 1H), 3.69 (s, 3H), 2.74 (dd, J = 12.8, 3.7 Hz, 1H), 2.58 (ddd, J = 14.6, 4.7, 1.9 Hz, 1H), 2.37 (ddd, J = 14.6, 13.2, 7.1 Hz, 1H), 2.30 – 2.16 (m, 1H), 2.08 – 1.98 (m, 1H), 1.97 – 1.88 (m, 1H), 1.86 (s, 3H), 1.84 – 1.73 (m, 2H), 1.53 – 1.39 (m, 1H), 1.04 (s, 3H).

^{13}C NMR (101 MHz, CHLOROFORM-*d*) δ ppm = 205.04 (C), 173.68 (C), 140.92 (C), 137.68 (C), 67.95 (CH), 52.49 (CH_3), 51.54 (CH), 41.80 (CH_2), 40.33 (C), 30.26 (CH_2), 26.97 (CH_2), 23.84 (CH_2), 18.75 (CH_3), 18.62 (CH_3).

HRMS (EI) m/z calcd for $\text{C}_{14}\text{H}_{20}\text{O}_4$ [M^+]: 252.1362; found 252.1372.

FTIR (neat, cm^{-1}): ν = 3445 (m), 2926 (m), 1723 (s), 1679 (s), 1147 (s).

7.3.3 Exploring the reactivity of the acetal / lactol



Compound 4.2.3

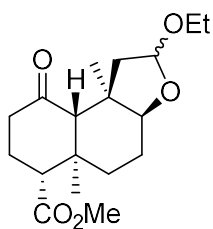
Ethyl vinyl ether (0.03 ml, 0.3 mmol) was added to NBS (57 mg, 0.3 mmol) in DCM (0.4 ml) at 0 °C and stirred for 1 hour. **4.2.4** (50 mg, 0.2 mmol) was added and the reaction mixture was stirred at room temperature for 16 hours. The solvent was evaporated under reduce pressure follow by the addition of Et₂O (10 ml). The organic layer was washed with water and brine. The organic layer was dried over anhydrous MgSO₄, filtered and the solvent was evaporated under reduce pressure. The crude was purified by flash column chromatography on basified silica gel (20% EtOAc in hexane with 1% Et₃N) to give the desired acetal **4.2.3** as a 1:1 mixture of diastereomer (75 mg, 96%).

¹H NMR (400 MHz, CHLOROFORM-*d*) δ ppm = 4.77 – 4.69 (m, 2H), 3.90 (q, *J* = 2.2 Hz, 1H), 3.75 (t, *J* = 3.1 Hz, 1H), 3.73 – 3.56 (m, 10H), 3.46 – 3.37 (m, 2H), 3.41 – 3.30 (m, 2H), 2.76 (ddd, *J* = 12.8, 4.6, 3.8 Hz, 2H), 2.56 (ddd, *J* = 14.8, 5.0, 2.0 Hz, 2H), 2.38 (dddd, *J* = 14.7, 13.3, 7.2, 3.2 Hz, 2H), 2.21 (qd, *J* = 13.3, 4.9 Hz, 2H), 2.07 – 1.85 (m, 5H), 1.83 (s, 3H), 1.83 (s, 3H), 1.73 – 1.51 (m, 2H), 1.50 – 1.36 (m, 2H), 1.23 (dt, *J* = 7.0, 4.0 Hz, 6H), 1.06 – 1.00 (m, 6H).

¹³C NMR (101 MHz, CHLOROFORM-*d*) δ ppm = 205.20 (C), 205.11 (C), 173.67 (C), 173.62 (C), 142.20 (C), 141.96 (C), 135.64 (C), 135.52 (C), 103.12 (CH), 100.23 (CH), 75.28 (CH), 72.58 (CH), 62.15 (CH₂), 62.09 (CH₂), 52.29 (CH₃), 52.28 (CH₃), 51.53 (CH), 51.52 (CH), 41.85 (CH₂), 41.81 (CH₂), 40.29 (C), 40.25 (C), 32.14 (CH₂), 32.01 (CH₂), 30.47 (CH₂), 30.17 (CH₂), 24.51 (CH₂), 23.95 (CH₂), 23.93 (CH₂), 22.72 (CH₂), 18.72 (CH₃), 18.63 (CH₃), 18.60 (CH₃), 18.52 (CH₃), 15.33 (CH₃), 15.13 (CH₃).

HRMS (ESI) *m/z* calcd for C₁₈H₂₇BrO₅ [*M*⁺ + Na⁺]: 427.0919; found 427.0942.

FTIR (neat, cm⁻¹): ν = 2970 (m), 2945 (m), 1731 (s), 1691 (s), 1009 (s)



Compound 4.2.2

[Au₂(dppm)₂]Cl₂ (570 mg, 0.56 mmol) was added to **4.2.3** (1.8 g, 4.6 mmol), DIPEA (4 ml, 5 mmol) in degassed MeCN (30 ml) and irradiated with 360 nm LED for 16 hours. The reaction mixture was quenched with H₂O and extracted with DCM (3x). The combined organic layers were dried over anhydrous MgSO₄, filtered and the solvent was evaporated under reduce pressure. The crude was purified by flash column chromatography on silica gel (20% EtOAc in hexane) to give the desired cyclic acetal **4.2.2** as a 1:1 mixture of diastereomer (1.30 g, 87%).

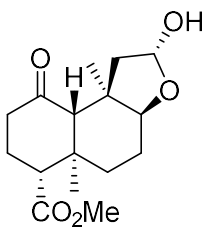
¹H NMR (400 MHz, CHLOROFORM-*d*) δ ppm = 5.02 – 4.94 (m, 2H), 3.81 – 3.59 (m, 9H), 3.51 (t, J = 2.8 Hz, 1H), 3.46 – 3.31 (m, 2H), 3.16 (s, 1H), 2.65 (dt, J = 12.6, 3.4 Hz, 2H), 2.40 (dddd, J = 14.7, 13.4, 5.2, 1.9 Hz, 2H), 2.33 – 2.08 (m, 7H), 2.05 – 1.90 (m, 3H), 1.89 – 1.68 (m, 5H), 1.59 (dd, J = 14.3, 4.4 Hz, 1H), 1.34 – 1.20 (m, 9H), 1.16 (dt, J = 7.1, 3.2 Hz, 6H), 1.01 (s, 6H).

¹³C NMR (101 MHz, CHLOROFORM-*d*) δ ppm = 209.40 (C), 208.99 (C), 173.77 (C), 173.58 (C), 102.96 (CH), 102.59 (CH), 84.60 (CH), 81.18 (CH), 63.54 (CH₂), 63.28 (CH₂), 59.98 (CH₃), 58.37 (CH₃), 55.22 (CH), 54.91 (CH), 51.38 (CH), 51.36 (CH), 50.25 (CH₂), 49.27 (CH₂), 42.05 (C), 41.59 (CH₂), 41.53 (CH₂), 40.97 (C), 40.89 (C), 39.31 (C), 31.99

(CH₂), 31.82 (CH₂), 24.72 (CH₂), 24.64 (CH₂), 21.19 (CH₂), 20.50 (CH₃), 20.36 (CH₂), 19.80 (CH₃), 15.63 (CH₃), 15.37 (CH₃), 15.27 (2xCH₃).

HRMS (EI) *m/z* calcd for C₁₈H₂₈O₅ [M⁺]: 324.1937; found 324.1957.

FTIR (neat, cm⁻¹): ν = 2931 (m), 1731 (s), 1708 (s), 995 (s).



Compound 4.2.25

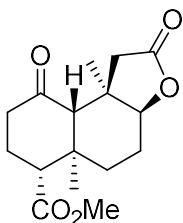
p-TSA (60 mg, 0.3 mmol) was added to **4.2.2** (100 mg, 0.3 mmol) in THF:H₂O (1:1, 1.5 ml) and refluxed for 3 hours. The reaction mixture was quenched with saturated NaHCO₃ and extracted with DCM (3x). The combined organic layers were dried over anhydrous MgSO₄, filtered and the solvent was evaporated under reduce pressure. The crude was purified by flash column chromatography on silica gel (70% EtOAc in hexane) to give the desired cyclic acetal **4.2.25** (77 mg, 87%).

¹H NMR (400 MHz, CHLOROFORM-*d*) δ ppm = 5.50 – 5.34 (m, 1H), 3.84 (d, *J* = 2.6 Hz, 1H), 3.66 (s, 3H), 2.96 (d, *J* = 3.5 Hz, 1H), 2.70 (ddd, *J* = 12.9, 3.5 Hz, 1H), 2.43 (ddt, *J* = 10.9, 5.6, 2.2 Hz, 1H), 2.36 – 2.13 (m, 3H), 2.02 – 1.91 (m, 1H), 1.89 – 1.71 (m, 3H), 1.63 – 1.54 (m, 1H), 1.34 (s, 3H), 1.31 – 1.25 (m, 1H), 1.02 (s, 3H).

¹³C NMR (101 MHz, CHLOROFORM-*d*) δ ppm = 208.97 (C), 173.59 (C), 97.12 (CH), 81.59 (CH), 59.83 (CH₃), 54.90 (CH), 51.50 (CH), 51.34 (CH₂), 42.70 (C), 41.58 (CH₂), 40.98 (C), 31.77 (CH₂), 24.63 (CH₂), 20.47 (CH₂), 19.87 (CH₃), 15.30 (CH₃).

HRMS (EI) m/z calcd for $C_{16}H_{24}O_5$ [$M^+ - OH$]: 279.1596; found 279.1600.

FTIR (neat, cm^{-1}): ν = 3430 (s), 2926 (m), 1723 (s), 1709 (s), 999 (s).



Compound 4.2.30

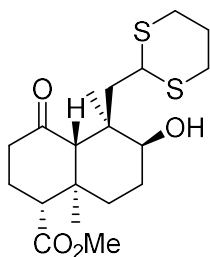
PCC (30 mg, 0.13 mmol) was added to **4.2.25** (20 mg, 0.068 mmol) and SiO_2 (30 mg) in DCM (0.34 ml). The reaction mixture was stirred for 3 hours and filtrated over cotton. The residue was evaporated under reduced pressure and purified by flash column chromatography on silica gel (40% to 60% EtOAc in hexane) to give the desired lactone **4.2.30** (18 mg, 91%).

1H NMR (400 MHz, CHLOROFORM-*d*) δ ppm = 4.13 (s, 1H), 3.66 (s, 3H), 2.67 (dd, J = 13.0, 3.6 Hz, 1H), 2.53 (d, J = 17.5 Hz, 1H), 2.48 – 2.40 (m, 1H), 2.39 – 2.26 (m, 2H), 2.24 – 2.10 (m, 2H), 2.09 – 1.93 (m, 2H), 1.90 – 1.69 (m, 2H), 1.42 (s, 4H), 1.06 (s, 3H).

^{13}C NMR (101 MHz, CHLOROFORM-*d*) δ ppm = 207.62 (C), 176.60 (C), 173.19 (C), 84.90 (CH), 58.39 (CH_3), 54.24 (CH), 51.58 (CH), 47.35 (CH_2), 41.09 (CH_2), 40.28 (C), 40.24 (C), 31.29 (CH_2), 24.34 (CH_2), 20.04 (CH_2), 19.75 (CH_3), 14.94 (CH_3).

HRMS (EI) m/z calcd for $C_{16}H_{22}O_5$ [M^+]: 294.1467; found 294.1444.

FTIR (neat, cm^{-1}): ν = 2940 (m), 1760 (s), 1700 (s), 1727 (s), 1160 (s),.



Compound 4.2.32

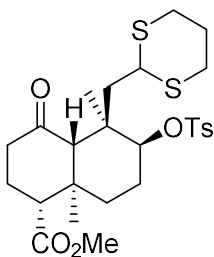
BF₃-Et₂O (0.23 ml, 1.85 mmol) was added to **4.2.2** (200 mg, 0.62 mmol) and 1,3-propanedithiol (0.19 ml, 1.85 mmol) in DCM (3 ml) at 0 °C. The reaction mixture was stirred for 1 hour at 0 °C and 30 minutes at room temperature. The reaction mixture was quenched with sat. NaHCO₃ stirred for 30 minutes. The aqueous layer was extracted with DCM (3x). The combined organic layers were dried over anhydrous MgSO₄, filtered and the solvent was evaporated under reduce pressure. The crude was purified by flash column chromatography on silica gel (20% to 40% EtOAc in hexane) to give the desired compound **4.2.32** (215 mg, 90%).

¹H NMR (400 MHz, CHLOROFORM-*d*) δ ppm = 4.07 (dd, *J* = 6.4, 3.0 Hz, 1H), 3.66 (s, 3H), 3.66 – 3.63 (m, 1H), 3.00 – 2.87 (m, 2H), 2.85 – 2.73 (m, 2H), 2.70 – 2.61 (m, 2H), 2.40 – 2.32 (m, 2H), 2.24 – 1.95 (m, 5H), 1.92 – 1.79 (m, 2H), 1.75 – 1.58 (m, 2H), 1.29 (s, 3H), 1.27 – 1.18 (m, 1H), 1.06 (s, 3H).

¹³C NMR (101 MHz, CHLOROFORM-*d*) δ ppm = 210.25 (C), 173.62 (C), 71.30 (CH), 58.98 (CH₃), 55.56 (CH), 51.38 (CH), 44.46 (CH₂), 42.60 (CH₂), 42.30 (C), 41.39 (CH), 40.24 (C), 31.48 (CH₂), 31.26 (CH₂), 31.19 (CH₂), 25.84 (CH₂), 25.10 (CH₂), 24.30 (CH₂), 18.66 (CH₃), 15.94 (CH₃).

HRMS (EI) *m/z* calcd for C₁₉H₃₀O₂S₂ [M⁺]: 386.1586; found 386.1598.

FTIR (neat, cm⁻¹): ν = 3462 (m), 3947 (m), 2362 (m), 1727 (s), 1707 (s), 669 (s).



Compound 4.2.33

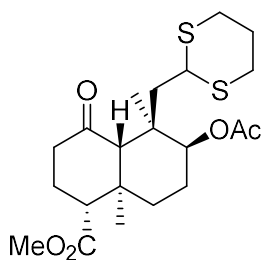
n-BuLi (0.12 ml, 0.28 mmol) was added to **4.2.32** (50 mg, 0.13 mmol) in THF (0.65 ml) at -78 °C and stirred for 5 minutes. TsCl (37 mg, 0.19 mmol) was added and the reaction mixture was warmed at room temperature. The reaction mixture was quenched with sat. NaHCO₃ and the aqueous layer was extracted with EtOAc (3x). The combined organic layers were dried over anhydrous MgSO₄, filtered and the solvent was evaporated under reduce pressure. The crude was purified by flash column chromatography on silica gel (20% to 30% EtOAc in hexane) to give the desired compound **4.2.33** (46 mg, 65%).

¹H NMR (400 MHz, CHLOROFORM-*d*) δ ppm = 7.89 (d, *J* = 8.3 Hz, 2H), 7.37 (d, *J* = 8.0 Hz, 2H), 4.58 – 4.46 (m, 1H), 4.20 (dd, *J* = 7.5, 4.6 Hz, 1H), 3.66 (s, 3H), 3.08 – 2.83 (m, 1H), 2.82 – 2.63 (m, 4H), 2.46 (s, 3H), 2.30 (ddd, *J* = 13.4, 5.2, 1.9 Hz, 1H), 2.12 (qd, *J* = 13.5, 5.2 Hz, 1H), 2.02 – 1.72 (m, 6H), 1.48 (dd, *J* = 15.2, 4.5 Hz, 1H), 1.43 (s, 3H), 1.33 – 1.20 (m, 4H), 1.03 (s, 3H).

HRMS (EI) *m/z* calcd for C₂₆H₃₆O₆S₃ [*M*⁺]: 540.1674; found 540.1674.

FTIR (neat, cm⁻¹): ν = 2953 (m), 1735 (s), 1711 (s), 1237 (s), 1044 (s).

7.3.4 En route towards the synthesis of salvinorin A



Compound 4.2.35

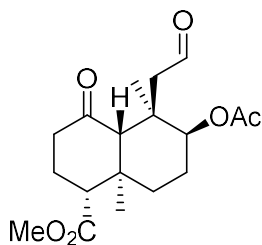
Ac₂O (0.13 ml, 1.3 mmol) was added to **4.2.32** (170 mg, 0.44 mmol), DMAP (11 mg, 0.08 mmol) and Et₃N (0.25 ml, 1.75 mmol) in DCM (2.2 ml) and stirred for 16 hours. The reaction mixture was quenched with H₂O and extracted with DCM (3x). The combined organic layers were dried over anhydrous MgSO₄, filtered and the solvent was evaporated under reduce pressure. The crude was purified by flash column chromatography on silica gel (20% to 30% EtOAc in hexane) to give the desired compound **4.2.35** (179 mg, 95 %).

¹H NMR (400 MHz, CHLOROFORM-*d*) δ ppm = 4.72 (dd, *J* = 3.4, 2.2 Hz, 1H), 3.94 (t, *J* = 5.0 Hz, 1H), 3.65 (s, 3H), 2.86 (dddd, *J* = 14.5, 12.2, 4.2, 2.5 Hz, 2H), 2.77 – 2.63 (m, 2H), 2.51 (s, 1H), 2.46 – 2.29 (m, 2H), 2.23 – 2.10 (m, 1H), 2.09 (s, 3H), 2.05 – 1.91 (m, 3H), 1.86 – 1.66 (m, 4H), 1.55 (dd, *J* = 14.9, 4.6 Hz, 1H), 1.38 (s, 3H), 1.33 – 1.17 (m, 2H), 1.04 (s, 3H).

¹³C NMR (101 MHz, CHLOROFORM-*d*) δ ppm = 209.24 (C), 173.25 (C), 170.26 (C), 75.03 (CH), 59.81 (CH₃), 55.77 (CH), 51.54 (CH), 44.40 (CH₂), 42.47 (CH₂), 42.14 (C), 41.97 (CH), 39.16 (C), 32.03 (CH₂), 31.57 (CH₂), 31.50 (CH₂), 25.77 (CH₂), 25.13 (CH₂), 21.71 (CH₃), 21.65 (CH₂), 19.02 (CH₃), 15.88 (CH₃).

HRMS (EI) *m/z* calcd for C₂₁H₃₂O₅S₂ [M⁺]: 428.1691; found 428.1698.

FTIR (neat, cm⁻¹): ν = 2947 (m), 2358 (m), 1728 (s), 1726 (s), 1715 (s), 1239 (s).



Compound 4.2.36

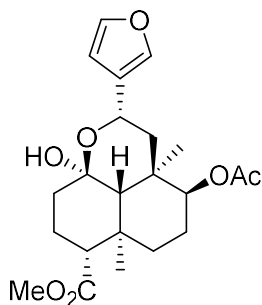
MeI (2.06 ml, 16.6 mmol) was added to **4.2.35** (178 mg, 0.415 mmol), CaCO₃ (750 mg, 7.5 mmol) in MeCN (20 ml) and H₂O (20 ml) and was vigorously stirred for 16 hours. The reaction mixture was quenched with saturated NH₄Cl and extracted with DCM (3x). The combined organic layers were dried over anhydrous MgSO₄, filtered and the solvent was evaporated under reduce pressure. The crude was purified by flash column chromatography on silica gel (40% to 50% EtOAc in hexane) to give the desired compound **4.2.37** (145 mg, 99 %).

¹H NMR (400 MHz, CHLOROFORM-*d*) δ ppm = 9.70 (dd, J = 3.2, 2.3 Hz, 1H), 4.69 (t, J = 2.7 Hz, 1H), 3.68 (s, 3H), 2.82 – 2.68 (m, 2H), 2.52 – 2.36 (m, 4H), 2.28 – 2.13 (m, 1H), 2.05 (s, 4H), 1.96 – 1.85 (m, 1H), 1.82 – 1.71 (m, 2H), 1.46 (s, 3H), 1.40 – 1.31 (m, 1H), 1.09 (s, 3H).

¹³C NMR (101 MHz, CHLOROFORM-*d*) δ ppm = 209.43 (C), 201.13 (CH), 173.17 (C), 169.83 (C), 76.96 (CH), 58.02 (CH₃), 55.54 (CH), 52.43 (CH₂), 51.59 (CH), 41.87 (C), 41.83 (CH₂), 39.66 (C), 32.12 (CH₂), 25.38 (CH₂), 21.74 (CH₂), 21.23 (CH₃), 20.82 (CH₃), 15.99 (CH₃).

HRMS (EI) m/z calcd for C₁₈H₂₆O₆ [M^+ -O]: 324.1937; found 324.6226.

FTIR (neat, cm⁻¹): ν = 2951 (m), 1729 (s), 1711 (s), 1706 (s), 1232 (s).



Compound 4.2.38

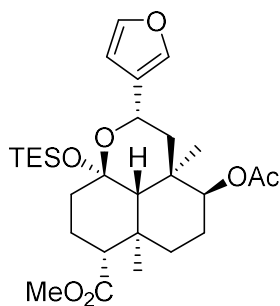
(3-furyl)Ti(OiPr)₃¹³² (0.72 ml, 0.3 mmol) was slowly added to **4.2.37** (50 mg, 0.15 mmol) and (*R*)-BINOL (2 mg, 0.007 mmol) in THF (3 ml) at 0 °C and stirred for 3 hours. The reaction mixture was quenched with 1M NaOH and extracted with EtOAc (3x). The combined organic layers were dried over anhydrous MgSO₄, filtered and the solvent was evaporated under reduce pressure. The crude was purified by flash column chromatography on silica gel (20% to 30% EtOAc in hexane) to give the desired compound **4.2.38** (42 mg, 70 %).

¹H NMR (400 MHz, CHLOROFORM-*d*) δ ppm = 7.46 – 7.31 (m, 2H), 6.34 (dd, *J* = 1.8, 0.9 Hz, 1H), 5.14 (ddd, *J* = 12.0, 2.0, 0.8 Hz, 1H), 4.56 (t, *J* = 2.7 Hz, 1H), 3.64 (s, 3H), 2.23 (dd, *J* = 12.9, 2.7 Hz, 1H), 2.17 – 1.95 (m, 6H), 1.89 – 1.56 (m, 7H), 1.51 (d, *J* = 0.9 Hz, 3H), 1.48 – 1.39 (m, 1H), 1.33 – 1.24 (m, 1H), 1.22 (s, 3H).

¹³C NMR (101 MHz, CHLOROFORM-*d*) δ ppm = 173.98 (C), 170.38 (C), 142.93 (CH), 138.83 (CH), 127.24 (C), 108.66 (CH), 97.35 (C), 76.16 (CH), 61.35 (CH), 56.80 (CH₃), 51.10 (CH), 48.85 (CH), 44.35 (CH₂), 40.98 (CH₂), 37.09 (C), 36.29 (C), 35.24 (CH₂), 22.23 (CH₂), 21.72 (CH₂), 21.56 (CH₃), 21.23 (CH₃), 15.42 (CH₃).

HRMS (EI) m/z calcd for $C_{22}H_{30}O_7$ [M^+]: 406.1992; found 406.1982.

FTIR (neat, cm^{-1}): ν = 3483 (m), 1936 (m), 1726 (s), 1707 (s), 1237 (s), 1022 (s).



Compound 4.2.39

4.2.38 (50 mg, 0.123 mmol) was slowly added to NaHMDS (30 mg, 0.16 mmol) in THF (1.2 ml) at $-78^\circ C$ and stirred for 30 minutes. TESCl (0.04 ml, 0.246 mmol) was then added and the mixture was brought to room temperature. The reaction mixture was quenched with sat. $NaHCO_3$ and extracted with Et_2O (3x). The combined organic layers were dried over anhydrous $MgSO_4$, filtered and the solvent was evaporated under reduce pressure. The crude was purified by flash column chromatography on basified silica gel (5% to 10% EtOAc in hexane with 1% Et_3N) to give the desired compound **4.2.39** (60 mg, 94 %).

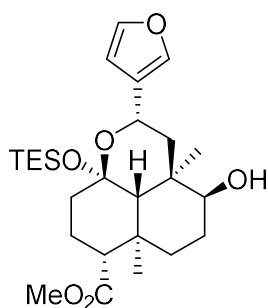
1H NMR (400 MHz, $CHCl_3-d$) δ ppm = 7.35 (t, J = 1.7 Hz, 1H), 7.32 – 7.29 (m, 1H), 6.33 (dd, J = 1.8, 0.9 Hz, 1H), 4.96 (d, J = 11.1 Hz, 1H), 4.54 (t, J = 2.7 Hz, 1H), 3.64 (s, 3H), 2.23 (dd, J = 12.9, 2.8 Hz, 1H), 2.06 (s, 3H), 2.05 – 1.85 (m, 2H), 1.84 – 1.55 (m, 5H), 1.48 (d, J = 0.8 Hz, 3H), 1.44 – 1.35 (m, 1H), 1.35 – 1.23 (m, 2H), 1.20 (s, 3H), 0.98 (dt, J = 15.9, 7.9 Hz, 10H), 0.77 – 0.69 (m, 6H).

^{13}C NMR (101 MHz, $CHCl_3-d$) δ ppm = 174.17 (C), 170.54 (C), 142.88 (CH), 138.79 (CH), 127.43 (C), 108.68 (CH), 99.31 (C), 76.53 (CH), 61.69 (CH), 56.96 (CH_3),

51.17 (CH), 50.34 (CH), 44.24 (CH₂), 39.87 (CH₂), 37.25 (C), 36.18 (C), 35.52 (CH₂), 22.25 (CH₂), 21.97 (CH₂), 21.33 (CH₃), 21.31 (CH₃), 15.63 (CH₃), 6.58 (3xCH₃), 5.80 (3xCH₂).

HRMS (EI) *m/z* calcd for C₂₈H₄₄O₇Si [M⁺-C₂H₅]: 491.2465; found 491.2445.

FTIR (neat, cm⁻¹): ν = 2952 (m), 1732 (s), 1240 (s).



Compound 4.2.40

K₂CO₃ (20 mg, 0.139 mmol) was added to **4.2.39** (60 mg, 0.115 mmol) in MeOH (1.2 ml) at room temperature and stirred for 24 hours. The mixture was filtrated and concentrated under reduce pressure followed by the addition of H₂O and extraction with DCM (3x). The combined organic layers were dried over anhydrous MgSO₄, filtered and the solvent was evaporated under reduce pressure. The crude was purified by flash column chromatography on basified silica gel (20% to 30% EtOAc in hexane with 1% Et₃N) to give the desired compound **4.2.40** (36.2 mg, 66 %).

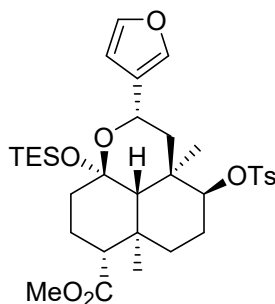
¹H NMR (400 MHz, CHLOROFORM-*d*) δ ppm = 7.36 (s, 1H), 7.35 (s, 1H), 6.38 (t, *J* = 1.4 Hz, 1H), 4.97 (dd, *J* = 12.0, 2.1 Hz, 1H), 3.64 (s, 3H), 3.32 (t, *J* = 2.7 Hz, 1H), 2.24 (dd, *J* = 12.9, 2.9 Hz, 1H), 2.19 – 1.83 (m, 4H), 1.75 (dt, *J* = 13.9, 3.8 Hz, 1H), 1.69 (s,

1H), 1.67 – 1.45 (m, 3H), 1.44 – 1.38 (m, 3H), 1.39 – 1.31 (m, 1H), 1.24 (dd, $J = 12.8, 2.1$ Hz, 1H), 1.19 (s, 3H), 1.00 (t, $J = 7.9$ Hz, 9H), 0.81 – 0.65 (m, 6H).

^{13}C NMR (101 MHz, CHLOROFORM-*d*) δ ppm = 174.42 (C), 142.83 (CH), 139.01 (CH), 127.62 (C), 108.93 (CH), 99.44 (C), 74.50 (CH), 61.67 (CH), 56.91 (CH₃), 51.11 (CH), 49.09 (CH), 44.40 (CH₂), 39.97 (CH₂), 37.37 (C), 37.00 (C), 34.78 (CH₂), 25.16 (CH₂), 22.01 (CH₂), 21.58 (CH₃), 15.69 (CH₃), 7.29 (3xCH₃), 6.34 (3xCH₂).

HRMS (EI) m/z calcd for C₂₆H₄₂O₆Si [M^+]: 478.2751; found 478.2739.

FTIR (neat, cm⁻¹): $\nu = 3500$ (m), 2952 (s), 2361 (w), 1731 (s), 968 (s).



Compound 4.2.41

4.2.40 (12 mg, 0.025 mmol) was added to NaHMDS (7 mg, 0.38 mmol) in THF (0.25 ml) at -78 °C and stirred for 20 minutes. TsCl (10 mg, 0.05 mmol) was added and the reaction mixture was warmed at room temperature. The reaction mixture was quenched with sat. NaHCO₃ and the aqueous layer was extracted with EtOAc (3x). The combined organic layers were dried over anhydrous MgSO₄, filtered and the solvent was evaporated under reduce pressure. The crude was purified by flash column chromatography on silica gel (10% to 20% EtOAc in hexane) to give the desired compound **4.2.41** (11 mg, 70%).

¹H NMR (400 MHz, CHLOROFORM-*d*) δ ppm = 7.77 (d, J = 8.3 Hz, 2H), 7.35 (t, J = 1.7 Hz, 1H), 7.28 (d, J = 8.0 Hz, 2H), 7.16 (dt, J = 1.7, 0.9 Hz, 1H), 6.21 (dd, J = 1.9, 0.8 Hz, 1H), 4.82 (d, J = 11.9, 1.6 Hz, 1H), 4.23 – 4.11 (m, 1H), 3.63 (s, 3H), 2.42 (s, 3H), 2.22 (dd, J = 12.9, 2.8 Hz, 1H), 2.10 – 1.82 (m, 3H), 1.79 – 1.56 (m, 6H), 1.55 (s, 1H), 1.39 (s, 3H), 1.16 (s, 3H), 0.98 (t, J = 7.9 Hz, 9H), 0.85 (dd, J = 13.1, 2.1 Hz, 1H), 0.77 – 0.64 (m, 6H).

¹³C NMR (101 MHz, CHLOROFORM-*d*) δ ppm = 174.09 (C), 144.61 (C), 142.71 (CH), 138.98 (CH), 134.27 (C), 129.81 (2xCH), 127.81 (2xCH), 127.00 (C), 108.83 (CH), 99.20 (C), 86.32 (CH), 61.29 (CH), 56.43 (CH₃), 51.17 (CH), 49.66 (CH), 44.18 (CH₂), 39.72 (CH₂), 36.99 (C), 36.85 (C), 34.75 (CH₂), 23.20 (CH₂), 21.91 (CH₂), 21.59 (CH₃), 21.19 (CH₃), 15.68 (CH₃), 7.23 (3xCH₃), 6.29 (3xCH₂).

HRMS (EI) m/z calcd for C₃₃H₄₈O₈SSi [M⁺ -C₂H₅]: 603.2448; found 603.2454.

FTIR (neat, cm⁻¹): ν = 2952 (m), 2361 (w), 1731 (s), 1177 (s), 595 (s).

-
- [122] S. Mukherjee, D. Kontolosta, A. Palti, S. Rallapalli, and D. Lee, *J. Org. Chem.*, **2009**, *74*, 9206-9209.
- [123] G. Bellavance, L. Barriault, *Angew. Chem.* **2014**, *126*, 6819-6822.
- [124] N. Kern, A. Blanc, S. Miaskiewicz, M. Robinette, J.-M. Weibel, P. Pale, *J. Org. Chem.*, **2012**, *77*, 4323-4341.
- [125] M. Morin, P. Levesque, L. Barriault, *Beislt. J. Org. Chem.*, **2013**, *9*, 2625-2628.
- [126] C. A. Miller, R. A. Batey, *Org. Lett.*, **2004**, *6*, 699-702.
- [127] M. E. H. Howden, A. Maercker, J. Burdon, J. D. Roberts, *J. Am. Chem. Soc.* **1966**, *88*, 1732-1737.
- [128] P. A. Grieco, P. Galatsis, R. F. Spohn, *Tetrahedron*, **1986**, *42*, 2847-2853.
- [129] S. F. Martin, S. A. Williamson, R. P. Gist, K. M. Smith, *J. Org. Chem.* **1983**, *48*, 5170-5180.
- [130] J. S. Bair, R. Palchaudhuri, P. J. Hergenrother, *J. Am. Chem. Soc.*, **2010**, *132*, 5469-5478.
- [131] V. Hickmann, M. Alcarazo, A. Fuerstner, *J Am. Chem. Soc.*, **2010**, *132*, 11042-11044.
- [132] S. Zhou, C.-R. Chen, H.-M. Gau, *Org. Lett.*, **2010**, *12*, 48-51.

**Collective Spectral Data: Application of Gold(I) Catalysis in the
Synthesis of Bridged Carbocycles, (±)-Magellanine and
(±)-Salvinorin A**

Philippe McGee

Supporting information for a thesis submitted in partial fulfillment of the
requirements for the Doctorate Philosophy degree in Chemistry

Department of Chemistry and Biomolecular Science
Faculty of Science
University of Ottawa

© Philippe McGee, Ottawa, Canada, 2018

